DEVELOPMENT OF DATA-DRIVEN, REDUCED-COMPLEXITY WATERSHED SIMULATION MODELS TO ADDRESS AGRICULTURAL NON-POINT SOURCE SEDIMENT POLLUTION IN SOUTHERN MINNESOTA

by
Se Jong Cho

A dissertation submitted to Johns Hopkins University in conformity with the requirements for the degree of Doctor of Philosophy in Environmental Engineering and Management

Baltimore, Maryland

January 2017

Abstract

Agricultural nonpoint source sediment pollution and management has been a subject of intensive modeling and economic research. Important challenges remain for the scientific and regulatory communities in understanding, not only the mechanisms of pollution, but also different options for environmental management. To better understand nonpoint source pollution at the watershed scale and to evaluate the impacts of various management options, a data-driven, reduced-complexity modeling framework is developed through a collaborative process involving multiple scientists, engineers, and economists, as well as local stakeholders in Southern Minnesota. The models in this framework are developed by making the most effective use of abundant information on soils, topography, and sediment loading in a platform that is transparent and accessible for decision-making. The models' simulation outputs are within the constraints provided by observation and tested against independent data, thereby providing reliable and robust predictions about management impact on water quality. This modeling framework can support evaluation of different conservation scenarios to address nonpoint source sediment pollution in an agricultural watershed with simulation outputs that are relevant to environmental and social needs.

Acknowledgement

Over the years I have received support and encouragement from many people. Dr. Wilcock and Dr. Hobbs have been my mentors, colleagues, and friends. Their guidance has made this a thoughtful and rewarding journey. I would like to thank Dr. Zaitchik for his support and advice on matters on earth and sky. I would also like to thank the Collaborative for Sediment Source Reduction (CSSR) team for supporting my research through teamwork and friendship, especially Dr. Gran, Dr. Belmont, Dr. Kumarasari, Martin Bevis, Nate Mitchell, Barbara Heitkempt, and Jeff Marr. Also, I would like to dedicate a special thanks to the stakeholders of the CSSR project; without them, this research would have been very different. Finally, I would like to thank my husband, Marc Miller for his constant encouragement, kindness, and love.

Table of Content

1. Introduction

1.1. Problem statement and research objective

Agricultural nonpoint source (NPS) sediment pollution is a leading cause of impairment in U.S. rivers and streams. Water quality management planning, required to allocate mitigation activities to effectively address NPS pollution, has been a subject of intensive modeling and research (Palmer et al., 2000; Shortle and Horan, 2001; US EPA, 2012a). However, we are still left with a number of important challenges in addressing and managing water quality: 1) reliable quantification of locations, mechanisms, and rates of sediment loading in order to assign appropriate management strategies (Belmont et al., 2011) , 2) accurate and practicable information on best available, economically achievable means in reducing agricultural NPS pollution (US EPA, 2012b), and 3) an accessible and reliable basis for evaluating the effectiveness and tradeoffs among different conservation strategies at the watershed scale (Tomer et al., 2015).

First, the challenges in providing background information about agricultural NPS pollution include difficulties in measuring and predicting the pollution sources and transport. Sediment erosion and transport processes are spatially dispersed, strongly contingent on local conditions, and inherently nonlinear (De Vente et al., 2007; Phillips, 2006). The Universal Soil Loss Equation (USLE) provides a basis for predicting soil erosion rates at the field scale based on research observations and extensive mapping of soil properties over the past century (Wischmeier and Smith, 1978). However, linking the USLE estimated soil erosion rates to watershed-scale sediment yield requires a reliable estimate of delivery and storage of sediment across the watershed. This problem has been

referred to as the *Sediment Delivery Problem* and remains an outstanding challenge in geomorphology and watershed modeling (Trimble, 2000; Walling, 1983).

Soil erosion from agricultural fields is not the only source of sediment pollution. Near-channel sediment supply (NCSS) associated with erosion of streambanks, bluffs, and near-channel gullies and ravines may contribute substantially to sediment loading from a watershed. For example, Belmont et al., (2011) use geochemical fingerprinting and a suite of geomorphic change detection techniques to demonstrate that the dominant sediment source in the Minnesota River Basin (MNRB) has shifted from agricultural soil erosion to NCSS associated with increased river discharge over the past 50 to 75 years (Novotny and Stefan, 2007). Reliable estimates of NCSS are difficult to obtain because the associated mechanisms are varied and highly episodic such that direct measurement requires substantial effort (e.g., erosion pins, close-range photogrammetry, terrestrial laser scanning, and traditional survey methods) (Day et al., 2013a; Westoby et al., 2012). A reliable and practical basis for estimating NCSS is another outstanding challenge in addressing NPS sediment pollution.

Water quality problems accumulate to the continental scale (water pollution in the upstream states will affect the downstream water quality in the Gulf of Mexico), yet the solution to these problems lies in the management of thousands of agricultural watersheds and millions of individual farm fields across the Midwest (Tomer et al., 2015). A second challenge in addressing NPS sediment pollution concerns the complex nature of the agricultural system, much of which is in private ownership and responds to both market and policy forces (Xepapadeas, 1992). Individual and collective responses of farmers to policy directives is difficult to forecast (Segerson, 1988), making it also difficult to define

the adoption or outcome of different programs intended to improve water quality at the watershed-scale. Critical dimensions of social, economic, and environmental concerns can be evaluated in the form of competing objectives, but the challenge remains to effectively forecast and communicate the tradeoffs among multiple objectives for different management scenarios at a scale relevant for policy decisions (Stoorvogel et al., 2004).

A third challenge for managing water quality links the physical and social components. What is the best approach for simulating NPS sediment pollution in a fashion that balances available information, model accuracy and clarity, and stakeholder engagement? Watershed simulation models have evolved to have a complex model structure that includes many different watershed processes and mechanisms (Tomer et al., 2015). Despite their complexity, such models may not include essential or valuable elements, such as a basis to evaluate NCSS or to incorporate the effect of uncertainty in decision support (see Chapter 2 for a review of watershed models). With many complex and inter-linked mechanisms, watershed models generally include very large numbers of boundary conditions and parameters, requiring extensive calibration such that the meaning, reliability, and uniqueness of model outputs are difficult to judge (Haag and Kaupenjohann, 2001; Korfmacher, 2001; Smith et al., 2011). Existing watershed simulation models are sufficiently slow and complex that decision-makers or stakeholders are often unable to utilize the model independently to evaluate new environmental conditions and management scenarios, introducing an important separation between decision-makers and management simulation results (Gaddis, 2010).

A reduced-complexity model that makes efficient use of available information and provides accessible and reliable predictions could be more useful in helping stakeholders make strategic investment decisions than complex watershed models. The overarching objective of this dissertation is to target the challenges associated with NPS pollution management by developing a watershed modeling framework for assessing conservation actions intended to reduce sediment loading from an agricultural watershed. This overarching research objective can be broken down to three modeling components:

1) **Develop a reduced-complexity sediment delivery model to better understand NPS sediment pollution transport and deposition at the watershed-scale.**

   This work is aimed at the challenges associated with predicting erosion and transport of NPS sediment pollution. The sediment delivery model combines spatially extensive information on soil erosion and topography with spatially integrated information on watershed sediment loads with the goal of extracting the effect of watershed topography on sediment delivery. The model is reduced in complexity because local sediment transport mechanisms are not modeled. Rather, two simple functions of topography, one for field transport and another for stream transport, are used to link the spatially distributed soil erosion data to the sediment loading measurements at gages. Although spatially explicit, the model is computationally simple such that it is possible to build a watershed-scale sediment delivery model without the burden of long computational time. The simplicity of the model allows for transparent demonstration of the

assumptions about the model structure, and the implications of its predictions and uncertainties.

2) **Evaluate the NPS sediment pollution from near-channel sources and its dependence on river discharge.**

This work is aimed at the challenges associated with estimating near-channel sediment supply (NCSS). Commonly used watershed simulation models do not directly estimate NCSS, although some have been adapted to use independent estimates of NCSS as a separate input (Smith et al., 2011). We develop sediment load estimates for paired stream gages that bracket stream reaches with large NCSS and find that the rate of NCSS can be estimated as a function of river discharge. This approach may provide important advantages as stream gaging is becoming more extensive, reliable, and cost-effective (Juracek and Fitzpatrick, 2009; Wahl et al., 1995). The NCSS empirical model provides a basis for predicting the effect on NCSS of water conservation measurements intended to reduce river discharge.

3) **Develop a watershed management simulation model for evaluating conservation actions across the watershed.**

This work is aimed at the challenges associated with providing a reliable and accessible basis to evaluate various portfolios of management alternatives at the watershed scale. The sediment delivery simulation in 1) and the NCSS model in 2) provide the core of a management option simulation model. This model is designed to evaluate different portfolios of conservation measures intended to reduce sediment sources and/or sediment delivery. Model outputs

are constrained by observed information of sediment loading under a wide range of user inputs of management scenarios. The model runs in seconds, thereby allowing immediate user feedback and permitting multiple simulation runs that can be used to evaluate tradeoffs among different management scenarios.

1.2. Contribution of the data-driven, reduced-complexity approach to watershed modeling

There is a paradigm in environmental simulation modeling that puts emphasis on building complex models to match the complex environmental system and regulatory demands (Thomann, 1998). Especially with the advent of computers, it became possible to deal with increasing model complexity with large number of parameters in dynamical simulations (Haag and Kaupenjohann, 2001). However, increasing model complexity requires more data input, which may or may not be available at the relevant scale, with results that are more difficult to interpret and understand, and not necessarily accurate (Korfmacher, 2001).

Modeling to support environmental decision-making should offer transparency and provide context-sensitive knowledge to support stakeholder engagement in specific decision problems (Haag and Kaupenjohann, 2001). When simulation models are developed with the participation of stakeholders, valuable learning occurs as the stakeholders participate in model development and execution (Yearley, 1999).

In this dissertation, we present an approach to watershed modeling for decision-making processes that is data-driven and of reduced-complexity. This approach aims to make the most effective use of existing information on soils, topography, and stream

gaging in a reduced-complexity platform that is transparent and relevant for decision-making. The resulting simulation model is meant to support ready evaluation of different conservation scenarios by providing *relevant*, *reliable*, and *robust* simulation outputs.

- The data-driven, reduced-complexity modeling approach is *relevant* to environmental and social needs in that it focuses on developing a model that is transparent and built on stakeholder input. Policy questions and stakeholder inputs are embedded in model development and only those watershed processes immediately pertinent to environmental decision-making are included, rather than trying to represent all possible physical processes.
- In this approach, observational data provide strong constraints on model predictions such that the model produces *reliable* predictions: the model predictions are credible and consistent with observations at the watershed scale.
- Lastly, individual model processes and uncertainties are traceable within the reduced-complexity structure and model predictions are bounded by observation data. Thus, this approach aims to provide *robust* solutions: the model is unlikely to produce solutions outside the realm of possibility under a wide range of user inputs.

The data-driven, reduced-complexity modeling approach distributes the results of the physical processes across the watershed using observed data within models with reduced-complexity structure, where only essential and measurable physical attributes are incorporated to make predictions about the effects of management options on NPS sediment erosion and transport.

1.3. Social context of the research

This dissertation presents a watershed-modeling framework to address widespread NPS sediment pollution in south central Minnesota. In the Minnesota River Basin (MNRB), turbidity due to excess sediment loading is a pressing environmental and social problem. For instance, coring records indicate that the sedimentation rate in Lake Pepin, a natural lake of recreational and popular importance on the Mississippi River, has increased by an order of magnitude over the past 150 years (Engstrom, 2009). The MNRB is a major culprit in the increased sedimentation rate in Lake Pepin contributing about 80-90% of suspended sediment (Belmont et al., 2011). Up to 50% of that sediment load comes from the Greater Blue Earth River Basin (GBERB), a south central watershed that comprises only about 20% of the MNRB (Wilcock, 2009) (more description of the study site in Chapter 2). When the watershed's total maximum daily load (TMDL) was issued in 2012, it listed 39 river reaches in the GBERB as impaired for turbidity under section 303d of the Clean Water Act (Minnesota State University, Mankato Water Resources Center, 2012).

Investment required to reduce sediment loading and other NPS water quality problems in the GBERB and the rest of Minnesota is potentially enormous (Belmont et al., 2011). In 2008, a substantial down payment was made when Minnesotans passed a state constitutional amendment that will raise over $3.5 billion in tax revenue through 2034, with approximately one-third directed toward protecting and mitigating water quality (Minnesota State Legislative Coordinating Commission, 2016). Effective use of these funds to effectively address sediment pollution will require accurate identification of sources and mechanisms of sediment supply (Belmont et al., 2011).

The work in this dissertation was developed within a broad stakeholder framework, termed Collaborative for Sediment Source Reduction (CSSR). The primary goal of CSSR was to develop a basis for evaluating and prioritizing different management actions for reducing sediment loading. The resulting product is intended to support watershed-scale prioritization addressing the challenges of agricultural NPS pollution management (Wilcock et al., 2016). CSSR operated in a collaborative environment in which scientists and stakeholders from multiple state agencies, industry groups, and individual farmers worked together towards the development of a consensus strategy to address the watershed's sediment pollution (Belmont et al., 2012). CSSR stakeholders provided guidance on local environmental, social, and economic factors and provided evaluation of components and outputs of the models as they were being developed. A further discussion on stakeholder involvement can be found in Chapter 2, including the types of participants and meeting processes.

1.4. Scope

Chapter 2 provides a description of the watershed and the regional water quality management requirements that have motivated and guided this project. The chapter also examines the limitations and advantages of different approaches to watershed modeling and environmental decision analysis, and argues that a reduced complexity approach tightly constrained by existing information is needed.

Sediment delivery and near-channel sediment supply components of the management simulation model are developed in Chapters 3 through 5. Each chapter reviews previous research efforts and founding principles, and describes the contributions made with our research. Chapter 3 introduces the sediment delivery model (termed Topofilter) that uses

spatially explicit soil erosion rates and topography to develop a model for determining the sediment delivery ratio (the fraction of eroded sediment that is delivered from the watershed). Chapter 4 extends the Topofilter approach to include near-channel source sediment loading in multiple subwatersheds. Chapter 5 develops a model for estimating near-channel sediment supply as a function of river discharge using paired gages, providing a predictive basis for evaluating the effects of water storage management on near-channel source sediment loading.

Chapter 6 develops the management option simulation model, which combines the sediment delivery models with a set of representative management options intended to reduce agricultural NPS sediment sources and delivery from the watershed. The model includes development of a management option database that is used to quantify available spatial extents for implementation. Chapter 7 examines model behavior for a range of management options and evaluates the tradeoffs between environmental and economic objectives among these management scenarios. Chapter 8 concludes the dissertation with a summary of how the research objectives are accomplished through the work described in the preceding chapters.

2. Background on Watershed Modeling and the Case Study Region

2.1. Introduction

This chapter provides background for the development of a management option simulation model to support decisions concerning rural sediment reduction. The chapter begins with a broad review of watershed models and their use in supporting decision analysis for nonpoint source (NPS) pollution control. Further background on specific modeling topics is provided in later chapters in this dissertation on sediment delivery (Chapters 3, 4), near-channel sediment supply (Chapter 5), and the development of the management option simulation model (Chapter 6).

We also describe in this chapter the geophysical characteristics and the history of anthropogenic influences in the study watershed. Some local factors play an important role in motivating and shaping model development.

The chapter closes with a description of watershed models intended to evaluate NPS sediment pollution and management options to reduce sediment loading within the context of collaborative modeling process. This approach involved multiple scientists and stakeholders as a part of the Collaborative for Sediment Source Reduction (CSSR). The collaboration builds on previous work establishing a sediment budget for the watershed, (Belmont et al., 2011; Gran et al., 2011), local environmental, social, and land use knowledge provided by the stakeholders, and experience with the previous application of watershed models, thus providing a background for the choices made in developing the watershed models presented in this dissertation.

2.2. Watershed simulation models

We describe a few environmental simulation models in terms of water quality evaluation and management assessment, and their use in decision analysis. Then, we describe and compared data-driven, reduced-complexity approach against these other models (Table 2.1).

Table 2.1: Comparison of various watershed simulation modeling approaches from process-based watershed models including spatially-lumped (Hydrological Simulation Program-Fortran (HSPF) and Soil and Water Assessment Tool (SWAT)) and spatially-distributed hydrologic models (Gridded Surface Subsurface Hydrologic Analysis (GSSHA)) to reduced-complexity models that are formula-driven (Prioritize, Target Measure Application (PTMApp) and Agricultural Conservation Planning Framework (ACPF)) and are data-driven(Management Options Simulation Model (MOSM))

Type	Spatially-lumped hydrologic models	Spatially-distributed hydrologic models	Formula-driven reduced-complexity models	Data-driven reduced-complexity models
Examples	HSPF, SWAT	GSSHA, MIKE SHE	PTMApp, ACPF	MOSM
General description	Hydrologic and NPS pollution models with three major components (hydrology, sediment, and chemical)	Gridded hydrologic and sedimentation process model build on mass-conserving solutions of partial differential equations	Curve Number (CN) method, USLE, and sediment delivery ratio (SDR) formulation are used to estimate flow, soil loss, and sediment delivery to characterize management suitability	SDR and sediment loading simulations are driven by observed data, and constrained by mass conservation
Pros	- Widely used for research and environmental management analysis -Robust long-term water yield analysis	Computationally robust from mass-conservation equations	-Relatively simple to use -Accessible	-Reliable, robust, and relevant
Cons	-Long computation time -Problem of identifiability and predictability -No formal evaluation near channel sediment supply (NCSS)	-Even longer computation time -Problem of identifiability and predictability -No formal evaluation NCSS	-Long computation time -No formal evaluation NCSS	-Requires historical data on flows and sediment loads; need to define watershed sediment balance

2.2.1. Spatially lumped hydrologic models

Watershed hydrology and water quality models such as the Soil and Water Assessment Tool (SWAT) and the Hydrological Simulation Program—Fortran (HSPF) predict water, sediment, and chemical yields for agricultural basins and can be used to evaluate the effects of different management options (Beeson, 2014; Krysanova et al., 1998; Singh et al., 2005). These models operate on spatially lumped functional modeling units, sometimes called Hydrologic Response Units (HRUs). Information on different land use and soil types is combined, or "lumped" within these units, such that spatial resolution is at the scale of HRU.

Published reviews of these models show that they have been widely used for research and evaluation of environment management scenarios. For example, SWAT has shown usefulness in studying the impacts of climate changes on long-term water yields (Borah, 2004). SWAT is widely used for hydrological analysis in agricultural watersheds with tile and ditch drainage, and can adequately represent water flows when calibrated appropriately (Krysanova and Arnold, 2008; Skaggs et al., 2012). SWAT uses the Muskingum method to route water through channels (Gassman, 2007), a well validated kinematic wave routing method for simulating flood wave propagation (Ponce et al., 1996). Also, these models are used widely to estimate sediment loading and effects of management scenarios. These models use the universal soil loss equation (USLE) to calculate the soil loss rates from agricultural field. Sediment transport on field with surface runoff for each time step over different HRUs is calculated using a surface runoff lag equation, and transport in lateral and groundwater flow is calculated using a linear function of the HRU area and flow (Arnold et al., 2011).

There are number of hindrances in utilizing these models to address the challenges associated with NPS pollution management outlined in Chapter 1. These include parameter input requirements, near-channel source evaluation, problems of undetermined systems, and uncertainty evaluation as discussed in the following paragraphs.

These models often incorporate very detailed representations of physical processes for water routing, sediment erosion and storage, and nutrient processing. Implementation of these models requires large numbers of boundary conditions and parameter inputs, and entails calibration to adjust parameters or inputs to minimize the difference between the predicted values to measured values (Krysanova et al., 1998; Smith et al., 2011). Heavily parameterized models like the SWAT and HSPF therefore face problems of *identifiability* and *predictability*:

- Problem of *identifiability*: it is often challenging to use these models to isolate any particular physical processes. So, it is difficult to quantify the impacts of any particular physical processes and input parameters on the overall sediment yield prediction (Krysanova and Arnold, 2008). In the context of environmental policy analysis, model complexity makes it difficult to trace how different management actions impact water quality (Krysanova and Arnold, 2008; Wu, 2006).
- Problem of *predictability*: model predictions have a strong reliance on the conditions used for calibration. For this reason, a calibrated set of parameters cannot be used with confidence to predict future conditions or to predict the conditions of other ungaged watersheds even if they are adjacent to the calibrated watershed (Folle et al., 2009).

In the agricultural watersheds of south central Minnesota, near-channel sediment supply (NCSS), such as ravine, streambank, and bluff erosion, is a major contributor of water pollution (Gran et al., 2011). However, hydrologic watershed simulation models typically only address the loading and transport of field-derived pollutants, and do not directly address NCSS (Folle et al., 2009; Smith et al., 2011). While downstream addition of sediment, particularly from near-channel sources is not included in these models, some have developed watershed models that incorporate near-channel sediment loading using independent information. For example, in using SWAT to conduct a cost-benefit analysis of environmental management scenarios in the Minnesota River Basin, Dalzell et al. (2012) used an external regression model to incorporate NCS sediment loading as a function of river discharge.

Even though these process-based models are missing some important processes (e.g., near-channel loading, transport, and mitigation), they nevertheless require a large number of input parameters. Many of these parameters cannot be obtained from field data, in which case, their values are selected from literature and refined through model calibration (Jia, 2006; Krysanova et al., 1998). Many of these parameter values can be adjusted over large ranges, and during the calibration of parameter values, a modeler often has little more than intuition upon which to base decisions about parameter tuning (Smith et al., 2011). It is important to note that any particular calibrated set of parameters may be just one of many possible combinations of parameters that can give equally good predictions even as they may indicate different combinations of watershed processes (i.e., problems of undetermined systems or *equifinality* defined by Beven (2001)).

Lastly, application of these models in the context of environmental decision analysis is hindered by the inherent sources of uncertainty from numerous parameter inputs, limitations of model structure, stochasticity of climatic data, and errors in observed data (Beven and Freer, 2001). Nevertheless, many process-based models do not offer a formal way to represent uncertainty in their predictions (Haag and Kaupenjohann, 2001). Thus, it is difficult to consider the role of uncertainty in model predictions when determining environmental management strategies (Wu, 2006).

2.2.2. Spatially-distributed hydrologic models

In addition to spatially-lumped hydrologic models, there are models with higher spatial resolution to represent various processes within a watershed. Gridded Surface Subsurface Hydrologic Analysis (GSSHA) and MIKE-Système Hydrologique Européen (MIKE-SHE) models are spatially distributed, physically based hydrologic models capable of simulating stream flow through multiple pathways, including surface runoff and subsurface flow (Downer, 2009; Singh and Frevert, 2005).

For example, GSSHA employs mass-conserving solutions of the governing partial differential equations (i.e., Richards equation), such that the hydrologic components are closely related to an overall mass balance (Downer and Ogden, 2006). GSSHA can be defined at a fine spatial scale intended to match the governing mechanisms.

Numerical implementation of the basic conservation equations allows the model to be solved relatively quickly, although computational speed becomes an issue for a spatially distributed models with increasing number of parameters, especially for larger watershed or when a variable time step is used (Singh and Frevert, 2005). Both GSSHA and MIKE-SHE require boundary conditions, parameter inputs, and calibration for numerous

watershed processes including distribution of rainfall, surface retention, infiltration, soil moisture, evapotranspiration, surface runoff, and channel flow (Christiaens and Feyen, 2001; Downer and Ogden, 2003). Thus, like the spatially-lumped hydrologic models, these models face the problems of *identifiability* and *predictability* as well as the problem of *equifinality* as described above. Also, the spatially-distributed models do not have built-in processes for simulating near-channel sediment loading (Downer and Ogden, 2006).

2.2.3. Formula-driven, reduced-complexity models

In contrast to the hydrologic models reviewed above, there are formula-driven, reduced-complexity models that were developed to evaluate agricultural conservation planning activities without requiring the expertise involved in complex modeling. Formula-driven, reduced-complexity models generally have a framework that can be informed by landowner and community preferences (Tomer et al., 2015). The model framework is simple, involving a limited set of empirical or physical formulations (e.g., curve number method to estimate water delivery), compared to the process-based models, and is accessible to a wide range of users due to its simplicity (Houston Engineering Inc., 2016; Tomer et al., 2015; Voinov and Bousquet, 2010).

Prioritize, Target, Measure Application (PTMApp) and Agricultural Conservation Planning Framework (ACPF) are reduced-complexity watershed models intended to support decisions regarding surface water quality planning and management. These two instances of reduced-complexity models use Digital Elevation Models (DEM) of a candidate watershed to prioritize specific locations for implementing management options. For example, ACPF conducts runoff risk assessment (i.e., identification of areas

susceptible for erosion) on fields based on topography and soil type, and evaluates riparian function based on defined stream reaches. Meanwhile, compared to ACPF, PTMApp has more formulas in evaluating surface and in-stream flow. The SCS curve number (CN) method is used to simulate surface runoff volume and peak discharge. PTMApp uses the USLE to calculate agricultural field soil loss, provides an estimate of sediment delivery ratio (SDR) from each raster to the watershed outlet as a function of catchment area, and calculates in-channel sediment loss based on travel time.

Based on these calculations using a set of formulas, these models identify management *target* sites for different management types given the topographic characterization of the watershed, and the users can select specific practices to evaluate their feasibility, effectiveness, and cost in different sites (Houston Engineering Inc., 2016; Tomer et al., 2015). However, in the case of these reduced-complexity models, there is little information on model validation or it is declared that the model lacks formal approaches for doing so (Houston Engineering Inc., 2016). Both of the examples of formula-driven, reduced complexity models do not address NCSS (Houston Engineering Inc., 2016; Tomer et al., 2015).

2.2.4. Data-driven, reduced-complexity models

Data-driven, reduced-complexity modeling is a method to simulate watershed processes within a simple structure, making the most effective use of abundant information on soils, topography, and gage information. The model simulation is transparent and relevant for decision-making processes because this modeling approach has a simple structure applying only the pertinent watershed processes in order to effectively assign appropriate management

As the reviews of the lumped- and distributed-hydrologic models illustrate, models that incorporate numerous explicit physical processes face considerable challenges associated with spatially variable, temporally episodic, and nonlinear nature of the rainfall-runoff and sediment transport processes. For example, landscape heterogeneity and process complexity within soil structure, vegetation, climatic conditions, soil moisture, geology, etc. are important in governing watershed responses, but they are intrinsically difficult to represent at the watershed-scale (McDonnell et al., 2007). Also, the process-based models are built on small-scale mechanisms (e.g., Darcy's law and Richards equation) that are often difficult to accurately represent at a larger scale relevant for environmental management due to the landscape heterogeneity, therefore, they must rely on calibration to account for this lack of understanding of landscape heterogeneity and multiple culminating complex watershed processes (Kirchner, 2006).

The complexity of the watershed processes and landscape heterogeneity at the watershed-scale is ubiquitous for all modeling efforts, but some of these limits may be alleviated by new measurement technologies and new hydrologic observatory networks (Kirchner, 2006). Observational data can expand our understanding of aggregate watershed processes as the basis for deriving macro-behavior involving simplified laws of interaction on the micro-scale and hypothetical probability estimates (Dooge, 1986). This aggregate method must satisfy the law of mass conservation, which states that matter is neither created nor destroyed (Leopold and Langbein, 1962). Observational data at gages can provide constraints for model prediction so the law of conservation is satisfied.

Date-driven, reduced-complexity approach distributes the results of the physical processes from observed data, such as sediment loading at stream gages, to understand the aggregate watershed processes using high-resolution spatial data. For example, sediment delivery ratio (SDR) can be formulated as a function of topography where specific SDR values across the watershed can be calculated with high-resolution DEM, and the resulting sediment loading is calculated using spatially distributed information about soil loss and spatially integrated information about sediment loading at gages. Similarly, near-channel sediment supply (NCSS) can be estimated using a simple metric, such as river discharge, given the information provided by paired gages that bracket river sections dominantly populated with near-channel sources, instead of modeling the numerous processes involved in slope failure at individual near channel sources.

We have adopted this modeling approach in this dissertation in order to project the potential sediment reductions from implementing various types of management options. Specifically, we develop models to distribute the observed results of physical processes across the watershed to estimate sediment storage and delivery from various sources across the watershed, including field and near-channel sources (the Topofilter approach in Chapters 3 and 4). The model is similar to PTMApp in the sense that its goal is to distribute sediment loading (and reduction) based on topography. The differences between our modeling approach and PTMApp include (i) Topofilter is based on observed loads, (ii) SDR depends on topography, not just area, and (iii) our approach explicitly incorporates one source of uncertainty (uncertainty due to equifinality of alternative parameterizations of SDR models).

Furthermore, using observations from paired gages, we generalize the relationship between peak river discharge and sediment loading from river segments dominated by NCSS. Again, there are multiple competing processes contributing to sediment loading from these sources, but the gage records indicate that most of the sediment loading occurs only during larger flows (see Chapter 5). Thus, we aggregate sediment loading as a simple function of river discharge without specifying the type and rates of the different erosion mechanisms producing this loading. Such specification would require detailed in-situ measurement that are difficult to access and costly (e.g., erosion pins, close-range photogrammetry, terrestrial laser scanning, and traditional survey method) (Day et al., 2013a; Westoby et al., 2012).

However, our modeling approach does not exclude representations of physical processes where they are especially needed and can be adequately represented (e.g., the standard Muskingum-Cunge method is used to route water through the channel network in order to capture the effect of water storage on river discharge). Our modeling approach is designed to be well constrained by observed sediment loads, with a focus on simulating the magnitude and distribution of sediment sources and sinks throughout the watershed, rather than trying to predict these quantities by integrating the result of local mechanisms operating over the entire watershed.

The simulation model described in Chapter 6 (also Section 2.4 provide an overview), the Management Option Simulation Model (MOSM), uses a simplified representation of management options, representing their functions as either: 1) reducing sediment production at sources, 2) reducing sediment delivery rates using the outputs of the sediment delivery models in Chapters 3 and 4, or 3) reducing sediment production at the

near-channel sources as a result of peak flow attenuation as evaluated using paired gages in Chapter 5.

2.3. Study site description

In this section, we describe the setting in which the data-driven, reduced complexity modeling approach is applied. The Greater Blue Earth River Basin (GBERB) consists of three major watersheds (Figure 2.1): Watonwan River Basin (WRB), Blue Earth River Basin (BERB), and Le Sueur River Basin (LSRB), with total land area of 3,540 square miles and approximately 3,384 miles of stream and rivers (Minnesota State University, Mankato Water Resources Center, 2012). Water quality records indicate that the GBERB contributes disproportionally large quantities of sediment to the Minnesota River (Matteson, 2006). As a result, the Minnesota River and 39 reaches in the GBERB have been listed as "impaired" for turbidity, and Total Maximum Daily Loads (TMDLs) have been established for all these reaches. State and local agencies are developing implementation plans to address the impairment (Minnesota State University, Mankato Water Resources Center, 2012).

Section 2.3.1 describes the geologic history of the study site, and Section 2.3.2 describes the anthropogenic influences that affected the landuse and landcover of the study watershed.

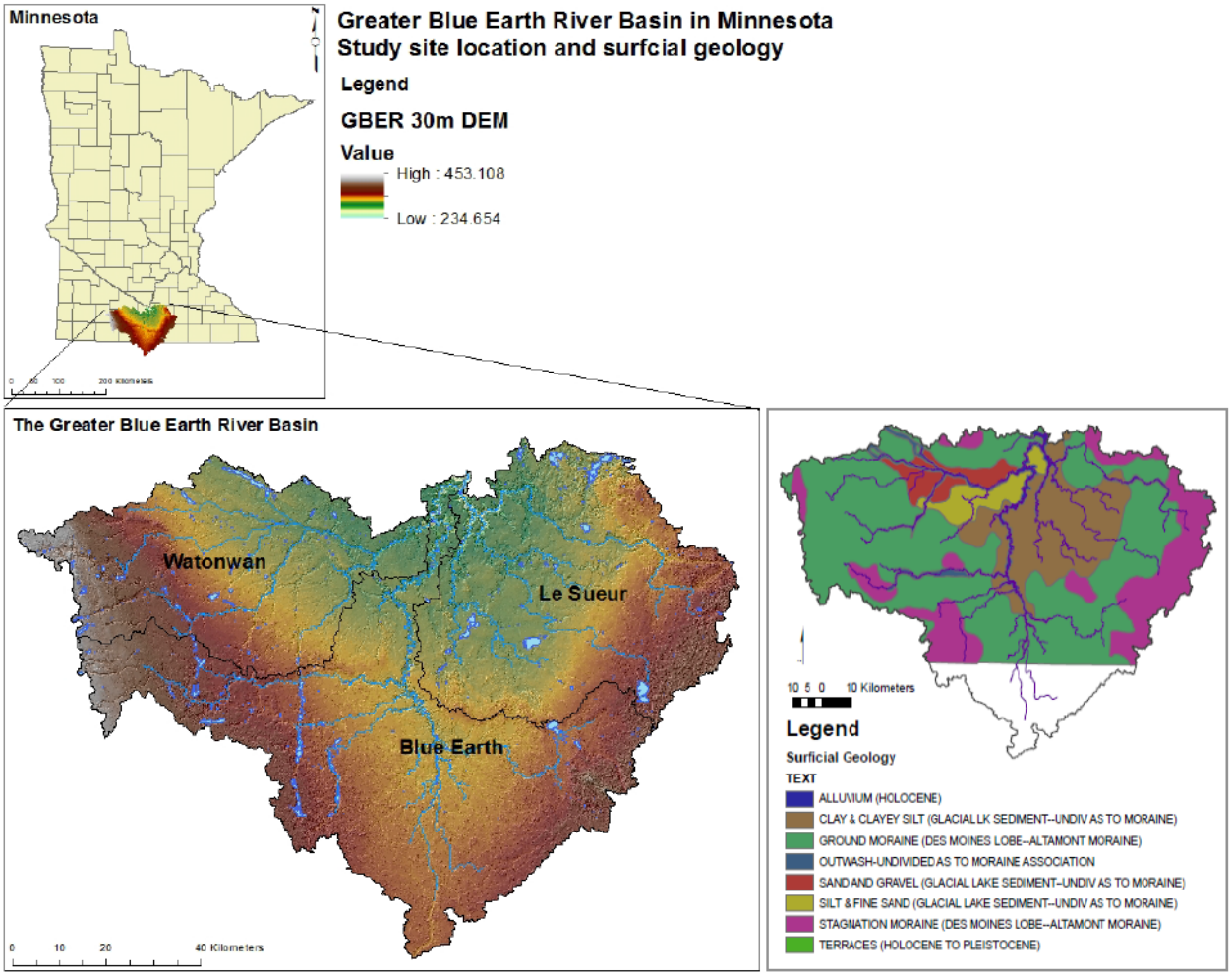

Figure 2.1: Greater Blue Earth River Basin (GBERB), located in south central Minnesota, consists of three major watersheds: Watonwan, Blue Earth, and Le Sueur River Basins (see watershed map and topography in bottom left). GBERB is located over poorly drained soils (see the surficial geology map on the bottom right) (provided through the courtesy of Dr. Karen Gran of University of Minnesota at Duluth)

2.3.1. Geologic influence on the accelerated sediment loading

The GBERB is primarily a very flat, poorly drained landscape of glacial till and glacial lake deposits. The significant exception to this flat landscape is found near the watershed outlet. Catastrophic drainage of the Glacial Lake Agassiz at the end of the last glacial period approximately 13,500 years ago produced an incision of 60 m in the ancestral Minnesota River Valley (Gran et al., 2009). This base-level drop for the GBERB triggered rapid downcutting and incision of a rejuvenated drainage network. The

upstream boundary of this incision has migrated upstream from the watershed outlet at an average rate of 3.0 to 3.5 m/yr with an average incision rate of 2.6 mm/yr over the Holocene (Day et al., 2013b). This channel incision into glacial deposits (see the surficial geology map in Figure 2.1) has resulted in the development of tall bluffs and steep ravines in the incised river valley (Gran et al., 2009). On the other hand, the upland topography of the GBERB is very flat, and composed of till and glacial lake deposits. This land is almost entirely in row crops (Figure 2.2b). Presently, cultivated crops cover about 85% of the GBERB (Minnesota State University, Mankato Water Resources Center, 2012).

Valley incision occurred throughout the Holocene and continues today, resulting in a landscape primed for large sediment loading (Gran et al., 2013). During the first part of the period since European settlement, field erosion was sufficiently large, and more of the sediment delivery from the watershed was derived from upland, agricultural fields. In the latter period since mid-twentieth century, with the advent of soil conservation measures and the persistent expansion of tile and ditch drainage systems, larger river flows have increased sediment supply from near-channel sources within the incised sections of the watershed (Figure 2.2a), such that they are again the largest sediment source in the watershed (Belmont et al., 2011).

Figure 2.2: a) An aerial view looking downstream (north) from just north of Mapleton between the Maple River and the Cobb River shows incised rivers responding to the base level drop (b) An aerial view from the same point looking upstream (south) shows flat terrain consisting of agricultural fields. (Source: Google Earth (Version 5.1.3533.1731))

2.3.2. Anthropogenic influence on the accelerated sediment loading

Sediment sources, storage, and loading in the GBERB are strongly influenced by its landcover/landuse (LCLU) changes in last two hundred years since the European settlement. Cultivation of the flat uplands of the GBERB required extensive drainage of native wetlands and prairie potholes over the past 170 years (Shepard and Westmoreland, 2011). Presently, the artificial drainage system consists of 719 miles of public open ditches; 2,665 miles of public tiles; and a larger, unknown extent of private ditches and tiles, resulting in approximately 86% wetland loss in the study site since the European settlement (Minnesota State University, Mankato Water Resources Center, 2012).

The row crop conversion and widespread alteration of the drainage system have significantly affected the watershed hydrology and sediment loading. For instance, stream gages have recorded increases in the river discharge in the past several decades in southern Minnesota where more frequent and higher peak discharges have escalated the valley excavation rates in the incised zones (Novotny and Stefan, 2007; Schottler et al., 2013). Consequently, according to a sediment fingerprinting analysis in the Upper Mississippi River, the dominant sediment source in the study region has shifted from

agricultural soil erosion, though its loading still remains significant, to the near-channel sources in the past several decades (Belmont et al., 2011).

2.4. Overview of MOSM and decision framework within the context of collaborative for sediment source reduction

In this section, we describe the overall structure of the management option simulation model (MOSM) within the context of the Collaborative for Sediment Source Reduction (CSSR) in the Greater Blue Earth River Basin (GBERB), building on the background provided above on existing modeling strategies and study site characteristics. In Chapter 6, we describe the computational modules of the MOSM.

Considerable attention and funding have been focused on sediment loading from the GBERB because the watershed has been identified as the largest source of sediment to the Minnesota River—the GBERB provides 80-90 percent of the sediment loading to the Upper Mississippi River (Kelley and Nater, 2000). In addition to concerns about the impact of turbidity on water quality and ecological health, the sediment loading is associated with the accelerated filling of Lake Pepin, a naturally dammed lake on the Mississippi River that is an important scenic and recreational amenity for Minnesota. In 2008, voters in Minnesota passed the Clean Water, Land and Legacy Amendment, which introduced a 3/8 cent sales tax for the next 25 years, raising over $3.5 billion in tax revenue, with one-third of the proceeds designated for improving water quality (The Minnesota State Legislative Coordinating Commission, 2016). Combined with other sources of environmental funding, the opportunity exists to make substantial investment in improving water quality.

In the context of a prominent nonpoint source water quality problem and the

emerging availability of funds to address the problem, the CSSR was created with the goal of developing a consensus strategy for reducing sediment loading and delivery from the GBERB (Belmont et al., 2012). A need was identified among various scientists and stakeholders of the watershed for an alternative approach to support the evaluation of investment priorities for sediment reduction for the purpose of effectively utilizing the Clean Water Legacy funds (Ibid.). This set an overall goal of developing a model that could support the ready and transparent evaluation of the cost and effectiveness of different management strategies. Supported by Clean Water Legacy funds, as well as funds from the agricultural industry and Clean Water Act implementation funds from the EPA, the stakeholder group was formed in 2012, and eight meetings were held between June 2012 and January 2016 (see Appendices 2.A for a list of attending stakeholders and 2.B for meeting agendas).

The CSSR collaboration played an important role in shaping and directing the research in this dissertation, where watershed models are built through collaborations with the scientists, engineers, and economists from three research universities (Johns Hopkins University, University of Minnesota, and Utah State University), and the stakeholder groups representing different environmental, social, and economic objectives from agricultural producers, conservation groups, and the members of local regulatory agencies (see Appendix 2.A for a complete list of the stakeholders and scientists). The watershed models are intended to support the ready and transparent evaluation of the cost and effectiveness of different management strategies (i.e., MOSM), and were built using a wide range of independent data and local watershed knowledge collected during these stakeholder meetings.

There are three major inputs that inform the development of MOSM, (Figure 2.3): 1) supporting research actions; 2) scientific collaboration, and 3) stakeholder participation.First, supporting research actions are conducted to characterize the sediment loading from multiple dominant sources in the study watershed. For instance, in chapter 4, we develop a model to simulate all plausible sediment delivery ratio (SDR) values across the watershed to make sediment-loading predictions, and identify subsets that are most consistent with gaging records. These values are needed by MOSM to translate local (e.g., field) sediment loss into changes in sediment loading at the watershed outlet. MOSM simulates the effects of management actions by changing the rates of sediment production from various sources, or by changing the SDR values in the areas affected by management action depending on the various functions of the defined management options.

In the previous section, we discussed the implication of geologic setting and anthropogenic influences on watershed hydrology and escalated sediment loading. A key issue in our case study region that is missing in standard watershed modeling approaches is near-channel sediment supply (NCSS) that is affected by stream flows. Thus in Chapter 5, we examine how peak river discharge affects sediment loading from streambanks and bluffs to develop a basis for evaluating the impacts of water conservation management and peak flow attenuation. Accordingly, these research actions inform the general model structure and provide input data for MOSM.

Second, we obtained data required to develop and validate the supporting research actions through collaboration with other scientists on the CSSR team, for example:

- In Chapters 3 and 4, we use the USLE calculation conducted in the calibrated SWAT model (Kumarasamy and Belmont, 2014) to estimate field soil erosion rates;
- In Chapter 3, we use a LiDAR-based analysis to detect changes in surficial topography to confirm the SDR predictions (Schaffrath et al., 2015);
- In Chapter 4, we use the integrated sediment budget to identify and quantify sediment sources across the watershed (Gran et al., 2011);
- In Chapter 5, we use the water quality and river discharge data from gages throughout the watershed provided by the Minnesota Pollution Control Agency (MPCA) and USGS; and
- In Chapters 6 and 7, we use the SWAT outputs of water yield data to simulate river routing, and confirm the reasonableness of MOSM's simulation of daily hydrograph (Mitchell, 2015).

Third, we gathered different aspects about sediment pollution and feasible management strategies in the study watershed from the stakeholders (see Appendix 2.B. for a detailed description of meeting discussions and workshops involving stakeholders). We also shared the progress of MOSM development and supporting research actions with the collaborating scientists and stakeholders through CSSR meeting processes held biannually from the year 2013 to 2015 (Table 2.2). Each meeting consists of collecting information about study watershed from stakeholders, reporting findings from research actions, progress update on model development, discussion, and workshop to inform the forthcoming research actions (see Appendix 2.B for meeting agendas and description of each meeting). Some of the key stakeholder involvement includes:

- Determination of necessary model complexity to accommodate specific environmental problems of concern;
- Acquisition of available scientific information and local knowledge in the study site;
- Exploration of potential management option scenarios that reflect geophysical, social, and economic concerns and constraints; and
- Development of management option portfolios (MOPs) with stakeholders and evaluation of MOSM outputs in the context of water quality mitigation objectives as well as other environmental, social, and economic objectives.

Table 2.2: Stakeholder meetings and summary of discussions that led to the development of the MOSM

Year	Meeting	Summary of meeting
2013	Summer	• Outlined the project objectives based on the understanding of the water pollution problem • Conceptualized watershed-scale simulation model and its functionality
	Winter	• Presented a simulation prototype with its functionality • Collected the stakeholder inputs to decide on the general structure of the model and to determine supporting research actions based on the exploration with the prototype model
2014	Summer	• Discussed typical and plausible best management practices (BMPs) at the study site that the simulation model should evaluate
	Winter	• Defined management option (MO) groups based on the stakeholder inputs about current practices that the simulation model would evaluate. • Presented the general structure of the watershed simulation model in the form of Management Option Simulation Model (MOSM)
2015	Summer	• Presented the first version of MOSM • Collected stakeholder inputs to revise MOSM
	Winter	• Presented the revised MOSM • Evaluated management option portfolios (MOPs) • Collected further stakeholder inputs to revise MOSM as presented in Chapter 6

Lastly, MOSM simulates the effects of different management choices, and is intended to help stakeholders develop a consensus regarding sediment management strategies. The model outputs are used to understand the implications of various environmental management option portfolios (MOPs) that include various strategies of addressing NPS sediment pollution by assigning different types of management options (MOs) at various extents and allocations across the watershed. Therefore, the last part of the watershed simulation model development consists of evaluating various management option scenarios and tradeoffs between sediment reduction and economic investment objectives that will be described in Chapter 7 (Figure 2.3).

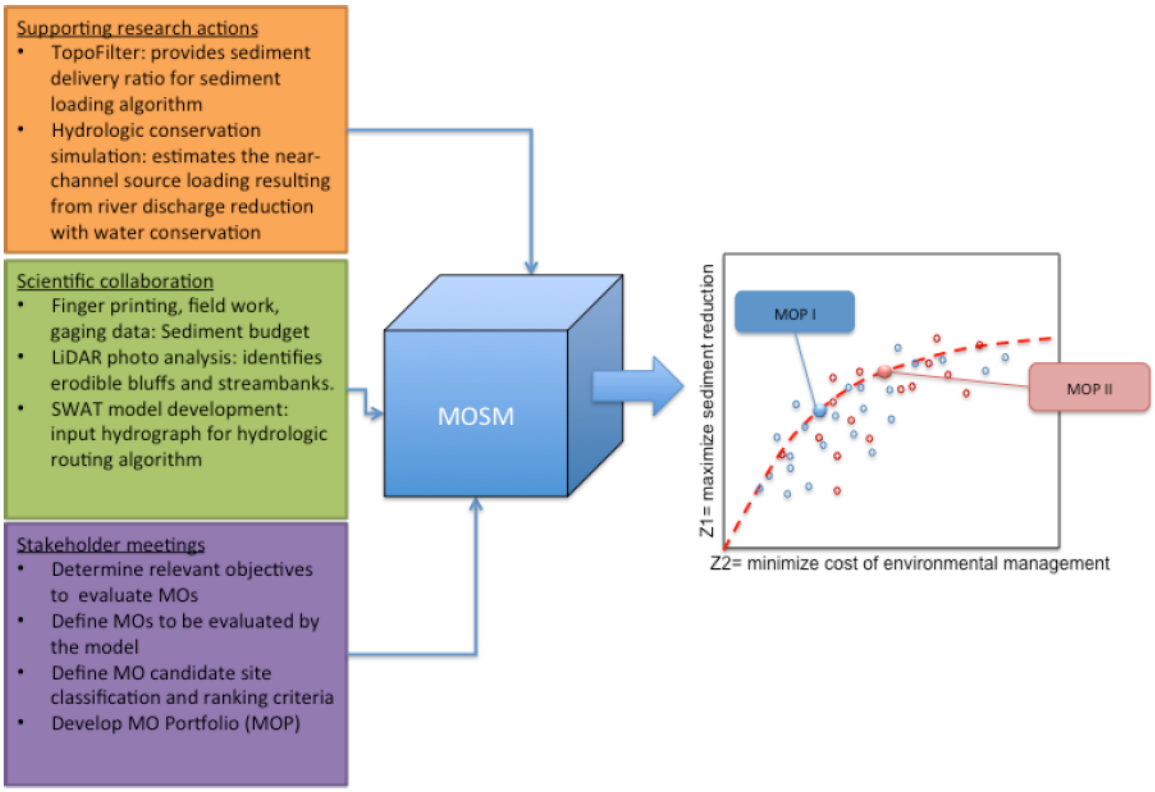

Figure 2.3: an overview of MOSM's data input structure and an illustration of tradeoffs among various management option portfolios (MOP) evaluated from MOSM outputs

Appendix 2.A: Stakeholder and CSSR member list

Organization/Occupation	Representative	Email
Minnesota Agricultural Water Resource Center (MAWRC)	Warren Formo	warren@mawrc.org
Minnesota Soybean Growers Association (MSBGA)	Steve Commerford	comagro@comcast.net
Greater Blue Earth River Basin Alliance (GBERBA)	Jill Sackett	sacke032@umn.edu
GBERBA	Dave Bucklin	david.bucklin@windomnet.com
Blue Earth County	Will Purvis	Will.Purvis@co.blue-earth.mn.us
Blue Earth County	Julie Conrad	Julie.Conrad@co.blue-earth.mn.us
Farmer	David Ward	drward@hickorytech.net
Farmer	Dave Craigmile	dacmile@mvtvwireless.com
Minnesota Pollution Control Agency (MPCA)	Larry Gunderson	larry.gunderson@state.mn.us
MPCA	Paul Davis	
MPCA	Bill Kell	william.kell@state.mn.us
Minnesota Department of Agriculture (MDA)	Adam Birr	adam.birr@state.mn.us
Minnesota Board of Water & Soil Resources (BWSR)	Al Kean	al.kean@state.mn.us
Department of Natural Resources (DNR)	Greg Eggers	greg.eggers@state.mn.us
University of Minnesota (UMN)	Ken Brooks	kbrooks@umn.edu
UMN	Joe Magner	
UMN, Collaborative for Sediment Source Reduction (CSSR)	Jeff Marr	marrx003@umn.edu
UMN, CSSR	Barbara Burkholder	bkb0811@umn.edu
University of Minnesota, Duluth (UMD), CSSR	Karen Gran	Kgran@d.umn.edu
Utah State University (USU), CSSR	Patrick Belmont	patrick.belmont@usu.edu
USU, CSSR	Peter Wilcock	wilcock@usu.edu
Johns Hopkins University (JHU), CSSR	Ben Hobbs	bhobbs@jhu.edu
JHU, CSSR	Se Jong Cho	sejong@jhu.edu
North Dakota State University (NDSU), CSSR	Stephanie Day	dayxx196@umn.edu

Appendix 2.B: Stakeholder meeting agenda, 2012-2016

Stakeholder meeting #1
June 14, 2012
9:00 A.M. – 5:00 P.M.
Mankato, Minnesota

In this first stakeholder meeting, CSSR members (see Appendix 2.A) held a broad discussion and exercise sessions to define the goals for CSSR project and environmental modeling. CSSR members also collected from the stakeholders information about current management options used in mitigating nonpoint source sediment pollution. Finally, CSSR members presented the structure of the project and meeting process for the next three years.

Time	Activity	Presenter
9:00	Welcome	Peter Wilcock (PW)
9:30	Exercise 1: Collaborative Goals	Ben Hobbs (BH)
9:45	Sediment Budget: Le Sueur (LSRB) to Greater Blue Earth River Basin (GBERB)	Patrick Belmont (PB)
10:45	Break	
11:00	Exercise 1: Collaborative goals	Se Jong Cho (SJC) and BH
11:45	Exercise 2: Management options	BH
12:00	Lunch	
1:00	Exercise follow-up: Discussion of collaborative goals and management options	BH
1:45	Predicting sediment response to management options	PW
2:30	Break	
2:45	Prediction targets and evaluating scenarios	BH
3:30	Collaborative structure and process	Barbara Burkholder Heitkemp (BBH)
4:30	Wrap up plans	
5:00	Adjourn	Adjourn

Stakeholder meeting #2
December 17, 2012
9:00 A.M. – 5:00 P.M.
Mankato, Minnesota

In this meeting, CSSR members reported on the status of the sediment and water budget in the Le Sueur River Basin (LSRB) and Greater Blue Earth River Basin (GBERB). CSSR members defined management options to be evaluated in the simulation model with the stakeholders, and presented a toy version of the management option simulation model. Lastly, CSSR members informed stakeholders on the principles of decision analysis and discussed some of the challenges in environmental modeling and decision-making.

Time	Presentation	Discussion
09:00	Welcome and goals of the meeting (Peter Wilcock)	
09:30	Sediment & water budget LSRB and GBERB (Karen Gran)	
10:15	Overview: CSSR simulation model (PW)	
10:45	Break	Break
11:00	Introduction of Management Option Database (BBH)	
12:00	Lunch	Lunch
1:00		Management Option Database: what are typical management options in the GBERB? (BBH)
2:00	Demo: Toy CSSR simulation model (SJC)	
2:45	Break	Break
3:00	Decision Support Options (BH)	
3:15		Management portfolios, scenario options (BH)
3:45		Review: management options, simulation challenges (BH)
4:30		Wrap-up; goals&, location for next meeting (PW)
5:00	Adjourn	Adjourn

Stakeholder meeting #3
June 13, 2013
9:00 A.M. – 5:00 P.M.
Mankato, Minnesota

CSSR members discussed possible model structure for evaluating environmental management and setting appropriate objectives. CSSR members presented the results of hydrologic assessment of the study watershed. Dr. Magner, a guest speaker, presented a case study involving a management option to reduce flow and trap sediment along stream. Finally, CSSR members held discussion sessions to define the structure of the simulation model and management option database.

	Presentation	Discussion/workshop
09:00	Welcome and goals of the meeting (PW)	
09:30		Watershed modeling for environmental management: stakeholder experience and targets
10:00	Watershed hydrology update (PB)	
10:30	Break	Break
11:00	A case study of management option: two-stage ditches and culvert sizing (Joe Magner)	
11:30		Modeling overview and discussion (PRW and SJC)
12:15	Lunch	Lunch
1:00		Management option (MO) workshop: identification of plausible MOs for modeling
4:30		Discussion session to wrap up meeting
5:00	Adjourn	Adjourn

Stakeholder meeting #4
January 21, 2014
9:00 A.M. – 5:00 P.M.
Mankato, Minnesota

CSSR members presented evaluation of river profile and near-channel source sediment contribution versus stream flow. They also presented the updates to the sediment budgets in the study site that were first presented in meeting #2, and discussed the implications on sediment management. Preliminary spatial analysis to identify candidate sites for management option was presented (these sites were first defined in meeting #2) and a simulation trial game evaluating impacts of different management strategies were conducted.

	Presentation	Discussion/workshop
09:00	Welcome: Mid-project check-in (PW)	
09:15	Blue Earth, Watonwan, and Le Sueur River profiles (PB)	
09:30	River discharge and sediment loading relationship (SJC)	
10:00	Sediment budget update (KG)	
10:30	Break	Break
10:45		Sediment budget discussion
11:30	Lunch	Lunch
12:30	Identification and prioritization of management option locations (SJC)	
1:30	Break	Break
1:45		Trial gaming among different management options (PW and SJC)
4:00		Summary discussion and next steps
5:00	Adjourn	Adjourn

Stakeholder meeting #5
August 8, 2014
9:00 A.M. – 4:00 P.M.
Mankato, Minnesota

CSSR members presented the completed GBERB sediment budget. They presented updates on identification of water conservation management option sites and hydrologic modeling to evaluate these sites. A modeling exercise with the stakeholders was conducted to determine the fundamental structure of the management option simulation model.

	Presentation	Discussion/workshop
09:00	Welcome: Mid-project check-in (PW)	
09:15	Status of GBERB sediment budget (Martin Bevis (MB) and PB)	
10:30	Break	Break
10:45	Updates on identification and delineation of water conservation management options sites	
11:45	Lunch	Lunch
1:00	Hydrologic modeling update (SJC)	
2:00		Modeling exercise (PW and BH)
3:00	Break	Break
3:15		Summary discussion and next steps
4:00	Adjourn	Adjourn

Stakeholder meeting #6
January 16, 2015
9:00 A.M. – 4:00 P.M.
Mankato, Minnesota

CSSR members presented the updates to the GBERB sediment budget that was presented in meeting #5. They presented the outcomes of the spatial analysis to identify candidate sites of management options that were defined in meeting #3. A general framework for simulating the impacts of these management options was evaluated with the stakeholders using the first version of MOSM.

	Presentation	Discussion/workshop
9:00	Welcome: Mid-project check-in (PW)	
9:15	Status of GBERB sediment budget (MB and PB)	
10:30	Break	Break
10:45	Management option identification and delineation update (SJC and Nate Mitchell (NM))	
11:45	Lunch	Lunch
1:00	Management option simulation model (MOSM) framework (SJC)	
2:00		Simulation model exercise (SJC and PW)
3:00	Break	Break
3:15		Summary discussion and next steps
4:00	Adjourn	Adjourn

Stakeholder meeting #7
August 14, 2015
9:00 A.M. – 4:00 P.M.
Mankato, Minnesota

CSSR members provided another update to the GBERB sediment budget. Marty Mechior, a guest speaker, held a group discussion on bluff and ravine stabilization options with the stakeholders. Updates on MOSM based on the stakeholder inputs from meeting #6 were presented. CSSR members collected the stakeholder feedback on MOSM for further revision.

	Presentation	Discussion/workshop
09:00	Welcome: overview and goals (PW)	
09:15	GBERB sediment budget update (MB and KG)	
10:00		Discussion on bluff and ravine stabilization options (Marty Mechior group)
10:30	Break	Break
11:00	Updates on MOSM development and demonstration (SJC and PW)	
12:00	Lunch	Lunch
1:00	Management options: implementation in MOSM (SJC and BBH)	
2:00	Working with MOSM (SJC and PW)	
3:00	Break	Break
3:15		Stakeholder feedback on MOSM and discussion on decision support framework
4:00	Adjourn	Adjourn

Stakeholder meeting #8
January 12, 2016
9:00 A.M. – 5:00 P.M.
Mankato, Minnesota

CSSR members presented the revised MOSM and conducted a workshop with the stakeholders who ran multiple management scenarios independently. The model outputs of stakeholder simulation session were used to demonstrate how different scenarios are evaluated in terms of minimizing annual investment against maximizing sediment reduction. A discussion session was held to collect the stakeholders' inputs on MOSM, and communicate the capability and limitation of the model.

	Presentation	Discussion/workshop
9:00	Welcome: overview and goals (PW)	
9:20	Summary of research	
10:45	Presentation of MOSM	
10:30	Break	Break
10:45		Exercise 1: working with MOSM—creating management scenarios to achieve 10% and 50% reduction in sediment load
12:00	Lunch	Lunch
1:00		Discussion of exercise 1
1:30	MOSM behavior: evaluating cost and efficiency inputs, and understanding reduction targets	
2:00		Exercise 2: Management option scenarios evaluation in sediment reduction
3:00		Discussion: accounting for other benefits and cost, and understanding management implementation challenges
4:00	Closing remarks	Discussion
5:00	Adjourn	Adjourn

3. Topographic Model for Sediment Source Apportionment

3.1. Introduction

Agricultural nonpoint source (NPS) pollution is a leading cause of impairment in many rivers and lakes in the U.S. including sediment pollution that causes widespread damages to water supplies and wildlife resources (US EPA, 2012a). This chapter presents an analytical framework to identify dominant sediment source areas through a development of the topographic filtering simulation model (Topofilter). The model links sediment erosion rates based on Natural Resources Conservation Services (NRCS) soil mapping to observed sediment loading from stream gaging using simple topographic functions derived from a high-resolution digital elevation model (DEM). The motivation for the model is to extract the topographic effect on sediment delivery, thereby addressing a long-standing challenge in estimating sediment transport, storage, and loading in a watershed (De Vente et al., 2007; de Vente and Poesen, 2005; Walling, 1983).

In Section 3.2, we survey some existing approaches used for estimating sediment loading from a watershed and provide an overview of the Topofilter concept, which is based on a formulation of sediment delivery ratio using topographic variables derived from high-resolution DEM. In Section 3.3, we describe the development of Topofilter, including the process used to determine model parameters and numerous plausible solutions. In Section 3.4 we evaluate the dominant sediment loading areas identified using the model outputs, demonstrate the model's sensitivity to extent of river mapping, and compare the model's estimates against independent data.

3.2. Approaches to estimating sediment erosion and delivery

3.2.1. Modeling approaches

Watershed simulation models including empirical soil erosion models (e.g., the Universal Soil Loss Equation(USLE) (Wischmeier and Smith, 1978)) and process-based hydrologic watershed models (e.g., the Soil and Water Assessment Tool (SWAT) (Arnold et al., 2011)) have been used to evaluate sediment loading in a watershed. In this section, we describe the USLE and revisit watershed-modeling approaches (Chapter 2) to provide a context for developing Topofilter.

The USLE database was compiled from over 11,000 plot-years of data from 47 locations in 24 states since the 1930s (Wischmeier and Smith, 1978). The large assemblage of data and major modifications of the model over the years improved the soil erosion estimates and expanded the use of the USLE (Zhang et al., 2009). Based on its fundamental data, USLE is relevant to erosion at the plot scale but does not effectively account for sediment transport and storage between the field plot and any point downstream. USLE by itself is an insufficient tool for identifying and evaluating watershed-scale sediment management policy, if minimizing sediment loadings at the watershed mouth is the objective (Boomer, 2008; Trimble, 1997). This has been referred to as the *Sediment Delivery Problem* (Walling, 1983) and remains one of the outstanding research problems in geomorphology and watershed management.

The *Sediment Delivery Problem* can be addressed using process-based models, which can be defined at a scale consistent with soil erosion and sediment transport, and be placed within a larger watershed accounting. These models employ multiple climatic, hydrologic, geologic, and vegetative components to route water and sediment (Gassman,

2007). If such models are defined at scale fine enough to capture the physical mechanisms driving erosion, transport, and storage, the demand for detailed information on parameter inputs can be overwhelming, limiting the application of these models to scales no larger than fields or small catchments (Krysanova et al., 1998). Implementation at larger scale requires estimation of boundary conditions, which can be defined only within typical bounds (Smith et al., 2011). This introduces limits to prediction defined solely by uncertainty in the necessary inputs. Combined with the complex structure of these models, this uncertainty leads to a calibration-driven approach that works against the original intent of capturing the physical processes at their operative scale (Jia, 2006; Krysanova et al., 1998). In such models, including spatially-lumped and -distributed watershed process models, in which physical processes are no longer linked to explicit locations or drivers, model parameters and processes become conceptual abstractions of watershed characteristics that must be determined through trial-and-error process to match the historical input-output data (Gupta, 1998). In these models, it is no longer possible to unambiguously link cause and effect or to demonstrate that a close calibration in fact represents the only one possible mix of processes actually occurring (Beven, 2006). Also, accepting an optimal parameter set, rather than considering multiple plausible parameter sets scattered throughout the parameter space, implicitly rejects the possibility that uncertainty associated with model prediction might be large (Beven and Freer, 2001).

A strong dependence on the amount and quality of calibration data suggests that watershed process models are no longer truly predictive and raises the question of whether other, simpler approaches, which are closely linked to available input data and

with our knowledge of the watershed processes, may offer advantages of simplicity and usefulness in environmental modeling (Jørgensen, 2002). Such a move toward *reduced-complexity* models is further motivated by the increasing availability of highly resolved field information (McMillan and Brasington, 2007). Of particular importance is the rapid expansion of high-resolution topography available from airborne laser swath mapping using Light Detection and Ranging (LiDAR). The availability of accurate and finely resolved topographic data facilitates the development of fine-scale, process-based models, of course, and ever increasing computing power suggests that such models might be capable of practical operation over reasonable time and space scales (McMillan and Brasington, 2007). But a high resolution DEM does not address the underlying problem of defining other boundary conditions that control soil erosion, transport, and storage. Thus, we develop a reduced-complexity model for sediment sources and delivery that combines high resolution DEM with the availability of soil maps that define soil erosion rates at the subfield scale. These maps are the result of an extensive, nationwide program to map soils (USDA, 2016). Together, DEM and soil maps provide local information on sediment sources and the topography between the source and the watershed outlet.

Our goal is to use the DEM to define a transfer function between spatially distributed estimates of soil erosion and spatially integrated measures of sediment loading at the watershed outlet. We do not aim to capture the physical processes acting at all times and every location of the landscape. Rather, we attempt to extract the influence of topography on the transfer of sediment from source to outlet. Further, we do not aim to find a single optimum solution for the topographic effect on sediment transfer, but rather to define many possible solutions, none of which are deemed correct, but all of which provide a

reasonable estimates. This forms the basis for a stochastic approach to estimating sediment delivery that accounts for uncertainties resulting from the fact that the data does not allow us to uniquely identify the parameters for the topographic effect.[1]

3.2.2. Conceptual approach of Topofilter

Topofilter evaluates the topographic influences in two parts: as sediment moves from the field source to stream, and as it moves downstream along the stream to the watershed outlet. This approach links sediment erosion (*SE*) mapped on the field to sediment loading (*SL*) at the watershed outlet using a sediment delivery ratio (*SDR*), which is the fraction of *SE* in *SL*.

Topofilter utilizes a stochastic simulation approach based on the Generalized Likelihood Uncertainty Estimate (GLUE) methodology, in which a plausible parameter space is determined through a *model conditioning* process rather than selecting a best-fit or optimum parameter combination through *model calibration* (Beven, 2006). A single, optimum parameter set found for a particular calibration exercise may be sensitive to small changes in the observations or model structure and cannot be demonstrated to be the correct answer. There can be more than one parameter set that provides solutions essentially as good as the optimum, which defines the problem of *equifinality*. Parameter sets providing similarly good solutions may be drawn from very different parts of the parameter space. The model conditioning process explores the parameter space using Monte Carlo (MC) simulations for different randomly chosen parameter values in order to identify multiple acceptable parameter sets that give acceptable predictions (Section 3.3.2). Thus, a conditioned parameter space allows the possibility of assessing the

[1] Other uncertainties, however, such as sample and measurement error in estimating annual average soil erosion and sediment loadings at gaging points, would not be accounted for and also contribute error to those parameter estimates.

uncertainty in model predictions, as defined by the observation data. That uncertainty can then be included as a part of a decision-making process (Beven, 2001). For instance, Topofilter can be used to identify dominant sediment source areas of various likelihoods based on the frequency of areal selections from all the possible solutions from the conditioned parameter space (Section 3.4.1). Thus, this framework can be used to identify potential sediment management strategies to target the dominant sediment source areas with the highest certainty for conservation actions.

Topofilter estimates the fraction of soil erosion delivered to the watershed outlet. We evaluate the plausibility of the simulation by examining the other portion of the eroded sediment, which must be stored between source and outlet (i.e., floodplains along stream). We calculate the magnitudes of sediment storage using the simulated sediment delivery ratio values and evaluate them against independent observations (Section 3.4.3).

3.2.3. Sediment delivery ratio

The term "sediment delivery ratio" (*SDR*) refers to the ratio of sediment loading (*SL*, [Mg y^{-1}]) delivered to a specified point in the watershed to gross soil erosion (*SE*, [Mg y^{-1}]) (De Vente et al., 2007):

$$SDR = \frac{SL}{SE} \qquad [3.1]$$

There have been numerous efforts to generalize *SDR* to predict *SL* at the basin outlet given estimates of *SE* using various watershed characteristics. For instance, the upland theory of Boyce (1975) generalizes that sediment delivery is inversely proportional to basin size because the average slope and sediment production per unit area both decrease with the increasing basin size (Ferro and Minacapilli, 1995; Dendy and Bolton 1976). Similarly, lumped *SDR* curve models with watershed size and fitting parameters to

encompass multiple unexplained transport and storage processes have been widely used because of their simplicity (Boyce, R.C., 1975; Jain and Singh, 2003; Lim, 2005; USDA, 1975; Vanoni, 2006)

However, characterization of sediment delivery as a general function of drainage area omits the topographic factors influencing the delivery process. A GIS-based, spatially-distributed simulation of erosion and deposition patterns indicates that topography has a major influence on sediment delivery process (Desmet, 1996). For instance, slope angle influences the runoff discharge by causing more rapid flows and consequently affecting the transport of sediment. After all, the gravity is the main force moving each particle of water and its associated load (Leopold and Langbein, 1962). The distance between source and outlet will also influence the fraction of sediment deposited and the magnitude of *SDR*. Thus, important environmental factors to consider when estimating sediment delivery include the flow length and slope between source and sink, as well as broader characteristics of the watershed such as drainage density (Ferro, 1995).

Modeling efforts using spatially distributed topographic variables to predict sediment delivery across the watershed include Ferro (1995) who sets the ratio of flow length and square root of slope as the travel time of eroded sediment. This approach predicts *SDR* values for all morphological units between field and the stream network as a decreasing function of travel time, but does not predict *SDR* values from when a particle enters a stream channel until it exits the watershed. More recently, Fernandez et al. (2003) developed a spatially distributed *SDR* model at a finer resolution, using travel time from each raster cell along the flow path. Here, the travel time is a function of flow length and velocity calculated from slope of each cell. Similarly, a spatially distributed *SDR* model

was formulated with relief and flow length from the point of soil production to the stream, but does not predict the sediment delivery in the stream network (Fistikoglu, 2002). Sediment loading from a watershed will depend on sediment storage and delivery both on field and in stream, the relative importance of which will be contingent on the respective environmental factors listed by Ferro (1995) above.

The approach developed here includes the effect of topography on potential sediment deposition on field and in stream network, in order to address the compete sediment delivery problem by linking local soil erosion to sediment delivery at the basin outlet (Walling, 1983). The relative importance of soil losses prior to reaching the stream network vs. losses in the network itself will strongly depend on the topography and lengths of travel, and will differ from watershed to watershed. The work presented here also focuses on validating the predicted sediment delivery against independent observational data and quantifies the uncertainties related to predictions.

We develop Topofilter using flow length and gradient for each 30-m raster cell to capture the topographic influences on sediment delivery. Based on a general negative exponential function of length and slope, the model calculates *SDR* from each field raster cell *i* to the nearest stream cell ($SDRf_i$), and then uses the same general function but with different parameters to obtain *SDR* from this nearest stream cell to the basin outlet ($SDRs_i$). The overall sediment delivery ratio of each field raster cell *i*, SDR_i is the product of $SDRf_i$ and $SDRs_i$ [3.2], where sediment delivery on field, $SDRf_i$ is calculated using flow length and gradient from field cell *i* to an adjacent stream cell with field parameters a_1 and b_1 [3.3], and sediment delivery in stream, $SDRs_i$ is calculated using flow length and gradient from the adjacent stream cell to the watershed outlet with stream

parameters a_2 and b_2 [3.4]. These individual parameter values are constant across the watershed cells but the topographic variables vary by the location of cell *i*. The topographic inputs are spatially variable, so their influences on sediment delivery would result in a spatially variable SDR_i over the entire watershed.

$$SDR_i = SDRf_i \cdot SDRs_i \quad [3.2]$$

$$SDRf_i = f\left(L_{f_i}, \frac{\Delta E_{f_i}}{L_{f_i}}\right) = exp\left[a_1 \cdot \left(\frac{\Delta E_{f_i}}{L_{f_i}}\right)^{b_1} L_{f_i}\right] \quad [3.3]$$

$$SDRs_i = f\left(L_{s_i}, \frac{\Delta E_{s_i}}{L_{s_i}}\right) = exp\left[a_2 \cdot \left(\frac{\Delta E_{s_i}}{L_{s_i}}\right)^{b_2} L_{s_i}\right] \quad [3.4]$$

where L_{fi} is the on-field flow length from an individual field source cell *i* to its nearest stream cell and L_{si} is the in-stream flow length from this nearest stream cell to the basin outlet. ΔE_{fi} is the change in elevation from field source cell *i* to its nearest stream cell and and ΔE_{si} is the change in elevation from this nearest stream cell to the basin outlet. These topographic variables are absolute values obtained from high-resolution surface topography, as described in the next section. In order to obtain the total sediment loading (*SL*) of the watershed, the soil erosion rate, A_i [Mg/yr] is multiplied by SDR_i from an individual raster cell *i* to the watershed outlet, and this product is summed over all raster cells (*N*) in the watershed:

$$SL = \sum_{i=1}^{N} SDR_i \cdot A_i \quad [3.5]$$

3.3. Method

Topofilter is developed for subwatersheds of the Le Sueur River Basin (LSRB), a tributary to the Minnesota River (Figure 3.1). Topofilter is developed first for a single subwatershed, Little Cobb (LC). The conditioned parameter set for LC is then

applied to an adjacent watershed, Upper Maple (UM), to evaluate the transferability of both the general methodology and the individual parameter sets.

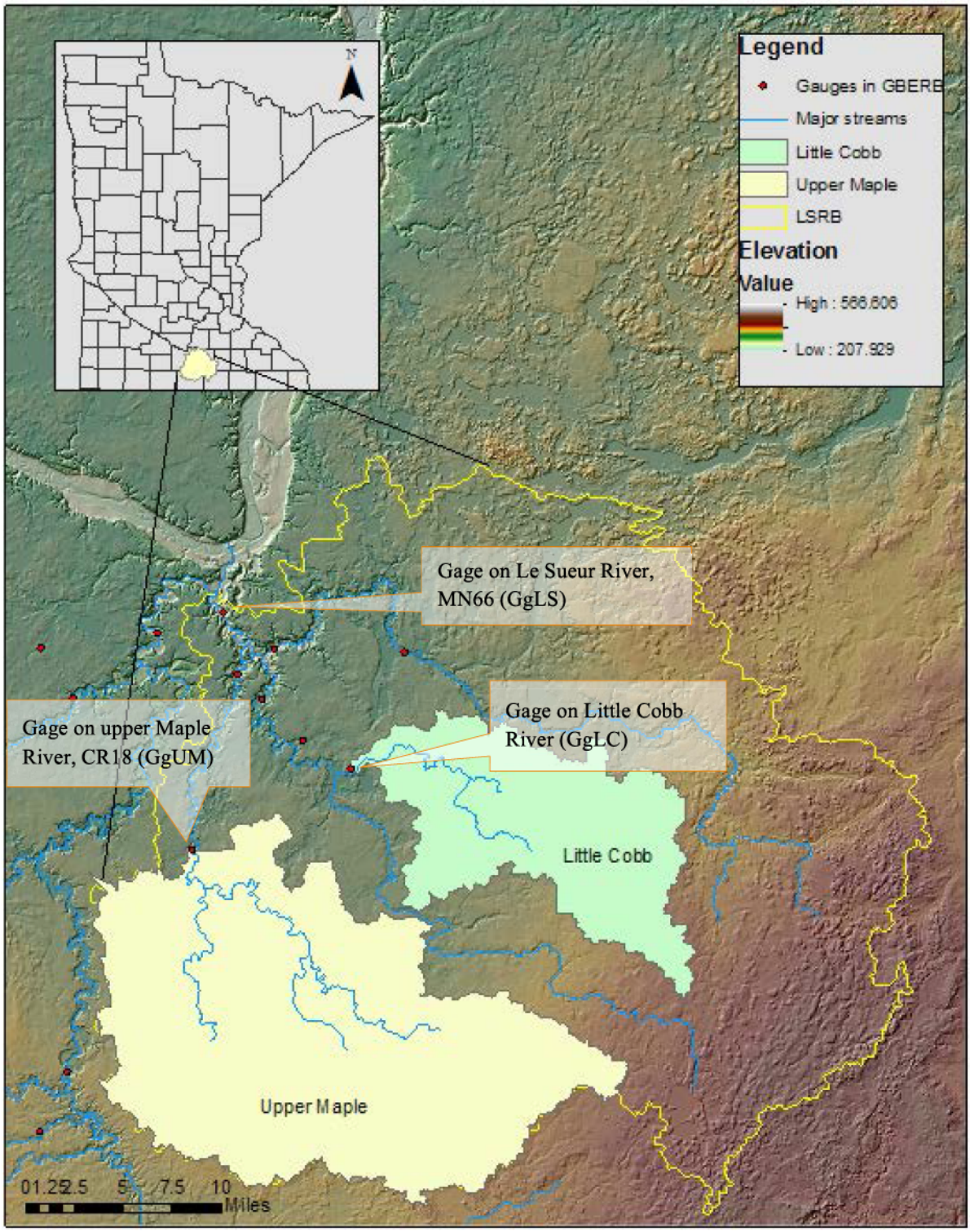

Figure 3.1: Study watersheds, Upper Maple (UM) and Upper Little Cobb (LC), are located in the uplands of the Le Sueur River Basin (LSRB) in South Central Minnesota (the study sites are identified by solid polygons). The gage locations are shown with red circles: gage at the outlet of UM (GgUM), gage at the outlet of LC (GgLC), gage at the outlet of LSRB (GgLS).

3.3.1. Input data

Input data consists of high-resolution surface topography, mean annual soil loss estimated at the sub-field scale from USLE, and stream gage records of total suspended solids (TSS) (used to estimate *SL*).

DEM map scale and topographic variables

Spatial resolution can affect the topographic assessment and parameterization of watershed models (Lane et al., 2004). Higher resolution DEM provides higher information content, which can influence the topographic metrics. A study comparing landscape representation of multiple DEM grid sizes demonstrates that a 10-m DEM will improve representation of topographic indices over 30- and 90-m DEM, but 2- or 4-m DEM data provide only a marginally additional improvement (Zhang and Montgomery, 1994). The choice of DEM resolution involves a tradeoff between improved accuracy in topographic metrics and increased computing time, and depends on the definition of model variables and the purpose of watershed modeling (Sørensen and Seibert, 2007). Using a higher resolution DEM (e.g., 3-m DEM instead of 30-m DEM or 100-m DEM) in a distributed hydrologic model can increase the number of computational elements, as well as computing time, by orders of magnitude. A higher resolution map may be re-sampled to a coarser resolution map to allow quicker simulation. Analysis of the impact of DEM accuracy and resolution on topographic indices indicates that the loss of spatial information by re-sampling a higher resolution DEM to a coarser resolution is small, and can offer much more detail than using a coarser resolution DEM (Vaze et al., 2010). Therefore, we re-sampled a 3-m DEM to develop a 30-m DEM to retain more topographic information while reducing the computational burden.

The watershed dimensions for the study sites are described in terms of the number of raster cells, map extents, and the spatial resolution (Table 3.1). Topographic variables, L_{fi} and $\frac{dE_{fi}}{L_{fi}}$ for calculation of field *SDR* in Equation [3.3], and L_{si} and $\frac{dE_{si}}{L_{si}}$ for stream *SDR* in Equation [3.4] for all raster cells of the study watersheds are obtained from the re-sampled DEM (Figure 3.2).

Table 3.1: This table shows the location coordinates and extents of the Upper Maple and Little Cobb. The watershed dimensions are calculated as the sum of raster cells making up the watershed. The cells outside of the defined watershed and stream cells have null raster value.

Watershed dimensions and map extents		
	Upper Maple	Little Cobb
Number of columns	1,481	950
Number of rows	1,078	802
X corner (Coordinates: NAD 1983 UTM zone 15N)	405,638.62	426,999.49
Y corner (Coordinates: NAD 1983 UTM zone 15N)	4,835,989.84	4,852,862.84
Cell size (30m x 30m)	900	900
Number of cells	1,596,518	761,900
Number of null cells	707,948	395,602
Number of watershed cells	888,570	366,298
Total area (sq. km)	800	330

Soil loss estimates at the field source

Mean annual soil erosion was estimated using USLE within a SWAT model running at a daily time step from 1981 to 2010. In SWAT, a watershed is divided into multiple subbasins, which are then further subdivided into Hydrologic Response Units (HRUs) that consist of homogeneous land use, management, and soil characteristics. Soil losses are calculated using USLE over the HRUs (i.e., soil loss polygons in Figure 3.2) (Gassman, 2007). The model was set up with 46,387 HRUs in the LSRB, and 4,768 and 9,264 HRUs in the LC and UM, respectively. The mean annual soil loss rates per unit

area for each HRU [Mg/yr-acre] are converted to the mean annual soil loss rate A_i [Mg/yr] at each raster cell over the watersheds (Figure 3.2).

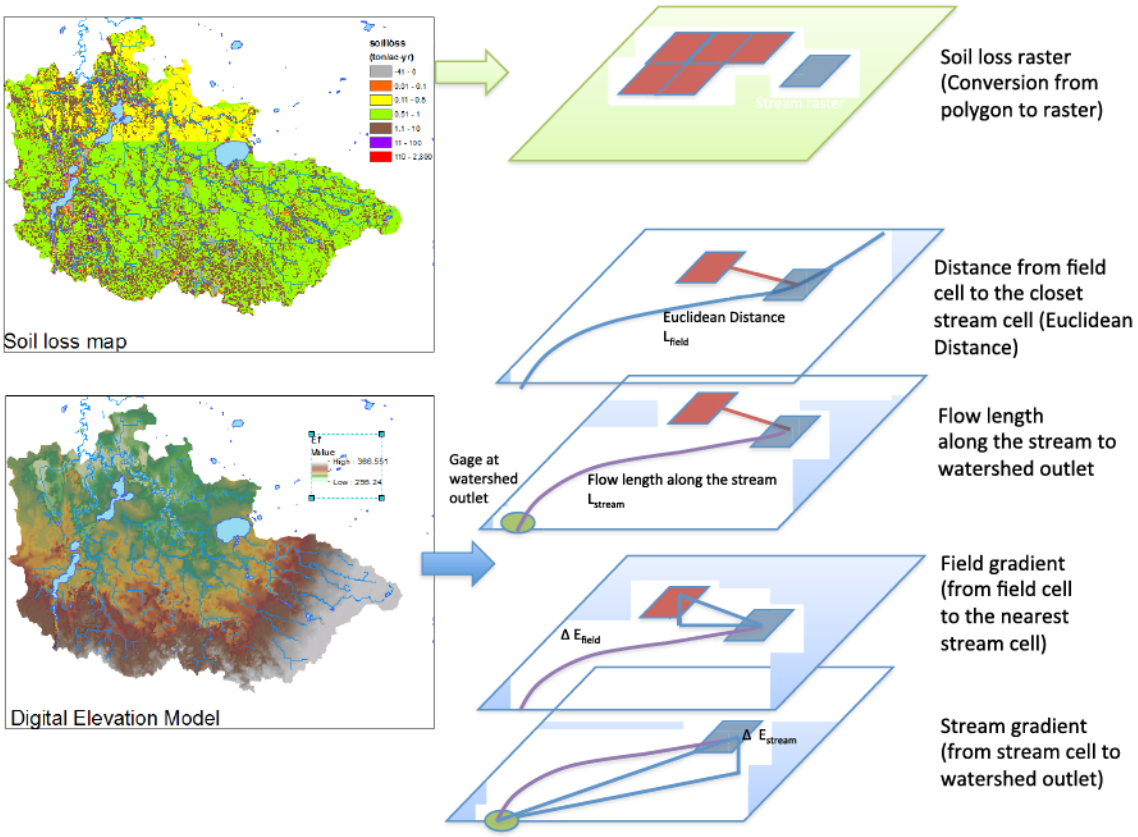

Figure 3.2: Topofilter input data are obtained from soil loss map that is converted to 30-m raster data, and from 30-m DEM, from which topographic variables, including elevation changes and flow lengths from field source rasters, are calculated

Observed sediment loading

Mean annual sediment loading was estimated from TSS observations at stream gages located at the mouths of the UM, LC, and LSRB (GgUM, GgLC, and GgLS in Figure 3.2). Suspended sediment is the major component of TSS measurements in the study watersheds (Minnesota State University, Mankato Water Resources Center, 2012), particularly at large TSS values. For example, for TSS concentrations greater than 500mg/L, the sediment fraction of TSS exceeded 90% for samples collected in 2008-

2009 (Gran 2016, personal communication, November 11). Thus, we use TSS values to represent sediment loading from the watershed.

Observations at the two upstream gages were available for the years 2006-2009. However, 2010 was an exceptionally large sediment loading year, as demonstrated by continuous monitoring from the entire LSRB at GgLS (column 10 of Table 3.2, below). In order to include a broader range of conditions in the estimated annual load, 2010 annual sediment loading for the study watersheds was estimated based on a regression of annual loads against the LSRB, for which 2010 observations are available (Figure 3.3). Sediment loading over the observation period are best described by lognormal distribution (Appendix 3.A) (Singh et al., 1997; Van Buren et al., 1997). For lognormal distribution, median represents the geometric mean (Daly and Bourke, 2008) so we used the sample median to condition the Topofilter parameters.

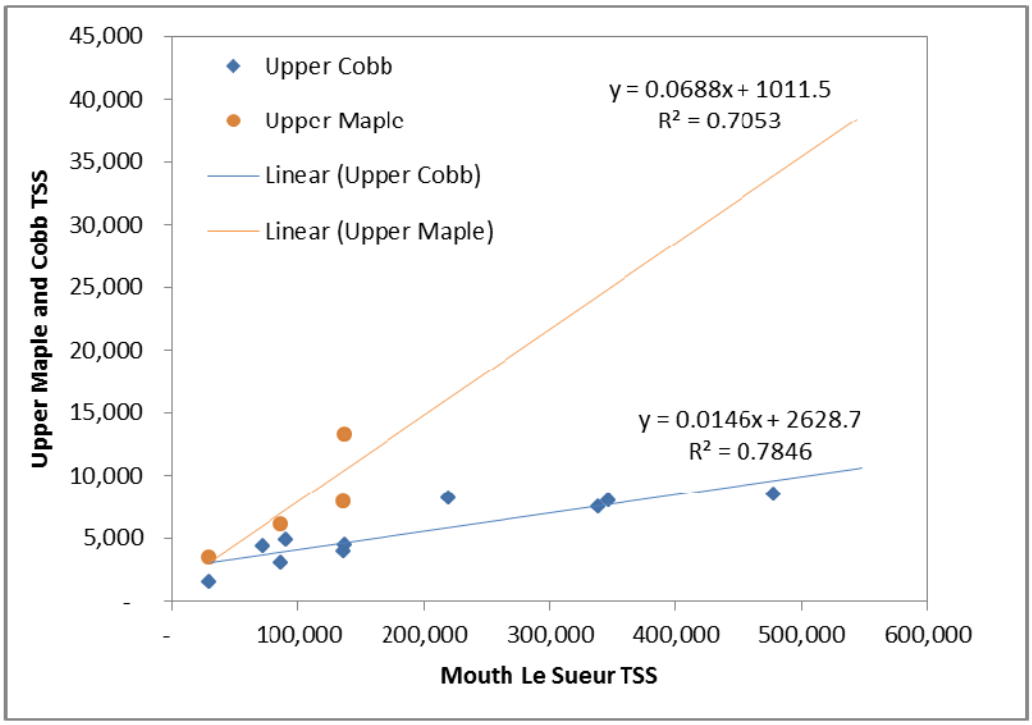

Figure 3.3: sediment loading observations at the GgLC and GgUM are linearly regressed against the observation at GgLS to estimate the sediment loading in 2010 that was not available at the time of this analysis. Extrapolated sediment loading in 2010 is shown in Table 3.2.

Sediment budget

An integrated sediment budget has been developed for the LSRB to quantify the average annual sediment loading rates from all major sediment sources: agricultural fields, ravines, streambanks, and bluffs (Gran et al., 2011). The Topofilter application developed here simulates the sediment delivery from only agricultural fields (Chapter 4 for extends Topofilter to all sediment sources). We used the sediment budget results to reduce observed loads to only the fraction derived from agricultural fields at GgUM (71%) and GgLC (82%) (Table 3.2).

Table 3.2: Total suspend solid (TSS is a reasonable proxy for sediment loading as discussed in this section) observed at GgUM, GgLC, and GgLS are shown in this table. Red fonts indicate extrapolated TSS values for the UM and LC. Sediment loading from field source is calculated using the sediment budget results where in UM field contribution is 71% and in LC it is 82%. Annual soil loss is calculated using the USLE over the entire watersheds from 2006 to 2010. Lumped *SDR* means the aggregate ratio of sediment loading from field over the soil loss in the field.

Basin	Upper Maple: DA=800 km^2				Little Cobb: DA=335 km^2				LSRB: DA=2880 km^2
	Observed TSS	Field contribution (71%)	SWAT USLE field soil loss	Lumped SDR	Observed TSS	Field contribution (82%)	SWAT USLE field soil loss	Lumped SDR	Observed TSS
Year	Mg	Mg	Mg	--	Mg	Mg	Mg	--	Mg
2006	7,875	5,591	59,565	0.09	3,965	3,252	43,772	0.07	135,362
2007	13,285	9,432	82,568	0.11	4,414	3,620	34,726	0.10	136,439
2008	6,060	4,303	214,369	0.02	3,061	2,510	141,374	0.02	86,285
2009	3,452	2,451	54,241	0.05	1,564	1,282	23,746	0.05	29,122
2010	38,384	27,252	136,741	0.20	10,559	8,659	76,994	0.11	543,198
Average for gaged record	13,811	9,806	109,497	0.09	4,713	3,865	64,122	0.06	186,081
Standard deviation	12,702	9,018	60,020	0.06	3,081	2,527	42,525	0.03	182,846.72
Median	7,875	5,591	82,568	0.09	3,965	3,252	43,772	0.07	135,361.70

3.3.2. Model conditioning

Topofilter uses four parameters to represent the sediment delivery from numerous raster cells in a watershed. It is likely that there are many combinations of parameters (a_1, b_1, a_2, and b_2) that result in a satisfactory fit between calculated and observed sediment loading, consistent with the concept of *equifinality* (Beven, 2001). We do not attribute particular significance to any combination of parameters; instead, we develop a stochastic simulation approach using a sediment-loading distribution for many plausible combinations of parameters.

The initial parameter space is determined based on the basic assumptions concerning the physics of sediment transport. First, *SDR* is assumed to be in the range [0, 1], which states that sediment delivery is positive and the maximum sediment loading is bounded by the gross soil loss. $SDR < 1$ requires that $a_1 < 0$ and $a_2 < 0$, such that the exponents in [3.3] and [3.4] are negative[2]. Second, *SDR* is assumed to increase with increasing slope for a fixed length: $\frac{d}{d\,(\Delta E)}[SDR] > 0$, such that $b_1 < 0$ and $b_2 < 0$[3]. Third, *SDR* is assumed to decrease with increasing flow length for a fixed elevation change: $\frac{d}{dL}[SDR] < 0$ (given fixed $(\frac{\Delta E}{L})$), such that $b_1 \leq 1$ and $b_2 \leq 1$[4]. Based on parameter values calculated with fixed flow length and elevation change, and a range of constant *SDR* values, we determined the

---

[2] Assuming that $SDR<1$ intrinsically indicates that sediment loading is no more than gross erosion. For instance given a general sediment delivery expression as a function of elevation change and flow length, $SDR = exp\left[a \cdot \left(\frac{\Delta E_i}{L_i}\right)^b L_i\right] < 1$ would imply that the coefficient, $a<0$

[3] Assuming that *SDR* increase with elevation change and is positive,
$\frac{d}{d\Delta E}[SDR] = \frac{d}{d\Delta E}\left(exp\left[a \cdot \left(\frac{\Delta E_i}{L_i}\right)^b L_i\right]\right) = \frac{d}{d\Delta E}\left(exp\left[aL_i^{1-b}\Delta E_i{}^b\right]\right) =$
$\exp\left(aL_i\left(\frac{\Delta E_i}{L_i}\right)^b\right) \cdot (ab) \cdot (L_i^{1-b}\Delta E_i^{b-1}) > 0$ indicates that $b<0$ since $a<0$.

[4] This assumption is also consistent with *SDR* decreasing with increasing flow length: $\frac{\partial}{\partial L}[SDR] =$
$\exp\left(aL_i\left(\frac{\Delta E_i}{L_i}\right)^b a(1-b)L_i^{-b}\Delta E_i^b < 0\right.$ indicates that $(1\text{-}b)>0$ since $a<0$, so $b<1$.

initial parameter space to be: a_1= [-1E-3, 0], b_1= [-1, 0], a_2= [-1E-3, 0], and b_2= [-1, 0] (see Appendix 3.B).

Model conditioning is used to narrow the initial parameter space by eliminating parameter ranges that produce few or no solutions with small error (i.e., 'behavioral' solutions have error smaller than some threshold value). In the first model conditioning simulation (MC1), *SDR* values for all field cells (i.e., $SDRf_i$ in [3.3]) and in stream (i.e., $SDRs_i$ in [3.4]) were calculated using randomly selected parameter values drawn from the initial parameter space using a uniform distribution for 10,000 MC realizations. The predicted watershed sediment loading (i.e., *SL* in [3.5]), based on the calculated *SDR* values (i.e., SDR_i in [3.2]) and soil loss for all raster cells in the watershed, is then compared to the observed sediment loading using a relative error calculation (rel.err.=abs($SL_{observed}$-$SL_{simulated}$)/ $SL_{observed}$ *100%). The relative errors associated with different parameter values can be displayed using scatter diagrams referred to as "dotty plots" (Figure 3.4). The dotty plots are not particularly useful for isolating particular parameter combinations that yield good predictions, but they are effective in illustrating the model sensitivity to parameter choice and identifying ranges in parameter space that produce few or no behavioral solutions.

The following analysis shows that the model behavior is more sensitive to stream parameters (a_2 and b_2) in that the dot distributions show distinct patterns indicating that the prediction accuracy depends on certain ranges of values. In particular, the model seems to be most sensitive to the stream parameter on gradient (b_2). In other words, in the study watershed, stream gradient has the strongest influence on the calculation of *SDR*. This result is conjectured to be reflective of the particular topographic setting of the

watershed wherein topographic relief is quite small in the upper watershed (providing little influence on sediment delivery) and stream gradient becomes larger near the watershed outlet, such that its influence on sediment delivery may be more significant.

The objective here is to determine an improved parameter space using MC simulation in order to observe the influence of parameter values on model predictions, and to develop a distribution of sediment loading from parameter space conditioned accordingly. We use a threshold value of 10% on the relative error to identify the ranges of parameter values that yield the most solutions that are behavioral (solutions with relative error smaller than or equal to the threshold value).[5] Parameter distribution functions (Figure 3.5 shows the cumulative density functions (CDFs)) of the parameter values that yield behavioral solutions versus the CDFs of parameters that yield non-behavioral solutions (the latter being solutions with relative error greater than the threshold value), together with the dotty plots, reveal which values of the parameters are most consistent with observed sediment loadings at the watershed outlet. This information allows us to update the parameter space to improve our prediction in the subsequent MC simulation.

In the following paragraphs, we describe the model conditioning process based on parameter performance at each of the MC simulation, MC1, MC2, and MC3:

MC1: The first set of dotty plots shows the relative errors of 10,000 sediment loading calculated from randomly chosen parameter values drawn from a uniform distribution over the initial parameter range. Among all the MC realizations, we identify only 10 behavioral solutions (relative error smaller than or equal to 10%). The dotty plots

[5] The terms "behavioral" and "dotty plots" are used in a fashion consistent with description of the Generalized Likelihood Uncertainty Estimate (GLUE) method (Beven, 2001)

illustrate that model performance is more sensitive to the stream parameters (a_2 and b_2) than the field parameters (a_1 and b_1). For all four parameters, non-behavioral solutions (relative error greater than 10%) are uniformly distributed over the entire range of values, whereas behavioral outputs can be found on a narrower range (see also the CDFs in Figure 3.5 (a)). For parameters a_1 and b_1, more behavioral models are distributed over (-6.0E-04,-1.25E-04) and (-0.5,-0.08), respectively. These narrower ranges for parameters a_1 and b_1 exclude 3 of the 10 behavioral solutions and a more lenient range could be adopted. For parameter a_2 and b_2, behavioral models are distributed over (-8.5E-05, 0) and (-0.5, 0), respectively. (Those ranges do not exclude any behavioral solutions.) With these observations, we update the parameter space to increase the number of behavioral solutions in the subsequent MC iteration (MC2).

MC2: With the conditioned parameter space derived from the outputs of the previous MC simulation, the MC2 simulation yields 313 behavioral solutions. Parameters interact with one another. For instance, in MC2, parameter b_2 no longer has the concentration of 100% relative errors on (-0.2, 0), indicating these non-behavioral solutions were associated with the values of other parameters eliminated with the updates on MC1 parameter space. Note that, for clarity, the dotty plots for MC1 don't show points having errors in excess of 150%. With the parameter space update, the MC2 simulation shows many more solutions with errors less than 150% (there are more dots shown in the MC2 simulations). The MC2 simulation also shows that the sediment loading outcomes show almost no sensitivity to parameters a_1 and b_1 (both behavioral and non-behavioral solutions exist on the entire range of parameter values) (Figure 3.5 (b)). On the other hand, parameters a_2 and b_2 show relatively more behavioral solutions on (-4.9E-05,-1.4E-

05) and (-0.17,-0.05), respectively. This narrower range for parameter a_2 excludes 100 out of the 313 behavioral solutions. A broader range of a_2 could be used.

MC3: With the more restrictive conditioned parameter space, there are 1,042 behavioral solutions out of 10,000 realizations in the MC3 realizations uniformly distributed over the entire ranges of the parameters (Figure 3.5 (c)). This indicates that we cannot significantly improve the performance of the model by conditioning the parameter space further, at least using rectangular subspaces (restrictions on values of individual parameters only[6]). Thus, we evaluate the population of the simulated sediment loadings using the MC3 parameter space.

[6] More complex subspaces, such as ellipsoids with axes that are not parallel to the parameter axes, might be used to restrict the space further, but this is left to future research.

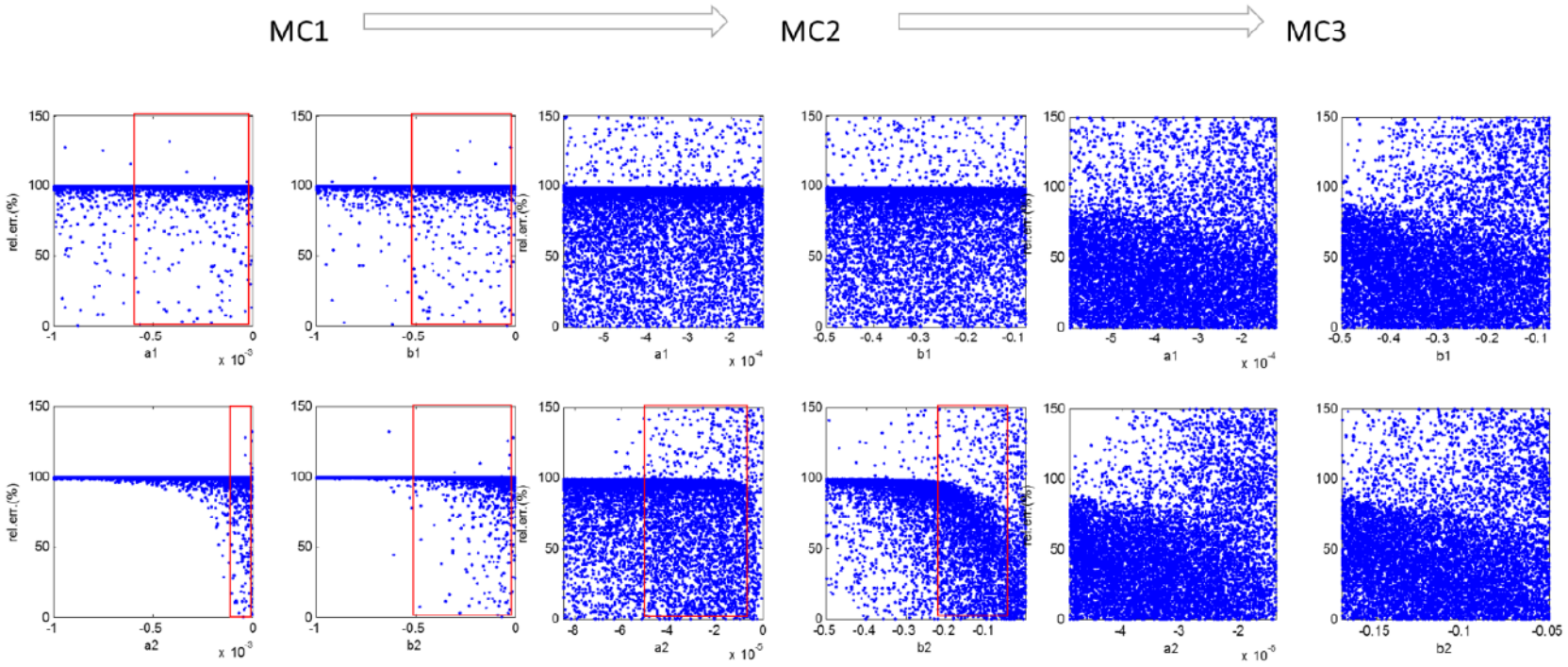

Figure 3.4: Dotty plots show the relative error as function of individual parameter values for iterations MC1, MC2, and MC3 conditioned against observed data in the Little Cobb. Red boxes indicate ranges of parameter values where behavioral values are concentrated. Note that in MC1, many of the non-behavioral solutions have relative error > 150% and are out of the range.

(a)

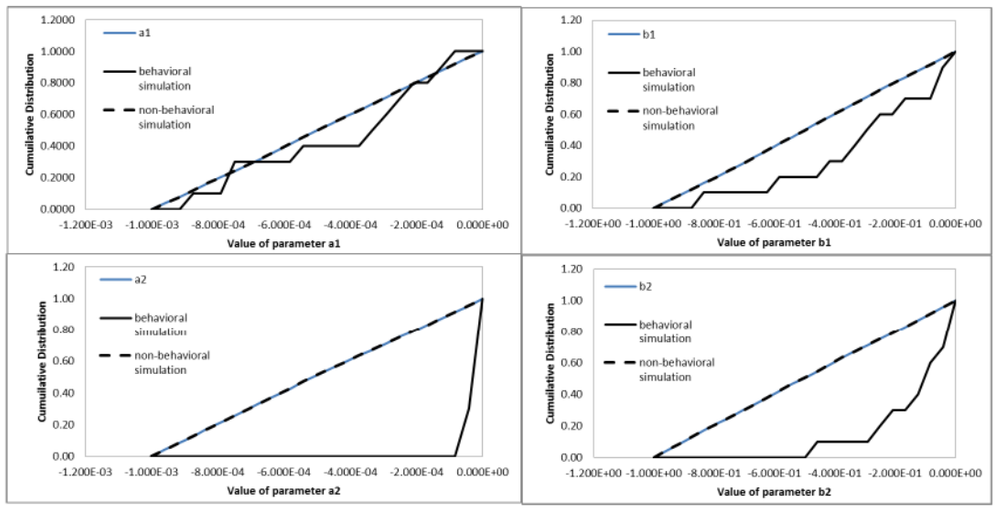

(b)

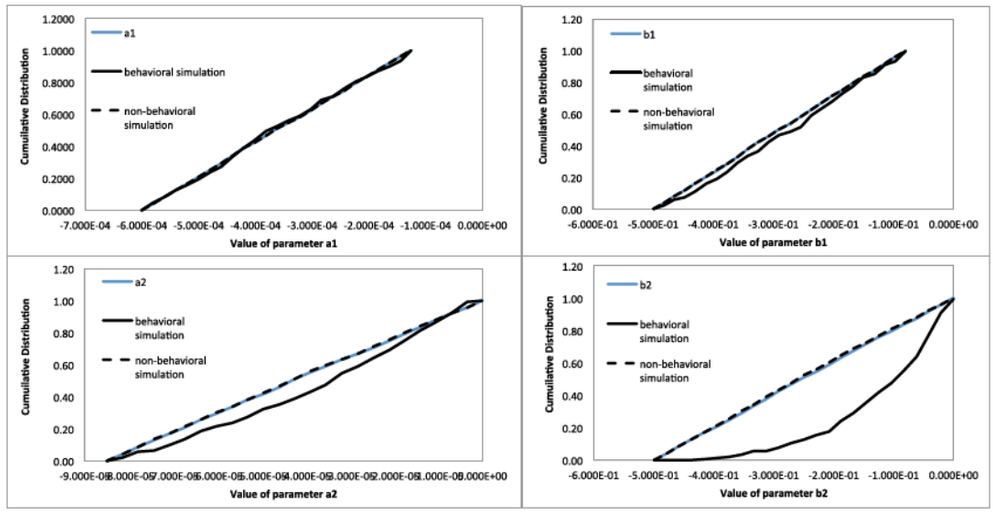

(c)

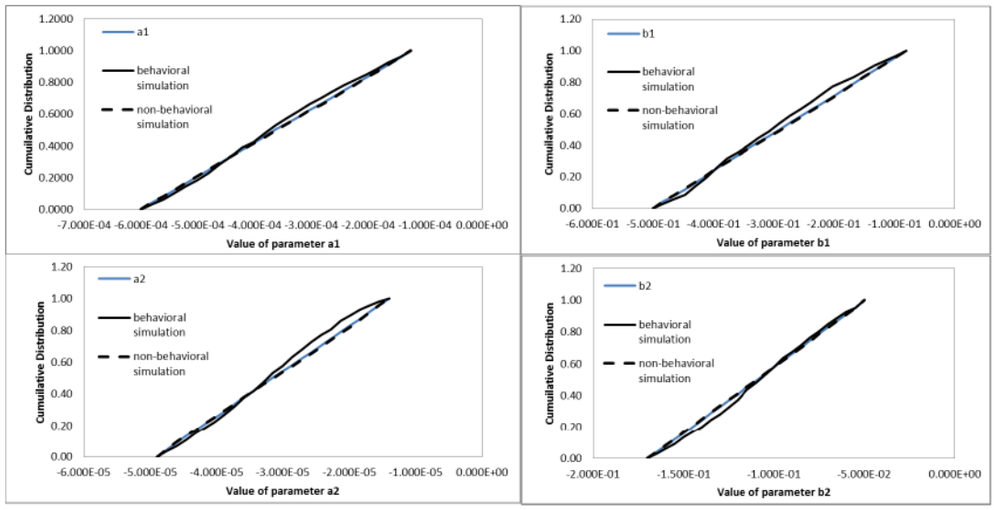

Figure 3.5: Cumulative Distribution Functions (CDFs) of all parameter values (blue line) compared to the behavioral (solid line) and non-behavioral (dotted line) values of all parameter realizations in MC1 (a), MC2 (b), and MC3 (c)

3.3.3. Evaluation of conditioned parameter space

The model conditioning process demonstrated that model solutions are much less sensitive to the field parameters, a_1 and b_1, compared to the stream parameters, a_2 and b_2. This may be attributed to topographic setting of the study watersheds. Most of the uplands are very flat such that water and sediment transport is slow. Stream channels are steeper and become increasingly steep toward the watershed outlet as the streams approach the lower, incised segments of the rivers. Thus, topographic influence on *SDR* and *SL* is likely to increase in downstream portions of the watersheds.

Most of the points in the initial parameter space, but not all, (MC1 outputs) estimate very small *SDR* values and consequently small sediment loading predictions (Table 3.3). Updated parameter spaces, mostly on the stream parameters, a_2 and b_2, improve the fit of the simulated population of sediment loading predictions. The median of 10,000 simulated sediment-loading values from the MC3 parameter space is slightly larger at 3,446 Mg/yr than the median of the observed sediment loading of 3,251 Mg/yr with the average simulated *SDR* values over the watershed at 0.09 (i.e., 9% of eroded sediment from field arrives at the watershed outlet) (see Fig. 3.6 for the distribution of estimated sediment loading outputs). Note however that most parameter values in MC3 are nevertheless "non-behavioral" (result in more than 10% error in estimating the total sediment discharge).

To evaluate whether a model conditioned for one watershed can be applied to a different watershed with similar topography and land use, we applied the MC3 parameter space conditioned for the Little Cobb to the Upper Maple (Table 3.3). The median value of simulated sediment loading is slightly smaller at 4,979 Mg/yr compared to the median

observed value at 5,591 Mg/yr with the average simulated *SDR* values over the watershed at 0.04 (i.e., 4% of eroded sediment from field arrives at the watershed outlet).

Frequency distributions of the simulated sediment loading values calculated with the MC3 parameter space are plotted for both watersheds (Figure 3.6 and 3.7). The probability distribution function that describes the simulated sediment loading the best is the lognormal distribution, determined from a goodness of fit test with maximum likelihood estimation method (*MATLAB and Statistics Toolbox*, 2016). Sediment loading predictions are spread over a wide range, which indicates that most of the parameter values even in the MC3's restricted subset are "non-behavioral." The objective of this exercise is not to provide a single calibrated prediction value, but to identify the conditioned parameter space that yields a population of values (median of this population is shown the green bars) representative of the observed value (median of this population is shown in red bars).

Table 3.3: MC simulation parameter spaces and simulated *SL* for the MC1 through M3 for the LC with the number of behavioral solutions and average *SDR* values at each MC iteration. The parameter space conditioned over three MC iterations is used to calculate *SL* in the UM and shows the number of behavioral solutions and average *SDR* value.

	10,000 Monte Carlo simulation with randomly selected from uniformly distributed parameter values								LC			UM			rel.err. =
									Obs SL	soilloss	SDRlump	Obs SL	soilloss	SDRlump	(SLobs-SLest)
	a1		b1		a2		b2		3251	64,122	0.05	5591	109,496	0.05	/(SLobs)
	min	max	min	max	min	max	min	max	Est SL (median)	Behav (#)	mean SDR	Est SL (median)	Behav (#)	mean SDR	rel.err. (%)
MC1	-1.00E-03	0.00E+00	-1.00E+00	0.00E+00	-1.00E-03	0.00E+00	-1.00E+00	0.00E+00	6	10	0.0003				
MC2	-6.00E-04	-1.25E-04	-5.00E-01	-8.00E-02	-8.50E-05	0.00E+00	-5.00E-01	0.00E+00	474	313	0.09				
MC3	-6.00E-04	-1.25E-04	-5.00E-01	-8.00E-02	-4.90E-05	-1.40E-05	-1.70E-01	-5.00E-02	3,446	1,042	0.09	4,979	1,108	0.04	8.50%

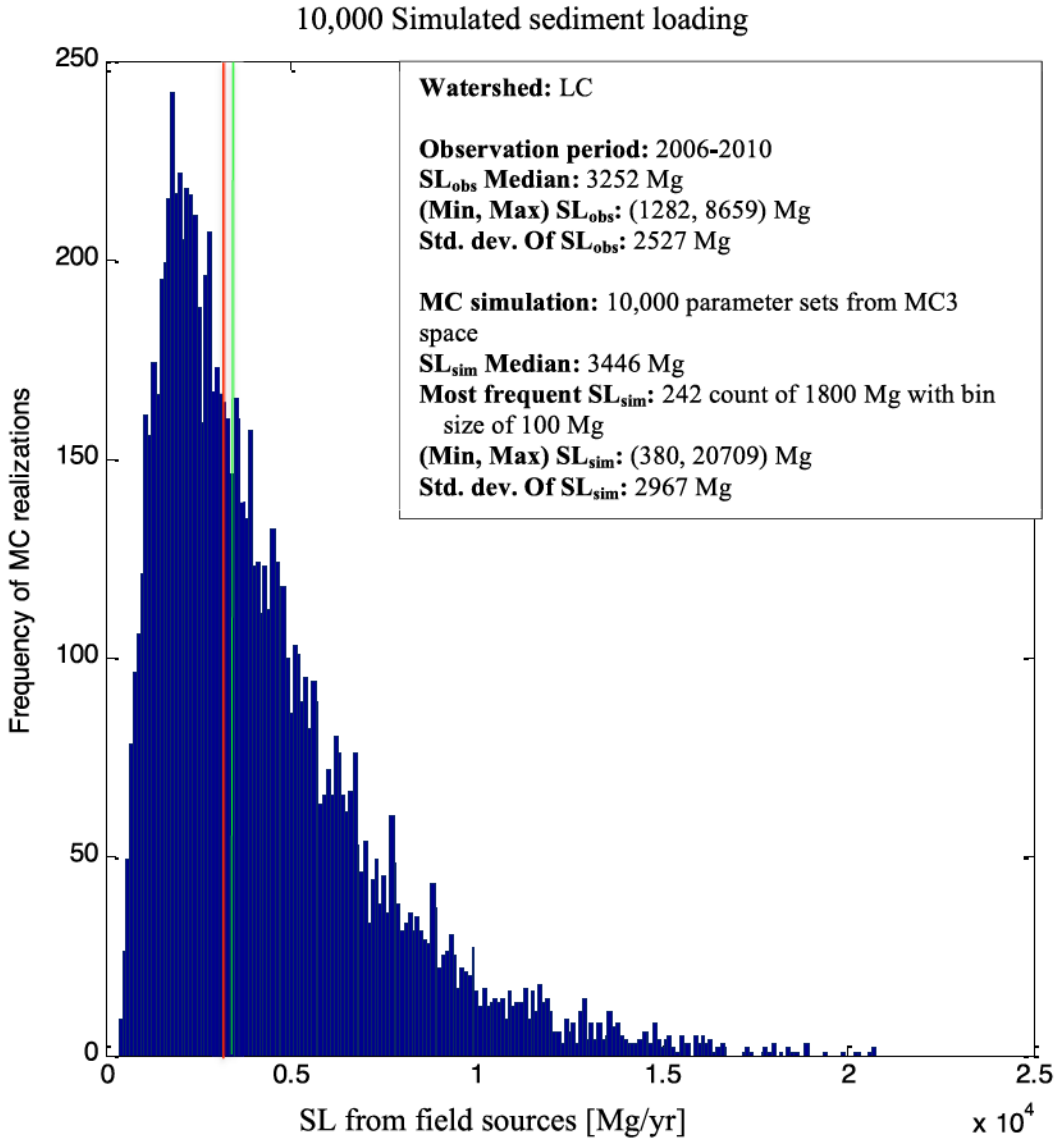

Figure 3.6: Histogram (Little Cobb) of 10,000 model outputs of sediment loading (*SL*) estimated using conditioned parameter space shows that the estimated *SL* has a lognormal distribution with the median value at 3,446 Mg/yr, which is an overestimate of the observed value at 3,252 Mg/yr

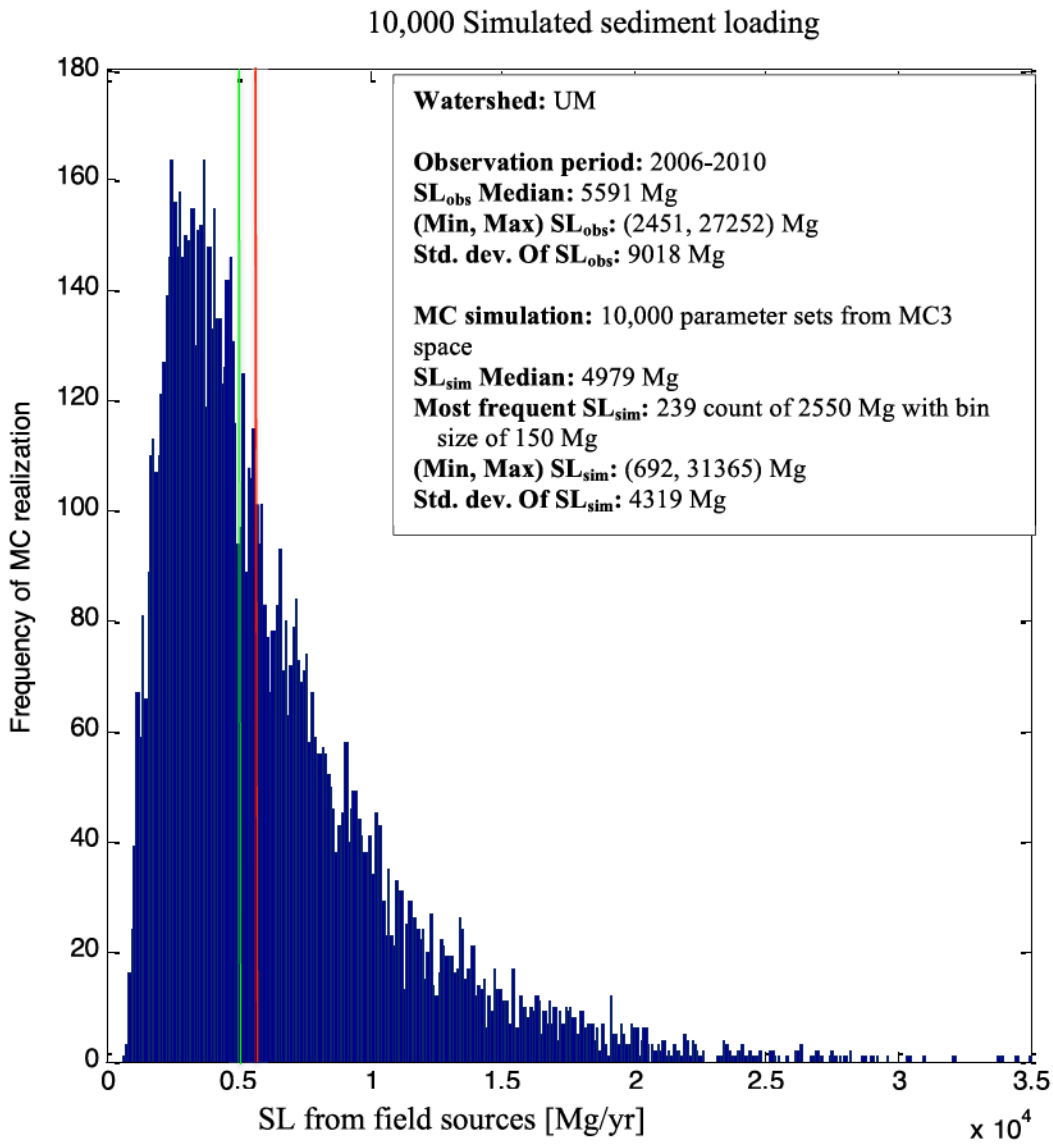

Figure 3.7: Histogram (Upper Maple) of 10,000 model outputs of sediment loading (*SL*) estimated using conditioned parameter space shows that the estimated *SL* has a lognormal distribution with the median value at 4,979 Mg/yr, which is an underestimate of the observed value at 5,591 Mg/yr

The MC3 set of the dotty plots (Figure 3.4) and distribution of sediment loading values (Figure 3.6) illustrate that the conditioned parameter space (Table 3.3) results in numerous non-behavioral solutions (those that yield sediment loading estimates that are too small or too large). The variability introduced in the sediment loading estimates by including all solutions from the MC3 simulation includes: 4,164 (5,057) and 4,794

(3,834) non-behavioral solutions that underestimate and overestimate sediment loading in the Little Cobb (Upper Maple) by more than 10%. In order to evaluate the sensitivity of the parameter space of including only the behavioral solutions among all 10,000 solutions derived from the conditioned parameter space, we removed those parameter combinations from the MC3 simulation outputs that yield non-behavioral solutions (Table 3.4).

With behavioral solutions only for the LC, the parameter space (the ranges of parameter values) remains about the same as the solutions from conditioned parameter space that contain both behavioral and non-behavioral solutions. We see the same ranges of parameter values when we extract behavioral solutions because the behavioral solutions are uniformly distributed over the entire conditioned parameter space (third set of plots in Figure 3.4). The estimated sediment loading values improve because we are only considering the behavioral solutions for which the mean *SDR* values are about the same (Table 3.4 compared to Table 3.3). By definition, for all of the behavioral solution, *SL* values are within 10% of the LC's target *SL* (historic value = 3252 Mg/yr). Likewise, we extracted only the behavioral solutions for the UM, and learned that the parameter space of behavioral solutions and the average *SDR* value are the same for those of all solutions derived from conditioned parameter space.

Table 3.4: Parameter space and mean estimated sediment delivery ratio and sediment loading of the behavioral solutions extracted from MC3 simulation outputs for the Little Cobb (1,042 behavioral solutions as shown in Table 3.3) and Upper Maple (1,108 behavioral solutions)

behavioral solutions extracted from MC3 simulation								LC		UM	
a1		b1		a2		b2		Est SL	SDR	Est SL	SDR
min	max	min	max	min	max	min	max	mean	mean	mean	mean
-6.00E-04	-1.25E-04	-4.90E-05	-8.03E-02	-4.90E-05	-1.40E-05	-1.70E-01	-5.00E-02	3244	0.08	5567	0.04

3.4. Results and discussion

3.4.1. Identification of dominant sediment loading areas

Topofilter analysis to this point provides the spatial distribution of sediment sources for 10,000 trials using the conditioned parameter space. This analysis provides a foundation for developing probability distributions of *SDR* for field and stream for the entire LSRB in Chapter 4. These distributions are used to provide stochastic input representing the uncertainty in sediment supply for the watershed sediment delivery and loading module in Chapter 6.

Although no single parameter set within the conditioned parameter space can be considered to be correct, the entire collection can be used to identify those locations that contribute to most of the sediment load. Locations that contribute to most of the total sediment load in most of the MC trials can be identified and are proposed as the dominant sediment source locations in the watershed.

We developed a spatial filtering algorithm that evaluates the sediment contribution from each raster in each MC trial. The spatial filtering algorithm incrementally eliminates cells with the smallest sediment loading until the sum of the remaining raster cells is equal to 90% of the total load from the watershed (90SL). The remaining cells contribute to most of the sediment load in that simulation. Spatial extent and distribution of areas that contribute to 90SL will vary according to one parameter set to another as they are drawn from the conditioned parameter space in each of the 10,000 MC trials. The areas contributing to 90SL are then collated over all MC trials to determine which areas are most frequently selected (i.e., cells selected 9,500 out of 10,000 trials have a 95% likelihood of being a 90SL area) (Figure 3.8).

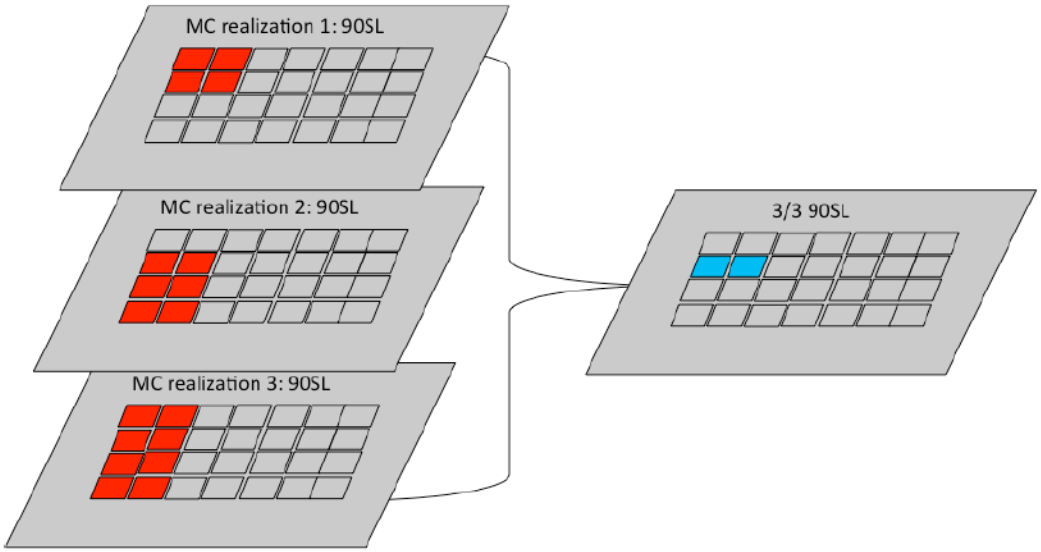

Figure 3.8: Topofilter identifies high sediment loading (*SL*) area for all outputs of the MC simulation. In this simple representation of spatially distributed outputs, we illustrate three MC outputs with 90SL areas indicated with the red cells. The Blue cells on the right illustrate the cells that always contribute to 90SL.

Application of the spatial filtering algorithm in the Little Cobb and Upper Maple determined that the areas that are within the 95% likelihood for contributing to 90SL (95-90SL areas) make up 4% (12.1 km^2) and 3% (22.6 km^2) of the respective watershed areas. Thus, a very small fraction of the watershed area is found to be highly likely to contribute to most of the sediment load. If the likelihood is reduced to 75%, the areas contributing to 90SL (75-90SL) increase to 7% (23.5 km^2) and 5% (43.9 km^2) of the watershed area. If the likelihood is further relaxed to 50%, the areas contributing to 90SL (50-90SL) increase to 11% (37.5 km^2) and 9% (75.8 km^2) of the watershed area (Figure 3.9). The extent of the areas contributing to 90SL increases with decreasing likelihood because the calculation includes cells that don't always contribute to 90SL. Parameter sets that simulate very large sediment loadings (the far right tail in Figure 3.6 and Figure 3.7) produce larger 90SL areas, including further uplands of the watershed. However, these far upland areas are picked less frequently over all MC simulation outputs than areas adjacent to streams and near the watershed outlet. Far upland areas have relatively a

small gradient over large flow length to the watershed outlet, thereby presenting more opportunities for storage along the sediment delivery paths. Areas near the watershed outlet have a larger gradient over a small flow length, such that more sediment is likely to make its way to the outlet.

The topographic characteristics of the study site contribute to the concentration of 90-90SL area identified using Topofilter: major contributing areas are mostly located near the watershed outlet where channel gradient is larger due to the broader patterns of relief in the watershed. For this reason, if we apply Topofilter in a watershed characterized by a high gradient upland and low gradient lowland, major contributing areas will not necessarily be concentrated near the outlet because the high gradient upland provides more opportunity for sediment delivery while the low gradient lowland provides more opportunity for sediment storage compared to the study sites illustrate in this chapter.

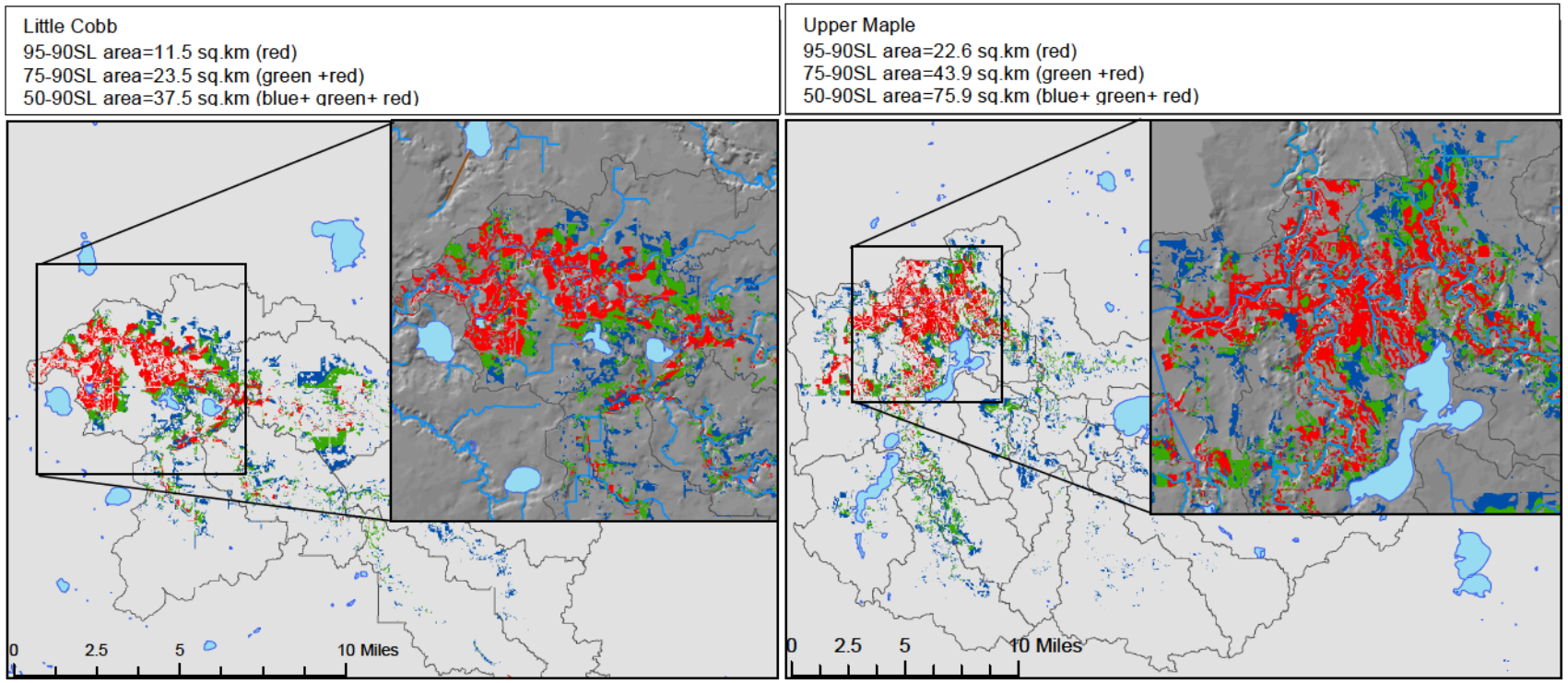

Figure 3.9: Areas that contribute 90% of total sediment loading in the watershed (90SL areas) for the Little Cobb and Upper Maple are calculated for all of 10,000 MC outputs each. The red cells show 90SL area with occurrence likelihood of 95% for all behavioral and non-behavioral parameter sets considered in MC3 (95-90SL area). The red and green cells together show 90SL area with occurrence likelihood of 75% (75-90SL area), and the red, green, and blue cells together show 90SL area with occurrence likelihood of 50% (50-90SL area).

The spatial distribution of locations contributing to most of the sediment load in most of the simulations may differ if only behavioral solutions are used, as discussed in the last part of Section 3.3.3. 90-90SL areas maybe different from using all 10,000 solutions from the MC3 parameter space (i.e., Figure 3.9) depending on the population of non-behavioral solutions that would be excluded from the evaluation of 90-90SL areas.

Those solutions that estimate smaller sediment loadings have 90SL areas consisting of raster cells only near the watershed outlet ; on the other hand, those solutions that estimate larger sediment loadings would have 90SL areas consisting of raster cells extending further upstream of the watershed. For example in Figure 3.10, a non-behavioral solution that underestimates the watershed sediment loading has those cells with larger SL_i values concentrated near the watershed outlet. On the other hand, a non-behavioral solution that overestimates the watershed sediment loading has those cells with larger SL_i values extending further upland. Based on these observations, exclusion of non-behavioral solutions, if they consist mostly of those that overestimate sediment loading, would lead to 90-90SL area concentrated more near the watershed outlet. Inversely, exclusion of non-behavioral solutions, if they consist mostly of those that underestimate sediment loading, would lead to 90-90SL area extending further upstream of the watershed.

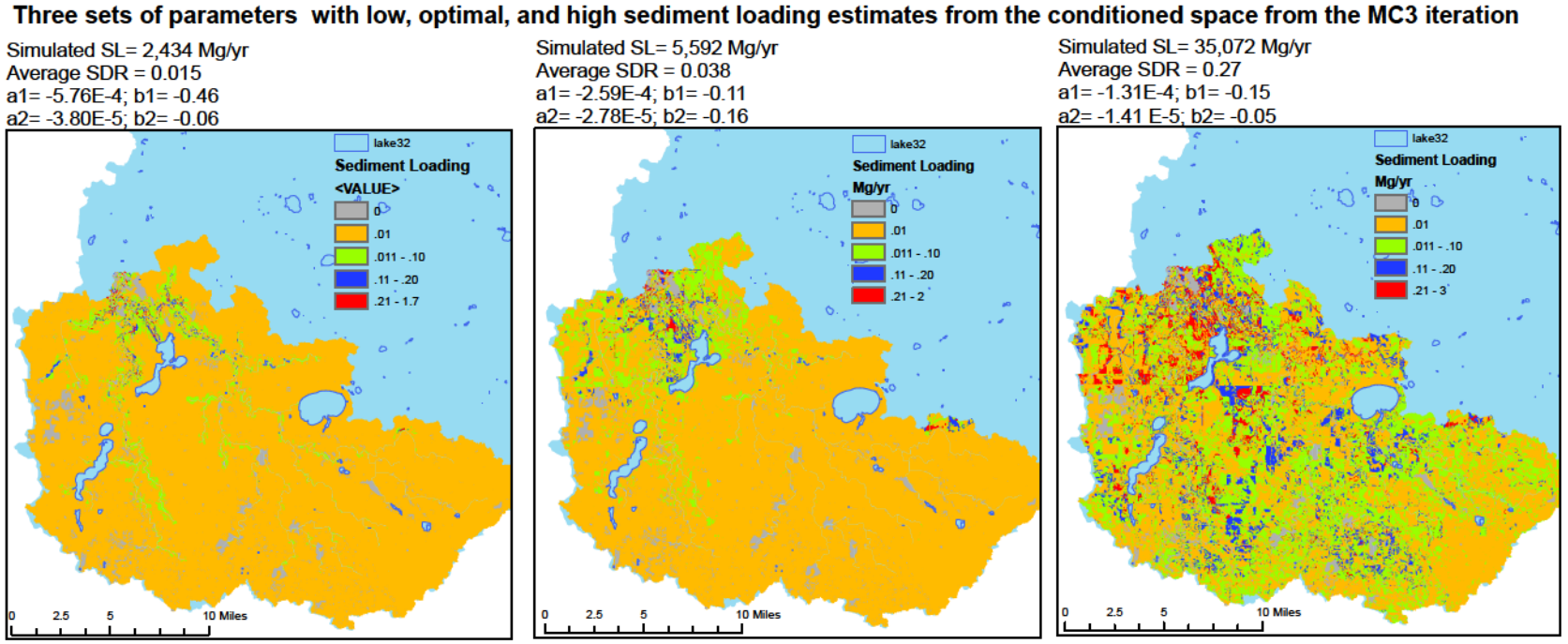

Figure 3.10: Spatial distributions of computed sediment loading using parameter sets that generate a non-behavioral solution that underestimates watershed *SL* (left), behavioral solution that estimates *SL* almost exactly (middle), and non-behavioral solution that overestimates *SL* (right) illustrate that those solutions that underestimate *SL* tend to have high contributing cells only near the watershed outlet; while, those solutions that overestimate *SL* tend to have high contributing cells extending further upstream.

The number of non-behavioral solutions that underestimate and overestimate the watershed sediment loading are about the same for the Little Cobb; therefore, the 90-90SL area, if non-behavioral solutions are excluded (which are about 90% of the parameter sets in MC3), would be about the same as including all solutions. For Upper Maple, there are more non-behavioral solutions that underestimate; therefore, the 90-90SL area, if non-behavioral solutions are excluded, would extend further upstream of the watershed. The effect on the spatial pattern of likely sediment source areas of using behavioral parameter sets or all parameter sets from the conditioned range is a subject for further research.

3.4.2. Sensitivity analysis on the drainage density

Drainage network definition or resolution may affect Topofilter simulation because the extent of the stream network will change the topographic variables and model parameters. In order to evaluate the sensitivity of the Topofilter analysis to stream network resolution, we repeated the model conditioning exercise using a more finely resolved drainage network based on field surveys and information from local drainage districts (MPCA, 2012). Compared to the NHD blue lines used in the first analysis, which shows streams and rivers, the second drainage network includes man-made structures such as canals and ditches. Comparison of the two networks shows that the network including canals and ditches includes more channel length at a greater resolution (Figure 3.11).

The conditioned parameter spaces for the Topofilter models defined by the NHD and the MPCA ditch blue lines are different because the topographic variables have been affected by the different resolutions of the blue lines. The MPCA ditch blue lines extend

further into the uplands, resulting in smaller values of flow length (L_f) and gradient on field (ΔE_f); at the same time, stream flow length (L_s) and elevation drop within stream (ΔE_s) are larger. Whereas the parameter space has shifted with different resolution of the blue lines, the distributions of the simulated sediment loading predictions are comparable (Table 3.5).

NHD blue line vs. Ditch blue line defined by the MPCA	
NHD blue lines in the Le Sueur River Basin **Number of river segments:** 538 **Segment types:** artificial path (49), canal ditch (52), connector (19), and stream/river (418) **Total length:** 1557 km	Ditch blue lines in the Le Sueur River Basin **Number of segments:** 4360 **Segment types:** public ditch open (536), public ditch tile (2503), and stream/river (1317) **Total length:** 2038 km

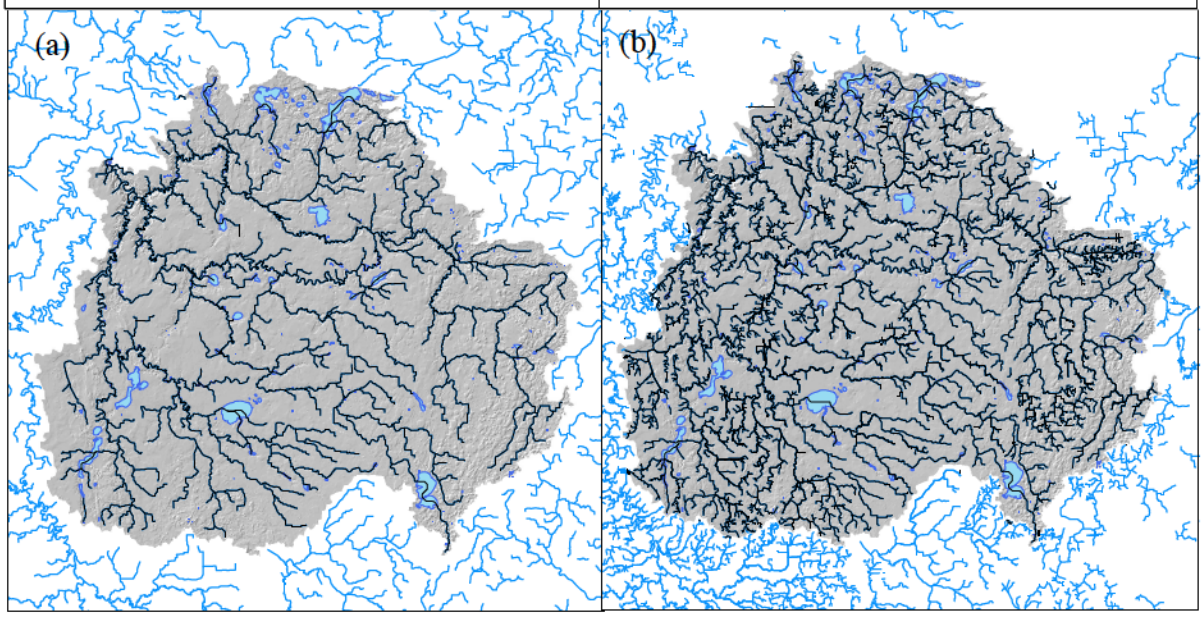

Figure 3.11: A comparison of drainage densities of (a) the National Hydrography Dataset (NHD) obtained from the USGS ("NHD blue line model"), and (b) Minnesota ditch blue lines obtained from the MPCA ("MPCA ditch blue line model")

Table 3.5: Comparison of Topofilter variables and parameter inputs to Little Cobb (LC) and Upper Maple (UM) with model outputs including median of simulated 10,000 *SL* and areas that contribute 90% of *SL* at different likelihood measures.

stream networks		NHD blueline				Ditch blueline			
watershed		LC		UM		LC		UM	
variables	units	max	avg	max	avg	max	avg	max	avg
Lf	[m]	6020	1315	5992	1249	1559	403	1917	349
dEf	[m]	28	9	43	7	19	3	21	3
Ls	[m]	57366	33570	76717	41476	61484	35723	81634	42995
dEs	[m]	57	20	54	21	64	25	65	26
Parameters		min		max		min		max	
a1	[-]	-6.00E-04		-1.20E-04		-7.00E-04		-4.50E-04	
b1	[-]	-0.5		0		-0.8		-0.2	
a2	[-]	-5.00E-05		-1.00E-05		-5.00E-05		-2.50E-05	
b2	[-]	-0.17		-0.05		-0.1		-0.01	
Median SLest	[Mg]	3445		4957		3365		5629	
Avg SLest	[Mg]	4244		6208		4272		6789	
STD SLest	[Mg]	2966		4318		2860		4636	
Mean SDR	[-]	0.09		0.04		0.07		0.04	
95-90SL area	[km2]	12.1		22.6		4.5		10.0	
75-90SL area	[km2]	23.5		43.9		12.7		49.9	
50-90SL area	[km2]	37.5		75.8		30.0		81.7	

We evaluated the 95-90SL, 75-90SL, and 50-90SL areas determined by applying Topofilter to the higher resolution drainage density from the MPCA ditch blue lines. There is more variability in the calculation of 90SL area from one parameter set to another when using the MPCA ditch blue line model. For instance, 95-90SL areas are much smaller for the MPCA ditch blue line model; whereas the 50-90SL areas for the MPCA ditch blue line model are comparable to the NHD blue line model (Figures 3.9 and 3.12, and Table 3.5). With the MPCA ditch blue line model, the 90SL areas remain close to the channel network but are less concentrated near the watershed outlet and more distributed in the uplands near the channel network (Figure 3.12). Particularly, the 50-90SL areas extend further upstream than the NHD blue line model. In other words, as a result of the extensive drainage network of the ditch blue line model, more raster cells in the further uplands have shorter L_f; thus, these raster cells in the further uplands contribute to 90SL for more parameter sets (i.e., 50% of all realizations). Nevertheless,

cells contributing to 95-90SL are still clustered near the watershed outlet even with more expansive drainage network.

This sensitivity analysis shows that higher-resolution drainage density (MPCA blue line model) provides more spatially-resolve predictions about high sediment loading areas compared to lower-resolution drainage density (NHD blue line model), but identification of general location of high sediment loading areas (i.e., near the mouth of the watershed adjacent to mainstem channels) did not change. In order to accurately identify high sediment loading area, drainage density map that realistically represents the path of surface runoff to stream network and routing of water within stream network should be used. However, in the study watersheds where large influences on sediment delivery and loading are made by steep topography near the watershed outlet, higher resolution of drainage network further in the upland didn't affect the simulation results significantly.

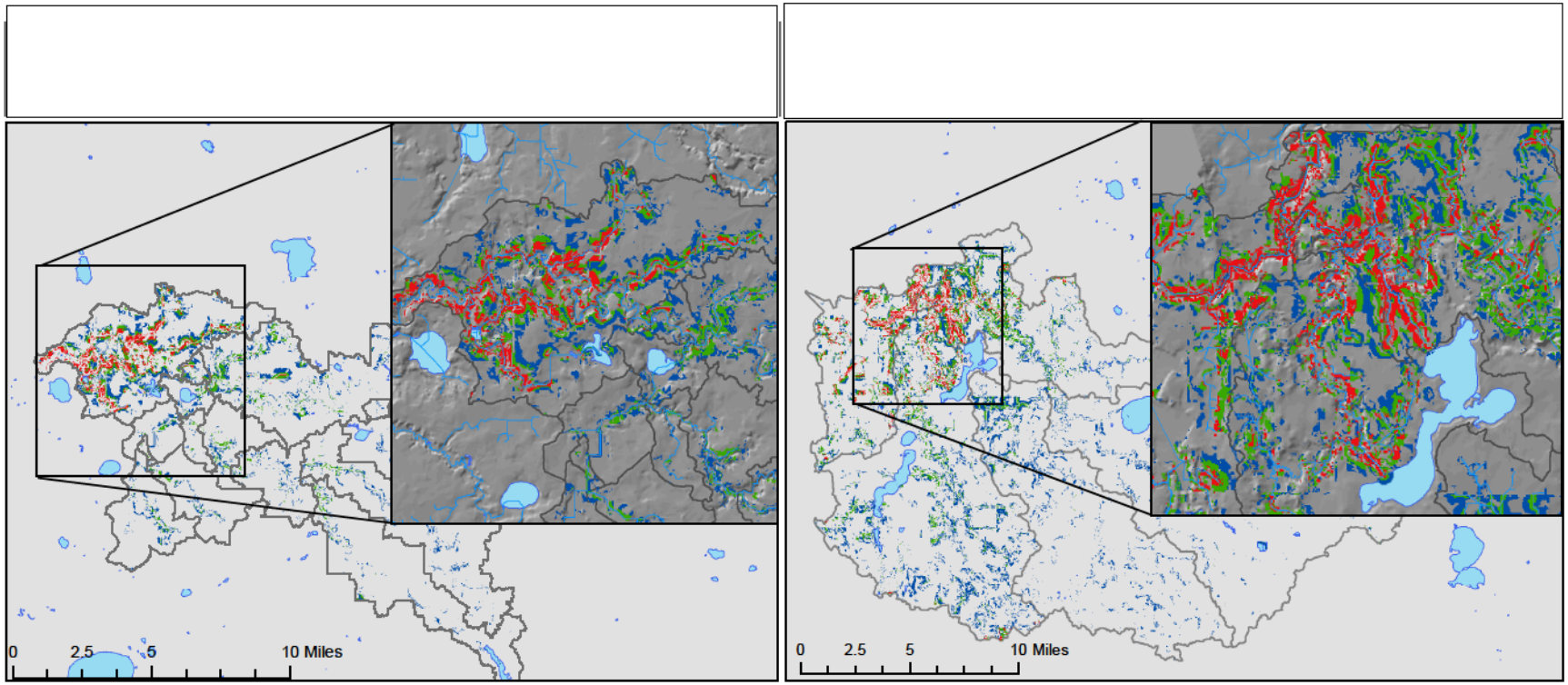

Figure 3.12: Sediment source areas identified using Topofilter based on the spatial filtering algorithm (Section 3.4.1) using the MPCA Ditch Blue lines: areas that contribute to 90% of the estimated sediment load (90SL) in 95% (95-90SL), 75% (75-90SL), and 50% (50-90SL) of 10,000 MC outputs are shown. Figure 3.12 shows the result of using a more finely resolved drainage density than the similar analysis in Figure 3.9.

3.4.3. Evaluation of magnitude of stream sediment supply and deposition

Topofilter provides an estimate of sediment delivery to the outlet of a watershed. The balance of the total soil erosion is necessarily deposited and stored somewhere between the sediment source and sink. Here we evaluate the magnitude of mean annual valley-bottom floodplain storage as a check on the overall function of the Topofilter approach. For example, if soil erosion rates calculated using USLE are much larger than the actual erosion rates, one may expect that the amount of sediment not delivered to the watershed outlet would produce unusually thick floodplain deposits. Similarly, if the conditioned parameter space yields unrealistically large field *SDR* and small stream *SDR*, calculated floodplain deposition will be unrealistically large, and vice versa.

Topofilter simulates $SDRf_i$ for all field cells ($i=1,\ldots, N$) in the watershed (i.e., *SDR* from any field cells to the stream cells) at each MC realization. The mean annual sediment input (*SI*) from a field cell *i* to the adjacent stream cell (SI_{F_i} [Mg/yr]) is calculated using the simulated $SDRf_i$ and mean annual soil loss rate (A_i):

$$SI_{F_i} = A_i * SDRf_i \qquad [3.6]$$

Mean annual sediment deposition rate along the floodplain from the point of sediment arrival from the field cell *i* to the watershed outlet (SD_{S_i} [Mg/yr]) is calculated using the simulated $SDRs_i$ (i.e., *SDR* from the stream cell to the watershed outlet):

$$SD_{S_i} = SI_{F_i} * (1 - SDRs_i) \qquad [3.7]$$

In other words, [3.6] calculates the fraction of sediment delivered from the field to the stream, and [3.7] calculates the fraction of sediment that is left (1-*SDR*) along the stream corridor. Sediment loads are calculated for all field cells $i=1\ldots N_j$ draining to the stream

cells in the path j. The mass of sediment deposition is converted to volume (SV_j [mm/yr]) over the floodplain area along the stream path j:

$$SV_j = \sum_{i=1}^{N_j} \frac{SD_{s_i}}{A_{s_j} * \rho_b} \quad [3.8]$$

where A_{s_j} is the cumulative floodplain area for the stream path j, and ρ_b is the bulk density of mud. This variable is defined over 39 reaches using 109 cross sections on a 3m DEM to identify the tops of streambanks and the floodplain area when the water overtops the streambanks by 1m (Figure 3.13).

Sediment deposition rates in the floodplains are calculated for 10,000 parameter sets from the conditioned parameter space for all the reaches. First, for each parameter set, mean annual sediment deposition rates are calculated for all raster cells in the floodplain area at each of the defined reaches. Then, the average mean annual sediment deposition rate over the entire floodplain area at each of the defined reaches is calculated for all 10,000 parameter sets. The average mean annual sediment deposition rate over all MC outputs is examined against the corresponding floodplain area (Figure 3.14). The simulated sediment deposition rates are smaller than 2 mm/year in many reaches. Deposition rates are generally larger for smaller floodplain areas. For example, a stream in a narrow valley with relatively small floodplain area (bottom middle insert of Figure 3.14) shows a sediment deposition rate of a little over 4 mm/year.

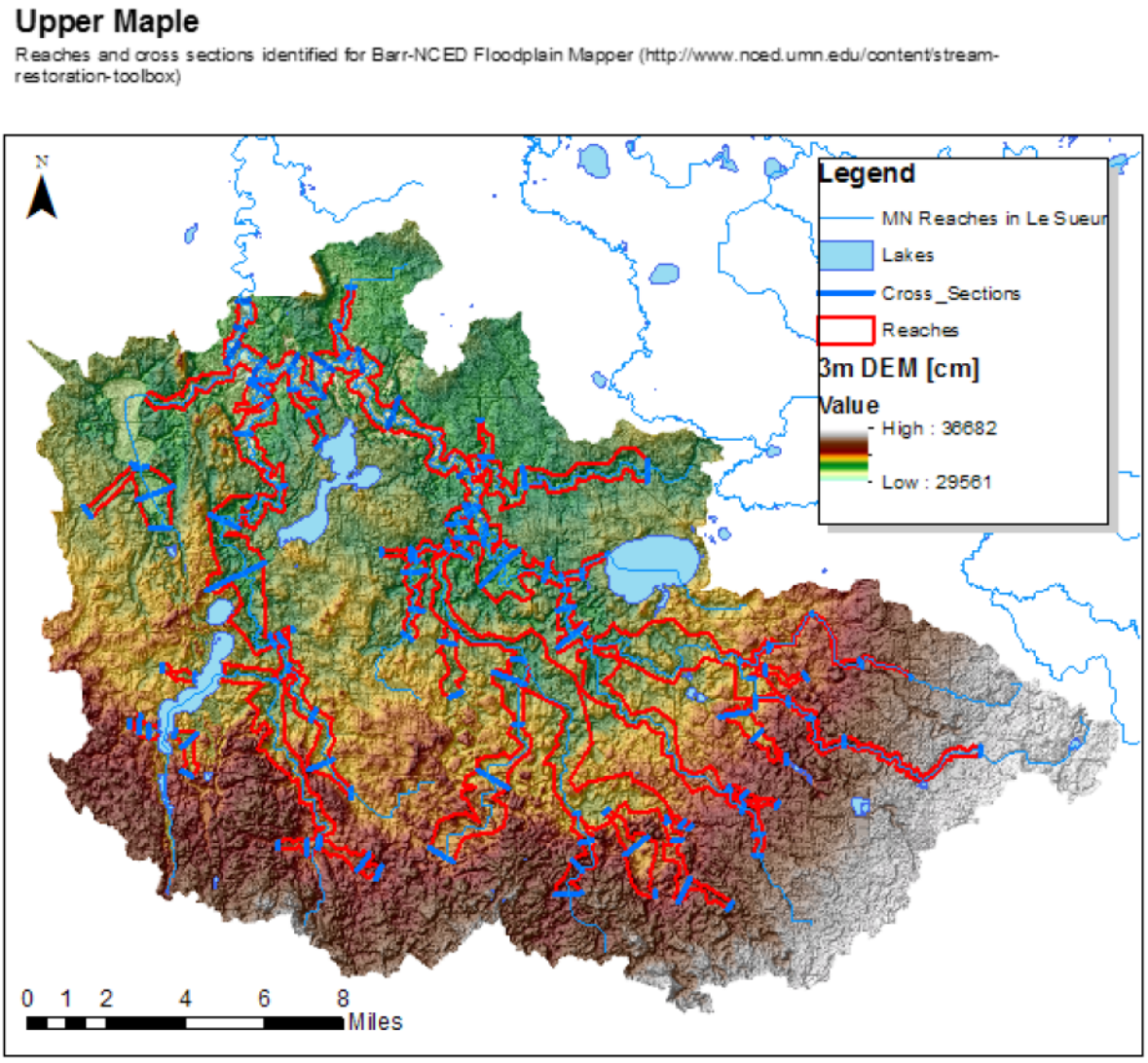

Figure 3.13: Reaches and cross sections in the UM defined using the *Floodplain Mapper Toolbox* (the toolbox is available for ArcGIS version 10.0 or higher as a part of the NCED stream restoration toolbox: http://www.nced.umn.edu/content/stream-restoration-toolbox) with the MN Reaches in the Le Sueur River Basin and 3m DEM

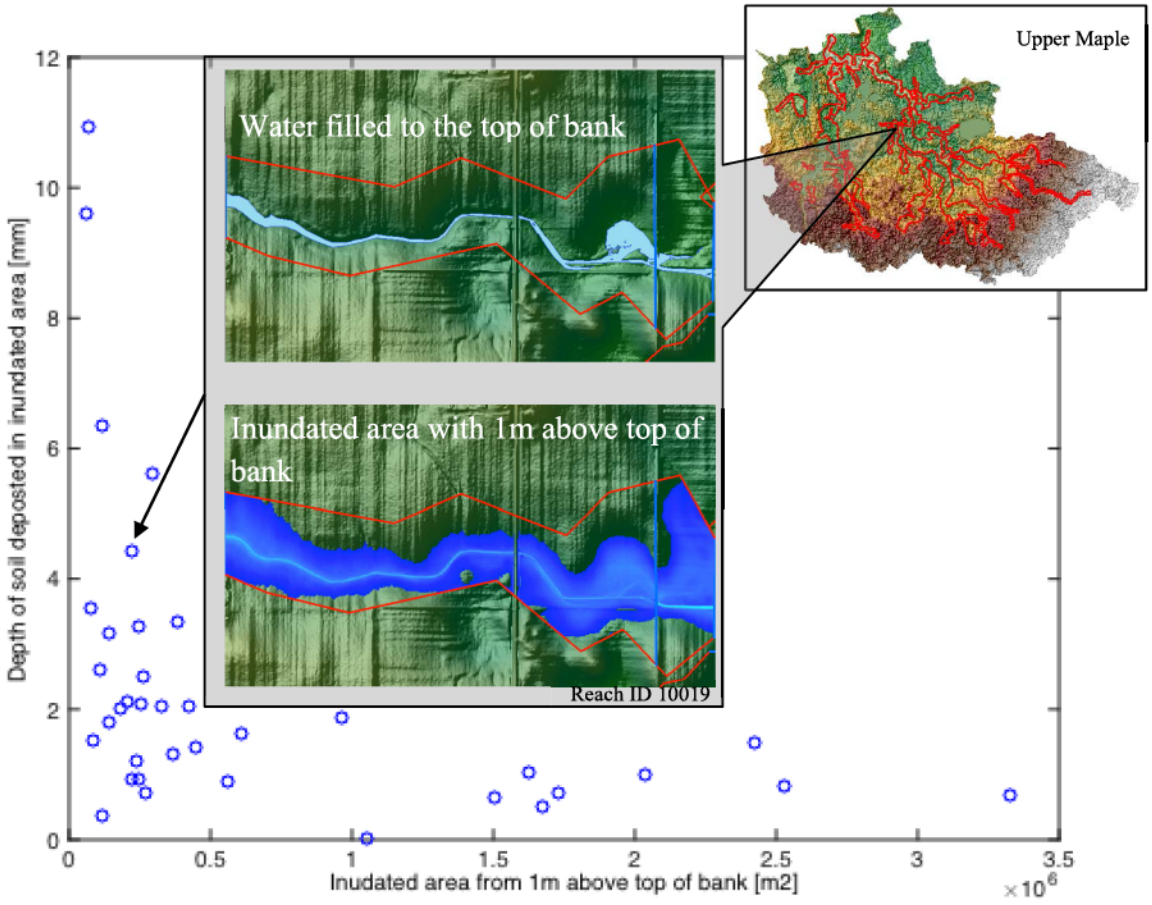

Figure 3.14: Mean annual sediment deposition rate as a function of inundated area with an insert to illustrate a reach and its inundated area. For many stream reaches, soil deposition rates along floodplain area are smaller than 2mm/yr, but for some stream reaches (those with smaller floodplain areas or larger soil erosion rates from their contributing areas) deposition rates are higher. The evaluation and graphic representation of the inundated floodplain area are made using the Floodplain Mapper Toolbox (the toolbox is available for ArcGIS version 10.0 or higher as a part of the NCED stream restoration toolbox: http://www.nced.umn.edu/content/stream-restoration-toolbox).

Although there are no direct observations of floodplain deposition in the immediate study area, a study of post-European settlement alluvial storage is available for the Indian Creek valley, located just southwest of Mankato, MN, with 7 valley transects (located near the incised zone of the LSRB) and Beaver Creek valley, located southeastern tip of the state along a tributary to the Root River, with 40 valley transects (located east of the LSRB) (Beach, 1994). In this study, the post-settlement (1851-1988) alluvial storage

(depth above paleosols) observed is 2.5 m (18.2 mm/yr when averaged over 137 years) in Beaver Creek and 50-120 cm (3.6 - 8.7 mm/yr when averaged over 137 years) in Indian Creek (ibid.). These observations are considerably larger than floodplain aggradation rates implied by Topofilter (Figure 3.14). One likely explanation for the difference is that soil loss from agricultural fields has declined in the last 80 years with soil conservation efforts (Belmont et al., 2011; Montgomery, 2007).

Another independent estimate of valley bottom storage is a recent repeat survey of high resolution topography data that enabled the analysis of geomorphic changes in the watershed (K. R. Schaffrath et al., 2015). This study utilizes airborne LiDAR collected in 2005 and again in 2012 to evaluate a DEM of elevation difference (DOD) for a 1-m resolution raster map showing the changes in the topography in the Blue Earth County, Minnesota (1,980 sq.km.). Blue Earth County covers the lower half of the Upper Maple, so floodplain soil accumulation values are checked for 11 lower reaches of this watershed.

The DOD estimates, extracted over floodplain areas and averaged over all raster cells, are in the range 5 mm/yr to 20 mm/yr. The Topofilter estimates fall toward the low end of the DOD estimates of surface elevation change (Table 3.6) (Figure 3.15). Comparison of floodplain deposition rates implied by application of Topofilter to USLE to the available observations of floodplain aggradation indicates that the implied Topofilter deposition falls within reasonable bounds. This indicates that the USLE estimates of soil erosion rate are also within reasonable bounds and that the Topofilter representation of the effect of topography on sediment delivery has been developed within erosion and loading estimates that are reasonable.

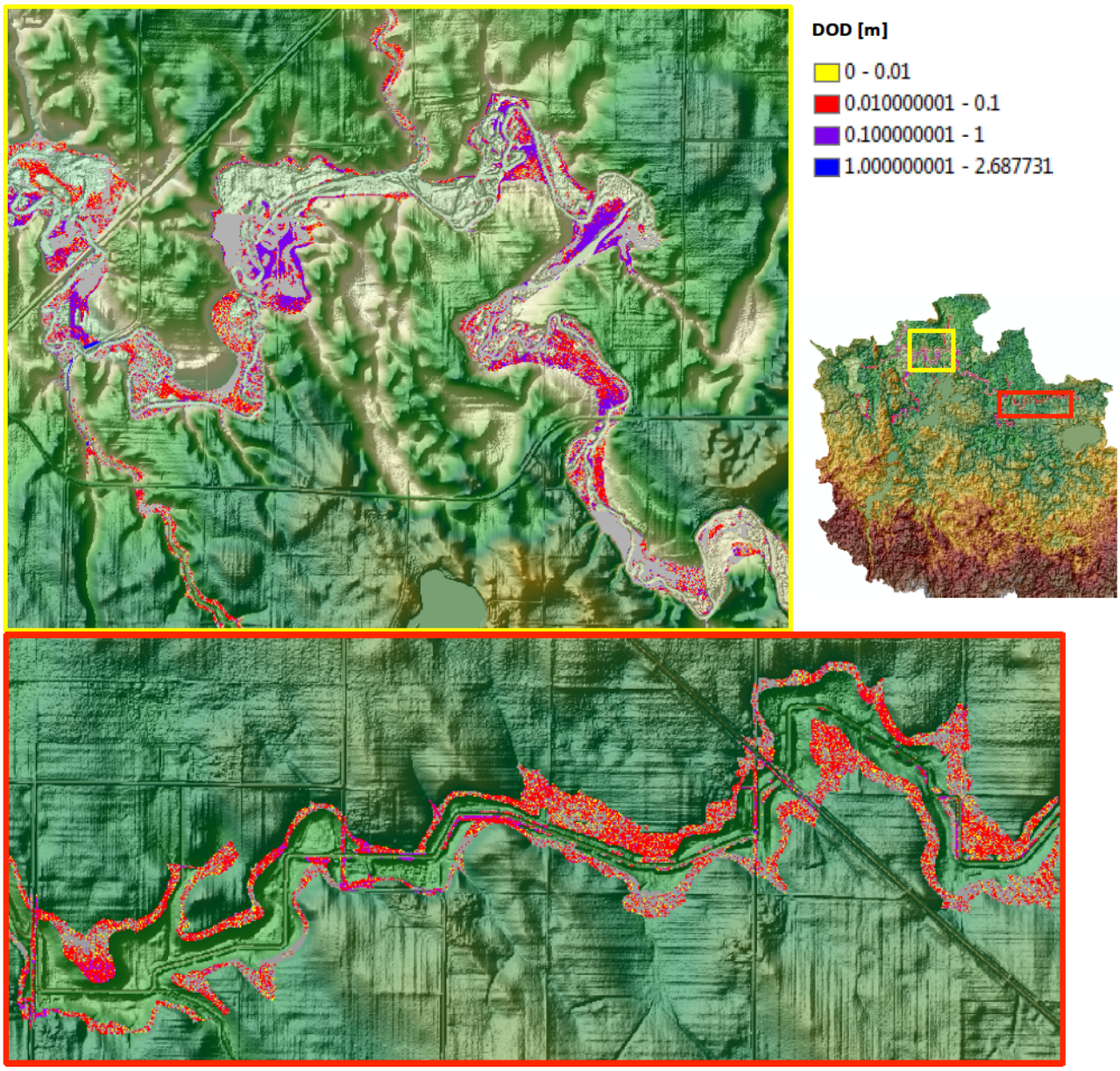

Figure 3.15: DEM of difference (DoD) results in the floodplains (yellow to blue cells) in the lower half of the Upper Maple (mapped with DoD data from the authors (K. R. Schaffrath et al., 2015)). Two example reaches show that in further upland aggradation along stream ranges between 0.01m-0.1m over the observation period (1mm/yr-14mm/yr), and near the watershed outlet the aggradation along stream ranges between 0.01m-1m over the observation period (1mm/yr-143mm/yr).

Table 3.6: comparison between Topofilter simulation of floodplain soil accumulation (column 2) and DEM of difference from 1-m spatial data from 2005 and 2012 (only the accretion is spatially averaged over the reaches and negative readings are omitted in columns 3 and 4, and both degradation and aggradation are average over the reaches in columns 5 and 6)

Models/ observation	Topofilter	DoD: positive changes only (Aggradation only)		DoD: all changes (Degradation and aggradation)	
Reaches	Floodplain soil accumulation (mm/yr)	Mean DoD (2005-2012) extraction over floodplain (m)	Mean annual DoD (mm/yr)	Mean DoD (2005-2012) extraction over floodplain (m)	Mean annual DoD (mm/yr)
SO1R16	0.891	0.066	9.371	0.019	2.714
SO1R17	9.595	0.038	5.382	-0.013	-1.857
SO1R25	2.587	0.049	7.039	0.009	1.286
SO1R26	3.164	0.059	8.452	0.005	0.714
SO1R27	3.278	0.067	9.531	0.006	0.857
SO1R28	6.367	0.047	6.728	-0.005	-0.714
SO2R1	0.367	0.067	9.627	0.007	1
SO3R1	0.708	0.106	15.146	0.022	3.114
SO3R2	0.926	0.142	20.294	0.088	12.529
SO3R3	0.808	0.102	14.641	0.029	4.129
SO4R1	1.472	0.103	14.661	-0.103	-14.709

3.5. Transferability of Topofilter

Topofilter's main function is to evaluate the effect of topography on sediment storage, delivery, and loading across a watershed, given distributed information about soil erosion and integrated sediment loading observation at the watershed outlet. Topofilter, as presented in this chapter, provides a description of sediment delivery and loading characterized by high-resolution DEM and USLE-predicted soil loss over the watershed for a reference period, 2006-2010, for which sediment gaging information was available.

Topography influences the spatial distribution of sediment delivery ratio in the watershed. Given the same topography, if soil erosion rate across the field is increased but sediment loading contribution from field at the watershed outlet is decreased (i.e., large fraction of field sediment is stored in river valleys), overall sediment delivery ratio (*SDR*) across the watershed would be smaller but the spatial distribution of *SDR* in the

watershed would remain essentially the same. For example, in the study watersheds, raster cells with larger *SDR* values will still be concentrated near the watershed outlet where the topography is steeper and flow length to the watershed outlet is smaller relative to raster cells further in the upland.

For this reason, as discussed in Section 3.4.1, the distribution of *SDR* and dominant source areas would be different in a watershed characterized by a high gradient upland and low gradient lowland. Upland, with higher gradient, provides more opportunity for sediment delivery while the low gradient lowland provides more opportunity for sediment storage. In this kind of watershed, larger *SDR* values and major contributing areas will not necessarily be concentrated near the watershed outlet as demonstrated in the study watersheds.

Both the distributed information about soil erosion rate across the watershed and the integrated information about sediment loading at the watershed outlet affect computation of sediment delivery ratio. Trimble describes shifting sediment budgets in a watershed with different topography but with similarities in land use history. During a period of maximum agricultural production with minimal soil conservation in 19th and early 20th centuries, soil erosion rates were very large and a large fraction of that sediment was stored in valley lowlands. After implementation of soil conservation, the amount of soil erosion was much smaller and the main source of sediment was shifted to the low lands (Trimble, 1999, 1981).

Let's consider the shifting sediment budgets in terms of Topofilter's computation of *SDR*. If a watershed has large soil erosion from field source while its field sediment contribution at the watershed outlet is small, the corresponding sediment delivery ratio

across the watershed will be small. If the same watershed has smaller soil erosion from field source while its field sediment loading at the watershed outlet remains the same, then the sediment delivery ratio across the watershed will be larger. In both cases, though the overall *SDR* value across the watershed is affected by sediment production and loading, the spatial distribution of sediment delivery will remain consistent where larger *SDR* will be populated in the areas with small flow length and steep gradient.

Topofilter and evaluation of spatial distribution of sediment delivery ratio depend on soil erosion, watershed sediment loading, and topography. High-resolution DEM is widely available with the advent of advanced monitoring tools and remote sensing technology (Osmanoğlu et al., 2014). While soil property data and erosion estimates are not as abundant in other parts of the world as in the U.S., there are methods to estimate soil erosion using geologic information (e.g., Amore et al., 2004; Fistikoglu, 2002; Munro et al., 2008). At the same time, stream gages are becoming more extensive, reliable, and cost-effective (Wahl et al., 1995). Even if stream gage data on sediment loading is not readily available, Topofilter may be applied using reasonable estimates based on watershed's geophysical characteristics (e.g., reservoir deposition and sediment fingerprinting).

3.6. Conclusion

This chapter presents a reduced-complexity framework to quantify the effect of topography on watershed-scale sediment delivery from agricultural field erosion. In a large watershed with sparse information about the drivers and mechanisms of sediment transport and storage, it is unlikely that any watershed simulation can provide a well-defined single model for sediment delivery. Topofilter does not aim to provide such an

answer, but instead combines spatially-rich information on soil erosion rates and topography with measured sediment load at the watershed outlet to provide an estimate of the magnitude and spatial distribution of sediment sources. The approach is based on the sediment delivery ratio, which is the fraction of eroded sediment that is delivered from the watershed. Sediment delivery ratio depends on the distance and slope of the pathway between each sediment source and the watershed outlet. The approach does not attempt to find a single best calibrated distribution of sediment delivery ratio, but instead uses a model conditioning approach to narrow the parameter range of the topographic model. Some of the estimates are likely to be poor, but the entire group is centered on the observed sediment load at the outlet. Because the underlying model is quite simple and anchored by reliable information on topography and relative soil erosion, we believe that the ensemble of simulations provides a reasonable representation of the possible sediment sources in the watershed.

The approach is particularly useful for identifying dominant sediment source areas. Even though there is not a single best model, if the same locations are found to contribute to most of the sediment load over a large number of model runs, that location is likely to be a dominant sediment source. The range of model solutions also allows for a stochastic representation of sediment supply that captures variability due to the uncertainty in sediment storage and transport throughout the watershed.

Appendix 3.A: Observed data distribution test

Natural log of TSS values in Table 3.2 is put to statistical test to determine the distributions. According Shapiro-Wilk test, we can't reject normal distribution of Natural log (LN) of TSS values (x).

Upper Maple (UM):

Summary statistics:

Variable	Observation	with missing	ithout missi	Minimum	Maximum	Mean	td. deviation
Ln(X_UM)	11	0	11	7.804	10.213	9.092	0.806

Shapiro-Wilk test (Ln(X_UM)):

W	0.940
p-value	0.526
alpha	0.05

Test interpretation:
H0: The variable from which the sample was extracted follows a Normal distribution.
Ha: The variable from which the sample was extracted does not follow a Normal distribution.
As the computed p-value is greater than the significance level alpha=0.05, one cannot reject the null hypothesis H0.
The risk to reject the null hypothesis H0 while it is true is 52.63%.

Little Cobb (LC):

Summary statistics:

Variable	Observation	with missing	ithout missi	Minimum	Maximum	Mean	td. deviation
Ln(X_LC)	11	0	11	7.157	9.066	8.362	0.560

Shapiro-Wilk test (Ln(X_LC)):

W	0.919
p-value	0.311
alpha	0.05

Test interpretation:
H0: The variable from which the sample was extracted follows a Normal distribution.
Ha: The variable from which the sample was extracted does not follow a Normal distribution.
As the computed p-value is greater than the significance level alpha=0.05, one cannot reject the null hypothesis H0.
The risk to reject the null hypothesis H0 while it is true is 31.09%.

Appendix 3.B: Determining the initial parameter space for Monte Carlo simulation 1 (MC1)

In Section 3.3.2, we determined that the parameters of *SDR* formulations in [3.3] and [3.4] are less than zero ($a1$, b_1, a_2, $b_2 < 0$) assuming that $SDR<1$, indicating that sediment loading of the watershed is no more than gross soil erosion; *SDR* increases with elevation change, indicating that steeper the slope more sediment travels; and *SDR* decreases with flow length, indicating that the longer the travel distance more likely for sediment to be trapped along its path. However, we have not established the lower bound based on these basic assumptions concerning the physics of sediment transport.

In this appendix, we demonstrate evaluation of general parameter space given constant topographic attributes (i.e., calculation of *SDR* at one raster location using [3.3] and [3.4]) for a range of *SDR* values. At the Little Cobb, the average field flow length (L_f) is about 1,500 meters and the average field elevation change (ΔE_f) is about 16 meters from field to stream over all raster cells (Figure 3.16); and the average stream flow length (L_s) is about 30,000 meters and the average stream elevation change (ΔE_s) is about 27 meters in stream to the watershed outlet over all raster cells (Figure 3.17).

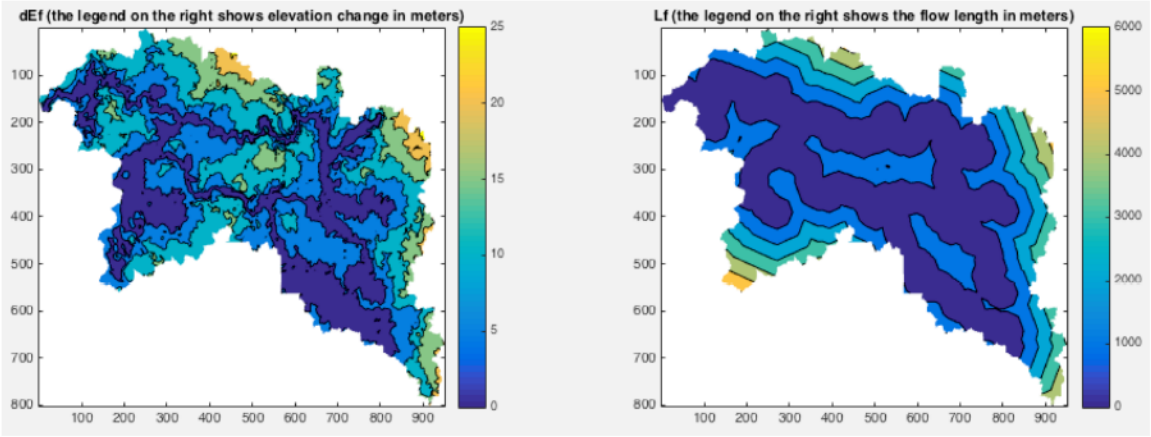

Figure 3.16: Elevation change (left) and flow length (right) from field cells to adjacent stream in meters

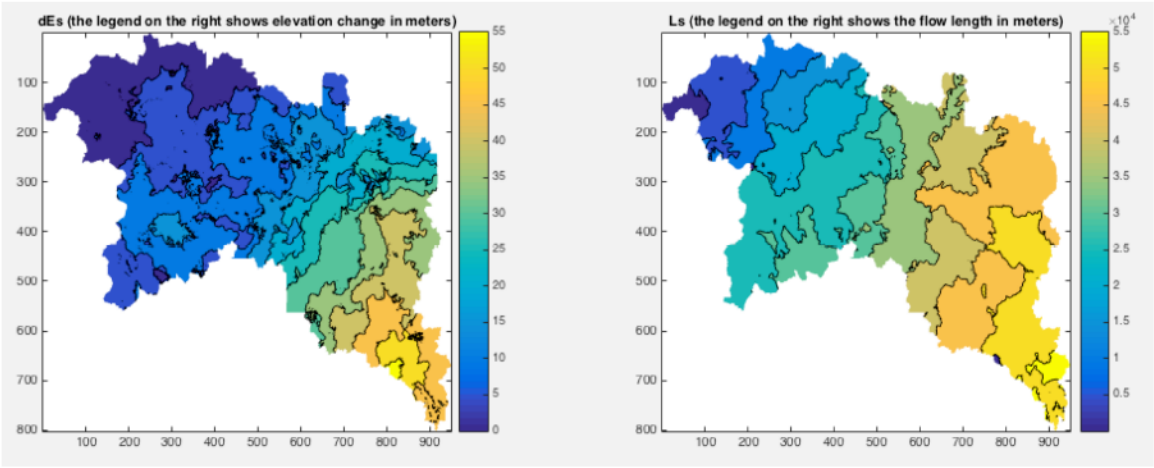

Figure 3.17: Elevation change (left) and flow length (right) in stream to the watershed outlet

We use the average topographic attribute values ($L_f = 1{,}500m, \Delta E_f = 16m, L_s = 30{,}000m$, and $\Delta E_{s=27m}$) and a range of *SDR* values (0.1, 0.2, 0.4, and 0.6) to back-calculate the parameter values a_1 and a_2 for a range of b_1 and b_2 values from -1 to 0 (Figure 3.18).[7] For a range of *SDR* values, parameter values a_1 and a_2 range between -1E-3 and 0. Both a_1 and a_2 spaces become narrow with larger *SDR* values. In the MC1 simulation, we want to allow a wide range of parameter values and consider correspondingly calculated *SDR* values. Thus, we determined based this analysis that the initial parameter space for a_1 and a_2 for MC1 simulation should be about (-1E-3,0) given the parameter space for b_1 and b_2 set at (-1,0).

a) *SDR* =0.1

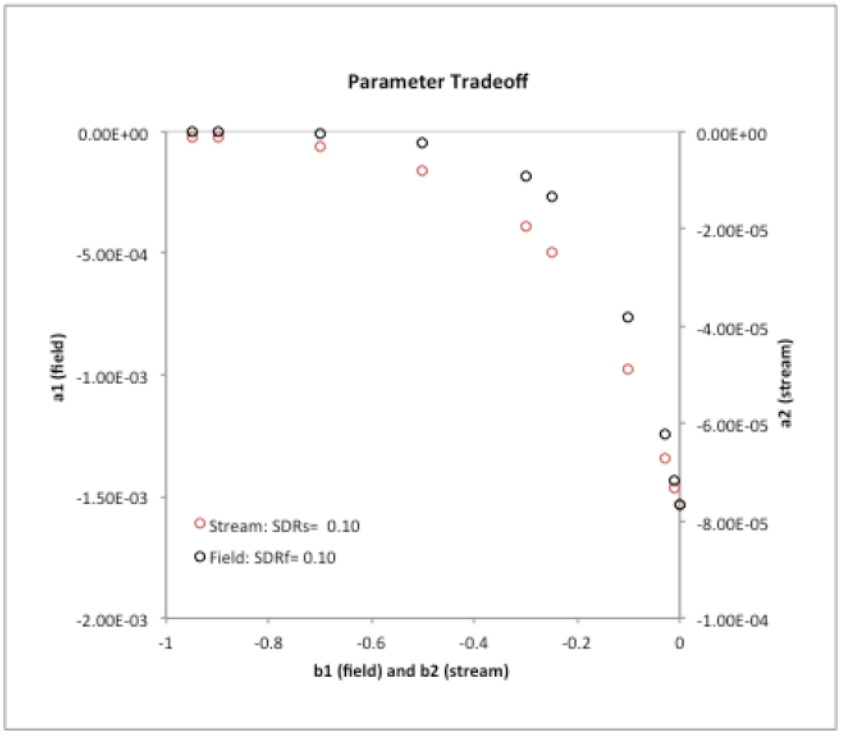

Figure 3.18: Parameter spaces given constant topographic attributes and a) *SDR*=0.1; continued next page

[7] To calculate a_1 and a_2 given a constant *SDR* values and average topographic attributes values ($L_f, \Delta E_f, L_s$, and ΔE_s) for a range of parameter values b_1 and b_2: $a_1 = \frac{Ln(SDR_{f_i})}{\left(\frac{\Delta E_{f_i}}{L_{f_i}}\right)^{b_1} L_{f_i}}$ and $a_2 = \frac{Ln(SDR_{s_i})}{\left(\frac{\Delta E_{s_i}}{L_{s_i}}\right)^{b_2} L_{s_i}}$

b) *SDR*=0.2

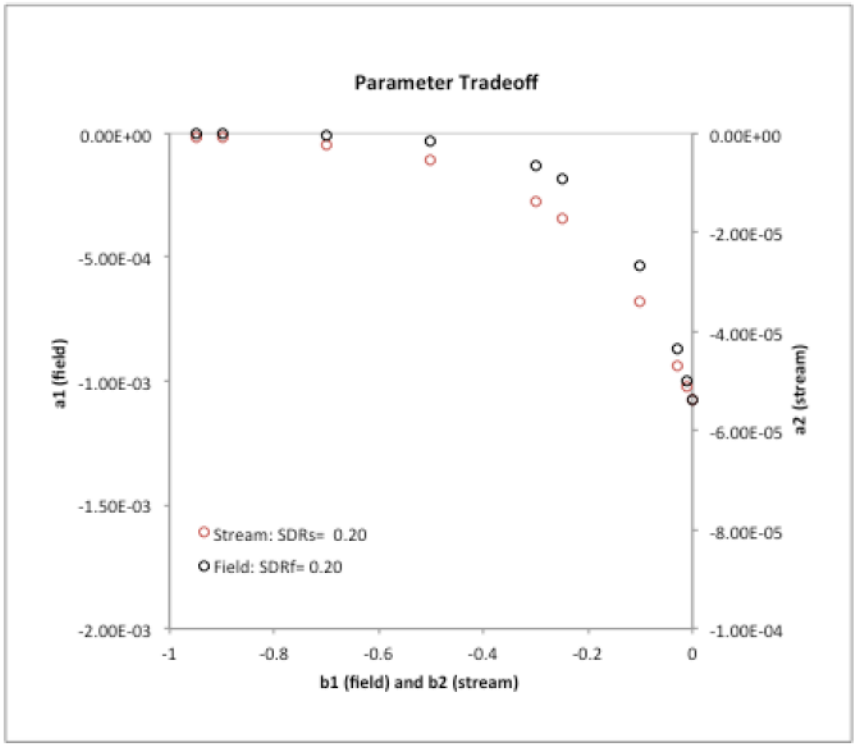

c) *SDR*=0.4

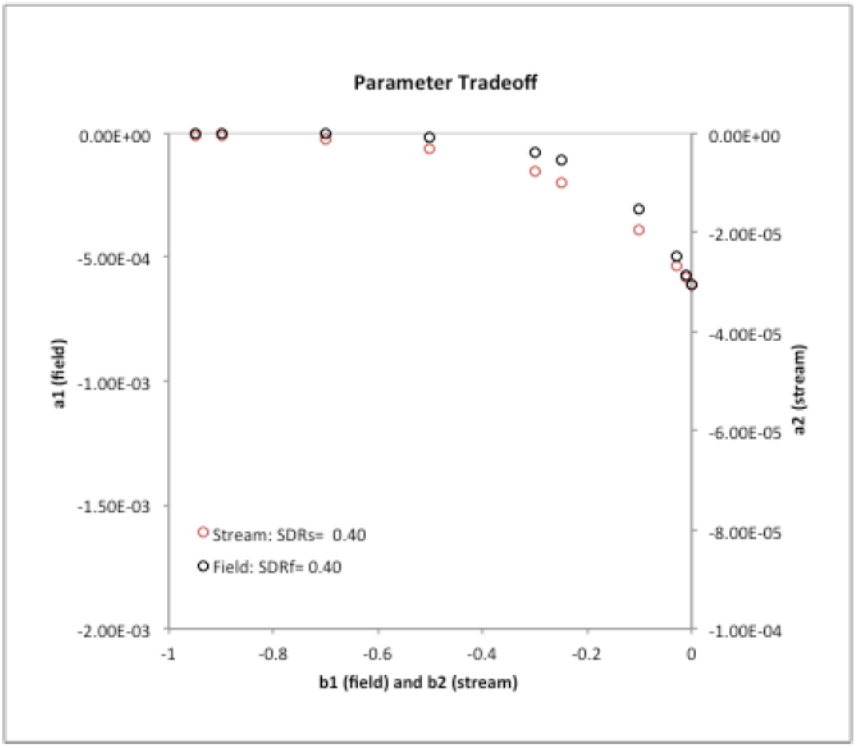

Figure 3.18: Parameter spaces given constant topographic attributes and b) *SDR*=0.2 and c) *SDR*=0.4;
continued next page

d) *SDR*=0.6

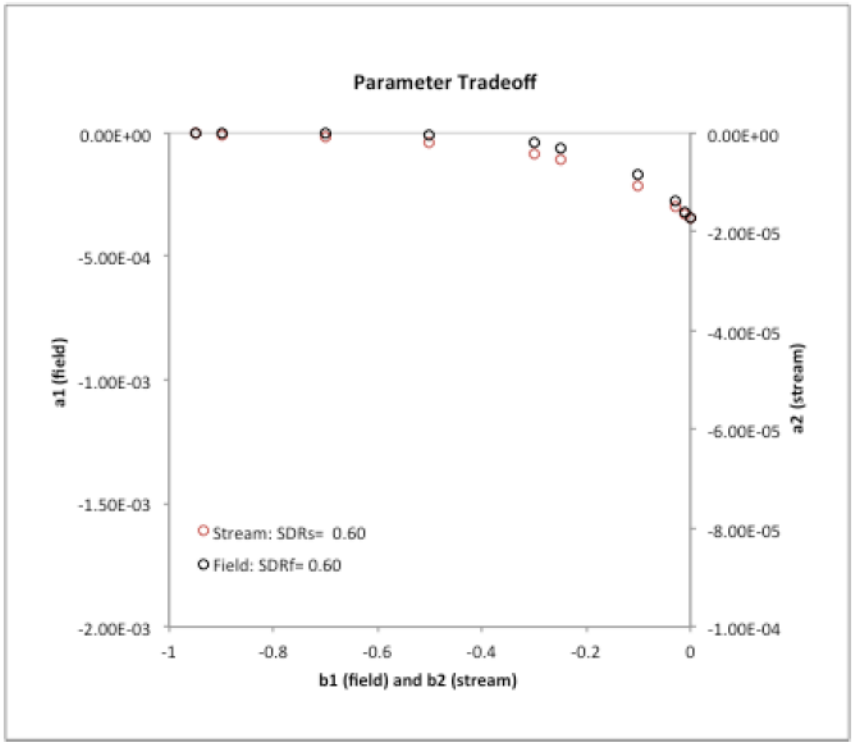

Figure 3.18: Parameter spaces given constant topographic attributes d) *SDR*=0.6;

4. Topofilter Implementation for All Sediment Sources

4.1. Introduction

Topofilter approach developed in Chapter 3 connects distributed upland sources of soil erosion to sediment load at the watershed outlet, accounting for topographic influences on sediment storage, delivery, and loading. In this chapter, we expand the structure of Topofilter to incorporate other sources of sediment found close to or along the stream channel network. These near channel sources (NCS: ravines, streambanks, and bluffs) are currently the largest fraction of the sediment budget for the Le Sueur River Basin (LSRB) (Gran et al., 2011), although this was not the case in earlier periods and may not be the case in other watersheds.

The application of Topofilter to upland field erosion in Chapter 3 used only that fraction of sediment load that is attributed to field erosion and has the advantage that it can be used to target field locations that contribute the most soil erosion to the watershed delivery. The context for this chapter is the entire sediment load with the goal of determining sediment delivery ratios (*SDR*) for all sediment sources. This broader view introduces additional considerations of sediment routing and the use of multiple stream gages, and provides a spatial distribution of *SDR* for all sediment sources throughout the watershed.

Topofilter uses the model conditioning approach, rather than calibration (Beven, 2001), to define a parameter space that yields a plausible distribution of simulated sediment loading as described in Chapter 3. The outputs of this analysis, distributions of *SDR* for all field and NCS support the sediment delivery and loading module in the watershed simulation model in Chapter 6.

In section 4.2, we list existing watershed models that account for pollution from field and near-channel sources. In Section 4.3, we describe study site delineation and spatial scale, input data including gage observation of watershed sediment loading and the watershed sediment budget used to allocate near-channel sediment supply (NCSS), and Topofilter formulation. In Section 4.4, we evaluate the Topofilter simulation outputs of field and stream *SDR* for field and near-channel sources.

4.2. Approaches for estimating sediment delivery from multiple sources

Understanding the sediment delivery process at the watershed-scale should entail consideration of all major sediment sources (de Vente and Poesen, 2005). The papers reviewed in chapter 3 on spatially-lumped and -distributed sediment delivery models using various watershed characteristics only consider sediment loading from agricultural fields (Fernandez et al., 2003; Ferro, 1995; Fistikoglu, 2002). In fact, very few studies include non-field sources such as gully and channel erosion, and spatial variability of sediment delivery and deposition processes (de Vente et al., 2008).

Those models that consider sediment transport from various sources often do not account for the spatial patterns of sediment delivery or have very high data requirements (de Vente and Poesen, 2005; Merritt et al., 2003). For example, the Chemical Runoff and Erosion from Agricultural Management Systems model (CREAMS) predicts erosion, deposition, and transport of sediment from field sources as well as from gullies, but the model is only appropriate for a field sized catchment with uniform soil topography and land use. The Environmental Management Support System (EMSS) is a reduced-complexity runoff model that predicts pollutant loading within channel network as a function of runoff volume and also operates at the scale of individual sub-catchments

(Merritt et al., 2003). The Agricultural Non-Point Source model (AGNPS) predicts runoff and pollutant transport using a grid cell representation of the catchment. The model estimates field soil erosion using the Universal Soil Loss Equation (USLE) and includes routines for gully erosion, sediment routing, and deposition. The model also requires specification of parameters describing catchment morphology, landuse, and climatic conditions for each grid cell. The Areal Non-point Source Watershed Environment Response Simulation (ANSWERS) is another gridded sediment transport simulation model, but differs from AGNPS in its representation of the erosion process with more physically-based relations. Both of these models have limited applicability due to large spatial and temporal input data requirements (de Vente and Poesen, 2005; Merritt et al., 2003).

4.3. Methods

In contrast to these models with high data requirements, Topofilter approach utilizes high-resolution topography in a reduced complexity model structure to evaluate the effect of topography on sediment delivery. Topofilter does not predict the rate of field soil erosion and near channel sediment supply (NCSS), but uses independent estimates of sediment supply as model input. The purpose of Topofilter is to link these sources with sediment loads at the watershed outlet, thereby extracting the effect of topography on the fraction of sediment supply that is delivered from the watershed.

In this chapter, Topofilter is applied to all sediment sources (field, ravines, streambanks, and bluffs) in the LSRB to estimate plausible sediment delivery values for field and NCS. Figure 4.1 provides a schematic of the essential elements of Topofilter and the manner in which field and NCS are treated. Top left of Figure 4.1 illustrates the

compilation of high-resolution topography, distributed information about soil loss across the watershed, and integrated information about sediment loading from Total Suspended Solid (TSS) data as demonstrated in Chapter 3. In addition to these data, we include a watershed sediment budget to quantify NCSS. Using these data, sediment delivery ratio (*SDR*) and sediment loading (*SL*) are calculated, and the corresponding model parameters are conditioned to identify plausible parameter space as exhibited in Chapter 3. Bottom left of Figure 4.1 shows the study watershed, Le Sueur River Basin (LSRB). Topofilter application in the LSRB is semi-distributed: soil loss and transport from agricultural field to the river network are evaluated on a 30-m raster grid. In contrast, sediment transport through the river network is lumped at the subbasin scale (each of these modeling units is referred to as a "sediment-subbasin (SEDSB)"). We use the LSRB sediment budget (Gran et al., 2011) to specify NCSS at the scale of each SEDSB because the budget quantifies some near-channel contributions based on channel length within each SEDSB. Top right of Figure 4.1 illustrates the Topofilter outputs of probability density function (PDF) of field *SDR* for SEDSBs. Bottom right shows the formulation of stream *SDR* where parameter combinations from conditioned space are used to estimate its quantity.

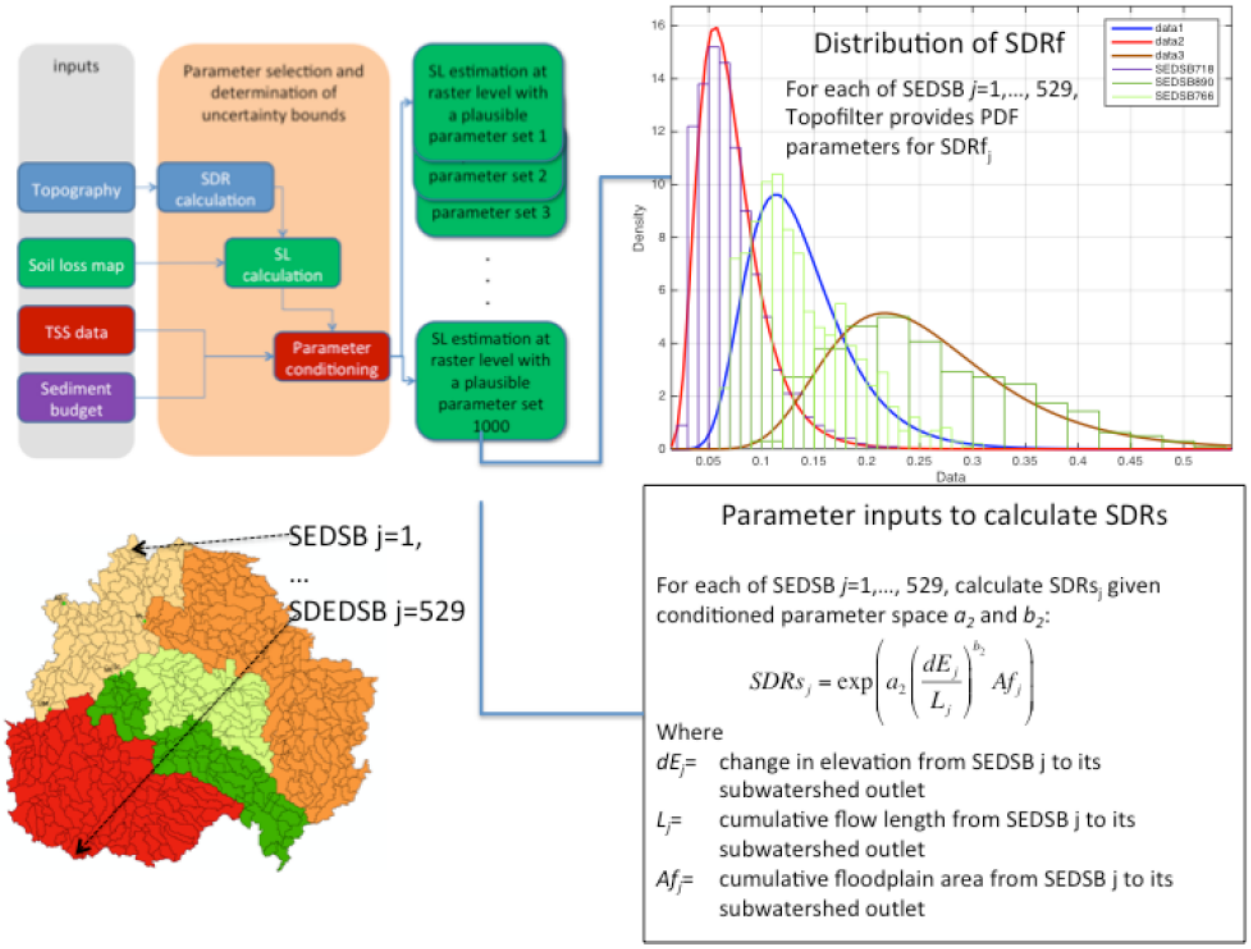

Figure 4.1: Schematic to illustrate utilization of Topofilter method (top left figure) scaled up to LSRB with five Toposheds, consisting of 529 sediment subbasin (SEDSB) units (bottom left figure). The model outputs consists of distribution of SDRf (top right) and SDRs parameter space (bottom right) at each SEDSB

4.3.1. Study site delineation and spatial scale definition

The LSRB can be divided into two major geophysical regions: a flat upland region and an incised region near the watershed outlet. Sediment delivery processes differ significantly between the regions, as described in Chapter 2. Stream gages on the major tributaries of the watershed are used to estimate mean annual sediment loading. These gages are also used to demarcate the LSRB into five Topofilter subwatersheds (Toposheds). The upland Toposheds consists of the Upper Maple (UM), Main Cobb (MC), Little Cobb (LC), and Upper Le Sueur (UL) as defined by the upper gages. The incised Toposhed is defined between the upper gages and the gage at the LSRB outlet (LO). LO Toposhed includes the drainage areas of the incised portions of the rivers (Le Sueur, Cobb, and Maple rivers), and of the Le Sueur River after the confluence with the Cobb and Maple Rivers just above the watershed outlet (Figure 4.2).

Individual Topofilter models are set up for each of the five Toposheds using topographic variables obtained from the 30-m DEM[1] and the National Hydrography Dataset (NHD). [1] Each Toposhed consists of multiple SEDSBs (smaller polygons within each Toposhed in Figure 4.2; there are 529 SEDSBs over the entire LSRB) with corresponding reach segments.

4.3.2. Input gage data

Existing gages located above the incised zone (upper gages) at the outlets of the UM, LC, and UL provide annual sediment loading rates from 2006 to 2010 (Minnesota State University, Mankato Water Resources Center, 2012). There are also gages located within the incised zone (lower gages) on the Lower Maple (LM), Big Cobb (BC), and Lower Le Sueur (LL), as well as at the watershed outlet (LO) (Figure 4.2). An existing gage on the

[1] USGS The National Map Viewer, http://viewer.nationalmap.gov/viewer/

Little Cobb River just before the confluence with the Cobb River defines the Toposhed LC above the incised zone. Another downstream gage, BC, defines the Big Cobb watershed including the LC and incised areas draining to the Cobb River. There is no gage defining the Toposhed MC, which is located at the confluence with the LC in order to define the area above the incised zone draining to the main Cobb River (see the virtual gage MC in Figure 4.2). To estimate the annual sediment loading at this virtual gage MC, we applied the average sediment load per unit area for UM and LC because MC is located between these Toposheds (Figure 4.2):

$$\frac{SL_{MC}^{t}}{A_{MC}} = avg\left(\frac{SL_{UM}^{t}}{A_{UM}}, \frac{SL_{LC}^{t}}{A_{LC}}\right)\left[\frac{Mg}{\square r \cdot m^2}\right];\ \forall\, t = 2006, \ldots, 2010 \qquad [4.1]$$

The UL gage record is missing sediment loading measurement from 2006. This record was estimated based on a regression between LL and UL mean annual sediment loading. Consequently, we used the average sediment loading rates from 2006-2010 to condition the Topofilter parameters space as described in Chapter 3 (Table 4.1).

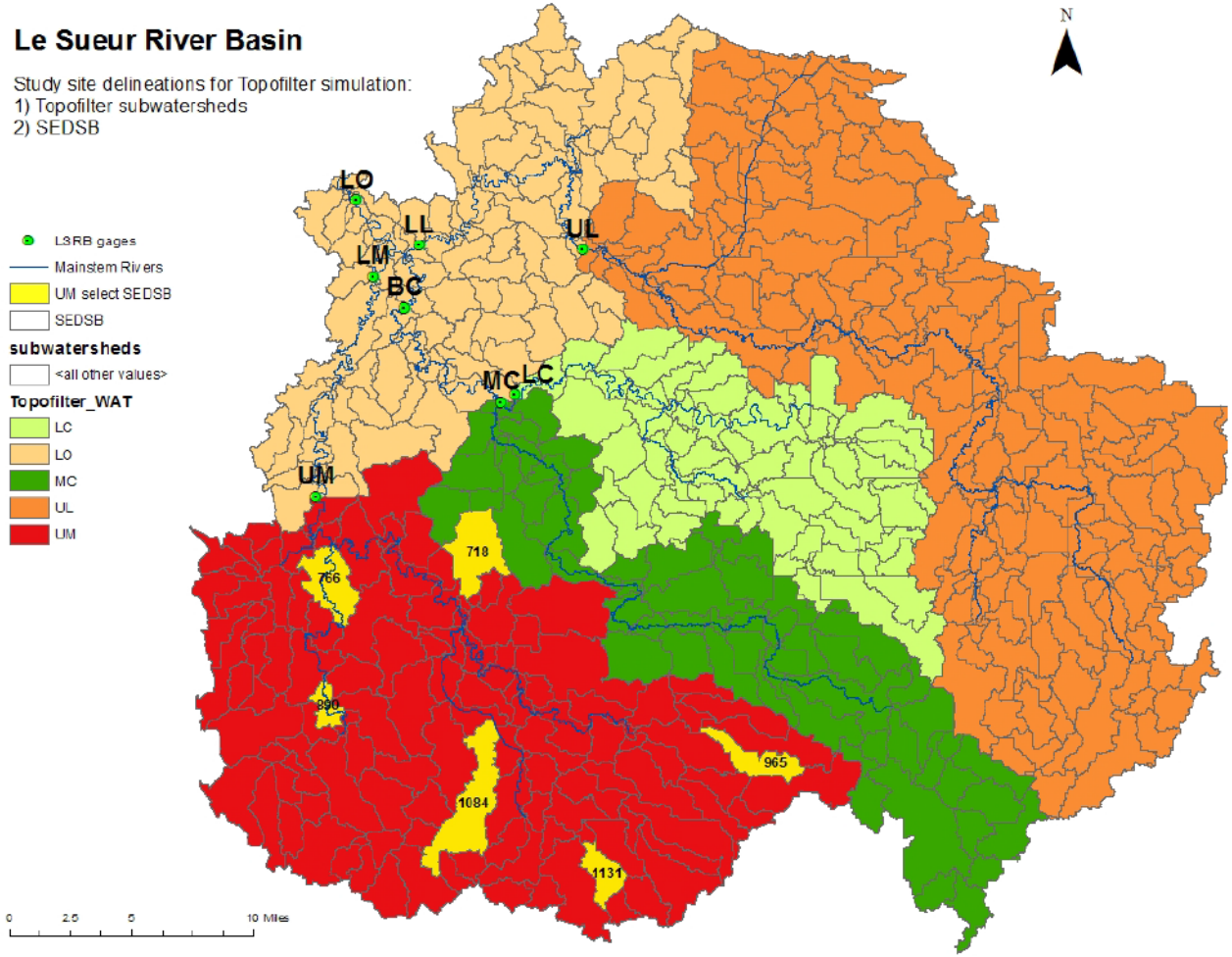

Figure 4.2: LSRB study site delineation for Topofilter simulation including five Toposheds defined by the five gage locations and SEDSBs defined by reach extent. Gages consists of upper gages at Upper Maple (UM), Main Cobb (MC), Little Cobb (LC), and Upper Le Sueur (UL), lower gages at Lower Maple (LM), Big Cobb (BC), and Lower Le Sueur (LL), and gage at the outlet of Le Sueur (LO). This figure also shows the SEDSBs in the UM selected in Section 4.3 to provide illustrative model results.

Table 4.1: Gage data showing annual sediment loading for the Toposheds (estimated values shown in grey cells)[2].

Gaging data from Minnesota Pollution Control Agency									
Basin		**Upper Maple (UM)**	**Lower Maple (LM)**	**Main Cobb (MC)**	**Little Cobb (LC)**	**Big Cobb (BC)**	**Upper Le Sueur (UL)**	**Lower Le Sueur (LL)**	**Le Sueur Outlet (LO)**
Contributing drainage area (km2)	**year**	**800**	**880**	**384**	**335**	**735**	**870**	**1210**	**2880**
Sediment Load (Mg/yr)	2000				8,532				477,888
	2001				8,020				346,506
	2002				4,833				90,246
	2003		18,607		4,385				71,132
	2004		101,243		7,479				337,976
	2005		85,099		8,187				219,315
	2006	7,875	22,326	4,163	3,965	33,390	36,000	86,558	135,362
	2007	13,285	37,909	5,718	4,414	21,829	38,098	74,662	184,874
	2008	6,060	22,326	3,209	3,061	14,632	20,705	42,786	88,495
	2009	3,452	4,916	1,725	1,564	6,312	4,289	13,404	36,381
	2010	19,755	185,875	10,961	10,853	47,137	44,751	127,762	539,208
Average (2006-2010)		10,085	54,670	5,155	4,771	24,660	28,769	69,034	196,864
STD (2006-2010)		5,811	66,428	3,180	3,193	14,330	14,554	38,914	178,115
median (2006-2010)		7,875	22,326	4,163	3,965	21,829	36,000	74,662	135,362

[2] Water quality data are obtained from Minnesota State University, Water Resources Center (2012), and also available at: https://public.tableau.com/profile/publish/WatershedPollutantLoadMonitoringNetworkWPLMNDataViewer/WPLMNBrowser#!/publish-confirm

4.3.3. Sediment input allocation

Total sediment loading from each Toposhed is calculated as the sum of all sediment inputs from SEDSBs within the Toposhed, discounted by the sediment delivery ratio to account for on-field and along-stream sediment storage. For each SEDSB, soil erosion rates from field sources are the same USLE estimates used in Chapter 3. Delivery of field sediment to the stream is the discounted soil erosion rate using the field sediment delivery ratio. The near channel sediment inputs are allocated to mapped reaches of the corresponding SEDSBs using the LSRB sediment budget results.

Field source sediment input

Mean annual sediment input rates from field sources (SI_F) are calculated by summing over the mean annual soil erosion rates discounted by the simulated field sediment delivery ratio (*SDRf*) for all field raster cells from each individual SEDSB. *SDRf* of a field raster cell *i* in SEDSB *j* $\left(SDRf_{ij}\right)$ is calculated based on the field raster cell *i*'s distance $(L_{f_{ij}})$ and gradient $\left(\left(\frac{\Delta E_f}{L}\right)_{ij}\right)$ to the nearest stream cell:

$$SDRf_{ij} = \exp\left(a_1 \left(\frac{\Delta E_f}{L}\right)_{ij}^{b_1} L_{f_{ij}}\right) \qquad [4.2]$$

The *SDRf* parameters (a_1 and b_1), along with the parameters for *SDRs*, are conditioned against the observed data at the outlets of the individual Toposheds (Table 4.1). In Chapter 3, we used the parameter set conditioned for a watershed (the Little Cobb) with similar topography and landuse to evaluate an adjacent watershed (the Upper Maple). The objective here is to provide reliable sediment delivery values for the entire LSRB for application in a sediment routing platform within the watershed simulation model (Chapter 6); thus, we conditioned the parameter space for individual Toposheds to

predict the sediment loading that is closest to the observed sediment loading at the corresponding stream gages instead of conditioning a common parameter space. The model conditioning process through Monte Carlo (MC) simulation is described in detail in Chapter 3.

We calculate the total SI_F of a SEDSB j (SI_{Fj} $\left[\frac{Mg}{yr}\right]$) by summing over the soil erosion rates at field raster cell i (SE_{ij}) multiplied by the simulated $SDRf_{ij}$ over all i=1,…,I_j field raster cells in SEDSB j [4.3]. SI_{Fj} indicates sediment delivered from field to stream network in SEDSB j. Then, we calculate the average *SDRf* over all field cells in SEDSB j ($SDRf_j$) by dividing the sediment delivered to the stream by the gross erosion over the SEDSB [4.4]:

$$SI_{F_j} = \sum_{i=1}^{I_j} SDRf_{ij} * SE_{ij} \quad \forall j \qquad [4.3]$$

$$SDRf_j = \frac{SI_{F_j}}{\sum_{i=1}^{I_j} SE_{ij}} \quad \forall j \qquad [4.4]$$

$SDRf_j$ calculated for all MC outputs over the conditioned parameter space are used to develop probability density functions at each SEDSB (Figure 4.1) (Section 4.4.1).

Stream source sediment input

Streams sources contribute sediment through a) channel widening, b) stream meander migration, and c) channel incision processes. The LSRB sediment budget quantifies the loading through these processes for fifth order streams and larger, with a minimum upstream contributing area of 100 km^2 ("mainstem reaches" indicated by blue and green reach segments in Figure 4.3(a)) (Gran et al., 2011). Equivalent mainstem reaches for this analysis are delineated using flow accumulation value at each stream cell, representing

the number of upstream contributing raster cells. Minimum flow accumulation values are set for the Le Sueur (LES), Cobb (COB), and Maple (MAP) River raster cells to identify SEDSBs with mainstem reaches to allocate sediment inputs from stream source (Figure 4.3(b)).

(a)

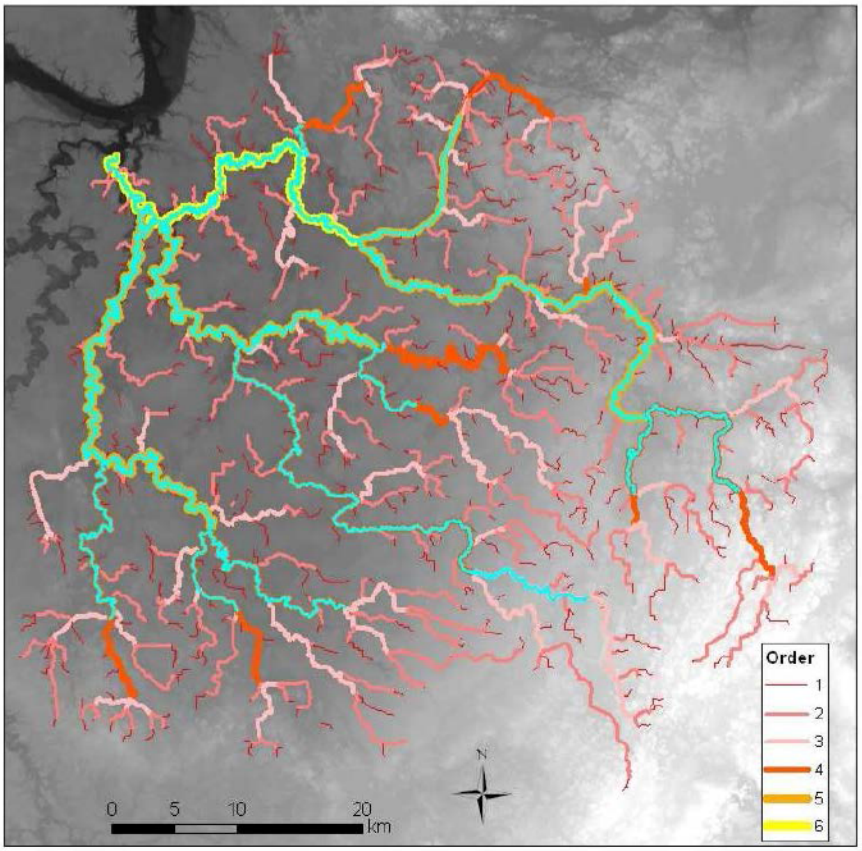

Figure 4.3 (a): Stream order delineation is used in the sediment budget to identify mainstem reaches shown in green lines (figure from Belmont et al., 2011);

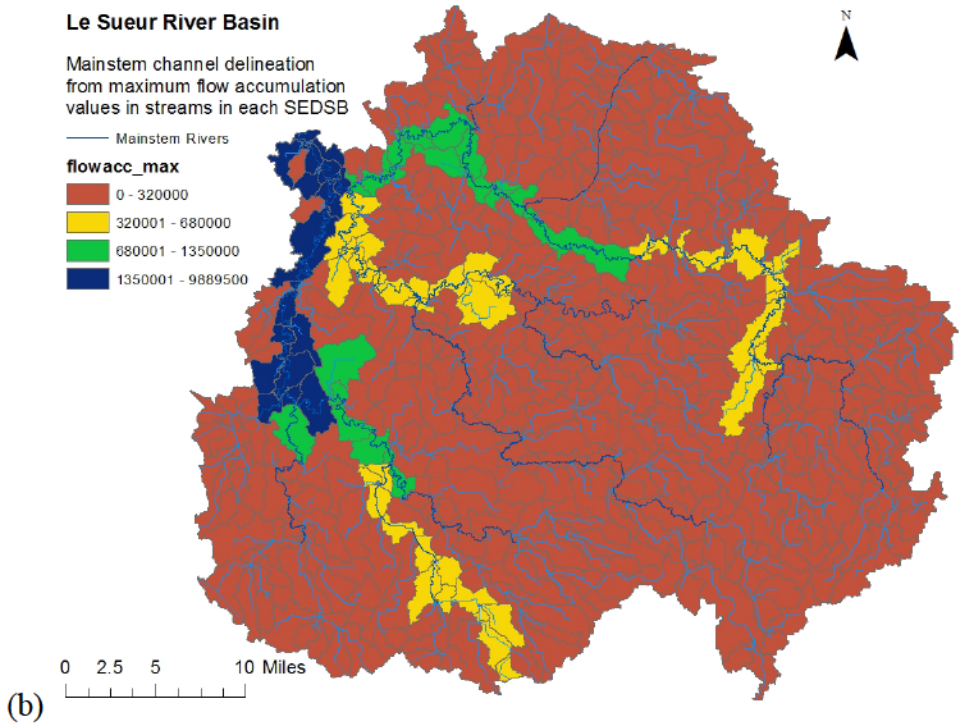

(b)

Figure 4.3 (b): SEDSBs with mainstem reaches (highlighted in blue for MAP, yellow for COB, and green for LES) are identified using the flow accumulation values along streams

a) Channel widening

The sediment budget evaluates channel widening using short-term measurements from ground-based LiDAR and long-term measurements from aerial photograph analysis for the time period between 1937 and 2009 (Gran et al., 2011). The channel widening rates [%/year] are averaged over three geomorphic regions: above upper gages (AB), between upper and lower gages (BT), and below lower gages (BL) for the mainstem reaches. AB indicates the drainage area above the upper stream gages (UM, MC, LC, and UL in Figure 4.2), BT between upper and lower gages (LM, BC, and LL in Figure 4.2), and BL below the lower gages and above the watershed outlet (LO in Figure 4.2) Channel widening rates over different geomorphic regions are applied to SEDSBs by their location. The volumetric loss of sediment from mainstem reaches [m^3/yr] from channel widening is calculated with the representative channel cross-section areas for

channel widening is calculated with the representative channel cross-section areas for different rivers and geomorphic regions according to the sediment budget. The sediment-loading rate in mass [Mg/yr] is calculated from volumetric loss [m^3/yr] using a bulk density of mud at 1.3 Mg/m^3.

b) Stream meander migration

The sediment budget quantifies net streambank sediment loading from channel meander migration (i.e., stream bank load from erosion minus floodplain storage from aggradation) using aerial photographs taken in 1938 and in 2005, and by interpolating the channel geometry along the direction and distance of lateral migration at a 10m interval (Gran et al., 2011). Again, the migration rates [Mg/year-meter] are defined for three geomorphic regions, AB, BT, and BL for the mainstem reaches along MAP, COB, and LES Rivers. Sediment loading from stream meander migration is calculated by multiplying the appropriate rates [Mg/year-meter] to the mainstem reach length at each SEDSB.

c) Channel incision

Channel incision occurs in the geomorphic regions BT and BL within the incised portion of the watershed. The sediment budget estimates sediment loading from channel incision using a vertical incision rate of 1.2 mm/yr along the mainstem reaches with an average channel width of 25m (Gran et al., 2011). The volumetric loss of sediment from mainstem reaches [m^3/yr] from channel incision is converted to mass [Mg/yr] using the bulk density of mud.

Finally, the net mean annual sediment input rates (SI_S [Mg/yr]) from stream due to a) channel widening, b) stream meander migration, and c) channel incision are allocated and summed over the SEDSBs containing mainstem reaches over all Toposheds (Figure 4.4).

Ravines

The sediment budget estimates mean annual ravine sediment erosion rates for each ravine use changes on aerial photography over a 67-year time period and direct monitoring of sediment output for two ravines in 2008 and four ravines in 2009 and 2010. Annual ravine erosion rate is expressed per unit area of ravines (0.0022 Mg/m^2-yr) (Gran et al., 2011). To quantify ravine loading, we used a ravine map developed from LiDAR data to calculate the total ravine area in each SEDSB. The ravine erosion rate from the sediment budget was then applied to the total ravine area in each SEDSB j to determine the mean annual sediment input rate from ravines (SI_{Rj}) (Figure 4.5 shows the ravines in red polygons and their sediment input rates along the reaches of SEDSBs).

Bluffs

Bluffs in the watershed were mapped from 3m DEM and bluff retreat rate was determined from aerial photographs in 1938 and 2005 (Gran et al., 2011). Mean annual sediment input rate from bluffs (SI_{Bj}) was calculated by summing the sediment contribution from the bluffs found in each SEDSB j (Figure 4.6 shows the bluff in red polygons and input rates along the reaches of the SEDSBs).

Combined Sediment Sources

Sediment input in each SEDSB j is the sum of the mean annual sediment input rates from field (SI_{F_j}), streambanks (SI_{S_j}), ravines (SI_{R_j}), and bluffs (SI_{B_j}) [4.5]. Sediment loading contributed from each SEDSB j is the sediment inputs from all sources (SI_j) reduced by the stream sediment delivery ratio ($SDRs_j$). The total sediment loading from a Toposhed T (SL_T) is the sum of sediment loading from all SEDSBs [4.6]:

$$SI_j = SI_{F_j} + SI_{S_j} + SI_{R_j} + SI_{F_j} \qquad [4.5]$$

$$SL_T = \sum_{j=1}^{N_T} SL_j = \sum_{j=1}^{N_T} SI_j * SDRs_j \qquad [4.6]$$

Where N_T indicates the number of SEDSBs in Toposhed T.

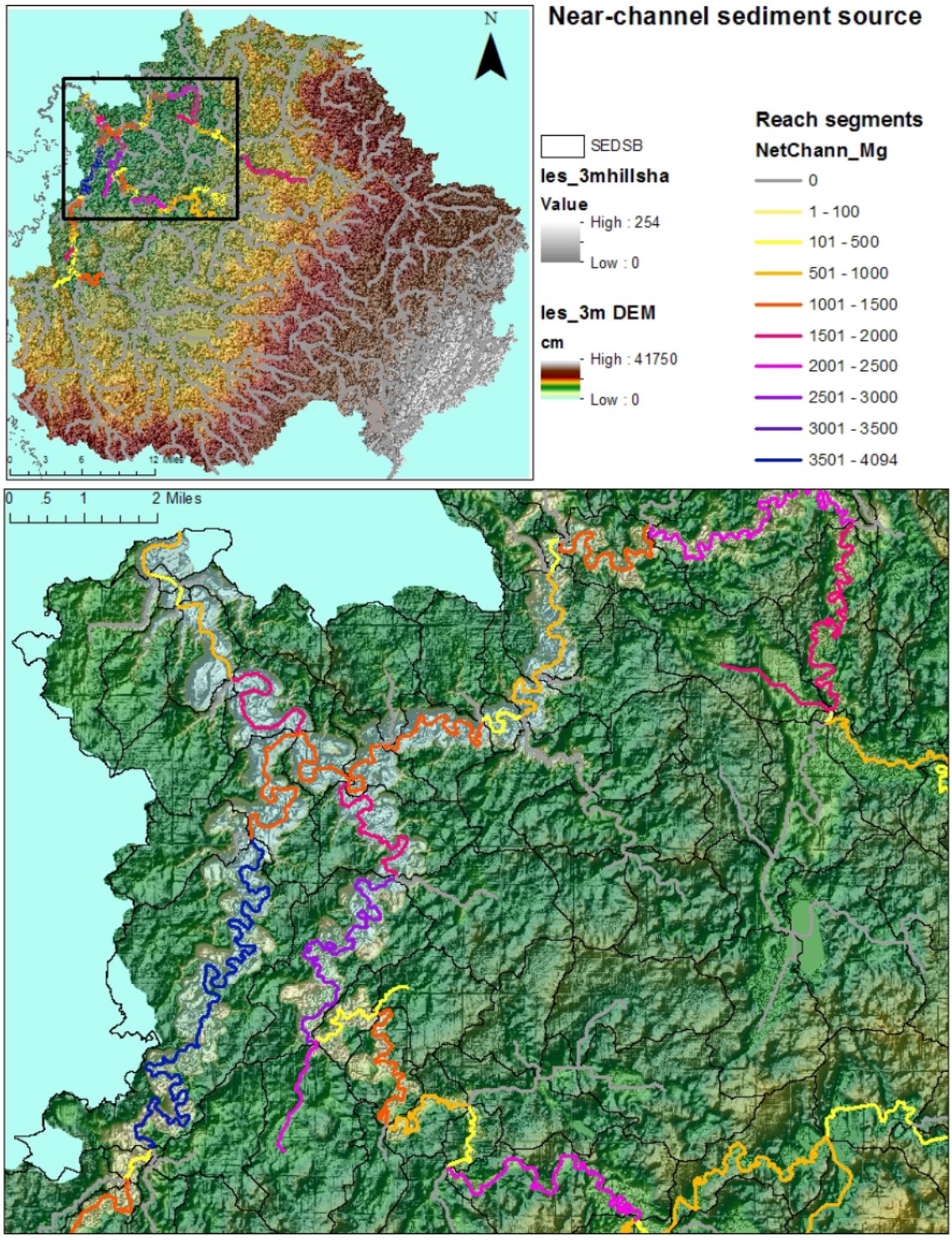

Figure 4.4: Total sediment loading from a) channel widening, b) meander migration, and c) incision calculated over the SEDSB streams qualified as mainstem channels

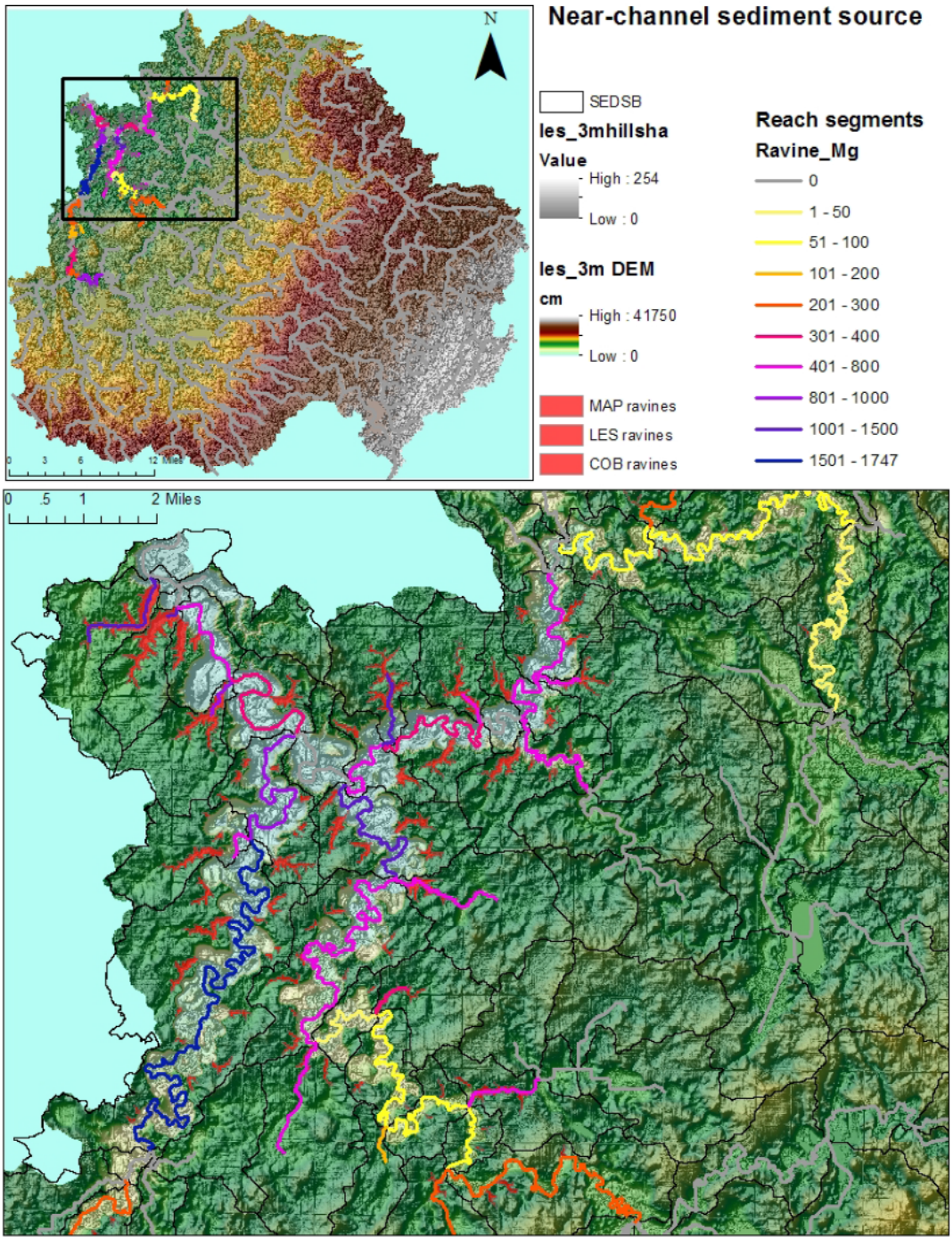

Figure 4.5: Ravines along MAP, COB, and LES are shown in red polygons and annual sediment input rate from ravines calculated over the SEDSB are shown in polylines.

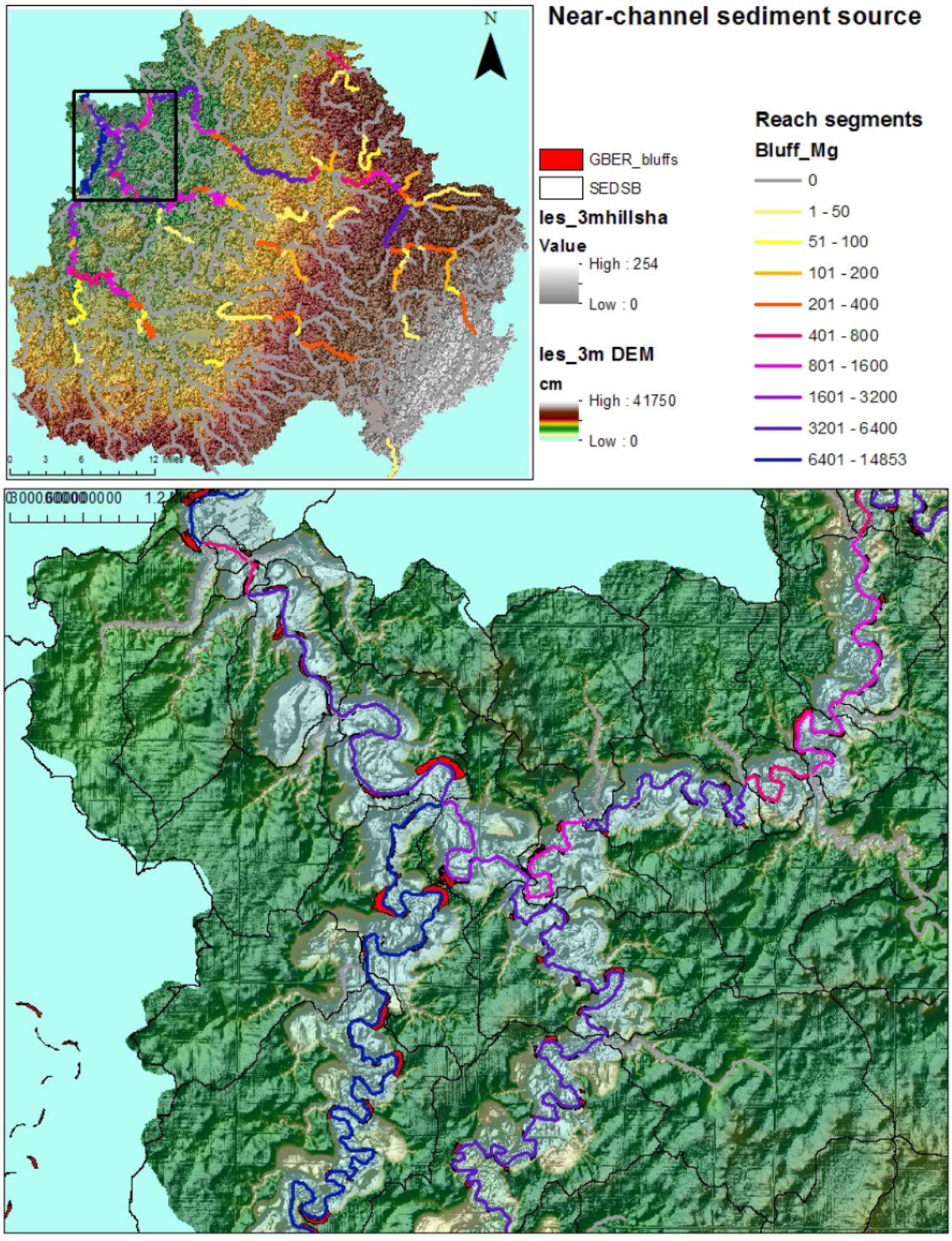

Figure 4.6: Bluffs along MAP, COB, and LES are shown in red polygons and annual sediment input rate from bluffs calculated over the SEDSB are shown in polylines.

4.3.4. Formulation of stream SDR

The stream channel network is the conduit of sediment inputs from all sources, including field, stream, ravines, and bluffs. The stream *SDR* for a SEDSB j ($SDRs_j$) expresses the proportion of sediment inputs that is delivered to the Toposhed outlet, accounting for sediment storage along the stream. The amount of storage depends not only on the amount of sediment inputted, but the location in the Toposhed; thus, $SDRs_j$ is defined as a function of stream length (L_j), elevation change (ΔE_j), and cumulative floodplain area (Af_j) from any given SEDSB j to the Toposhed outlets:

$$SDRs_j = \exp\left(a2\left(\frac{\Delta E_{s_j}}{L_{s_j}}\right)^{b2} Af_j\right) \qquad [4.7]$$

The stream flow length (L_{s_j}) is calculated as the total flow length from the centroid of a SEDSB j to the Toposhed outlet. The stream elevation difference $\left(\Delta E_{s_j}\right)$ is calculated by subtracting the elevation at the Toposhed outlet from the elevation at the centroid of a SEDSB j. The cumulative floodplain area (Af_j) is calculated as the product of reach length (l_j) within a SEDSB j and floodplain width (Bf_j) summed over all downstream SEDSBs following the flow path m to the Toposhed outlet, where J^m is the set of SEDSBs in this flow path to the watershed outlet.

$$Af_j = \sum_{j \in J^m} Bf_j \cdot l_j \qquad [4.8]$$

The floodplain width of a SEDSB j (Bf_j) depends on the geomorphic characteristics of the watershed. For instance, the width of active floodplain in the incised zone tends to be smaller than the floodplain in the upper watershed (Gran et al., 2013). Thus, Bf_j is

expressed in terms of the location of the SEDSB j and boundary conditions on the flood plain widths:

$$Bf_j = B_{\min} + \frac{B_{max} - B_{\min}}{1+\exp\left(-k\left(x_j - x_o\right)\right)} \qquad [4.9]$$

where x_o is the measured distance from the knick points to the Minnesota River along the Maple, Cobb and Le Sueur Rivers, and x_j is the variable distance from a SEDSB j to the mouth of the LSRB. Thus, river segments below the knick points have $x_j < x_o$. $B_{\min}$ and $B_{\max}$ are the measured minimum and maximum floodplain widths along the rivers, respectively (Table 4.2). The fitting parameter, k controls the rate at which floodplain area increases with distance above the knick point. These parameters are determined based on a survey of stream channel geometry along the Maple and Le Sueur rivers (Belmont, 2011). Equation [4.9] constrains the floodplain width of the rivers by $B_{\min}$ below the knick points where the river corridor is characterized by tall bluffs with smaller floodplain areas connected to the rivers. Above the knick points, river corridors reside on a flat terrain with increasing floodplain areas with the maximum area constrained by the $B_{\max}$ (Figure 4.7).

Table 4.2: Toposhed floodplain width parameters determined based on a stream channel geometry survey data (Belmont, 2011)

River	MAP, COB	LES
B_{max}[m]	150	150
K [-]	0.1	0.05
x_o [m]	55,000	80,000
B_{min} [m]	40	60

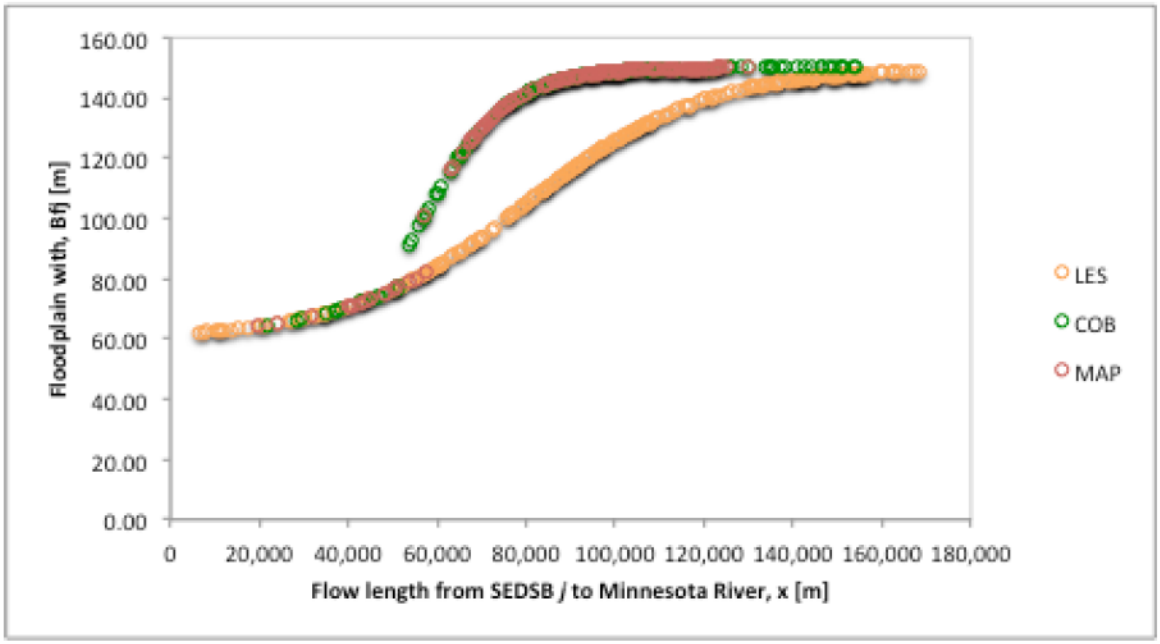

Figure 4.7: Floodplain width of each SEDSB j estimated as a function of distance to the Minnesota River to accommodate steep incised zone with small floodplain area and flat upland with more floodplain area. Floodplain width is calculated using [4.9] with parameter values in Table 4.2 based on the stream channel geometry survey conducted by Belmont (2011)

4.3.5. Conditioned parameter space

Parameter spaces for Topofilter parameters a_1 and a_2 for *SDRf* and a_2 and b_2 for *SDRs* are conditioned against observed data according to the method described in Chapter 3 for each of Toposhed. We used Monte Carlo (MC) simulation to calculate 1000 $SDRf_{ij}$, $SDRs_j$, and SL_j over all SEDSBs from randomly generated parameter combinations from the conditioned parameter space (Table 4.3)[3]. In Section 4.4, we demonstrate the distributions of the simulated *SDR* values. In this section, we examine the conditioned parameter space and average simulation outputs.

[3] The model outputs include both behavioral and non-behavioral solutions calculated from the conditioned parameter space. These outputs, both stochastic (all solutions discussed in Sections 4.4.1 through 4.4.3) and deterministic (a solution that yields an optimal sediment loading prediction as discussed in Section 4.4.4) data on sediment delivery, are supplied to the sediment delivery and loading module in Chapter 6. Evaluation of only the behavioral solutions including development of probability distributions of *SDRf* and *SDRs* is a subject of future research.

For all Toposheds, the average *SDRf* over all MC outputs in each Toposhed ranges around 10% except in the UL where uplands have more topographic relief (Table 4.3). The average *SDRs* over all MC outputs in each Toposhed ranges between 20% to 60% in the upper Toposhed above the knick points, and ranges about 84% in the steeper incised zone.

The volume of sediment that is not delivered to the watershed outlet must necessarily be deposited between source and outlet. A comparison of the magnitude of this deposition with independent information on rates of topographic changes across the watershed provides a useful check on the reasonableness of the Topofilter results (see Chapter 3.2.1).

Given the soil loss from field source and simulated *SDRf* values, the average annual sediment deposition rates on field (SD_f) over all SEDSB areas in each Toposhed ranges between 0.1 to 0.14 mm/year when averaged over all MC outputs. Similarly, for the sediment input rate to stream and simulated *SDRs* values, the average annual sediment deposition rate along stream in the floodplain areas (SD_s) over all SEDSBs in each Toposhed ranges between 0.09 to 1.13 mm/year when averaged over all MC outputs (Table 4.4).

An independent observation using 1-m LiDAR for Blue Earth County examines the Difference of DEM (DoD) between the years 2005 and 2012 (Schaffrath et al., 2015) (see Chapter 3 for the description of this data). Actual erosion and deposition rates through changes in surficial topography vary spatially as shown in Figure 4.8. The DoD shows that the average aggradation over the Blue Earth County areas overlapping with SEDSBs of the study site is about 9 mm/year (only the positive elevation changes), and the

average overall change (positive and negative elevation changes) in elevation is -0.514 mm/year. The DoD in floodplain areas ranges from -15 mm/year (net degradation) to 13 mm/year (net aggradation) over the 7 years between the data collection (see Table 3.5, Chapter 3). When spatial distribution of DoD (Figure 4.8), over the agricultural field area is examined, most of the raster cells have changes in elevation of about 0.001-0.1 meters over the 7 years (0.1-14 mm/year). Along the floodplain area most of the elevation change ranges about 0.11-1 meters over 7 years (2-143 mm/year) (Figure 4.8). Overall, the mean sediment deposition rates inferred from non-delivered sediment in TopoFilter are consistent with the observed topographic elevation change.

Table 4.3: Conditioned parameter spaces for the Toposheds are presented. The table also shows the summary 1000 simulation (sim) outputs calculated using the conditioned par space, including average *SDR* in field (*SDRf*) and on stream (*SDRs*), and average simulated sediment loading (*SL*) against observed (obs) data

Watershed	UM		MC		LC		UL		LO	
Parameters	min	max	min	max	min	max	min	max	min	max
a_1	-1.00E-02	-3.00E-03	-8.00E-03	-3.00E-03	-1.00E-02	-5.00E-03	-3.00E-03	-1.00E-03	-1.00E-02	-7.00E-03
b_1	-9.00E-01	-7.00E-02	-8.00E-01	-1.00E-01	-5.00E-01	-5.00E-02	-9.00E-01	-1.00E-01	-2.00E-01	-5.00E-02
a_2	-1.20E-07	-5.00E-08	-7.00E-08	-1.00E-08	-1.00E-07	-5.00E-08	1.25E-07	-1.50E-08	-5.00E-08	-1.00E-10
b_2	-1.50E-01	-3.80E-03	-1.00E-01	-2.00E-04	-2.50E-01	-1.00E-01	-1.00E-01	-7.00E-04	-1.00E-01	-1.00E-02
SDRf	0.10		0.11		0.12		0.27		0.11	
SDRs	0.36		0.62		0.23		0.50		0.84	
Sim *SL* [Mg/yr]	10,057		5,048		4,653		29,608		184,856	
Obs *SL* [Mg/yr]	10,085		5,155		4,771		28,769		186,081	

Table 4.4: Using the *SDR* values calculated with conditioned parameter space, annual sediment deposition rate on field (SD_F), annual sediment input rate from field source (SI_F), near-channel sediment input rate (NCS soil loss), annual sediment deposition rate along stream (SD_S), and annual sediment loading at the Toposhed outlet (*SL*) are calculated for realizations, and then averaged over 1000 MC simulations in this table.

Topofilter (Mg,mm/yr)							
	Total soil loss at field source (Mg/yr)	Average SD_F (mm/yr)	Simulated SI_F to reach (Mg/yr)	Sum of total NCS SI_{NCS} (Mg/yr)	Average SD_S (mm/yr)	Simulated *SL* at the watershed outlet (Mg/yr)	Observed *SL* at watershed outlet (Mg/yr)
UM	143,753	0.12	13,205	4,496	0.18	10,057	10,085
MC	58,056	0.10	6,532	1,416	0.09	5,048	5,155
LC	66,517	0.14	6,269	7,383	0.23	4,653	4,771
UL	126,268	0.07	32,991	21,572	0.28	29,608	28,769
LO	84,383	0.14	8,213	205,821	1.13	184,856	186,081

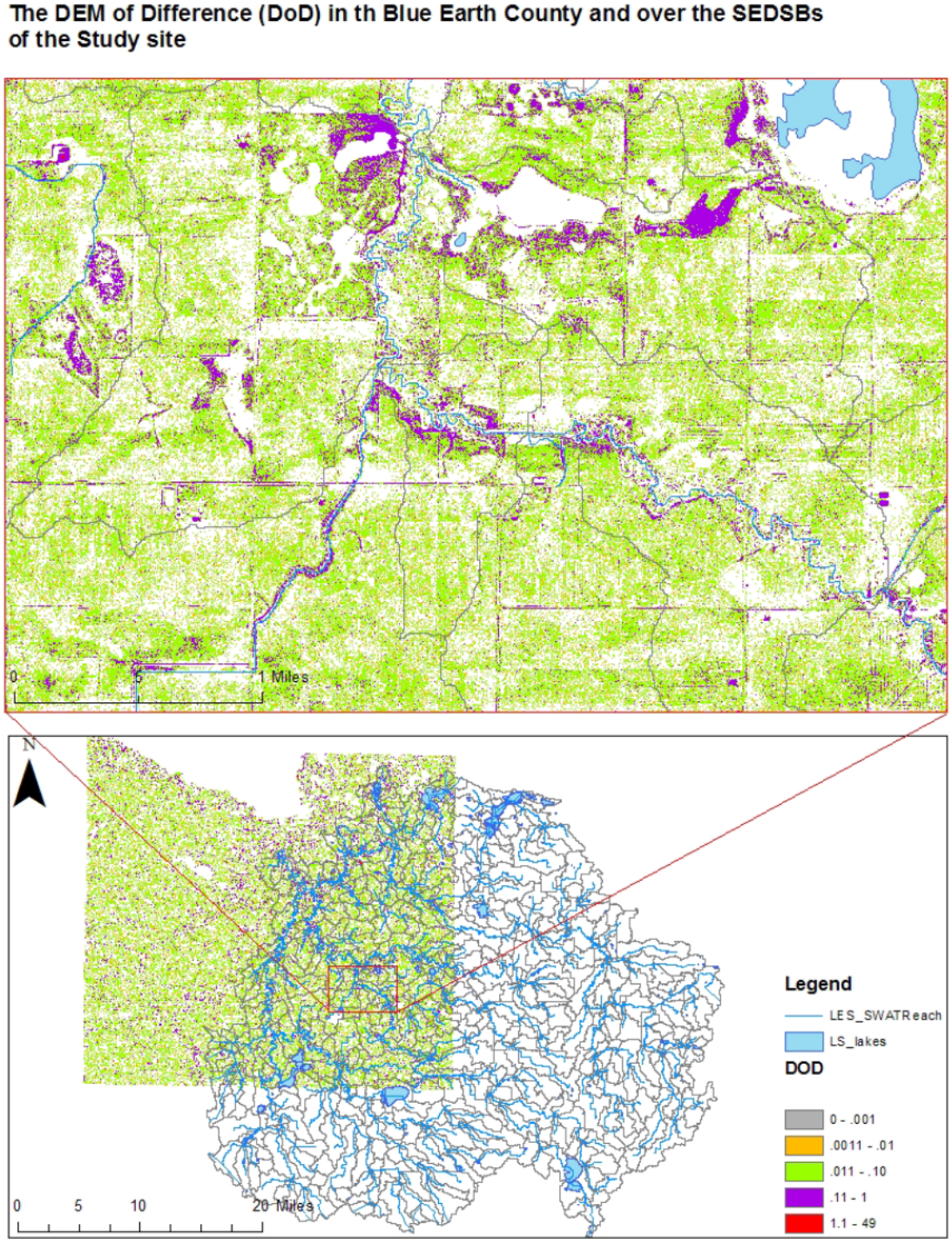

Figure 4.8: The DEM of Difference (DoD) from LiDAR collected between 2005 and 2012 (only the positive elevation change are shown in meters) mapped over the Blue Earth County is displayed over the SEDSBs of the study site to illustrate the spatial distribution of change in surface elevation over 7 years (mapped with DoD data from the authors (Schaffrath et al., 2015)

4.4. Results and discussion

The expanded, network-based Topofilter accounts for all major sediment sources and calculates field and stream sediment delivery values from the conditioned parameter space. The outputs of this simulation provide probability distributions of sediment delivery ratios as a sediment routing platform for the watershed simulation model described in Chapter 6.

4.4.1. Field *SDR* simulation results

Sediment delivery from every field raster cell to the adjacent stream is calculated by randomly selecting parameter sets from the conditioned parameter space for 1000 MC iterations. $SDRf_{ijk}$ represents the sediment delivery of field-eroded sediment from field raster cell i contributing to the stream network of SEDSB j for the k^{th} MC iteration. The product of the annual soil erosion rate of raster cell i of SEDSB j (SE_{ij}) and $SDRf_{ijk}$ is the mean annual sediment input rate from field cell i of SEDSB j for k^{th} MC iteration ($SI_{F_{ijk}}$). The sum of $SI_{F_{ijk}}$ over all field cells in SEDSB j is the total sediment input from field to stream ($SI_{F_{jk}}$) for k^{th} MC iteration (MC_k):

$$SI_{F_{jk}} = \sum_{i=1}^{I_j} SI_{F_{ijk}} = \sum_{i=1}^{I_j} SE_{ij} * SDRf_{ijk} \;\; \forall \, SEDSB_j; MC_k \qquad [4.10]$$

where I_j is the total number of field raster cells in SEDSB j.

We do not attribute particular significance to any particular parameter combination from the MC simulation. Rather, the simulated parameter combinations capture the range of possible field *SDR* values by evaluating the entire MC outputs. Average field *SDR* over all field raster cells in a SEDSB j for the k^{th} MC iteration ($SDRf_{jk}$) is calculated by dividing the $SI_{F_{jk}}$ by the sum of soil erosion over the field cells ($\sum_{i=1}^{I_j} SE_{ij}$) (see [4.4]).

The variation in simulated field *SDR* is captured using the cumulative density function (CDF) of 1000 $SDRf_{jk}$ values at each SEDSB.

The results of this analysis are illustrated with six SEDSBs (j= 718, 890, 965, 1084, and 1131, locations highlighted in yellow in Figure 4.2 with topographic characteristics summarized in Table 4.5). Variation in the *SDRf* and CDFs reflects the influence of different topography across the SEDSBs in the watershed (Figure 4.9). The flow length on field plays ($L_{f_{ij}}$) a major role in determining field *SDR* values, particularly on a flat terrain such as the uplands of the LSRB where the field gradient is very small throughout the SEDSB area. For example, SEDSB 1084 is about five times larger than SEDSB 890; thus flow length on field to stream is generally larger in SEDSB 1084 (Figure 4.9). Accordingly, field *SDR* of SEDSB 1084 has 50% exceedance probability at approximately 0.04; on the other hand, in SEDSB 890 field *SDR* has 50% exceedance probability at approximately 0.24 (Figure 4.9).

In SEDSB near the incised sections of the LSRB, the distribution of field *SDR* values is more significantly influenced by the elevation change from field to stream ($\Delta E_{f_{ij}}$). SEDSB 766 is about two times larger than the SEDSB 1131 and is populated with many cells with longer flow lengths that would have attributed to smaller field *SDR* values over the SEDSB area. However, these SEDSBs have similarly distributed *SDRf* values because SEDSB 766 is located near the watershed outlet and along the incised mainstem river where many cells have a steep field gradient, resulting in larger *SDR* values over the entire MC outputs of the conditioned parameter set.

Table 4.5: Six SEDSBs with different area (A), average elevation change ($\overline{dE_{f_j}}$) and flow length ($\overline{L_{f_j}}$) over field raster cells to adjacent stream cells, and the elevation change (dE_{sj}) and flow length (L_{sj}) in stream from SEDSB j to watershed outlet at UM gage

SEDSB j	A (km^2)	$\overline{dE_{f_j}}$ (m)	$\overline{L_{f_j}}$ (m)	dE_{s_j}(m)	L_{sj} (m)
718	14.71	0.78	215.12	15.24	32,478.76
766	12.29	4.70	287.73	9.40	11,742.88
890	4.20	4.28	264.01	15.64	28,143.89
965	8.58	2.07	304.54	48.75	71,688.31
1084	20.45	2.46	297.91	26.37	53,168.83
1131	6.66	2.70	204.26	36.61	64,580.16

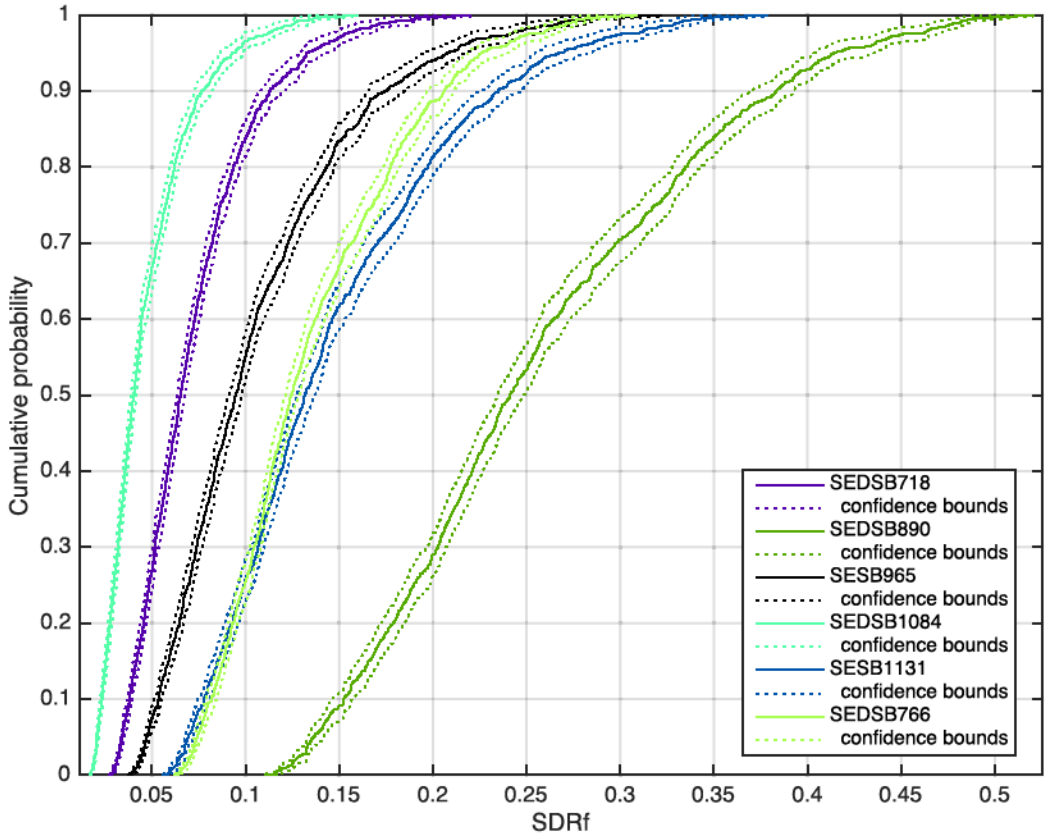

Figure 4.9: Cumulative probability distribution *of SDRf* for SEDSBs shown in Figure 4.2

4.4.2. Field *SDR* in the buffer area of the SEDSB

Field raster cells near the stream network generally have larger field *SDR* values because they have smaller flow lengths and steeper gradient to the stream network

compared to the further upland areas. It is important to recognize that the areas proximal to the stream network (A_p) have larger field *SDR* values than areas further away (A_f) when evaluating different management options. For example, buffer strip management options treat sediment loading from A_p compared to other field management options such as grassed waterways that could be implemented in further upland. Operationally, we define A_p as the areas within 100m of the stream network (approximately 11% of the LSRB area) and A_f as the remainder of the SEDSB area.

Topofilter simulation calculates mean annual sediment input rate from field in SEDSB j for the k^{th} MC iteration ($SI_{F_{jk}}$), from the proximal area ($SI_{F,p_{jk}}$) and from the further upland ($SI_{F,f_{jk}}$). Average *SDR* values over the proximal area in SEDSB j for the k^{th} MC iteration ($SDRf_{p_{jk}}$) and further upland area ($SDRf_{f_{jk}}$) are calculated by dividing the sediment input rates ($SI_{F,p_{jk}}$ and $SI_{F,f_{jk}}$) by the sums of soil erosion in the respective areas ($\sum_{i=1}^{I_{p_j}} SE_{p_{ij}}$ and $\sum_{i=1}^{I_{f_j}} SE_{f_{ij}}$ where I_{p_j} and I_{f_j} are the total numbers of field raster cells in proximal and further areas, respectively in SEDSB j) for k^{th} MC iteration. $SDRf_{p_{jk}}$ is generally larger and $SDRf_{f_{jk}}$ is smaller than the overall field *SDR*, SDR_{jk}. For example, in SEDSB 1131 the 50% exceedance probabilities for the entire SEDSB area, proximal area, and further upland area occur at: $SDRf_{1131k} = 0.13$, $SDRf_{p_{1131k}} = 0.42$, and $SDRf_{f_{1131k}} = 0.06$ (Figure 4.10).

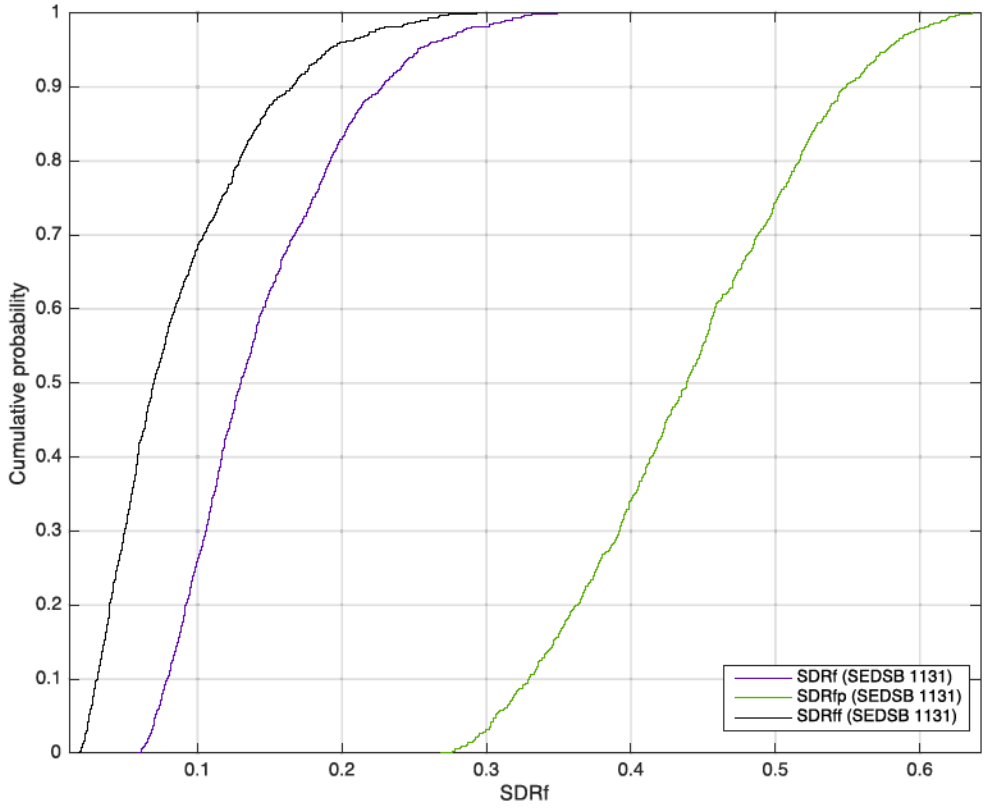

Figure 4.10: Cumulative density distributions of *SDRf* and partitioned *SDRf* in the proximal area ($SDRf_p$) and further upland ($SDRf_f$) from the 1000 MC outputs of the Topofilter simulation for the SEDSB 1131

4.4.3. Stream *SDR* simulation results

Stream *SDR* values depend on the location of SEDSB j, which influences the gradient $\left(\frac{\Delta E_{s_j}}{L_{s_j}}\right)$ and cumulative floodplain area (Af_j) (Equation [4.7]). The CDF developed from the range of possible stream *SDR* values over all MC simulation outputs for each SEDSB j ($SDRs_j$) provide information about how the distributions of the simulated *SDR* values differ by the SEDSB location. For example, SEDSB 766, which is located very near the Toposhed outlet, has a largest elevation change (Table 4.5), and a relatively small floodplain area because its flow length to the outlet is small. Its stream *SDR* values are larger than other sampled SEDSBs (Figure 4.11). In fact, stream *SDR*

values decrease as we move further away from the mouth of the Toposhed, from SEDSB766, 890, 718, 1084, 1131, then 965.

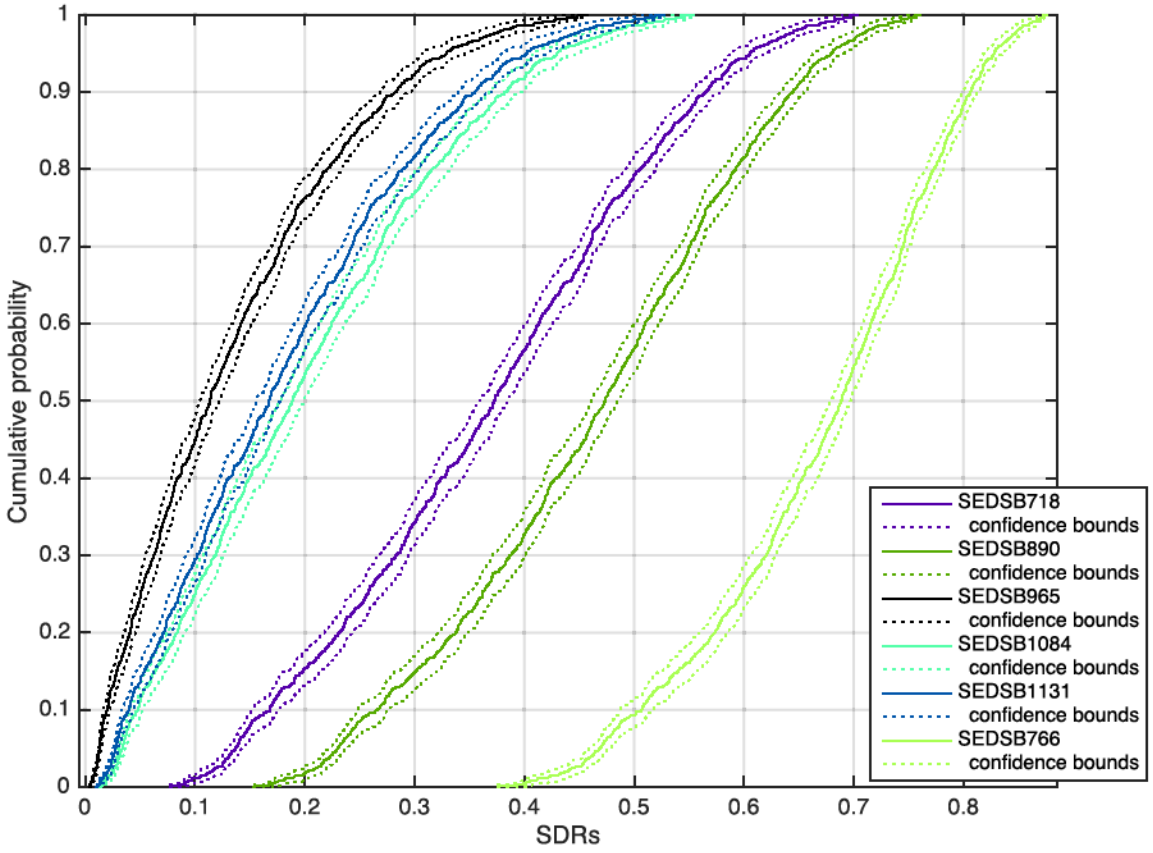

Figure 4.11: Cumulative probability distributions of *SDRs* for SEDSBs show in Figure 4.2

4.4.4. Optimal simulation outputs

In sections 4.4.1 through 4.4.3, we discussed the stochastic outputs of the Topofilter simulation and demonstrated the variability in simulated *SDR* values in different SEDSBs across the watershed. For the purpose of discussing the broad pattern of *SDR* in the watershed, here we focus on an 'optimal' parameter combination for each Toposhed that generates the most accurate sediment loading prediction against measured values among all MC realizations from the conditioned parameter space (Table 4.6). The optimal

parameter combination yields *SDR* and *SL* predictions that are comparable to the average among all MC realization (Table 4.3). It is important to note that the parameter combinations shown in Table 4.6 are one of many possible combinations that yield comparably accurate predictions against observed data due to *equifinality* (Beven, 2006). We profile these parameter sets as an example of a solution in terms of *SDRf, SDRs,* and *SDR* simulation across the watershed. Also, the "deterministic" management option simulation in Chapter 7 utilizes these particular sets of parameters to calculate the effects of management options and sediment loading.

Table 4.6: Optimal parameter sets for the Toposheds that result in the most accurate sediment loading estimate among all 1000 MC realizations from the conditioned parameter space shown in Table 4.3

Watershed	UM	MC	LC	UL	LO
a_1	-8.24E-03	-3.31E-03	-7.81E-03	-2.44E-03	-8.68E-03
b_1	-5.41E-01	-4.28E-01	-3.03E-01	-7.16E-01	-9.82E-02
a_2	-8.99E-08	-9.83E-08	-9.41E-08	-4.68E-08	-2.68E-08
b_2	-2.18E-02	-1.80E-02	-1.28E-01	-3.77E-02	-1.42E-02
SDRf	0.07	0.17	0.11	0.18	0.11
SDRs	0.46	0.47	0.24	0.60	0.90
Sim *SL* [Mg/yr]	10,079	5,155	4,768	28,783	138,909
Obs *SL* [Mg/yr]	10,085	5,155	4,771	28,769	137,301

Sediment delivery ratios across the field raster cells, $SDRf_{ij}$ (see [4.1]) are calculated using the optimal parameter combinations (a_1 and b_1) and averaged over each SEDSB (see [4.3]) for each Toposhed (top left map in Figure 4.12). SEDSBs with higher $SDRf_j$ are mostly located along Upper Le Sueur where its topography is characterized by presence of moraines (Gran et al., 2011). Along Cobb River, SEDSBs near Upper Le Sueur show relatively high $SDRf_j$. The patterns of high *SDRf* values correspond to greater topographic relief in that portion of the watershed (see top right 3m DEM in Figure 4.12).

Stream sediment delivery ratios (middle left map in Figure 4.12) depend most strongly on each reach segment's distance to the watershed outlet, such that the smallest *SDRs* are in the reaches furthest upstream and larger *SDRs* are near the watershed outlet, particularly in the incised zone below the upper gages.

The composite sediment delivery ratio for each SEDSB *j* (bottom map in Figure 4.12) is the product of $SDRf_j$ and $SDRs_j$. These *SDR* values combine the effect of both topographic relief (e.g. larger *SDRf* in Upper Le Sueur) and proximity to watershed outlet that result in higher *SDR* in the incised zone and along the Le Sueur River.

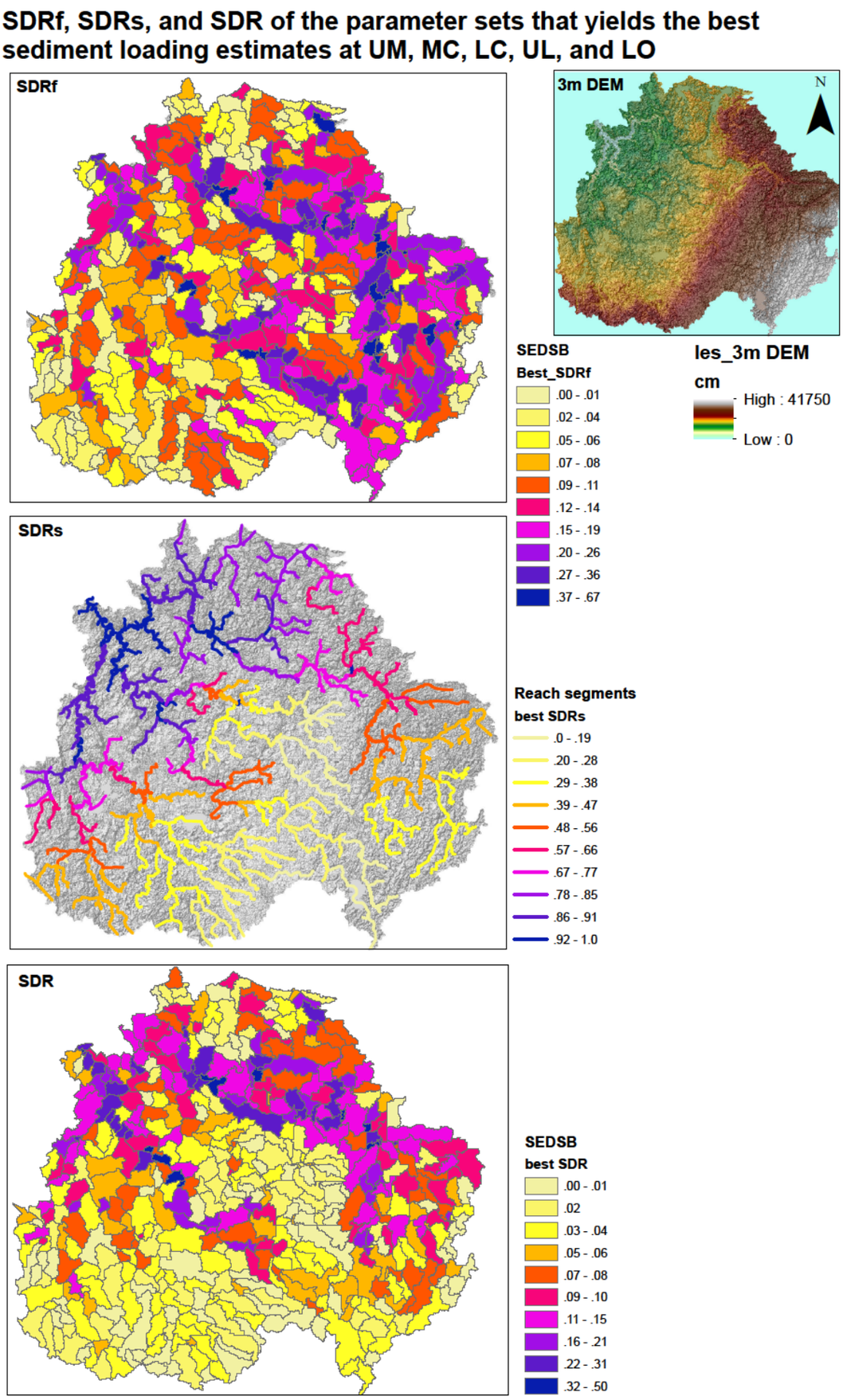

Figure 4.12: Spatial distributions of the *SDRf*. *SDRs*, and *SDR* calculated with parameter sets yielding the best sediment loading estimates at the UM, MC, LC, UL, and LO outlets.

4.5. Conclusion

The Topofilter approach can be used to extract the effect of location and topography on the delivery of sediment from all sediment sources. In this chapter, we expand the structure of Topofilter to include both field and near channel sediment sources. The latter are currently the largest fraction of the sediment budget for the Le Sueur River Basin (Gran et al., 2011). This broader context introduces additional considerations of sediment routing and the use of multiple stream gages and provides a basis for evaluating the importance of all sediment sources (and their possible management) in terms of actual delivery from the watershed.

The analysis divides the study watershed into 529 individual sediment subbasins (SEDSB) and provides distributions of plausible sediment delivery ratio (*SDR*) values for each SEDSB. In general, field flow length influences the field *SDR* more significantly than the gradient between source and stream, particularly in the flat uplands of the LSRB. Exceptions are found in SEDSBs near the incised zone where the terrain becomes steeper and the delivery process is more significantly influenced by the gradient on field. Field SDR values can be separately determined for areas proximal (i.e., within 100m of stream) and far from the stream network for the purpose of supporting evaluation of stream buffer management in Chapter 6. Proximal *SDR* are larger than in the areas in further upland, indicating an opportunity to capture sediment in the proximal area with more effectiveness than further upland.

Stream *SDR* values are generally larger for SEDSBs located near the watershed outlet where stream gradient is generally larger and floodplain area available to store sediment is smaller. This indicates that management options that reduce field sediment supply will

be most effective in locations close to the stream network in SEDSBs near the watershed outlets. The distributions of *SDRf* and *SDRs* over the SEDSBs are used in estimating sediment loading and delivery in the watershed simulation model in Chapter 6.

5. Near-Channel Sediment Sources

5.1. Introduction

Sediment loading in the Upper Mississippi River has increased 10-fold over the past two hundred years since the European settlement based on the analysis of sediment core records from Lake Pepin, a natural impoundment on the Mississippi River downstream of its confluence with the Minnesota River (Belmont et al., 2011; Kelley and Nater, 2000). Geochemical fingerprinting of the Lake Pepin sediment cores and a suite of geomorphic change detection techniques demonstrate that, while sediment loading has remained large through the past 70 years, the dominant source of sediment has shifted from agricultural soil erosion to accelerated erosion of streambanks and bluffs, driven by increased river discharge (Belmont et al., 2011; Novotny and Stefan, 2007). In this chapter we develop a general relation between near-channel sediment loading and river discharge using measurements of river discharge and sediment concentration at paired stream gages on the same river. This relation can be used to estimate changes in near channel sediment supply (NCSS) as a result of past or future changes in river discharge.

A number of different mechanisms produce NCSS. Determining the net contribution from near channel sources by measuring and aggregating the output from individual locations faces difficult challenges of accessibility, accuracy, and cost for in-situ measurement (e.g., erosion pins, close-range photogrammetry, terrestrial laser scanning, and traditional survey methods) (Day et al., 2013; Westoby et al., 2012). On the other hand, sediment measurement from stream gaging is becoming more extensive, reliable, and accessible: more than 90% of U.S. streams have gages that provide daily streamflow records, and the USGS online National Water Information System

(http://water.usgs.gov/nwis) provides access to real-time and historical surface water, groundwater, and water quality data (Hirsch and Costa, 2004; Juracek and Fitzpatrick, 2009; Wahl et al., 1995). A motivation for developing a relation between river discharge and near-channel sediment loading is to utilize these readily available gage observations to develop a practical method to estimate the magnitude of near-channel supply and its variation with discharge. This analysis also provides a basis for estimating how management actions taken to reduce river discharge might reduce NCSS.

In Section 5.2, we provide background information about the Upper Mississippi watersheds that motivated this analysis. In Section 5.3, we describe the study site and gage data availability, and in Section 5.4, we explain the methods to compile gage data and estimate NCSS. In Section 5.5, we provide results of the analysis, examine outliers of the general relation between river discharge and sediment loading, and describe a model for estimating effects of peak flow attenuation on NCSS. In Section 5.6, we discuss how this method might be transferable to other watersheds and discuss factors that might influence whether the relation between sediment supply and river discharge is stationary.

5.2. Background information

Excess sediment loading in the Greater Blue Earth River Basin (GBERB) may be attributed to the watershed's history over the Holocene as well as anthropogenic influences on the landscape since the European settlement in the region (Chapter 2). The GBERB is characterized by deeply incised river valleys in the lower portions of the watershed ("incised zone"), created by a 65m drop in base level of the ancestral Minnesota River approximately 13.5 thousand years ago (Gran et al., 2009). Lowering of the base level triggered the incision of the lower portions of the GBERB with rapid

upstream expansion of a larger and more dissected channel network. Near-channel materials in the lower watershed are primarily erodible glacial tills and lake sediments; thus, the river basin is naturally primed to produce a large sediment supply (Gran et al., 2009).

Hydrologic changes in the GBERB have been observed since the European settlement when the upland landscape was largely changed from native wetlands and prairie to almost exclusive row-crop agriculture. This drastic transformation of the landscape in mere two hundred years was possible through installation and maintenance of an extensive and widespread artificial drainage system of subsurface tiles and ditches that drain the watershed for crop production (Shepard and Westmoreland, 2011). Alterations of the drainage system and row crop conversion, coupled with increased precipitation in recent decades, have contributed to increases in both peak flow magnitude and duration in the GBERB (Novotny and Stefan, 2007; Schottler et al., 2013).

The combination of highly erodible steep river valleys and increased river discharge has contributed to the intensification of sediment loading in the GBERB. For example, a recent study in the Le Sueur River Basin (LSRB), a subwatershed of the GBERB, indicates that valley excavation rates and the overall contribution from near-channel sources (streambanks, bluffs, and ravines) have dramatically increased during the past decades: estimated erosion rates from the near-channel sources from 2000 to 2010 are three times larger than pre-settlement erosion rates (Gran et al., 2013). Also, a sediment mass balance study demonstrates that the dominant source of sediment has shifted from agricultural soil erosion, which still remains significant, to near-channel sources,

particularly tall bluffs below the knickpoints that mark the slope change in the river profile adjusting to the base level drop (Belmont et al., 2011).

Observations of increased river flows over the latter half of the 20th century (Novotny and Stefan, 2007) and the shift in dominant sediment source from field to near-channel (Belmont et al., 2011) have led to a hypothesis that sediment loading from the GBERB can be reduced by decreasing the magnitude of peak flows in the streams and rivers passing through the incised zone. The heart of any evaluation of this hypothesis must be a relation between river discharge and the rate of near-channel sediment loading. Although sediment budgets developed for the watershed (Bevis, 2015; Gran et al., 2011; Wilcock et al., 2016) indicate that near-channel sources provide the most sediment to the river network and that their location means that a large fraction of this sediment is delivered to the watershed outlet, a sediment budget provides no basis for assessing the relation between river discharge and sediment input.

Sediment supply from near-channel sources is complex, intermittent, contingent on previous events, and highly difficult to quantify. Here, we develop an approach that does not depend on estimating and cumulating local sources of sediment, but uses instead *paired observations of sediment loadings* at two stream gages on the same river, thereby providing a measure of total sediment loading as a function of river discharge. This approach may prove promising because it supports a reliable estimate of near-channel sediment supply at a reasonable cost while also providing a basis for estimating the relative magnitude of near-channel versus upland sources.

In addition to the three main tributaries in the Le Sueur watershed, each of which had two operating gages for some time period, we also examined the results from paired

gages in three other watersheds that bracket the incised portions of the Minnesota River Basin (MNRB). By examining six different rivers within and outside of the GBERB, we were able to explore whether a common pattern of near-channel sediment loading exists.

5.3. Study site

The specific focus of this work is the development of a quantitative relation between near-channel sediment supply (NCSS) and river discharge for the Le Sueur River watershed, the largest tributary and largest source of sediment to the Blue Earth River (Wilcock, 2009). The Le Sueur River has three subwatersheds: the Maple (MAP), Cobb (COB), and Le Sueur (LES) Rivers (Figure 5.1). Each of these rivers has two gages operating simultaneously for a period of time. In each case, one gage is located toward the upper end of the incised zone and a second gage located toward the lower end of the incised zone but above the confluence of the three rivers. There is also a gage on the Le Sueur River below the confluence with the Cobb and Maple Rivers. Although the entire incised zone on each river is not fully contained between the gages, the near-channel sediment loading may be determined per unit length of river between the gages and used to estimate sediment loading in the balance of the incised sections.

To explore the available data set and assess whether a general relation for near-channel loading exists, we also examine paired gages on High Island Creek (HI), Rush River (RUS), and Seven Mile Creek (SMC) (Figure 5.1). These subwatersheds drain into the incised portion of the Minnesota River Valley downstream of the mouth of the Le Sueur and Blue Earth Rivers. Thus, multiple subwatersheds are included in the analysis in order to evaluate whether a general relation exists between river discharge and

sediment loading from near channel sources (NCS) in the incised portion of the Minnesota River basin.

5.4. Method

5.4.1. Compiling data at the upper gages and lower gages

River discharge and water quality data (grab samples) from the paired stream gages on MAP, COB, LES, HI, RUSH, and SMC were collected and compiled (Table 5.1). Observations from the upper gage (UG) and lower gage (LG) were paired if they were collected within 60 minutes of one another. In cases without a reported river discharge accompanying the water quality data, the discharge was estimated using the time of sampling and the 15-minute river discharge data (Table 5.2).

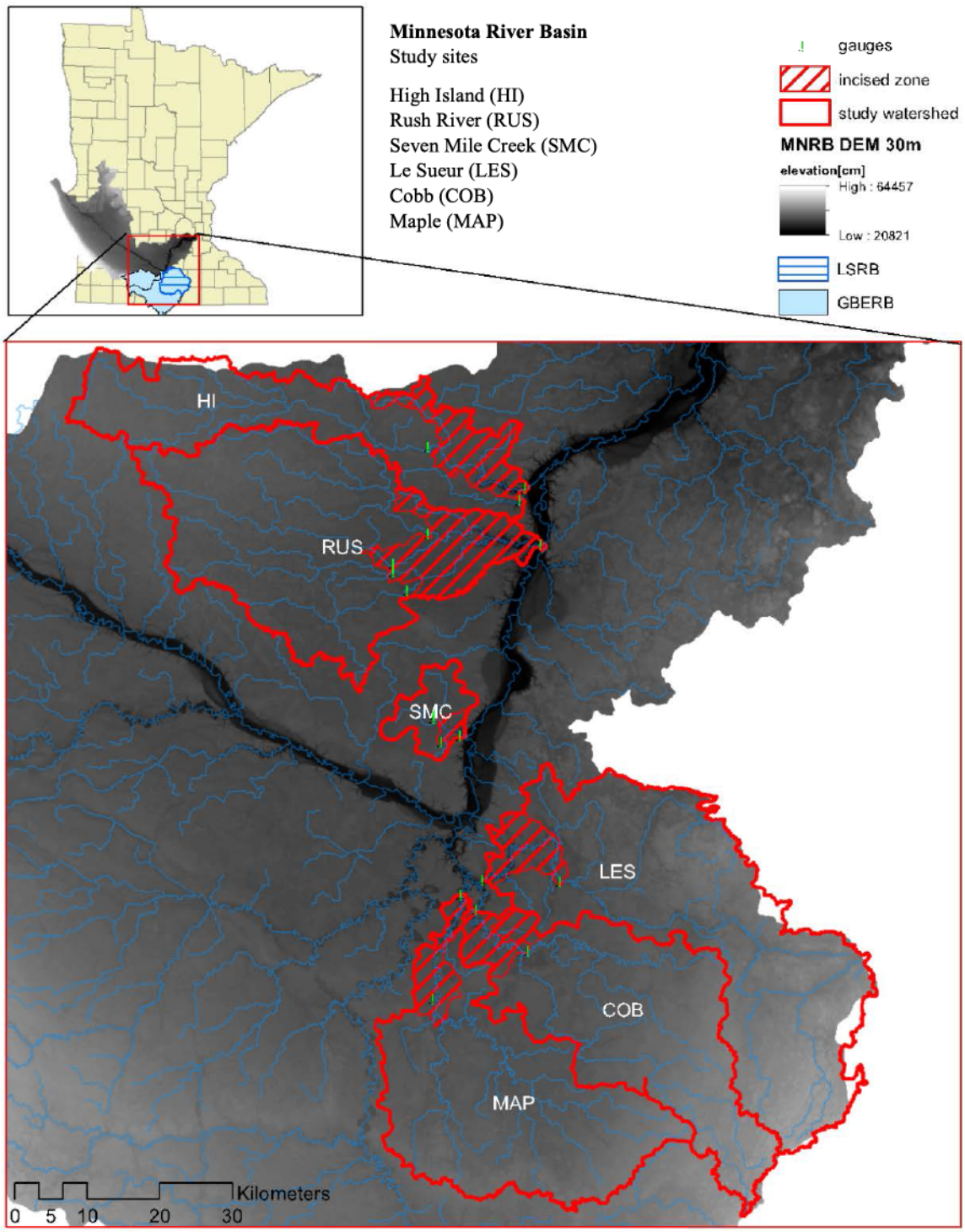

Figure 5.1: Study sites and their locations with indications of the incised zones (red cross hatched areas) and the gage locations over 30-m topography and National Hydrography Dataset (NHD)

Table 5.1: This table lists the gage data sources used in the analysis. Note: SMC1, SMC2, and SMC3 data from Brent Dalzelle of the University of Minnesota and Pat Baskfield of the Minnesota Pollution Control Agency (MPCA) are combined in the analysis. Brent Dalzelle provided data from 2000 to 2007 and Pat Baskfield provided data from 2007 to 2011 or 2012. When there are duplicate data, I used the data compiled at a later date.

Rivers	Gauge Field Code	Hydra ID	Storet station ID (MPCA)	U/M/D/O	drainage area (km2)	incised length (km)	data	start date	end date	Sample type	Sample size	source
Maple	MAP nr Sterling Center, CR18	H32062001		U	790.00	N.A.	TSS	4/3/2006	9/23/2011	grab sample	282	http://www.dnr.state.mn.us/waters/csg/index.html
Maple	MAP nr Sterling Center, CR19	H32062001		U			Q	3/29/2006	12/17/2011	15-min data		email from Pat Baskfield
Maple	MAP nr Rapidan, CR35	H32072001		D	877.15	9.88	TSS	5/2/2003	10/5/2011	grab sample	594	http://www.dnr.state.mn.us/waters/csg/index.html
Maple	MAP nr Rapidan, CR35	H32072001		D			Q	4/24/2003	10/13/2011	15-min data		email from Pat Baskfield
Cobb	Little COB	H32069001		U	332.89	N.A.	TSS	2/2/2006	6/26/2012		285	http://www.dnr.state.mn.us/waters/csg/index.html
Cobb	Little COB	IDA USGS 05320270		U			Q	4/1/1996	10/1/2007	15-min data		http://ida.water.usgs.gov/ida/available_records.cfm?sn=05320270
Cobb	Little COB	NWIS USGS 05320270		U			Q	10/2/2007	10/15/2012	daily		http://nwis.waterdata.usgs.gov/nwis/uv/?site_no=05320270
Cobb	Beauford	H32073001		M	22.37	N.A.	Q	3/7/2010	10/28/2011	15-min data		email from Pat Baskfield
Cobb	Beauford	H32073001		M			TSS	3/27/2005	8/30/2011	grab sample	295	http://www.dnr.state.mn.us/waters/csg/index.html
Cobb	Big COB, CR16	H32071001		D	784.12	7.67	TSS	10/11/2005	10/5/2011	grab sample	594	http://www.dnr.state.mn.us/waters/csg/index.html
Cobb	Big COB, CR16	H32071001		D			Q	4/24/2003	10/13/2011	15-min data		email from Pat Baskfield
Le Sueur	LES at St. Clair	H32079001		U	914.39	N.A.	Q, TSS	3/29/2007	9/28/2011	grab sample	179	email from Pat Baskfield, 12/11/2013
Le Sueur	LES at St. Clair	H32079001		U			Q	3/25/2007	10/4/2011	15-min data		email from Pat Baskfield
LeSueur	LES nr Rapidan, CR8	H32076001		D	1156.56	13.80	TSS	3/31/2006	10/5/2011	grab sample	244	http://www.dnr.state.mn.us/waters/csg/index.html
LeSueur	LES nr Rapidan, CR8	H32076001		D			Q	3/28/2006	10/5/2011	15-min data		email from Pat Baskfield
Seven Mile Creek	SMC1 (CD13A)	H28062001		U	40.29		Q	4/2/2002	10/6/2011	15-min data		email from Pat Baskfield, 1/24/2013
Seven Mile Creek	SMC1	H28062001	S002-934	U			Q, TSS	4/26/2000	10/25/2007	grab sample	118	email from Brent Dalzelle, 11/22/2013
Seven Mile Creek	SMC1	H28062001	S002-934	U		N.A.	Q, TSS	3/14/2007	8/17/2011	grab sample	67	email from Pat Baskfield, 12/10/2013
Seven Mile Creek	SMC2	H28066001	S002-936	U	36.90		Q	4/3/2002	10/6/2011	15-min data		email from Pat Baskfield, 1/24/2013
Seven Mile Creek	SMC2	H28066001	S002-936	U			Q, TSS	4/26/2000	10/25/2007	grab sample	122	email from Peter Wilcock 12/2/2013
Seven Mile Creek	SMC2	H28066001	S002-936	U		N.A.	Q, TSS	3/14/2007	9/28/2011	grab sample	76	email from Pat Baskfield, 12/10/2013
Seven Mile Creek	SMC4	H28063002	S002-464	M	18.11	N.A.	Q, TSS	3/30/2006	7/6/2009	grab sample	60	email from Pat Baskfield, 12/10/2013
Seven Mile Creek	SMC3	H28063001	S002-937	D	95.31	2.93	Q	3/13/2007	9/13/2011	15-min data		email from Pat Baskfield, 1/24/2013
Seven Mile Creek	SMC3	H28063001	S002-937	D			Q, TSS	4/10/1996	10/25/2007	grab sample	219	email from Peter Wilcock 12/2/2013
Seven Mile Creek	SMC3	H28063001	S002-937	D			Q, TSS	3/14/2007	5/24/2012	grab sample	175	email from Pat Baskfield, 12/10/2013
High Island	HI at Arlington (5P)			U	415.92	N.A.	Q, TSS	4/10/2002	9/17/2012	grab sample	255	email from Pat Baskfield, 12/10/2013
High Island	HI at Buffalo (9P)			M	71.85	N.A.	Q, TSS	4/3/2002	9/17/2012	grab sample	254	email from Pat Baskfield, 12/10/2013
High Island	HI at Outlet (10P)			D	615.73	25.64	Q,TSS	4/3/2002	9/17/2012	grab sample	289	email from Pat Baskfield, 12/10/2013
Rush River	RUS North Branch (2RP)			U	256.34	N.A.	Q, TSS	3/25/2003	10/13/2005	grab sample	64	email (combined results) from Pat Baskfield and Scott Mattison, 12/9/2013
Rush River	RUS Middle Branch (3RP)			U	208.86	N.A.	Q, TSS	3/25/2003	10/13/2005	grab sample	65	email (combined results) from Pat Baskfield and Scott Mattison, 12/9/2013
Rush River	RUS South branch (4RP)			U	212.65	N.A.	Q, TSS	3/25/2003	10/13/2005	grab sample	61	email (combined results) from Pat Baskfield and Scott Mattison, 12/9/2013
Rush River	RUS at JC1 (5RP)			U	196.00	N.A.	Q, TSS	3/25/2003	10/13/2005	grab sample	63	email (combined results) from Pat Baskfield and Scott Mattison, 12/9/2013
Rush River	RUS at Outlet (1RP)			D	1043.18	17.30	Q, TSS	3/25/2003	9/17/2012	grab sample	271	email from Pat Baskfield, 12/10/2013

Table 5.2: Data extracted for the analysis from data sources (Table 5.1): river and gage locations (column 1 and 2); unprocessed water quality sample size (column 4); number of water quality samples with total suspended solids (TSS) readings but with no water discharge readings (column 5); number of water quality samples supplemented with 15-min river discharge data (column 6); and number of samples with no recordable TSS reading (Data shows either TSS=0 or N/A) (column 7); total number of candidate data at the UG and LG that would be paired if their collection times were similar (column 8); the number of discarded data due to missing TSS or river discharge data (column 9). The highlighted cells indicate the number of paired gage data matched by data collection time in the UG and LG.

River	UG/LG	GaugeID	total # WQ data	TSS<>0, Q=0	15min Q supp	TSS=0	Data used to find matching UG, MG, and LG measurements by date and time	Discarded data (TSS=0 or no Q data)	Discarded due to mismatched date and time	#data match by date and time	Data discarded (%)
Maple CR18	UG	H32062001	282	95	91	53	225	57	64	161	43%
Maple CR35	LG	H32072001	594	97	93	212	378	216	217	161	73%
LittleCobb	UG	H32069001 / NWIS 05320270	285	121	113	59	218	67	79	139	51%
Big Cobb	LG	H32071001	594	209	191	157	419	175	280	139	77%
LeS StClair	UG	H32079001	179	0	0	0	179	0	89	90	50%
LeS RapidanCR8	LG	H32076001	244	110	98	29	203	41	113	90	63%
7mile_SMC1	UG	H28062001	185	2	0	0	183	2	124	59	68%
7mile_SMC2	UG	H28066001	198	6	0	0	192	6	133	59	70%
7mile_SMC4	UG	H28063002	60	1	0	0	59	1	0	59	2%
7mile_SMC1, 2, 4	UG	above three	59	0	0	0	59	0	8	51	14%
7mile_SMC3	LG	H28063001	394	24	0	21	349	45	298	51	87%
HighIS Arlington	UG	5P	255	2	0	0	253	2	1	252	1%
HighIS Buffalo	MG	9P	254	0	0	0	254	0	2	252	1%
HighIS Buffalo, Arlinton	LG	above two	252	0	0	0	252	0	12	240	5%
HighIS Henderson	LG	10P	289	1	0	0	288	1	48	240	17%
Rush River north branch	UG	2RP	64	0	0	0	64	0	7	57	11%
Rush River middle branch	UG	3RP	65	1	0	0	64	1	7	57	12%
RUsh River south branch	UG	4RP	61	0	0	0	61	0	4	57	7%
Rush River junction 1	UG	5RP	63	0	0	0	63	0	6	57	10%
Rush River 2, 3, 4, 5RP	UG	above four	57	0	0	0	57	0	40	17	70%
Rush River at outlet	LG	1RP	271	2	0	0	269	2	252	17	94%

5.4.2. Estimating sediment loading from NCS in the incised zone

The paired stream gage data enabled quantification of sediment loading between UG and LG by subtracting the sediment-loading rate (in mass/unit time) of the UG ($Q_{s_{UG}}$) from the LG ($Q_{s_{LG}}$). Sediment loading, Q_s [Mg/day] at each of these gages is calculated from the reported sediment concentration multiplied by the river discharge Q. Because the water quality samples are "grabbed" during different storm events, these are estimates of instantaneous sediment loading at these storm events. Some error is introduced because of travel time between the gages as the hydrograph can vary over the time between paired samples are collected.

The incised zone receives sediment not only from direct erosion of near-channel sources, but also from sediment delivered from field areas between the gages. The goal of this analysis is to identify that portion of the inter-gage supply that is directly related to river discharge, which includes sediment supply from ravines, streambanks, and bluffs. Hence, it is necessary to reduce the observed inter-gage loading by the sediment supplied from sources not directly related to near-channel erosion. This contribution includes sediment from upland area (referred to as "side area") draining to the inter-gage zone or incised zone (see Table 5.3 for side area (A_{side}) estimates). Using the sediment loading recorded at the UG (QS_{UG}), sediment loading from the side areas (QS_{side}) is estimated:

$$QS_{side} = \frac{QS_{UG}}{A_{UG}} A_{side} \qquad [5.1]$$

where $\frac{QS_{UG}}{A_{UG}}$ indicates sediment loading from upland sources per unit area, and A_{UG} and A_{side} indicate drainage area above the UG and side area in the inter-gage zone, respectively. Sediment contributed from NCS in the incised zone (QS_{NCS}) is then

$$Q_{s_{NCS}} = Q_{s_{LG}} - Q_{s_{UG}} - Q_{s_{side}} \quad [5.2]$$

The general relation between peak river discharge and sediment contribution from NCS in the inter-gage zone is developed using the river discharge at the LG, Q_{LG}.

Because we are comparing multiple watersheds with different geographic scales, Q_{LG} and $Q_{s_{NCS}}$ are scaled by the upstream drainage area at the LG and length of the river in the inter-gage zone, respectively. This allows examination of the sediment loading per unit length of the incised river versus river discharge per unit area of the watershed:

$$Q'_{LG} = \frac{Q_{LG}}{A_{LG}} \quad [5.3]$$

$$Q_s{}'_{NCS} = \frac{Q_{s_{NCS}}}{L_{inc}} \quad [5.4]$$

where A_{LG} is the upstream drainage area at the LG, and L_{inc} is the length of the incised river between gages calculated by tracing the river maps (Table 5.3). The entire length of the incised river (between UG and LG) is used to scale the sediment loading because below the knickpoints, steep valley walls characterize the entire length of the rivers.

Table 5.3: Watershed drainage area at the UG and LG, side area, and incised river length of study watersheds

Watersheds	A_{UG} (km^2)	A_{LG} (km^2)	A_{side} (km^2)	L_{inc} (km)
LES	914.40	1156.56	171.13	40.84
MAP	790.00	877.15	20.15	35.79
COB	332.89	784.12	403.10	31.91
SMC	95.30	178.71	0.00	10.30
HI	487.77	615.73	44.29	60.72
RUS	873.85	1043.18	34.87	90.02

5.5. Results and discussion

5.5.1. River discharge and sediment loading from incised zone

In this section, the relation between river discharge and sediment loading from the incised zone for individual storms for all study subwatersheds is observed. Then, seasonal

and monthly patterns, and outliers in terms of various environmental factors are examined.

Sediment contributed from NCS in the incised zone, scaled by the length of incised river (Q'_{NCS}) is plotted against the river discharge at the LG, scaled by the upper drainage area (Q'_{LG}) for all study subwatersheds (Figure 5.5). Sediment loading in the incised zone is negative, zero, or very small for low to moderate flow events. Negative sediment loading indicates that there is more sediment entering the reach than leaving; sediment is being stored in the incised zone. There are 175 observations of negative sediment loading in this study period (out of 698 paired observations). Many of negative sediment loading in small absolute magnitude occur when flow is smaller than 1mm/day; while a number of negative sediment loading in large absolute magnitude occurs when flow is larger than 1mm/day. In other words, majority of large sediment storage between gages occur during large flows (a detailed observation of this phenomenon is described in Section 5.5.3).

Another observation made from Figure 5.5 is that as the river discharge increases, near-channel sediment supply (NCSS) in the incised zone increases sharply when the river discharge exceeds approximately 1 mm/day (threshold river discharge, Q_t). Because of this pronounced kink in the relationship, we refer to this as "hockey stick relation".

Flow duration curves for the Le Sueur, Cobb, and Maple Rivers are developed using the 15-minute river discharge data collected over several years (Table 5.1) to evaluate the frequency of the river discharge exceeding the Q_t. The exceedance probabilities of 1mm/day are about 30% for all three rivers. In other words, Q_t is equaled or exceeded at

about 30% of all flow occurrences (Figure 5.3). It is important to note that Q_t is not just the peak flow but the flows that occur at about 30% of all time; this is not an infrequent flow event.

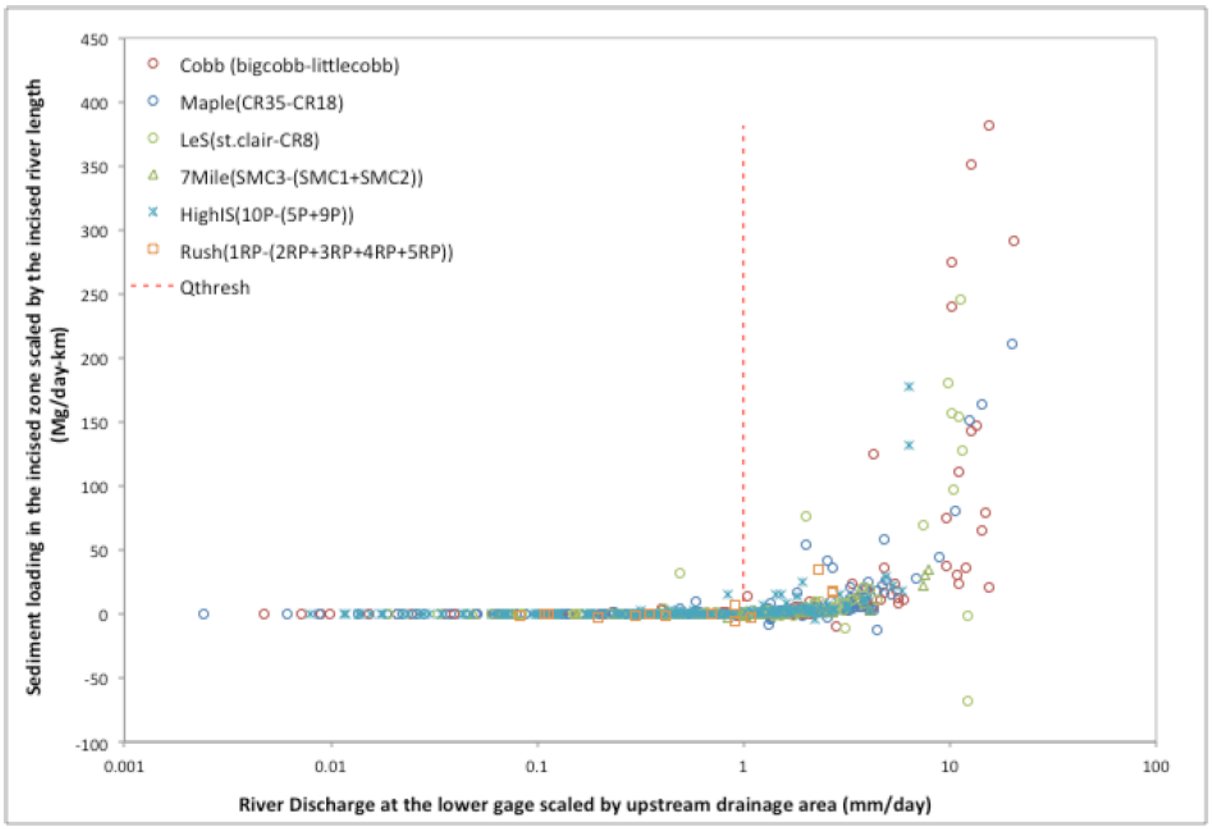

Figure 5.2: Sediment loading from NCS in the incised zone of the Maple, Cobb, Le Sueur, Seven Mile Creek, High Island, and Rush Rivers scaled by the length of incised river against river discharge at the LG scaled by the upstream drainage illustrates that the sediment loading increases with river discharge particularly when it exceeds 1 mm/day

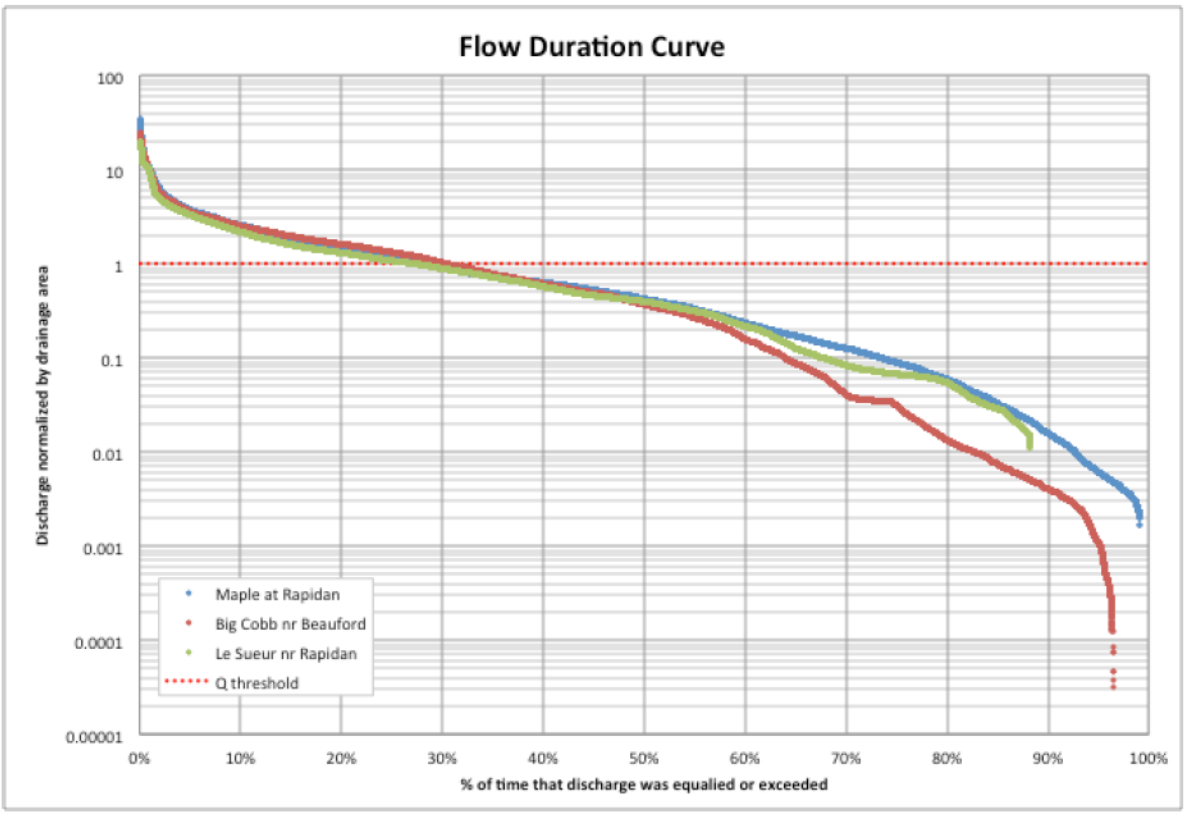

Figure 5.3: Flow duration curve for the MAP, COB, and LES at the LG locations shows that Q_t at 1mm/day have exceedance probabilities of 31%, 31%, and 32%, respectively.

5.5.2. Mean monthly and seasonal sediment loading

To understand the seasonal variability of river discharge and sediment loading, we calculated the mean monthly values from the paired gage data. The paired gage data at the UG and LG (Table 5.2), from which ${Q_s}'_{NCS}$ and Q'_{LG} are calculated, are sorted by the month according to the data collection time. For example, there are 90 paired observations for the LES. Among these, 15 observations are made in June. Thus, average monthly ${Q_s}'_{NCS}$ and Q'_{LG} are calculated by summing the data for each month and then dividing by the number of observations (Figures 5.4 and 5.5).

Highest sediment loading and river discharge are generally observed in the spring months (March to May) and lowest in the summer months (July and August). High spring flow can be attributed to snowmelt runoff (Novotny and Stefan, 2007), and low summer

flow can be attributed to higher agricultural water demands during growing season and decreased runoff from fields (Garbrecht et al., 2004). High monthly average sediment loading and river discharge in the LES, COB, and MAP are observed in the fall months (September and October). This is mainly a result of a particularly large storm event that occurred from 9/22/2010 through 9/29/2010.

To evaluate the seasonal trends, the paired gage data of the LES, COB, and MAP are sorted by season according to the date of data collection (see Appendix 5-A for demarcation of dates for different seasons) (Figure 5.6). In general, large sediment loading occurred during the spring whereas most of the low flows are observed in the fall and summer. High sediment loading observations in fall occurred during the large flood 9/22/2010 through 9/29/2010 as demonstrated by three data points in this figure.

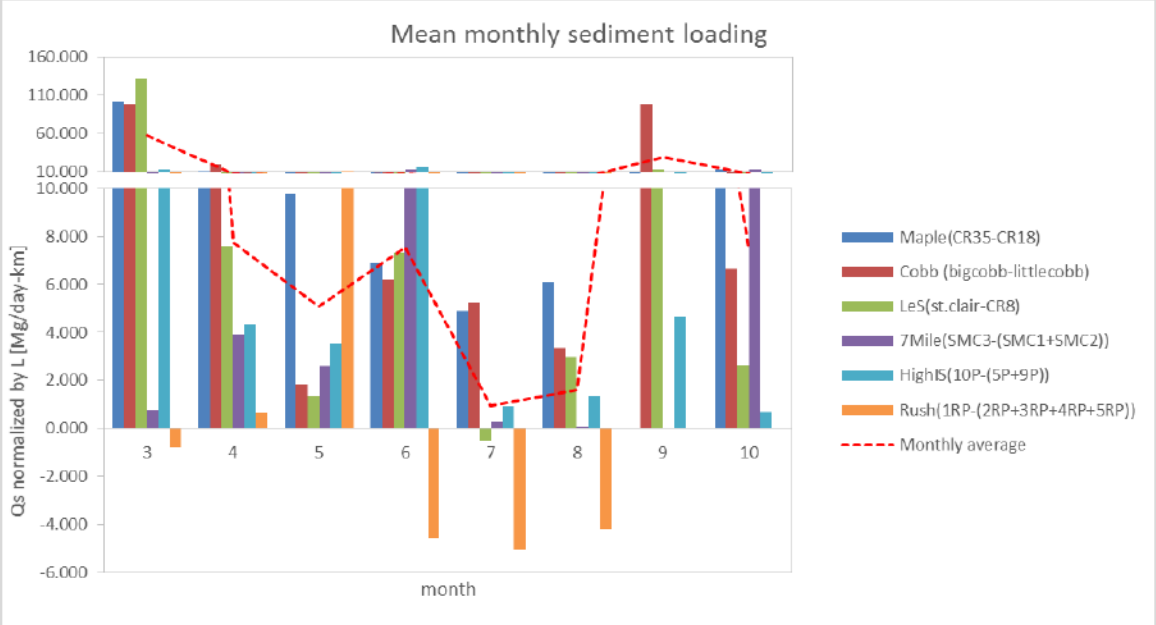

Figure 5.4: Mean monthly sediment loadings from incised zone of the individual watersheds are shown by the bar charts. Red dotted line shows the mean monthly sediment loading from incised zone among all watersheds.

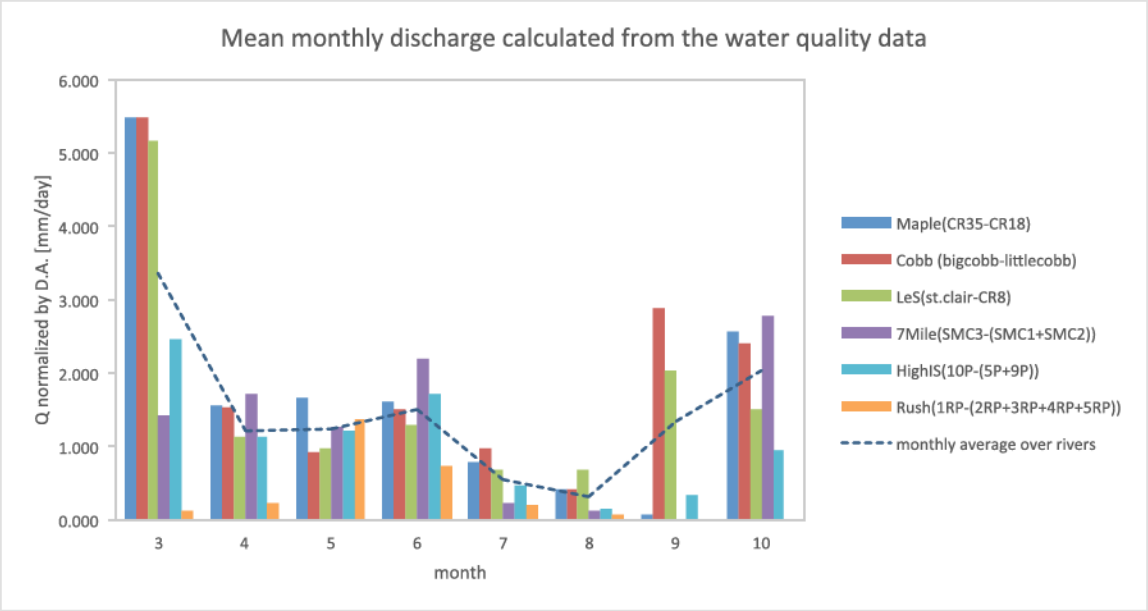

Figure 5.5: Mean monthly river discharges at the LG of the individual watersheds normalized by upstream drainage area (DA) are shown by the bar chart. Blue dotted line shows the average river discharge among all the rivers.

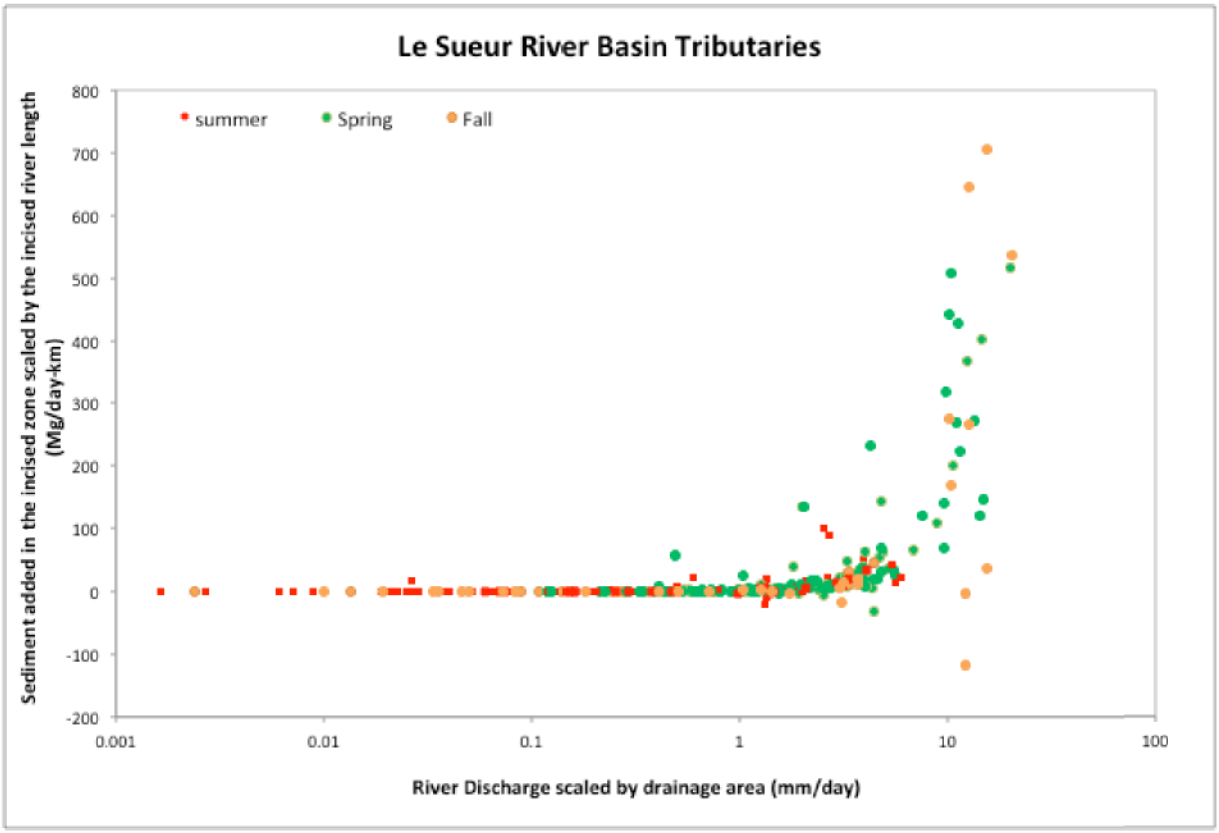

Figure 5.6: Seasonal plot of normalized sediment loading in the incised zone vs. river discharge for MAP, COB, and LES shows that major NCSS occurs mostly in Spring. Large NCSS in Fall occurred in one storm event in September of 2010.

5.5.3. Sediment delivery during a large flood event

To evaluate the large fall storm event that occurred from 9/22/2010 through 9/29/2010, sediment loading in the incised zone is plotted along with the hydrograph from 15-min river discharge data at the LG (Figure 5.7). During this storm event, the NCS in the incised zone of the Big Cobb River begins contributing sediment on the rising limb of the hydrograph and continues to contribute sediment in multiple pulses throughout the storm event. For instance, near the peak of the storm event, near-channel loading is small; then, on the falling limb of the hydrograph near-channel loading increase again.

Similar observations can be made in the Le Sueur River (Figure 5.8). There is a pulse of sediment input on the rising limb of the hydrograph on 9/23/2010, followed by negative sediment loading indicating storage of sediment on 9/24/2010. Then, the sediment loading picks up again on the falling limb on 9/29/2010.

In general, there is a pattern of large near-channel loading on rising limb, followed by a reduction in loading at the highest flows, followed by a spike in sediment loading on falling limb of hydrograph. From this observation, we can speculate that accumulated colluvium is being removed on the rising limb, followed by reduced sediment loading as most colluvium has been removed. On the falling limb of the hydrograph, sediment loading can increase again from collapsing or slumping of large blocks of material (Hooke, 1979). During the falling limb of a hydrograph, subsurface failures are commonly observed when river levels drop faster than the slopes can drain. In such cases, the loss of the counterbalancing weight of the elevated streamflow can exceed the

subsurface soil strength, which remains reduced due to higher pore pressures and lower effective stress (Ibid.).

Although this observation of aggregate inter-gage sediment loading mechanics from paired gages is speculative, a similar conclusion about bluff erosion processes in the study watershed has been made from a direct observation of bluff slope erosion using repeat in-situ photographs at various stages of storm events (S. Kelly 2016, personal communication, November 13). The repeat photographs indicate removal of colluvium on the rising limb of floods, followed by less rapid erosion at high flows, finally followed by the observation of occasional subsurface failures as river stage drops. Similarly, Hooke (1979) observed multiple phases of sediment removal from riverbanks through field studies in six river sites in Devon, England over the period of 2.5 years. Hooke indicates that slumping of large blocks of material after the storm peak has passed could contribute to higher sediment loading. Vertical seepage loss of confining pressure with declining hydrostatic forces and reduced soil strength from elevated pore pressures on the falling limb of the hydrograph result in bank-hydrology conditions that are favorable for mass failure (Simon et al., 2000). Particularly in incised rivers with tall banks or bluffs, negative pore pressure, or matric suction, in the unsaturated banks above the groundwater table can play an important role in initiation of bank instability following a period of rain fall (ibid.). These factors may have contributed to increase in near-channel loading on falling limb of hydrograph we observe in our dataset.

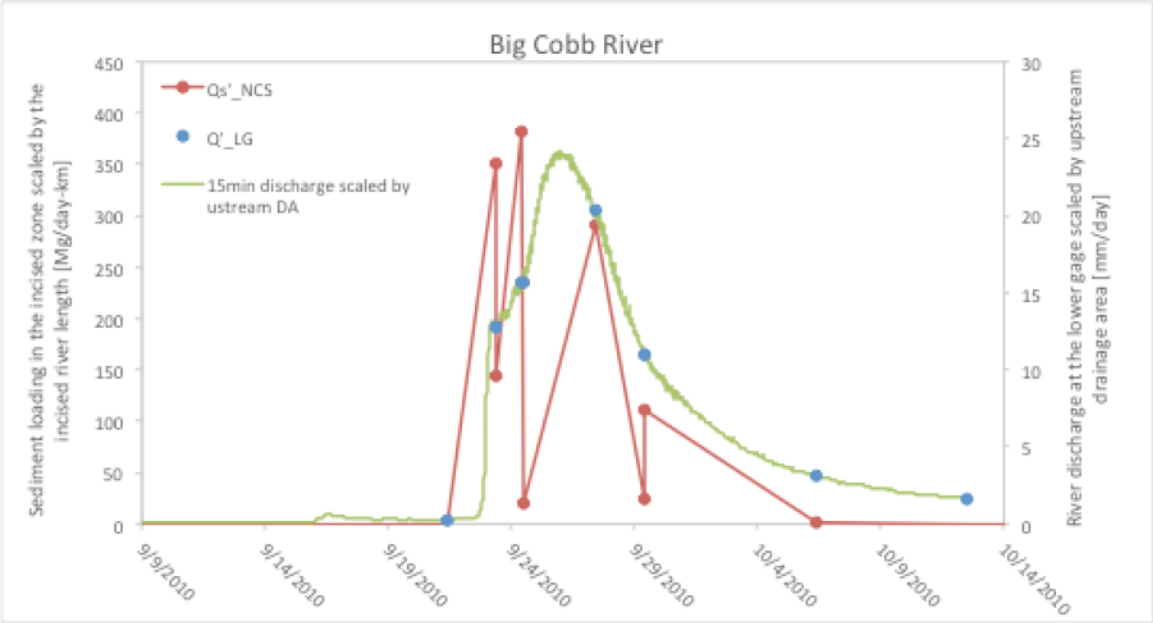

Figure 5.7: Observed near-channel sediment supply (NCSS) in the incised zone and hydrograph at the lower gage (LG) for the storm event from 9/20/2010 to 10/5/2010 on the Cobb River shows that sediment loading happens at multiple pulses through the storm event

Figure 5.8: Observed NCSS and hydrograph for the storm event from 9/20/2010 to 10/5/2010 on the Le Sueur River shows that sediment loading happens at multiple pulses through the storm event

5.5.4. Other factors influencing sediment loading in the incised zone

Factors other than river discharge can influence NCSS in the incised zone. For instance, several observations of sediment loading (Figure 5.2) do not follow the general

trend of sediment loading increasing as a function of the river discharge. These outliers include 1) low sediment loading with high river discharge and 2) high sediment loading with low river discharge.

1) Sediment loading is low when river discharge is high

Sediment loading can vary due to availability of sediment. During a long and large flood event, river discharge initially removes accumulated colluvium at the toe of bluffs on the rising limb of storm events. During the colluvial removal, sediment loading may be transport-limited. Once the colluvial material is removed, further sediment loading may be supply-limited at the height of the storm because most of loose or erodible sediment has already been carried out with the initial phase of the flood event. For example, negative sediment loading of -67.88 Mg/day-km in the incised section of the Le Sueur River is recorded on 9/24/2010 (green circle far below the hockey stick relation in Figure 5.9). This occurrence happened at the peak of the storm event (Figure 5.8).

Sediment loading can vary by season. River discharge is generally large in spring (Figure 5.5) when large river discharge can induce soil erosion. Large amounts of snowmelt and excess soil pore water, soil water piping, and rill/gully flow can cause mass soil failure and provide colluvium for transport during the spring flood event (Gatto, 1995). However, when the soil is frozen, it has a high resilient modulus (Figure 5.10) (Johnson et al., 1978). The resilient modulus measures the stiffness of the soil (low strength soil usually has a low resilient modulus) that is affected by seasonal variation in water content and temperature of soil (Drumm, 1997). Thus, in the early spring months, when soil is still frozen, even high river discharges may not yield significant sediment loadings from NCS. In particular, the storm event in March 2011 with $Q>Q_t$ yielded low

sediment loading in contrast to a comparable storm event in March 2010, which occurred during warmer weather (table insert in Figure 5.9). There are two factors to consider: i) following the large floods of fall 2010 (Figure 5.7), there may have been little colluvium left to remove in March 2011, and ii) the recorded mean daily temperature at Mankato weather station, located near the mouth of the LSRB, shows that the mean daily temperature was well below freezing for many days preceding and during the storm event in March 2011 (temperature time series insert in Figure 5.9).

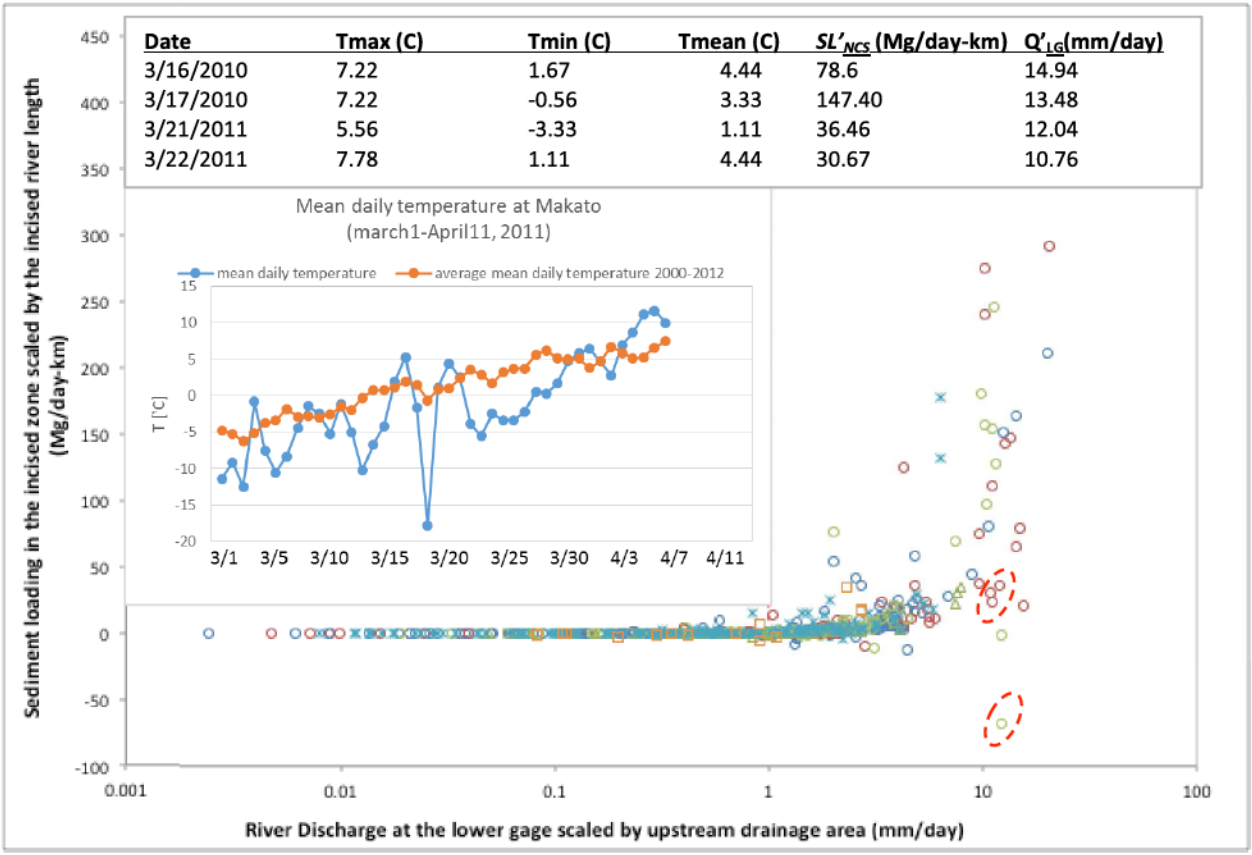

Figure 5.9: Low sediment loading is observed when river discharge is high in the COB and LES (Red dotted ovals around red and green points). Top insert show the mean daily temperature from 3/1/2011 to 4/7/2011 at the Mankato weather station (orange points showing the average mean daily temperature and blue points showing mean daily temperature observed from March to April 2011). Bottom table shows the sediment loading from NCS in the incised zone scaled by the length of river for a spring storm event in 2010 and another in 2011 to illustrate decrease in sediment loading following a large storm event in Fall 2010.

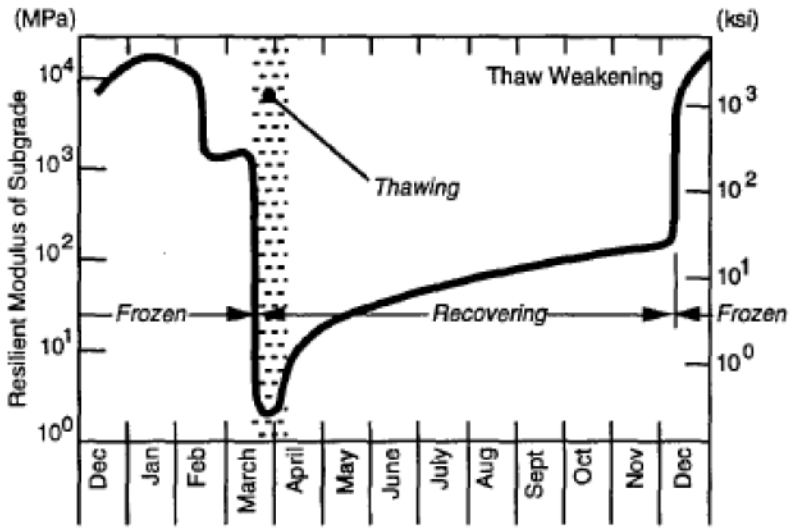

Figure 5.10: Changes in the resilient modulus of low plasticity silt (Johnson et al., 1978)

2) Sediment loading is high when river discharge is low

Freeze-thaw process influences the NCS resilience, erosion, and failure. Repeated freeze-thaw cycles cause soil pore water to swell and shrink, weakening the soil stability and causing slumping or mass failure. A weakened soil matrix, loss of soil, and mass failure can deliver sediment to the slope toe and the river (Gatto, 1995). For example, a relatively large sediment loading of 36.96 Mg/day –km was recorded when the river discharge was well below the Q_t of 1 mm/day on 3/23/2009. During this storm event, the temperatures were above normal and above freezing for several days before the event of large sediment loading. This temperate weather could have led to thawing of NCS, thereby increasing sediment supply prior to the moderate storm event on 3/23/2009 (Figure 5.11).

Another large sediment loading event with moderate stream flow occurred on 4/11/2008 after a number of days with mean daily temperatures alternating above and below freezing. The storm event on 4/6/2008 had a modest magnitude (1.03mm/day) and the average daily temperature was about 2°C (hydrograph and temperature plot in Figure

5.12). Freeze/Thaw processes may have weakened the NCS, thereby increasing sediment loading in that modest flood event. The next, larger storm of 2.03 mm/day on 4/11/2008 also produced a relatively large sediment loading of 76.73 Mg/yr-km (Figure 5.12).

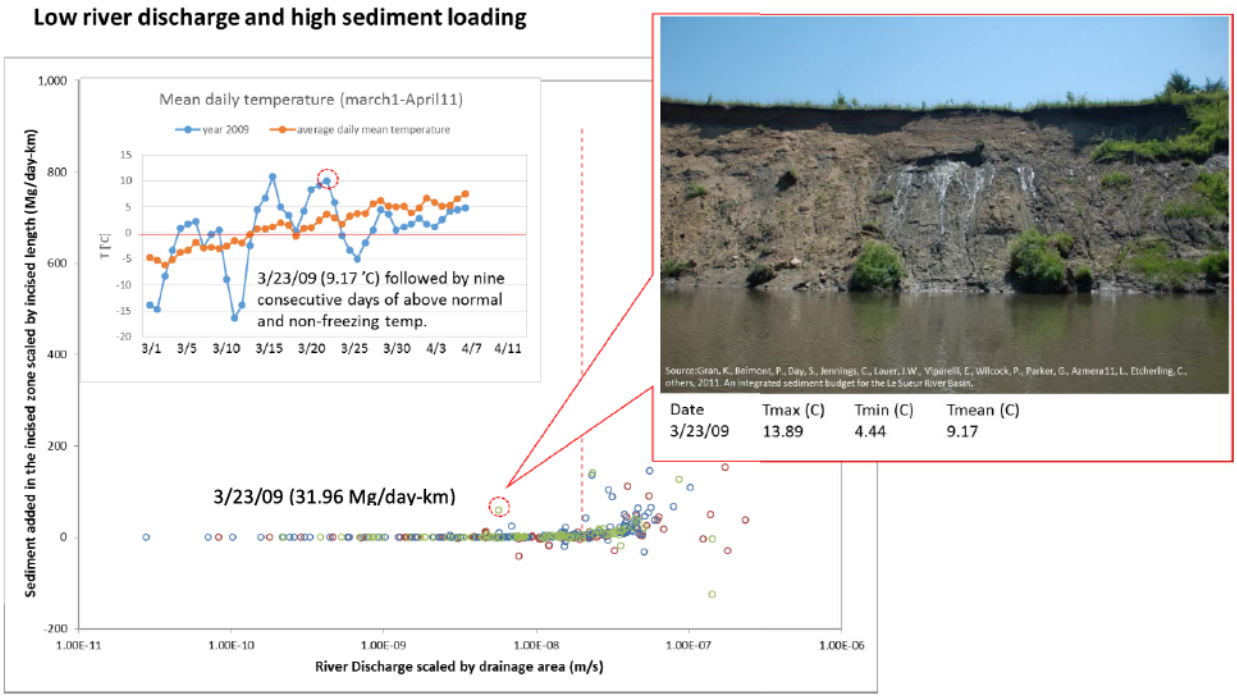

Figure 5.11: observed high sediment loading occurrence when river discharge is below Q_t in the Le Sueur River in March, 2009. Upper right figure illustrates a terrace along the Maple River with exposed truncated till bluff overlain by alluvium and seeps at contact (Gran et al., 2009). Upper left is the temperature time series (orange points showing the average mean daily temperature and blue points showing mean daily temperature observed from March to April, 2009)

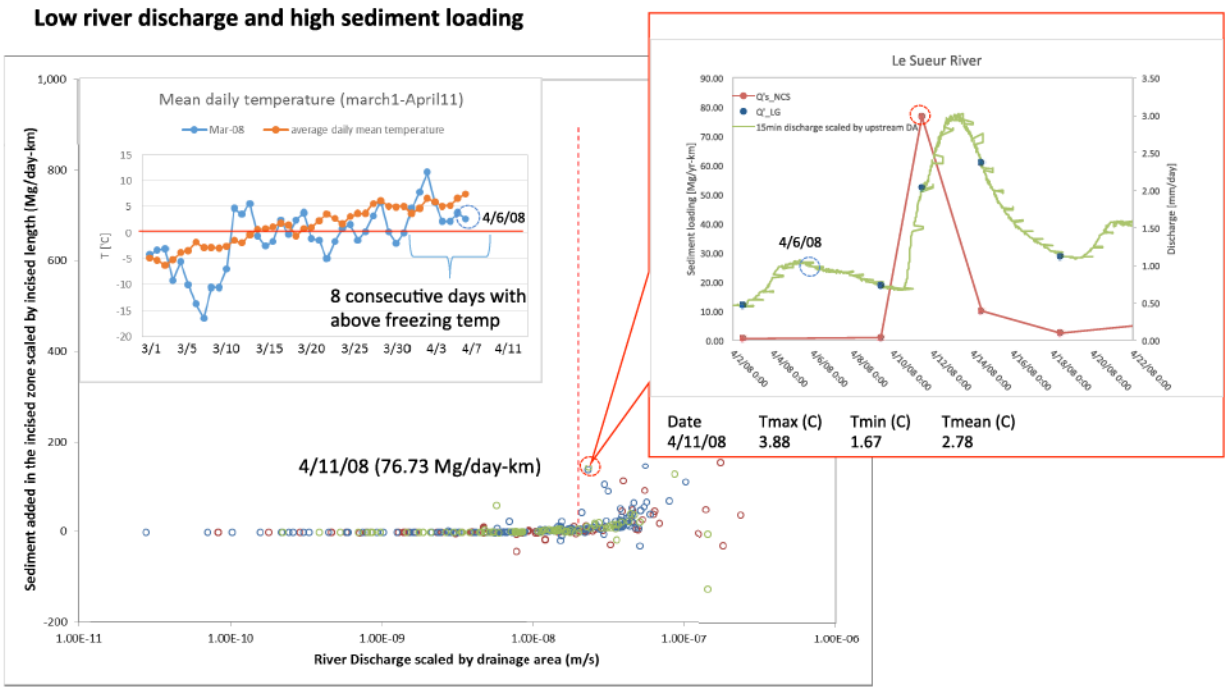

Figure 5.12: observed high sediment loading when river discharge is low in the Le Sueur River in March-April, 2008. Upper right is the hydrograph and sediment loading time series. Upper left is the temperature time series (orange points showing the average mean daily temperature and blue points showing mean daily temperature observed from March to April, 2008)

5.5.5. Estimating average near-channel sediment supply for the Le Sueur Basin

A primary motivation for developing a relation between river discharge and NCSS is to provide a basis for estimating how management actions taken to reduce river discharge might result in sediment loading reduction from NCS. The common trend observed in scaled sediment loading and river discharge suggests that a general relation can be defined. Discharge is clearly a strong driver of near channel sediment loading. The relation between river discharge and sediment loading from NCS in the incised zone (SL_{NCS} model) is developed using a power function regression fitted to the observed sediment loading occurrences for sufficiently large river discharge (i.e., $Q>Q_t$) (Figure 5.13).

We test that relation against independent information for the LSRB by calculating the annual NCSS predicted by the loading-flow relationship integrated over the years against a watershed sediment budget (Gran et al., 2011). Using the SL_{NCS} model, NCSS in the incised zone is calculated using 15-minute river discharge data for the MAP, COB, and LES at the LG locations (Table 5.1). The NCSS at 15-minute interval is then summed over each year to estimate total annual sediment loading, and mean annual NCSS rate is calculated from the total annual loadings over the observation periods of these watersheds. We then compare the predicted mean annual NCSS rate against the sediment budget's estimates of loading rates from ravines, streambanks, and bluffs (Gran et al., 2011) (Table 5.4 and Figure 5.14).

The SL_{NCS} estimate falls within 30% of the sediment budget values for NCSS, producing values smaller by 18% and 10% in the LES and COB basins by larger by 30% in the MAP basin. The similarity in these estimates suggests that sediment loading estimates based on instantaneous gage observations provide a consistent comparison with long term estimates of sediment loading based on multiple line of evidences including sediment fingerprinting, gage data analysis, and suite of geomorphic change detection techniques utilized to develop the watershed sediment budget (Gran et al., 2011).

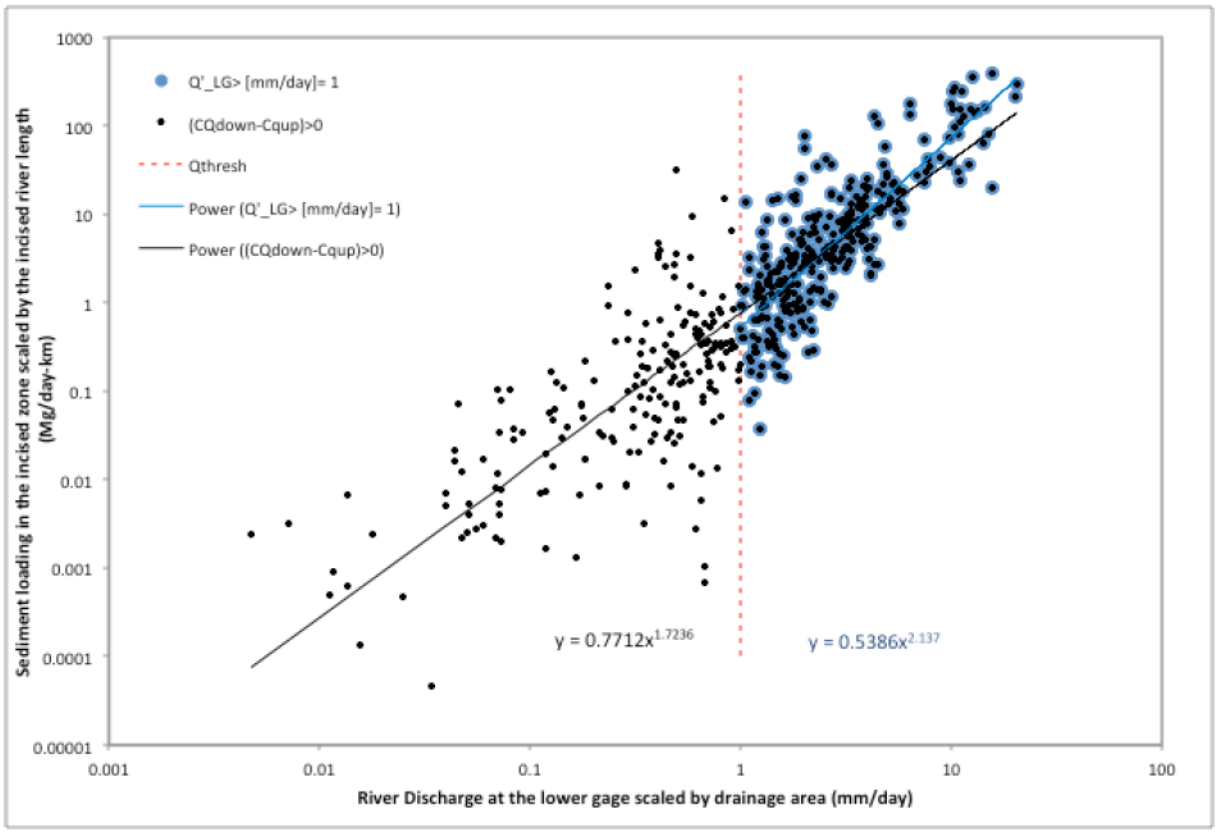

Figure 5.13: Near channel sediment supply in the incised zone scaled by the river length versus river discharge at the LG scaled by upstream drainage area on log-log scale with fitted power regression for flows above Q_t at 1mm/day indicated by the red dashed line.

Table 5.4: Prediction of annual sediment loading in the Le Sueur River Basin using the 15-minute discharge data. For each river, sediment loading predicted at 15-minute interval is summed over each year (first column for each river) and average daily sediment loading is calculated (third column for each river). Average annual sediment loading rate is calculated (red cells) and compared to the sediment budget estimates (green cells).

	Le Sueur near Rapidan CR8 (H32076001)			Big Cobb (H32072001)			Maple River nr Rapidan, CR35(32072001)		
year	sum(CQ Mg)	count 15min data	CQ [Mg/day]	sum(CQ Mg)	count 15min data	CQ [Mg/day]	sum(CQ Mg)	count 15min data	CQ [Mg/day]
2003							2,286	15,603	14.06
2004							22,790	20,718	105.60
2005							28,049	20,652	130.38
2006	8,854	19,973	42.56	8,045	19,589	39.43	13,910	18,444	72.40
2007	12,209	25,143	46.62	13,085	25,146	49.95	12,209	22,745	51.53
2008	5,769	23,133	23.94	4,445	23,142	18.44	6,808	21,142	30.91
2009	642	27,839	2.21	700	21,599	3.11	959	22,227	4.14
2010	79,416	21,696	351.40	96,336	24,948	370.70	161,251	22,179	697.96
2011	33,617	19,469	165.76	25,054	19,465	123.56	25,060	20,167	119.29
sum	140,506			147,666			273,321		
average(Mg/yr)	23,418			24,611			30,369		
Sed. Budget(Mg/y	28,553			27,262			23,288		

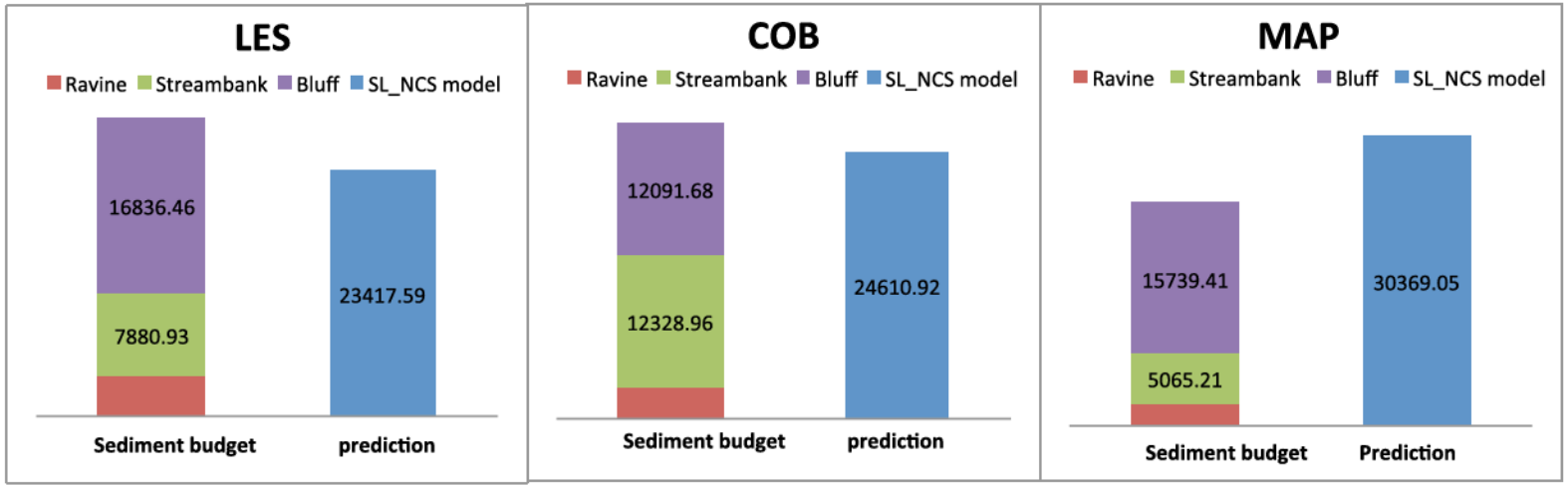

Figure 5.14: Model estimate (blue column on right) vs. sediment budget estimates (purple and green column on left) of sediment loading from bluffs, streambanks, and ravines in the incised zone

5.6. Transferability and stationarity

Sediment loading estimated from paired stream gages can be a useful approach for estimating the cumulative magnitude of complex processes of sediment erosion. The study sites in this chapter are in incised river valleys where near-channel sediment supply (NCSS) is now the dominant sediment source (Belmont et al., 2011). The paired gage analysis allows the assessment of aggregate sediment loading in the incised zone in relation to river discharge.

Paired gages may also be used to evaluate aggregate watershed process in a watershed without such distinct geomorphic characteristics. For example, in a watershed for which sediment storage on floodplains roughly balances sediment supply from bank erosion, the net sediment supply between gages would be small. Paired stream gages, in this example, will not generate a clear relation between sediment loading and river discharge; instead, they will provide an evidence that sediment flux in that stream reach is operating at a steady state.

This approach may be also transferrable to a watershed with partial paired gage data. A watershed might have partial data where only one of the two gages bracketing a stream reach has both river discharge and water quality data, and the other gage has only river discharge data. A sediment rating curve may be developed for the latter gage given some partial water quality observations. For gages with a stable sediment rating curve, continuous sediment loading between the gages can be estimated from continuous river discharge data.

Application of the NCSS model developed in this chapter to predict future changes in sediment loading requires an assumption of stationarity. That is, changes in flow may be

applied to the same NCSS model. Whether increases in peak river discharge over recent decades or possible future reductions in river discharge from water conservation actions, direct calculation of the associated sediment loading requires an assumption that the relation between discharge and NCSS does not change. The analysis in this chapter shows that increased river flows are associated with elevated NCSS, and this relation is consistent over multiple rivers in and near the study watershed. Technically, this relation is a correlation, and does not specifically denote cause and effect. There are, however, some observations that indicate that river discharge does in fact influence near channel erosion process.

First, a sediment fingerprinting analysis (Belmont et al., 2011) demonstrates that sediment contribution from near-channel sources has increased in more recent decades along with river discharge in south central Minnesota (Novotny and Stefan, 2007). These observations further reinforce the connection between increased river discharge and increased NCSS in recent decades.

Second, an independent, in-situ observation of repeat photographs of bluffs in the study watershed at various stages of storm events (S. Kelly 2016, personal communication, November 13) shows that slope material accumulated at the base of the river slopes as well as in-situ material are eroded during high flows. Therefore, decreasing river discharge may prevent further steepening of bluffs and susceptibility to block failure. Bluffs can develop gentler slope over time without persistent erosion at toe, and subsequent propagation of vegetation on the face of bluffs can provide further erosion control.

It is difficult to state whether the relation between river discharge and near channel sediment supply is stationary at this time. Future research can contribute to this question, including evaluation of bluff slope and vegetation before and after significant storm events using historic aerial photographs. More data on the physical attributes of bluffs have been collected more recently, and future work would include evaluation of bluff attributes in connection with significant storm events.

5.7. Conclusion

Sediment loading from NCS is complex, intermittent, contingent on previous events, and highly difficult to quantify. Approaches based on direct measurement of near-channel erosion face require considerable effort (Day et al., 2013; Westoby et al., 2012), and require estimation and upscaling from specific sites to a larger region in order to understand the aggregate effects of near channel contribution. This chapter presents an approach that does not depend on estimating and cumulating local sources of sediment but uses instead paired observations of sediment loading at two stream gages on the same river. This provides a measure of net sediment loading as a function of river discharge. This approach may prove promising because it supports a reliable estimate of near channel sediment supply, and provides a basis for estimating the relative magnitude of sediment loading resulting from river discharge at a reasonable cost of computation and effort.

Sediment loading from near channel sources in the incised zone shows strong dependence on peak river discharge based on the paired gage data analysis. The rate of near-channel sediment loading increases as a function of river discharge when discharge exceeds a threshold of approximately 1 mm/day. Other environmental factors, such as

season, temperature, and the timing of storm events can also influence sediment loading rates, producing occasional outliers about the general trend with river discharge. The outliers of the observed data set, particularly the occurrences of low sediment loading with high river discharge and high sediment loading with low river discharge may be due to the availability of erodible material near the slope toe and the occurrence of strong freeze/thaw cycles.

The results of this analysis can be used to evaluate the effects of water conservation (e.g., wetland restoration, water retention ponds, etc.) on near channel sediment supply. For instance, water conservation measures higher in the watershed may reduce the magnitude and frequency of larger river discharges. Estimates of the river discharge under future flow scenarios can be coupled with the SL_{NCS} model to estimate sediment loading reduction. This approach will be used to evaluate the effects of water conservation on sediment loading in the watershed simulation model in Chapter 6.

Appendix 5.A: Definition of seasons and data allocation

Dates of beginning of season are defined based on the mean daily temperature measured at the Mankato weather station. The first day of spring is the day when the average daytime temperature exceeds zero degree Celsius for seven consecutive days. Beginning of other seasons are determined using the same logic. I used the threshold temperature of 20 degree Celsius to determine the first day of summer. The first day of the fall is followed by seven consecutive days with temperature below 20 degree Celsius. Finally, the first day of winter is followed by seven consecutive days with temperature below 0 degree Celsius.

Year	Spring		summer		fall		winter	
2000	3/19/2000	6/29/2000	6/30/2000	9/10/2000	9/11/2000	11/11/2000	11/12/2000	3/28/2001
2001	3/29/2001	6/22/2001	6/23/2001	9/5/2001	9/6/2001	12/17/2001	12/18/2001	4/4/2002
2002	4/5/2002	6/17/2002	6/18/2002	9/9/2002	9/10/2002	12/1/2002	12/2/2002	3/12/2003
2003	3/13/2003	6/29/2003	6/30/2003	9/17/2003	9/18/2003	11/20/2003	11/21/2003	3/21/2004
2004	3/22/2004	7/8/2004	7/9/2004	9/22/2004	9/23/2004	12/15/2004	12/16/2004	3/25/2005
2005	3/26/2005	6/16/2005	6/17/2005	9/12/2005	9/13/2005	11/28/2005	11/29/2005	3/3/2006
2006	3/4/2006	5/22/2006	5/23/2006	9/7/2006	9/8/2006	11/28/2006	11/29/2006	3/7/2007
2007	3/8/2007	6/8/2007	6/9/2007	9/6/2007	9/7/2007	11/25/2007	11/26/2007	4/2/2008
2008	4/3/2008	7/3/2008	7/4/2008	9/1/2008	9/2/2008	11/14/2008	11/15/2008	3/13/2009
2009	3/14/2009	6/16/2009	6/17/2009	9/24/2009	9/25/2009	12/1/2009	12/2/2009	3/6/2010
2010	3/7/2010	6/15/2010	6/16/2010	8/31/2010	9/1/2010	11/15/2010	11/16/2010	3/28/2011
2011	3/29/2011	6/28/2011	6/29/2011	9/12/2011	9/13/2011	11/30/2011	12/1/2011	3/8/2012
2012	3/9/2012	6/20/2012	6/21/2012	9/14/2012	9/15/2012	11/22/2012	11/23/2012	4/2/2013
2013	4/3/2013	6/15/2013	6/16/2013	9/9/2013	9/10/2013			

6. Management Option Simulation Model (MOSM)

6.1. Introduction

Effective implementation of environmental management plans to meet water quality standards requires accurate predictions about how different management strategies will change the source, transport, and fate of target pollutants. For nonpoint source (NPS) pollution, water quality prediction and management requires analysis at the watershed level, accommodating spatially variable sources, land management, and often sparse information (Korfmacher, 2001). Watershed simulation models that endeavor to predict pollution response to management actions have become a central scientific tool in most watershed management efforts (Korfmacher, 2001; Thomann, 1998).

As reviewed in Chapter 2, many existing watershed simulation models have grown in complexity and size, accommodating multiple environmental processes and dimensions (i.e., physical, chemical, and biologic processes over different spatial and temporal scales with a number of interacting state variables), and regulation specifications (i.e., increase in both salience and complexity of modeling to meet various regulation needs) (Korfmacher, 2001; Thomann, 1998). These watershed simulation models are often overly calibrated due to heterogeneity of the natural environment and difficulties involved with parameter estimation of numerous physical processes embedded in them (Oreskes et al., 1994). These models are not accessible to a wide range of users and their predictions are difficult to judge with the number of different complex and inter-linked processes (Haag and Kaupenjohann, 2001; Korfmacher, 2001; Smith et al., 2011) (See Chapter 2 for more description of watershed simulation models). Challenges associated with use and evaluation of these watershed simulation models hinder the building of

consensus in environmental management decision-making (Thomann, 1998). Thomann (1998), after reviewing the development of increasingly complex surface water quality models, concludes:

> *The success of water quality models will not necessarily be due to "bigness" and complexity but rather to increases in understanding, which can contribute to building consensus in water quality management decision-making.*

In this chapter, we present a management option simulation model (MOSM) that is designed to increase stakeholders' understanding of NPS sediment pollution in a large watershed and to support development of a consensus strategy for sediment reduction. The model is intended to balance the needs for detail and simplicity in developing a representation of the dominant processes that is *reliable* (provides results that are sufficiently accurate and well-constrained by independent observations), *robust* (provides reliable solutions for a range of conditions and input), and *relevant* (accessible to stakeholders and incorporates policy questions) (see Chapter 1.2 for the description of data-driven, reduced complexity modeling approach and definition of these modeling criteria).

MOSM simulates movement of water and sediment in the watershed and evaluates the effects of various management option scenarios on sediment loading. It is a reduced-complexity watershed model where many components (i.e., spatial and temporal grids, and number of interacting state variables) and the degree of complexity (i.e., range of physical, chemical, and biological processes) have been reduced to include those processes essential to represent sediment transport and surface water routing. MOSM is

designed to be constrained by the best available existing information including stream gaging records, a complete watershed sediment budget, historical trends in the watershed, and independent measures of outputs, such as sediment fingerprinting and a suit of geomorphic change detections.

MOSM, like many previous watershed simulation models, is subject to uncertainties from model structure, as well as natural variability and data observation errors (Beven, 2001). Such sources of uncertainty are inherent in environmental decision-making and can profoundly affect the quality of decisions, so the uncertainties in model predictions associated with all aspects of the decision-making should be expressed explicitly (Ascough II et al., 2008). As described in Chapters 3 and 4, which present Topofilter concept and simulation of sediment delivery from various sources, we address the issue of model equifinality by using a wide range of plausible solutions rather than a single calibrated optimal solution. MOSM tracks a subset of uncertainties associated with evaluating sediment delivery (those due to equifinality resulting from limited gaging records of sediment and model structure), and explicitly quantifies their effects on model predictions of sediment loadings.

MOSM was developed in a collaborative environment of scientists, engineers, and economists from three research universities (Johns Hopkins University, University of Minnesota, and Utah State University), and with stakeholder groups familiar with the watershed (agricultural producers, conservation groups, and members of local regulatory agencies). This collaborative development helped to identify relevant and plausible environmental management alternatives to include in the model, and guided development of the model structure, input data, and decision analysis.

The framework for developing MOSM, including collaboration with stakeholders and scientific experts (Chapter 2), and development of Topofilter (Chapters 3 and 4) and the near-channel source (NCS) sediment loading model (SL_{NCS} model) (Chapter 5) provides a broader template for water quality models that can provide a practical representation of the watershed processes for the purpose of watershed scale environmental management evaluation.

In this chapter, we start by describing the overall structure of MOSM (Section 6.2). We then provide details on computational modules of MOSM: sediment loading and delivery module (6.3), water routing module (6.4), and management option allocation module (6.5). The chapter concludes by documenting the procedures to compute the management scenario cost (6.6). Appendix 6.A outlines all the management options considered and describes spatial analysis to determine their extents. Appendix 6.B. shows the Visual Basics for Application (VBA) codes corresponding to the computational modules described in this chapter.

6.2. Model structure

MOSM consists of three primary modules: 1) management option (MO) allocation, 2) hydrologic routing, and 3) sediment delivery and loading modules. MOSM allocates MO sites first, then simulates river discharge to estimate impacts on near-channel sediment supply (NCSS) from peak flow attenuation. Finally, the model calculates the total sediment loading resulting from MOs that reduce peak flow and MOs that reduce sediment production or delivery.

First, the user specifies the extent and location of different MO and the model allocates individual MO sites according to the rules to be defined in Section 6.5 (i.e., the

model allocates MO sites according to site selection prioritization rules determined using different geospatial characteristics such as geographic location, landuse/landcover, and topographic characteristics). The user specifies the amount of each MO within three zones within each of the three main subwatersheds of the Le Sueur River Basin (LSRB): Maple (MAP), Cobb (COB), and Le Sueur (LES) subwatersheds. The incised portion of each subwatershed is defined as one zone (zone 3) and the larger, upper, flat part of the watershed is divided into two zones (zones 1 and 2), one closer and one further from the incised zone, in order to capture the aggregate effect of travel time on model results (see Figure 6.1 for subwatershed and zone delineation). The maximum extent for each MO across the watershed was determined from a spatial analysis using topography and land use as described in Appendix 6.A. The maximum extent for each MO serves as an upper extent of total available sites to implement management. MO allocation module is described in detail in Section 6.5.

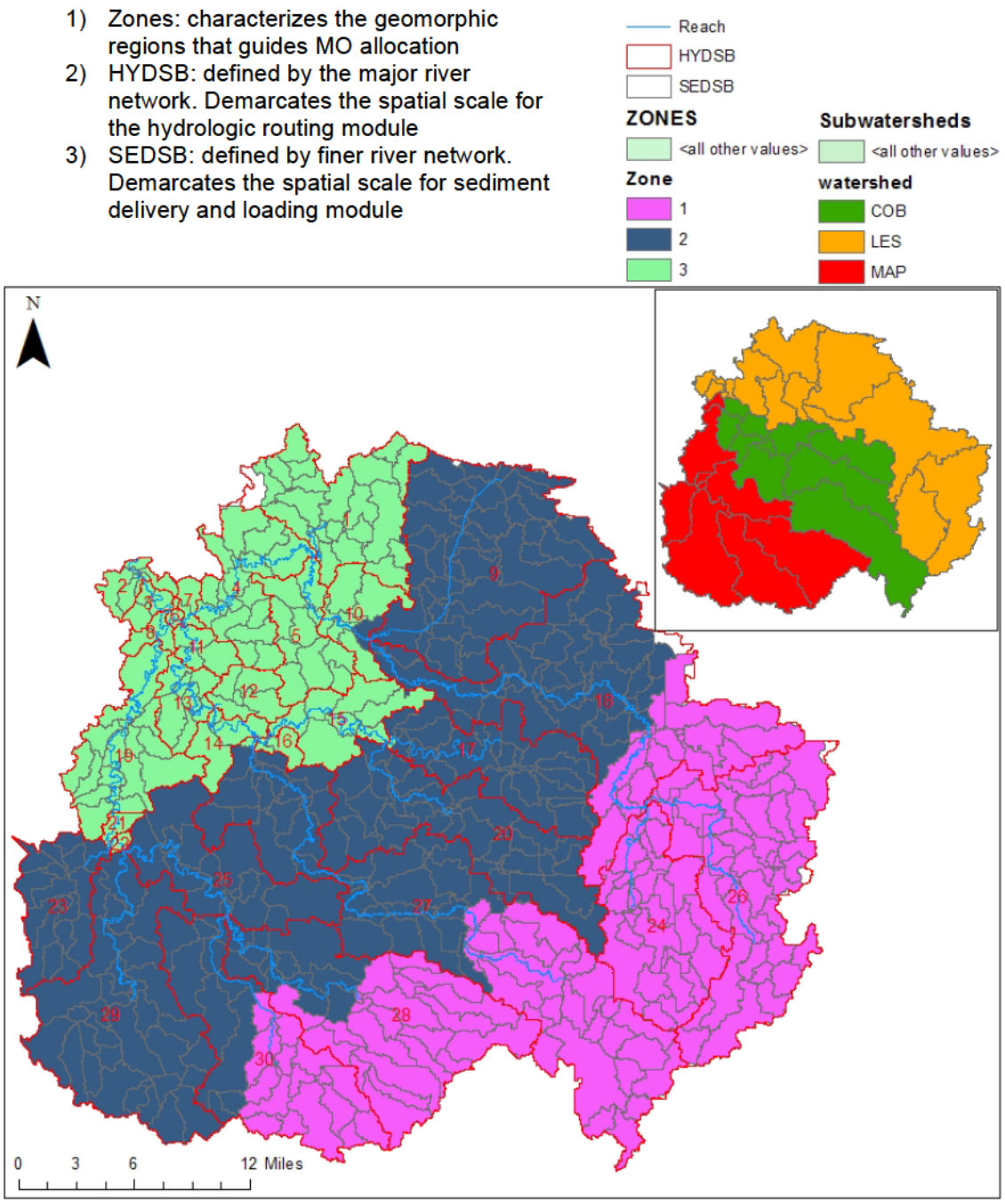

Figure 6.1: The Le Sueur River basin (LSRB) is divided into three zones: upland zone (zone 1), transitional zone (zone 2), and incised zone closest to the moth of the watershed (zone 3). The LSRB is divided into three watersheds: Maple (MAP), Cobb (COB), and Le Sueur (LES). The watershed and zone locations of management options can be specified for site allocation (Section 6.5). The LSRB is further divided into HYDSBs and SEDSBs, functional delineations applied for Hydrologic routing (Section 6.4) and for sediment delivery and loading (Section 6.3)

The second primary module simulates movement of water through hydro subbasins (HYDSBs) to watershed outlet. The LSRB is divided into 30 HYDSBs (Figure 6.1) to simulate daily discharge over multiple years at a reasonable computation time so the delineation for water routing is coarser than the one for sediment routing. Water routing module evaluates management options (MOs) whose purpose is to reduce sediment loading from near channel sources (NCSs) by storing water in the watershed. Such options are water conservation MO (WCMO) and in-channel water conservation MO (ICMO) that store water in the field or in ditches, respectively. Thus, an important function of MOSM is to calculate the sediment loading reduction from near-channel sources (NCS) using the simulated daily river discharge and SL_{NCS} model from Chapter 5 (together with MOs implemented to make near-stream sources less vulnerable to erosion (e.g., hardening of toes of bluffs), which is simulated in the sediment delivery and loading module). Hydrologic routing module, along with definition of SL_{NCS} model, is described in Section 6.4.

The third primary module simulates average annual sediment loading from sediment subbasins (SEDSBs) across the watershed. This is the other primary function of MOSM: to address the impact of MOs implemented in the watershed either to prevent erosion in fields, edges of ravines, and bluffs, or to trap sediment in its path on field. There are 529 SEDSBs in the LSRB that allows higher resolution in annual sediment delivery simulation. This spatial scale is consistent with Topofilter, from which this module obtains the distribution of plausible sediment delivery ratio (*SDR*) values and aggregate soil loss in each SEDSB. MOSM is tuned to a reference period of 2006-2010 to simulate mean annual sediment loading because the Topofilter simulation depends on observation

data and the LSRB watershed sediment budget that was available for this period. This module predicts sediment-loading reduction from 1) reducing soil erosion with tillage MOs (TLMO); 2) reducing field sediment delivery to stream with agricultural field MO (AFMO) such as grassed waterways, WCMO such as wetland or sediment pond, buffer MO (BFMO) such as stream buffers; and 3) reducing NCS loading with ravine MO (RAMO) by protecting ravine tips and buffer MO (NCMO) such as bluff toe protection or repair. Sediment delivery and loading module is described in Section 6.3.

6.3. Sediment loading and delivery

As described in Section 6.2, there are three primary modules in MOSM. In this section, we describe sediment loading and delivery module first as this is the core of the model. In Sections 6.3 and 6.4, we describe the water routing and management option allocation modules.

MOSM allocates soil erosion and storage across the watershed based on gage data, a watershed sediment budget, and Topofilter simulation outputs with the reference observation period of 2006-2010. The central challenge was to develop a model that provides a reasonably accurate accounting of sediment sources reflecting the sediment budget results and observational data. MOSM utilizes high-resolution topography through Topofilter to simulate highly resolved and stochastic sediment delivery across the watershed (see Chapter 4). This approach, in contrast to spatially-lumped or – distributed, process-based models (Section 2.2), offers the simplest possible routing model using sediment delivery ratio values that rely explicitly on observation data.

The sediment loading and delivery module estimates the effects of an individual management option by altering the relevant sediment production rates and/or *SDR* values at each SEDSB (Figure 6.2):

(1) If tillage management option (TLMO) is implemented in SEDSB j, consisting of different proportions of conventional, reduced, and conservation tillage, then the sediment module calculates the changes in soil erosion rate (SE_j, Mg/yr) compared to the reference period rate (defined from 2006-2010 observation data) (Section 6.3.2).

(2) If AFMO, WCMO, and/or BFMO type of MO is implemented in SEDSB j, the sediment module calculates the changes in the field sediment delivery ratio ($SDRf_j$) for areas controlled by these MOs. NOMO is the area unaffected by management that is incorporated in the overall calculation of aggregate sediment delivery from the SEDSB (Section 6.3.3).

If a RAMO or NCMO type of MO is implemented in SEDSB j, then the sediment module calculates the changes in the sediment input rates from ravines (SI_{R_j}) and bluffs (SI_{B_j}), along with sediment input from field (SI_{F_j}), and calculates the resulting sediment loading (SL_j) using the stream sediment delivery ratio ($SDRs_j$) (6.3.4).

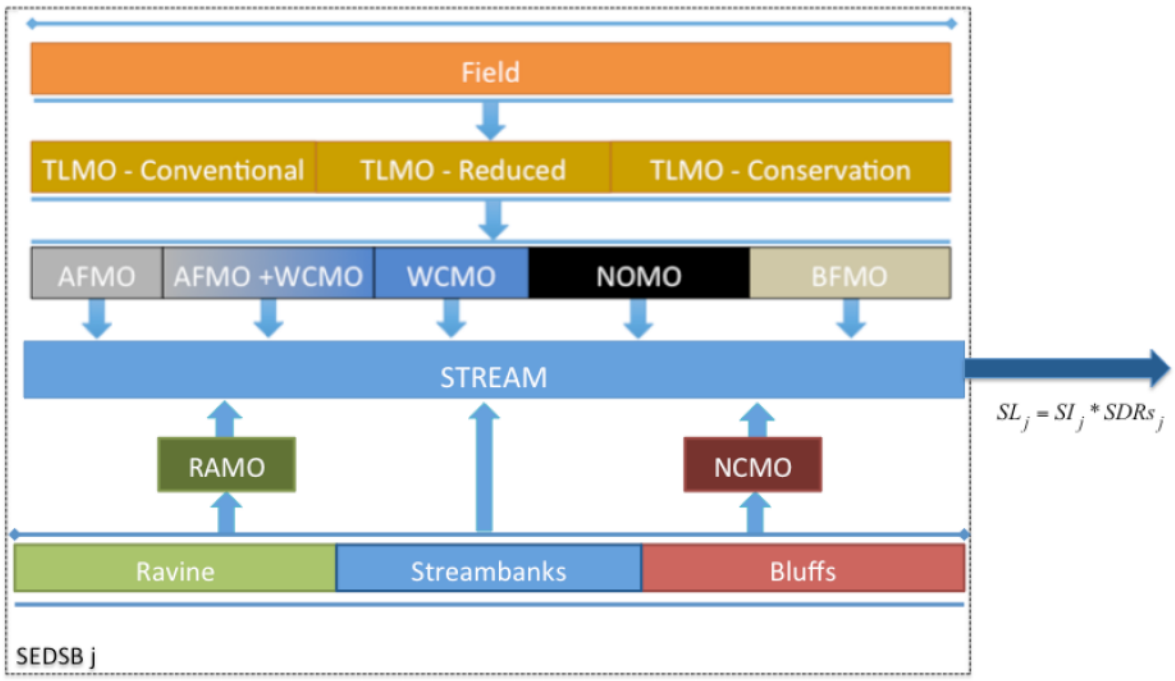

Figure 6.2: a schematic of sediment loading simulation in the MOSM. Sediment inputs (SI) consist of sediment loading from field, ravines, streambanks, and bluffs. Detailed elements in the figure are described in Section 6.3.2 through 6.3.4.

We do not assign a MO that directly reduces sediment input from streambanks. It is difficult to identify specific candidate streambank management sites along with potential sediment supply rates because streambank loading rates are determined at the regional

scale where the loadings were defined for the entire regions above, between, and below upper and lower gages (see Chapter 4.3.3). Since bluffs contribute more significantly to near-channel sediment supply (NCSS) compared to streambanks (i.e., bluff loading in the incised and transitional zones of the LSRB is about nine time greater than streambank loading) (Gran et al., 2011), it is likely to be more effective to focus environmental investment on bluffs rather than other types of streambank erosion control measures.

6.3.1. Uncertainty and its propagation in sediment loading prediction

MOSM may be executed using the deterministic setting where the optimal set of *SDRf* and *SDRs* over all SEDSBs is used. The optimal set of *SDRf* and *SDRs* predicts watershed sediment loading that is closest to the observed loading (see Section 4.4.4). MOSM may be executed using the stochastic setting where *SDR* values are obtained from all plausible solutions of *SDRf* and *SDRs* at each SEDSB (see Chapter 4.4.1 through 4.4.3). The variability in the observed sediment loading at the gages may be caused by the variability in soil erosion rates and the transport process. Thus, we evaluate the uncertainty associated with sediment transport process and consequent variability in sediment loading (*SL*) predictions using Topofilter. In the following paragraphs, we first describe the sediment loading calculation followed by sediment delivery ratio calculation.

The sediment loading and delivery module calculates the fraction of eroded sediment delivered to the watershed outlet from each SEDSB j (see Figure 6.1 for all SEDSB j=1,…529) by randomly selecting from the plausible *SDR* values within the probability distribution determined from Topofilter. First, the module accesses the Topofilter simulation outputs of plausible field *SDR* values ($SDRf_j$) to calculate sediment input to stream (SI_{F_j}) at each SEDSB j [6.1]. Additionally, the module accesses the sediment

input from streambanks (SI_{S_j}), ravines (SI_{R_j}), and bluffs (SI_{B_j}) to stream at each SEDSB j [6.2]. Then, the fraction of total sediment input to stream (SI_j) delivered to the watershed outlet is calculated using $SDRs_j$[6.3]. Total sediment loading at the outlet of each Topofilter watershed (Toposhed) (SL_T) is calculated by summing over the SEDSBs in each Toposhed. Toposheds are conglomeration of SEDSBs defined by the stream gages located above the incised zone (equivalent to areas covered by zones 1 and 2), and another at the mouth of the LSRB (equivalent to areas covered by zone 3) (Chapter 4, Figure 4.2). Following are reiteration of sediment loading formulations introduced in Chapter 4:

$$\square I_{F_j} = SE_j * SDRf_j \qquad [6.1]$$

$$SI_j = SI_{F_j} + SI_{S_j} + SI_{R_j} + SI_{B_j} \qquad [6.2]$$

$$SL_T = \sum_{j=1}^{N_T} SL_j = \sum_{j=1}^{N_T} SI_j * SDRs_j \qquad [6.3]$$

where SE_j is the annual soil loss rate and SL_j is the sediment loading from SEDSB j. The calculations of [6.1] to [6.3] are repeated for a user-specified number of Monte Carlo (MC) iterations up to 1000 times where $SDRf_j$ is randomly selected from its probability density function (PDF), and $SDRs_j$ is calculated using a random combination of parameter values selected from the conditioned parameter space identified in Topofilter simulation (see Chapter 4.3.5 for the conditioned parameter space and Chapter 4.4 for the resulting distributions of $SDRf_j$ and $SDRs_j$).

As discussed in detail in Chapter 4.3.3, sediment delivery ratio on field is calculated for all raster cells i in each SEDSB by applying parameter sets, a_1 and b_1 within

conditioned parameter space (see Chapter 4.3.3 equation [4.1] for $SDRf_{ij}$). Then, the average *SDRf* of a SEDSB j ($SDRf_j$) is calculated by dividing the total sediment input to stream from all raster cells in the SEDSB by its total soil erosion at each Monte Carlo (MC) realization (see Chapter 4.3.3 equation [4.2] and [4.3]). PDF of $SDRf_j$ is developed from all MC realizations (examples can be found in Chapter 4, Figure 4.9). For this reason, we couldn't directly apply parameter sets, a_1 and b_1 from conditioned parameter space to calculate *SDRf*. Rather, we use the mean and standard deviation of PDF at each SEDSB j to calculate $SDRf_j$.

SDRs of a SEDSB j ($SDRs_j$) is calculated by applying parameter sets a_2 and b_2 given the flow length, cumulative floodplain area, and elevation change to Toposhed outlet at the SEDSB. So, the module randomly generates parameter values a_2 and b_2 from the conditioned parameter space to directly calculate $SDRs_j$ at each SEDSB j using:

$$SDRs_j = \exp\left(a2\left(\frac{\Delta E_{s_j}}{L_{s_j}}\right)^{b2} Af_j\right) \qquad [6.4]$$

Where $\frac{\Delta E_{s_j}}{L_{s_j}}$ and Af_j are gradient and cumulative floodplain area from SEDSB j to Toposhed outlet, which are topographic variables defined at each SEDSB (Section 4.3.3).

To summarize, MOSM utilizes Topofilter outputs at each SEDSB to estimate *SL* at the Toposhed outlets: 1) the model uses the mean and standard deviation derived from a PDF of average $SDRf_{ij}$ over all raster cells in SEDSB j ($SDRf_j$); and 2) the model randomly generates plausible parameter sets, a_2 and b_2 within the conditioned parameter space to calculate *SDRs* at each MC iteration. There is an inconsistency introduced by this design decision where *SDRf* is calculated from its PDF and *SDRs* is calculated using

its parameters with topographic variables using [6.4]. For future model development, we recommend utilizing the PDF of *SDRs* as well as *SDRf* to calculate *SL*.

The model doesn't consider all the uncertainties associated with attributing *SL* to particular locations in the watershed. It doesn't consider uncertainties in USLE prediction of mean annual soil erosion rates (*SE*) (Parysow et al., 2003; W. C. Hession et al., 1996). Different *SE* values will affect the calculation of *SDR* values (see Chapter 3.5); a larger *SE* given the same *SL* observations at the watershed outlet will result in distribution of generally lower *SDR* values across the watershed, and vice versa. One way to include uncertainty analysis in *SE* is to assign another uncertainty parameter that could similarly be conditioned along with parameters on the topographic variables. This has not been done here, but could be the subject of future research; instead we used daily application of modified USLE for 33 years to calculate the mean annual *SE* as a constant boundary condition for Topofilter simulation. Given the extensive field work to develop and verify the USLE, and fairly constant landcover/landuse and land management in the recent years, we assumed that mean annual soil erosion will be constant over the reference period. Of course, there are observations of changing rainfall patterns in the study watershed (Novotny and Stefan, 2007) that will affect the USLE calculation. So, for the prediction of future conditions, given the possibility changing rainfall patterns and widespread landcover/landuse change as well as the well-documented uncertainties in USLE (Parysow et al., 2003; W. C. Hession et al., 1996), modeling uncertainty in *SE* within the Topofilter will be advisable.

6.3.2. Sediment erosion reduction by three TLMO types

TLMO's primary function that is simulated by MOSM is reduction in sediment erosion rates *SE* at individual SEDSB (Figure 6.3). Tillage practice is typically simulated in watershed models by imposing different sediment loss under different tillage scenarios (Folle et al., 2009). Similarly, this subsection describes how we calculate soil erosion under different composition of conventional, reduced, and conservation tillage practices.

To begin with, all agricultural land is assigned to one of three classes of tillage (Appendix 6.A). The three types, in decreasing order of sediment erosion rate, are conventional tillage, reduced tillage, and conservation tillage. The effect of tillage practice on soil erosion rate *SE* [Mg/yr] at each SEDSB is expressed as an area-weighted average for each practice:

$$SE = \left| T_1 \frac{A_{a1}}{A_a} + T_2 \frac{A_{a2}}{A_a} + T_3 \frac{A_{a3}}{A_a} \right| SE_{mx} \qquad [6.5]$$

where SE_{mx} is the soil erosion rate for conventional tillage; T is a tillage factor (Table 6.1) and the agricultural area A_a of each SEDSB is composed entirely of the three tillage types ($A_a = A_{a1} + A_{a2} + A_{a3}$). The tillage factor is derived from the USLE C factor that represents the cover-management including landuse, crop canopy, surface cover, and surface roughness (Renard, 1991).

Table 6.1: Reference C factor of the USLE (Stone and Hilborn, 2000)

Tillage Method	Equivalent TLMO	Factor
Fall plow	T_1	1
Spring plow	T_1	0.9
Mulch tillage	T_2	0.6
Ridge tillage	T_2	0.35
Zone tillage	T_3	0.25
No-till	T_3	0.25

The mean annual soil erosion rate at each SEDSB is a model input and based on a USLE simulation within SWAT model for a 33 yr period (1981-2014)(Kumarasamy and Belmont, 2014). These erosion rates were used to develop sediment delivery ratios for the reference period 2006-2010 over which the Topofilter parameter space is conditioned against observed water quality data (see Chapter 4, Table 4.1). Soil erosion rates of the non-agricultural area in the SEDSB are unaffected by TLMO application, where the reference period soil erosion rates are not changed.

Tillage class proportions were not explicitly defined in the SWAT USLE runs for each area (Kumarasamy and Belmont, 2014), so assumptions are needed to account for the tillage practice in place during the reference period. According to a 2007 tillage transect survey report by the Water Resources Center of the Minnesota State University, conventional, reduced, and conservation tillage were of approximately equal area in the Le Sueur River Basins (Fisher and Moore, 2008). Based on this assumption, and using [6.5] , the soil erosion rate for the reference period is then:

$$SE_R = \left[T_1 \frac{1}{3} + T_2 \frac{1}{3} + T_3 \frac{1}{3}\right] SE_{mx} \qquad [6.6]$$

where SE_R is the USLE estimate of soil erosion rate cumulated over each SEDSB and we assume no spatial correlation between tillage practice and local SE.[1] Using erosion factors of $T_1 = 1$ (conventional tillage), $T_2 = 0.5$ (reduced tillage), and $T_3 = 0.25$ (conservation tillage) from Table 6.1 in [6.6] gives (i.e., the reference period tillage scenario of equal distribution of conventional, reduced, and conservation tillage practices produces 7/12 of soil erosion compared to solely implementing conventional till):

[1] This is a strong assumption because in fact less erosive tillage practices might be more attractive in more erosive areas.

$$SE_R = \frac{7}{12} SE_{mx} \quad [6.7]$$

Using [6.6] to replace SE_{mx} in [6.7], we can evaluate the new soil erosion rate, SE_N under conditions different from the reference condition (i.e., different combinations of T_1, T_2, and T_3) relative to the reference period using:

$$SE_N = \left\lceil T_1 \frac{A_{a1}}{A_a} + T_2 \frac{A_{a2}}{A_a} + T_3 \frac{A_{a3}}{A_a} \right\rceil \frac{12}{7} SE_R \quad [6.8]$$

[6.8] indicates that if only conservation tillage is implemented, 3/7 of soil erosion of solely implementing conventional till would be produced.

6.3.3. Sediment delivery reduction from AFMO, WCMO, and BFMO

After calculating the mean annual soil erosion rate from implementing TLMO in agricultural land of each SEDSB using [6.8], the next step is to calculate the effects of management options on reducing delivery of field-eroded sediment (Figure 6.3). Three on-field MOs are defined for this purpose: agricultural field management options (AFMO) for which grassed waterways serve as a typical example, water conservation management options (WCMO), which can store sediment as well as water, and buffer strip management options (BFMO), which can store sediment in buffer areas along waterways. For each MO, the reduction in sediment delivery is accomplished by reducing *SDRf* in [6.1] by an efficiency *E* defined for each MO or combination of MOs. The model output depends on MO effectiveness and cost inputs, and these inputs can be changed to represent different specific management alternatives.

In general, BFMO operates in different areas than AFMO and WCMO; BFMO acts to trap sediment eroded from areas proximal to streams, whereas AFMO and WCMO generally act to trap sediment derived higher in the SEDSB, further from streams. To

accommodate this distinction, we divide the contributing area A of the SEDSB into two parts: $A = A_p + A_f$, where A_p is the portion of SEDSB area that is proximal to the stream network and A_f is the remaining SEDSB area further from waterways. Different sediment delivery ratios on field are defined: SDR_{fp} and SDR_{ff} for the proximal and far field locations, respectively. Operationally, we define A_p as the area within 100 m of the stream network and A_f as the balance of the SEDSB area. This distinction is important because the Topofilter analysis shows that the field sediment delivery ratio is much larger closer to waterways than it is further away (see Chapter 4, Figure 4.10 for the comparative distributions of SDR_f, SDR_{fp}, and SDR_{ff}). With partitioned sediment inputs from A_p and A_f, sediment input from field to stream for the reference period (SI_{FR}) with on-field MO implementation is:

$$\left[\begin{array}{l}\left(\begin{array}{l}(1-E_g)\frac{A_{gR}}{A}+(1-E_g)(1-E_w)\frac{A_{gwR}}{A}+(1-E_w)\frac{A_{wR}}{A}+\\ \frac{\left(A_f-(A_{gR}+A_{gwR}+A_{wR})\right)}{A}\end{array}\right)SDRf_f+\\ \left((1-E_b)\frac{A_{bR}}{A}+\frac{A_p-A_{bR}}{A}\right)SDRf_p\end{array}\right]SE_R = SI_{FR} \qquad [6.9]$$

where E_g, E_w, E_b are efficiencies for AFMO, WCMO, and BFMO, and A_{gR}, A_{wR}, and A_{bR} are the contributing areas to AFMO, WCMO, and BFMO in the reference period, respectively. A_{gwR} accounts for overlapped contributing area of A_{gR} and A_{wR} (see Section 6.3.3; in Figure 6.2 indicated as AFMO+WCMO) under the assumption that combined effectiveness is less than the sum of individual effects. Equation [6.9] may be rearranged and simplified:

$$\left[\frac{\left(A_f - E_g A_{gR} - (E_g + E_w - E_g E_w)A_{gwR} - E_w A_{wR}\right)SDRf_f + \left(A_p - E_b A_{bR}\right)SDRf_p}{A}\right] SE_R = SI_{FR} \quad [6.10]$$

The quantity in the square brackets of [6.9] and [6.10] is the area-weighted, or lumped field sediment delivery ratio for the reference period, $SDRf_R$. That is, it is the delivery ratio calculated based on the watershed-scale topographic analysis linking SE_R to sediment loading observed over the reference period at the stream gages.

For future conditions with different TLMO implemention, using subscript *N*, we rewrite Equation [6.9]:

$$\left[\begin{array}{l}\left((1-E_g)\frac{A_{gR}+A_{gN}}{A} + (1-E_g)(1-E_w)\frac{A_{gwR}+A_{gwN}}{A} + (1-E_w)\frac{A_{wR}+A_{wN}}{A} + \right.\\ \left.\frac{\left(A_f - (A_{gR}+A_{gN}+A_{wR}+A_{wN})\right)}{A}\right)SDRf_f + \\ \left((1-E_b)\frac{A_{bR}+A_{bN}}{A} + \frac{\left(A_p - (A_{bR}+A_{bN})\right)}{A}\right)SDRf_p\end{array}\right] SE_N = SI_{FN} \quad [6.11]$$

where A_{gN}, A_{wN}, and A_{bN} are *additional* contributing areas to AFMO, WCMO, and BFMO, respectively, relative to the reference period (Note: while we don't know the areas allocated to these MOs during the reference period in [6.9], we know the sediment loading so we attribute MO extent inputs in MOSM as *additional* areas to the reference condition). A_{gwN} is the contributing area in overlap between A_{gN} and A_{wN} (see Section 6.3.4). SE_N, the soil erosion from agricultural areas of SEDSB with TLMO practice scenario specified in MOSM. SE_N is determined by Equation [6.8] and accounts for the effect of a TLMO distribution different from the reference condition (which assumes 1/3 of the watershed under each type of tillage, as explained above). The term in the bracket of [6.11] is SDR_{fN}, area-weighted field sediment delivery ratio for the future conditions of MO implementation simulated in MOSM:

$$SDRf_N = \left[\begin{array}{l} \left((1-E_g)\frac{A_{gR}+A_{gN}}{A} + (1-E_g)(1-E_w)\frac{A_{gwR}+A_{gwN}}{A} + (1-E_w)\frac{A_{wR}+A_{wN}}{A} + \right. \\ \left. \frac{\left(A_f - (A_{gR}+A_{gN}+A_{wR}+A_{wN})\right)}{A} \right) SDRf_f + \\ \left((1-E_b)\frac{A_{bR}+A_{bN}}{A} + \frac{\left(A_p - (A_{bR}+A_{bN})\right)}{A} \right) SDRf_p \end{array} \right] \quad [6.12]$$

A relation is needed to define this $SDRf_N$ in terms of sediment delivery ratio during reference period, $SDRf_R$ ($SDRf$ with unknown management extent during the reference period in the bracketed term in [6.9]), which is available from the TopoFilter analysis (see Chapter 4.3.3) as described in the beginning of Section 6.3. Thus, SDR_{fN} is further decomposed and expressed in terms of SDR_{fR}:

$$\begin{aligned} SDRf_N &= \left[\begin{array}{l} \left((1-E_g)\frac{A_{gR}+A_{gN}}{A} + (1-E_g)(1-E_w)\frac{A_{gwR}+A_{gwN}}{A} + (1-E_w)\frac{A_{wR}+A_{wN}}{A} + \right. \\ \left. \frac{\left(A_f - (A_{gR}+A_{gN}+A_{gwR}+A_{gwN}+A_{wR}+A_{wN})\right)}{A} \right) SDRf_f + \\ \left((1-E_b)\frac{A_{bR}+A_{bN}}{A} + \frac{\left(A_p - (A_{bR}+A_{bN})\right)}{A} \right) SDRf_p \end{array} \right] \\ &= \left(\frac{A_f - E_g(A_{gR}+A_{gN}) - (E_g + E_w - E_gE_w)(A_{gwR}+A_{gwN}) - E_w(A_{wR}+A_{wN})}{A} \right) SDRf_f + \\ &\quad \left(\frac{A_p - E_b(A_{bR}+A_{bN})}{A} \right) SDRf_p \\ &= \left[\begin{array}{l} \frac{\left(A_f - E_gA_{gR} - (E_g + E_w - E_gE_w)A_{gwR} - E_wA_{wR}\right) SDRf_f + \left(A_p - E_bA_{bR}\right) SDRf_p}{A} - \\ \frac{\left(E_gA_{gN} + (E_g + E_w - E_gE_w)A_{gwN} + E_wA_{wN}\right) SDRf_f + E_bA_{bN}SDRf_p}{A} \end{array} \right] \\ &= SDRf_R - \frac{\left(E_gA_{gN} + (E_g + E_w - E_gE_w)A_{gwN} + E_wA_{wN}\right) SDRf_f + E_bA_{bN}SDRf_p}{A} \end{aligned} \quad [6.13]$$

After calculating sediment erosion as a result of TLMO implementation (SE_N) using [6.8], sediment delivery rate from field to stream as a result of implementing AFMO, WCMO, and BFMO is calculated using [6.13]. The area affected by these management

options is calculated based on topographic analysis and described in Section 6.3.4. Sediment loading from field to stream with on-field MO implementation is (Figure 6.3):

$$SI_{FN} = (SE_N)(SDRf_N) \qquad [6.14]$$

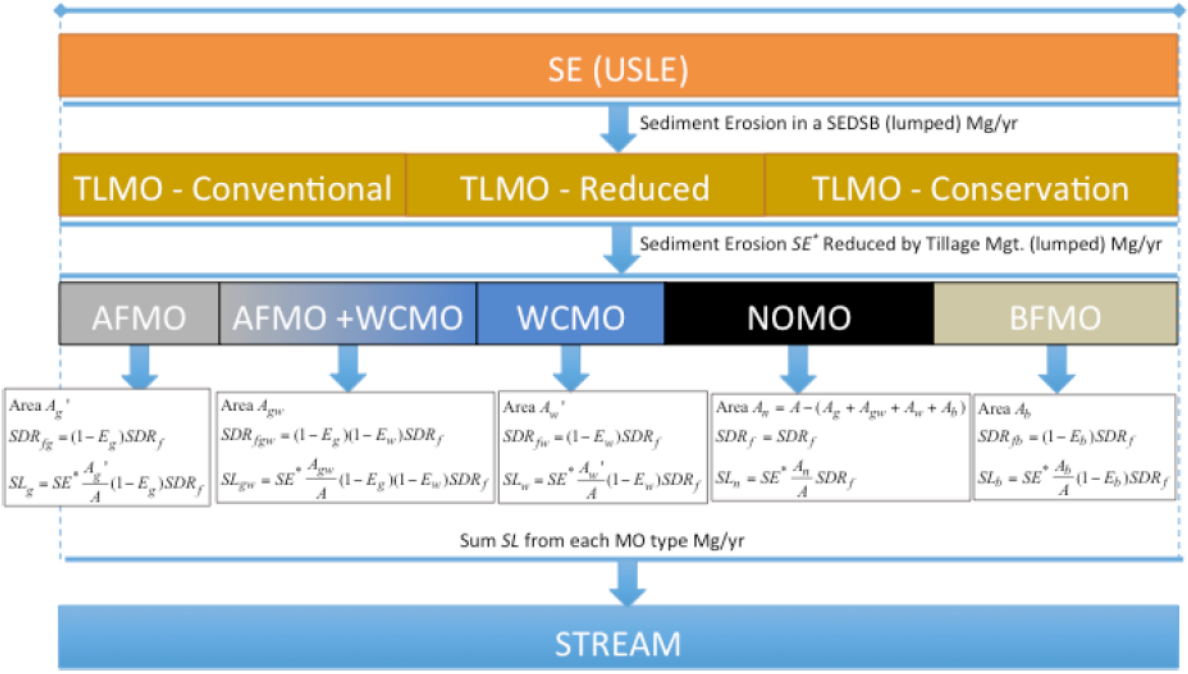

Figure 6.3: This figure shows the part of Figure 6.2 containing the on-field management options (MOs) including agricultural field MO (AFMO), water conservation MO (WCMO), and buffer strip MO (BFMO). This figure illustrates the individual effects of these MOs described in Section 6.3.3.

6.3.4. Contributing areas of BFMO, AFMO, and WCMO

Above section describes calculation of how on-field MOs, BFMO, AFMO, and WCMO change sediment delivery from field, and an important part of the calculation involves the areas contributing sediment to on-field MOs. In this section, we explain how the contributing areas (A_{gN}, A_{wN}, At_{wN}, and A_{bN} in [6.13] in Section 6.3.3) are calculated at each SEDSB.

Each MO affects the sediment loading from its contributing area. Considering first BFMOs, for an individual BFMO site k, contributing area, A_{bN_k} is calculated assuming that it intercepts sediment traveling with runoff from adjacent parallel area within some

uniform sheet flow length (in other words, the extent of drainage area is calculated by assuming that BFMO drains the surrounding area determined by some uniform length perpendicular to BFMO). BFMO contributing area from all selected sites in each SEDSB is the sum of individual contributing areas of sites, A_{bN_k}, $k \in K$.

$$A_{bN} = \sum_{\in K} A_{bN_k} = \sum_{k \in K} L_{b_k} \left(U + w_{b_k}\right) \quad [6.15]$$

where L_{b_k} and w_{b_k} are the length and width of a BFMO site k. BFMO site length is determined from the spatial analysis (Appendix 6.A.2.3), and width of individual site k is determined according to the buffer law that states 16.5-foot buffer is required for public ditches and 50-foot buffer is required for public waters (MNDNR, 2017). U is the assumed uniform sheet flow length of the surrounding area, and its default value is set at 100m, so for example, if a BFMO site is 1,000 meters long, then its drainage area would be 100,000 m^2 plus the surface area of the BFMO.

Meanwhile, an AFMO, such as a grassed waterway, would intercept and store sediment inflow from its upstream contributing area (Fiener and Auerswald, 2003). A_{gN} is calculated using the mean flow accumulation values over the AFMO sites with a 3-m DEM (i.e., the upstream contributing area is flow accumulation value multiplied by the area of raster cell, in this case $9m^2$). Flow accumulation of a cell indicates the number of upstream cells that flow into that cell according to surface topography defined by the DEM (Jenson and Dominque, 1988). Upstream contributing area generally increases with the length of individual AFMO sites while there are AFMO sites with wide range of drainage area given same extent (Figure 6.4 shows the length of individual AFMO sites and corresponding drainage area). Within each SEDSB, multiple individual AFMO sites

(A^o_{gNk} for $k \in K$) may be selected, in which case the contributing area of all selected AFMOs sites, not affected by WCMO's drainage area, (A^o_{gN}) is the sum of individual contributing areas of selected AFMO sites $k \in K$:

$$A^o_{gN} = \sum_{k \in K} A^o_{gNk} \qquad [6.16]$$

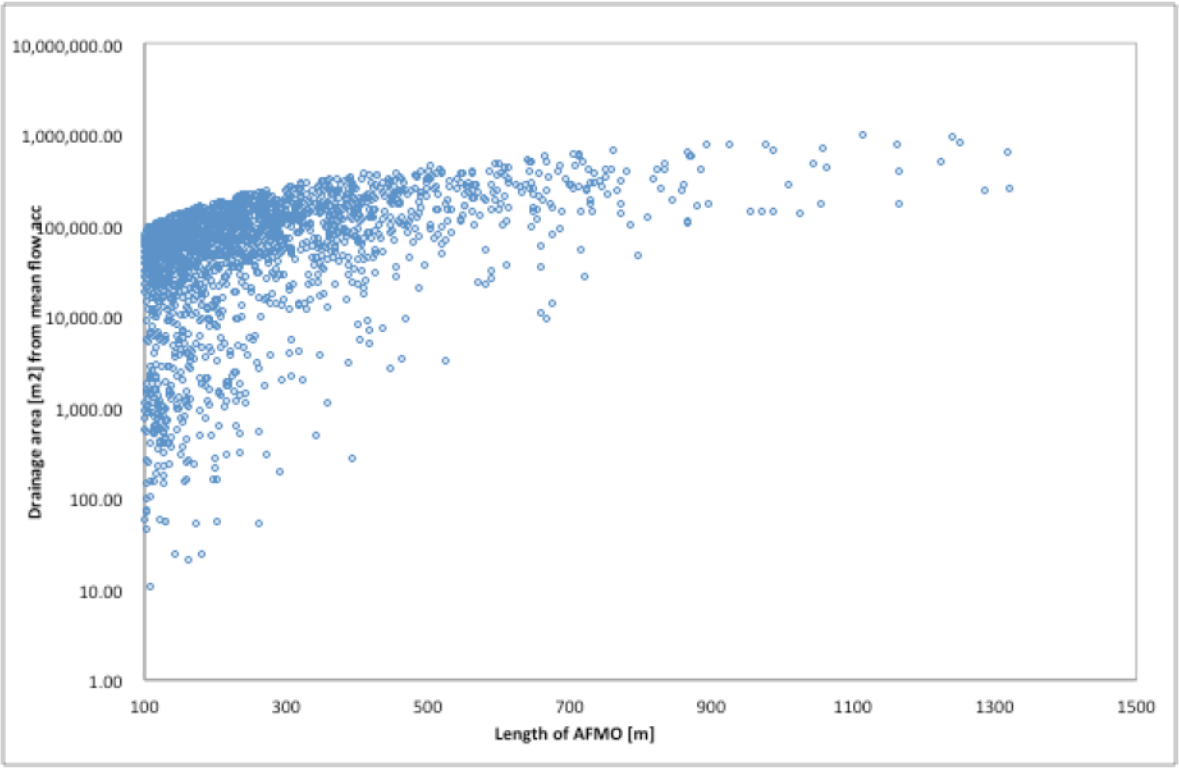

Figure 6.4: Contributing drainage area of individual AFMO site is estimated using flow accumulation values of 3-m DEM (product of flow accumulation and area of raster cell), and varies with length of AFMO sites. The AFMO sites in the entire Le Sueur River Basin are shown in this figure. They are identified using spatial analysis described in Appendix 6.A

Total contributing areas of WCMO sites selected for simulation in each SEDSB are calculated in MOSM. It is assumed that when only a few WCMO sites are selected, the collective contributing area is close to the sum of individual sites' contributing areas (i.e., their contributing areas do not overlap). Individual WCMO's contributing area can be calculated using the relationship proposed by Mitchell (2015), a linear function fitted to

individual WCMO's surface area versus contributing area determined from a flow accumulation analysis.

However, as more WCMO sites are selected, their contributing areas begin to overlap one another because one WCMO is increasingly likely to be upstream from another. Thus, the contributing area of multiple selected WCMO sites (A^o_{wN}) is approximated using a negative exponential function with an upper bound equal to the total contributing area when all potential WCMO sites are implemented (A^o):

$$A^o_{wN} = A^o\{1 - \exp[-c \sum_{i=1}^{K} SA_k]\} \qquad [6.17]$$

where $A^o = A - A_{bN} - A_{n,min}$. A^o, the area in the further upland that is affected by WCMO (i.e., excluding the area affected by BFMO). $A_{n,min}$ is the user inputted minimum area not affected by any management options. This allows the user some flexibility to simulate the impact of areas in the subbasin that will remain outside of any contributing areas of MOs, no matter the extent of implementation). SA_k is the surface area of an individual WCMO (see Appendix 6.A for an explanation of the procedure used to determine individual WCMO sites in each SEDSB). The calibration parameter c is determined such that the slope of the exponential function when only a few WCMO sites are considered matches the linear relation Mitchell (2015) proposes for each individual WCMO site's contributing area.

When both AFMO and WCMO sites are selected in a given area j, their respective contributing areas (A^o_{gN} and A^o_{wN}) may overlap, and the area of overlap (A_{gwN}) is estimated assuming that the decisions to site them have a dependency. The below function generalizes this relationship, and accounts for minimum area not affected MO:

$$A_{gwN} = P_{gw} \cdot Min\left(A^o{}_{gN}, A^o{}_{wN}\right) + \left(1 - P_{gw}\right) \cdot Max\left(0, \left(A^o{}_{gN} + A^o{}_{wN}\right) - \right. \qquad [6.18]$$

$$\left(A - A_{bN} - A_{n,min}\right)\Big)$$

where: P_{gw} determines the degree of overlap between A°_{gN} and A°_{wN}; P_{gw} is a user input dictating the relative locations of AFMO and WCMO and the degree to which their contributing areas would overlap (Figure 6.5 shows an example where WCMO has larger contributing area than AFMO over the SEDSB, but the opposite case also applies in this module). For example, if P_{gw} is 0.5, then the larger contributing area of AFMO or WCMO subsumes half of the smaller contributing area of AFMO or WCMO. The complementary proportion, (1- P_{gw}) is applied only if $A^{\circ}_{gN} + A^{\circ}_{wN}$ does not exceed the available area of the watershed to prevent unrealistically large contributing area relative to the total available area in the SEDSB. Thus, the areal extents of AFMO and WCMO used to calculate SDR_{fN} in [6.13] are:

$$A_{gN} = A^{o}_{gN} - A_{gwN} \qquad [6.19]$$

$$A_{wN} = A^{o}_{wN} - A_{gwN} \qquad [6.20]$$

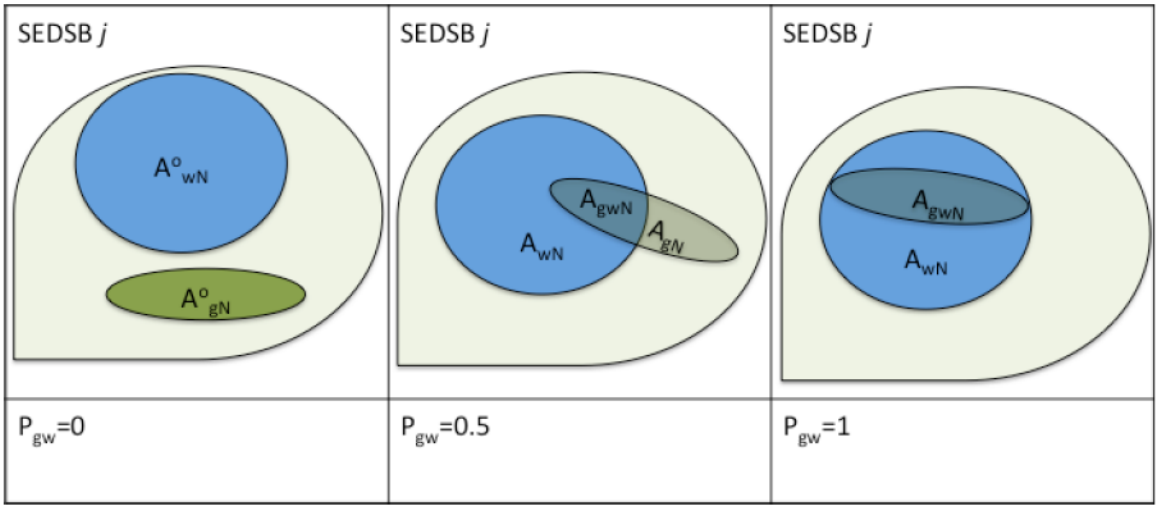

Figure 6.5: An illustration of application of Equation [6.18] for the case in which the contributing area of AFMO is smaller than WCMO (the equation works for the opposite case too) to approximate the overlapping contributing areas of the AFMO and WCMO with different overlapping factor, P_{gw}

6.3.5. Sediment loading reduction from RAMO

Ravines are one of the most prolific sediment sources in the watershed, although the total extent of ravines is small relative to bluffs, such that ravine sediment contribution to the overall sediment budget is smaller than that of bluffs (Gran et al., 2011). Ravines erode through incision and enlargement driven by concentrated flow that is often augmented by discharge from the outlets of field drainage tile systems (Ibid.).

Most commonly, ravine management is accomplished by arresting the extension of ravine tips into farmland using berms and ponds to capture the field runoff (Tran, 2015). Sediment reduction in MOSM is represented by ravine tip stabilization. There are 106 mapped ravines in the LSRB. Each ravine has between 1 and 39 tips (tips refer to steep, near vertical headcuts at the ravines), depending on the extent and location of the ravines (see Appendix 6.A.2.6). An estimated sediment loading rate per unit area of the ravine (0.002 Mg/m^2-yr)(Gran et al., 2011) is used to calculate the total annual loading rate from each mapped ravine. For each mapped ravine, sediment-loading rate per tip is calculated by dividing the ravine's loading rate by its number of tips. The fraction of sediment loading not associated with tip extension (i.e., sediment sourced from outside of ravine) is represented by the input parameter, (1-F_r). The ravine load affected by RAMO is calculated using the following equation for each SEDSB:

$$SI_R = \sum_{k \in N_r} L_k(R_k - r_k) + L_k \cdot F_r(1 - E_r)r_k + L_k \cdot (1 - F_r)r_k \qquad [6.21]$$

where

SI_R = Sediment input from N_r ravines to stream in a SEDSB [Mg/yr]

L_k = Ravine loading rate per tip [Mg/tip-yr] for ravine $k \in N_r$

R_k = Total number of tips in ravine k=1, …, N_r

r_k = Number of tips selected for RAMO implementation for ravine k

E_r =Effectiveness of RAMO

F_r = 0.8, Proportion of sediment generated within Ravine addressed by RAMO

Sediment delivery from ravines to the watershed outlet is calculated by multiplying SI_R [6.21] by SDR_s for each SEDSB and summed over all SEDSBs to estimate the total sediment loading from ravines (Figure 6.6).

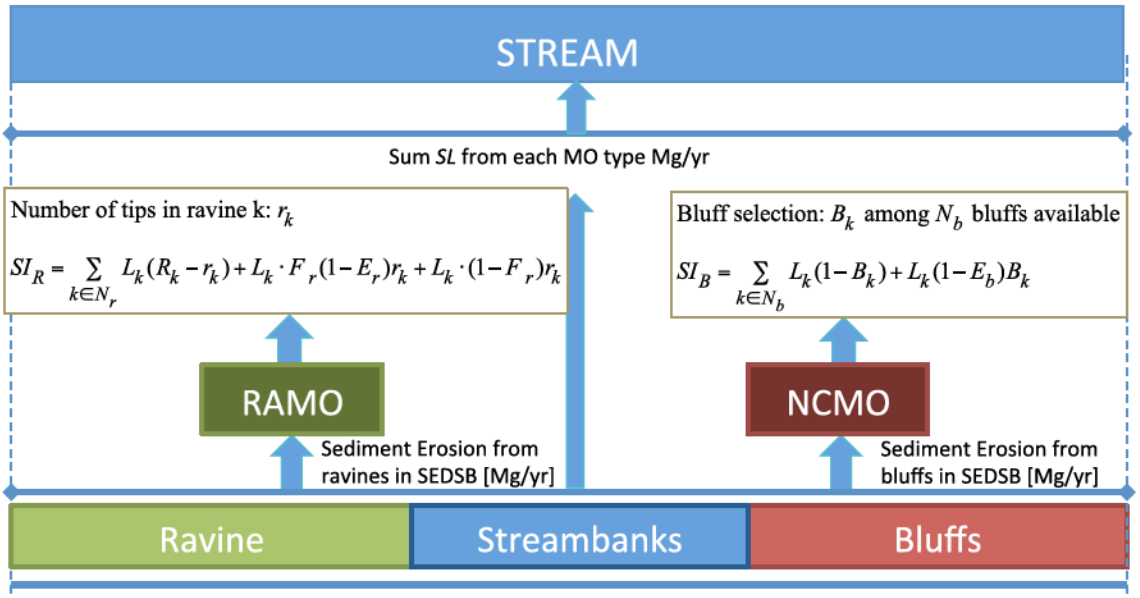

Figure 6.6: RAMO and NCMO reduce sediment inputs to stream directly. This figure Illustrates sediment inputs from ravines and bluffs and evaluation of RAMO and NCMO with the sediment reduction formulation at individual MO described in detail in Sections 6.3.5 and 6.3.6

6.3.6. Sediment loading reduction from NCMO

Bluffs are the largest source of sediment in the Le Sueur watershed (Gran et al., 2011). They are also located close to the watershed outlet, such that a larger fraction of the supply is delivered to the outlet, compared to other sources.

Reduction of sediment delivery from bluffs can be accomplished in two ways. The first is by reduction of river discharge, which reduces sediment loading as represented by the near-channel source sediment loading model (SL_{NCS}) (Chapter 5 and Section 6.4.3).

Second, sediment loading from bluffs can also be accomplished by directly stabilizing the bluffs. Although bluff erosion mechanisms are many and complex, continued bluff erosion is ultimately controlled by removal of bluff debris and erosion of the bluff toe. If toe erosion is eliminated, bluffs will naturally stabilize and re-vegetate, eliminating most future erosion.

Bluff toe stabilization is represented in MOSM in terms of 1,112 mapped bluffs adjacent to the rivers in the LSRB, and they are assigned to individual SEDSBs. NCMO represents management options to reduce sediment input from these mapped bluffs (Appendix 6.A.2.7). Sediment input reduction from NCMO implementation is calculated discretely for all mapped bluffs in each SEDSB:

$$SI_B = \sum_{k \in N_b} L_k(1 - B_k) + L_k(1 - E_b)B_k \qquad [6.22]$$

where

SI_B = Sediment input from the set of bluffs N_b next to streams [Mg/yr]

L_k = Bluff loading rate [Mg/yr] for bluffs $k \in N_b$

B_k = 1 if bluff k is selected for NCMO, and 0 otherwise

E_b =Effectiveness of NCMO

Consequently, sediment loading from bluffs with or without NCMO is calculated by multiplying SI_B [Eq. 6.28] by SDR_s at each SEDSB (derived from the Topofilter analysis of chapter 4) and summed over all SEDSBs to estimate the total sediment loading from bluffs.

In addition, if a WCMO or ICMO is implemented upstream (Section 6.4), any reductions in loadings from bluffs resulting from peak flow reductions will be discounted by implementing NCMO. In other words, SI_B in [6.22], which is already reduced by

NCMO, would be adjusted downwards by WCMOs/ICMOs; thus, the effectiveness of water conservation is reduced by the sediment reduction already applied by NCMO.

6.4. Water routing module

In the previous section, we described how MOs affect sediment loading and delivery. In this section, we describe how water storage MOs such as water conservation on field and in-channel (WCMO and ICMO) affect river discharge and consequent sediment loading from streambanks and bluffs. In Section 6.4.1 we describe the input data for water routing module; in Section 6.4.2, we describe water storage at each SEDSB and river routing through SEDSBs across the watershed; and in Section 6.4.3, we describe how we estimate sediment loading reduction from peak flow attenuation.

6.4.1. Database: SWAT water yield data

Water storage in the uplands can attenuate peak flow and consequently reduce sediment loading from NCSs (SL_{NCS} model developed in Chapter 5). In the LSRB, there are good gaging records for flow and sediment, but these records are limited at readings at seven stream gage locations above and below the incised zone along the Maple, Cobb, and Le Sueur Rivers, and another one after the confluence of these rivers at the mouth of the LSRB. Thus, a SWAT model that was calibrated using these gaging records is used to distribute the flows throughout the watershed among 30 subbasins. The resulting water yield data represents the net amount of water that leaves each of the subbasin contributing to stream flow downstream. We used the results of this SWAT analysis as an input to a flow routing analysis described below.

In order to estimate the downstream effects of implementing water storage, there is a need for hydrologic routing within MOSM. MOSM utilizes the daily water yield

simulated by the SWAT model (1/1/1985 to 12/31/2009) (developed by Kumarasamy and Belmont, 2014; Mitchell, 2015) to implement simple routing methods to capture the effects of water storage in reducing large flows downstream (i.e., flows exceeding the threshold river discharge (Q_t) determined in Chapter 5). To do this, it is necessary that the SWAT model's subbasin delineation corresponds to the HYDSB delineation in MOSM, as described Section 6.2.

6.4.2. Water storage and river routing algorithms

The water routing algorithm simulates the changes in the time and magnitude of peak river discharge as a result of implementing water conservation managements (WCMO and ICMO) in HYDSBs of the watershed. In this section, we describe the *level pool routing method* to estimate the effects of water storage on the HYDSB water yield, and the *Muskingum-Cunge method* to route the HYDSB water yield downstream.

6.4.2.1. Storage-outflow calculation: Level pool routing

Level pool routing is a method for calculating the outflow hydrograph from a water storage structure with horizontal water surface given the inflow hydrograph (i.e., SWAT's water yield data) and storage outflow characteristics (i.e., WCMO and ICMO's storage capacity and spillway design) (Chow et al., 1988).

To model the effects of water storage at each HYDSB, we made a few simplifying assumptions. First, we assume a cylindrical shape for the WCMOs with the user-specified design inputs on depth and outflow structure; and a rectangular prism shape for the ICMOs with the design inputs on depth and width together with a fixed outflow weir design. Second, a water routing algorithm is applied to lumped storage for each HYDSB. This lumped calculation involves using the average WCMO and ICMO dimensions,

including mean surface area ($\overline{A_{s_j}}$) and depth ($\overline{D_j}$), to represent all implemented MO sites in a HYDSB *j*. We calculate the inflow hydrographs, storages, and outflow hydrographs for the average WCMO and ICMO dimensions, and then we multiply the simulated outflows of the average structures by the number of selected sites (Figure 6.7).

Lastly, water storage simulation is done in series: we first calculate the inflow (total water yield from HYDSB), storage, and outflow of the WCMOs, and then we calculate the inflow, storage, and outflow of the ICMOs, assuming that the inflows to ICMO equal the water yield affected by WCMOs, as ICMOs are usually downstream from locations where WCMOs would be implemented.

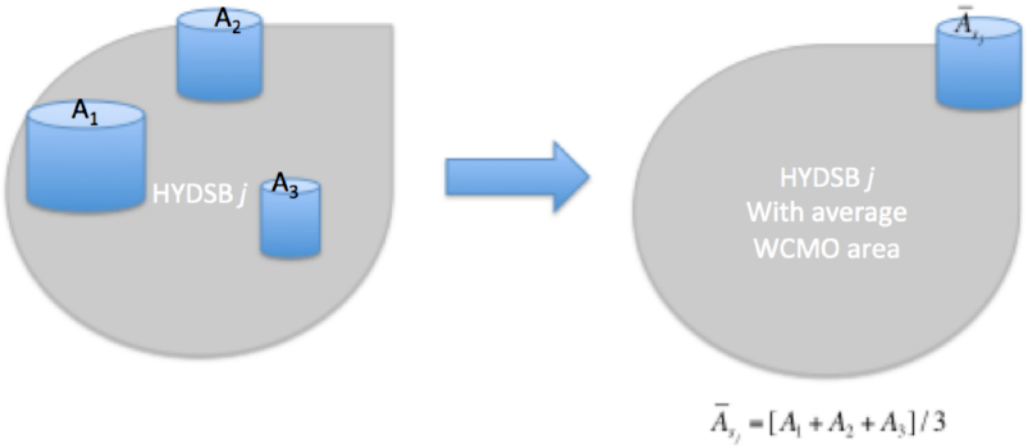

Figure 6.7: In this schematic example, three WCMO sites with areas, A1, A2, and A3 are implemented in HYDSB *j*. The model is lumped at HYDSB level, thus, to use the level pool routing method to estimate the outflow hydrograph of HYDSB *j*, the model takes the average area (Asbar) of the selected WCMOs to calculate the inflow from its drainage area, storage, and outflow. The outflow from average structure is multiplied by the number of WCMOs.

The inflow hydrograph is assumed to be uniformly distributed over the HYDSB; hence, the inflow to the water storage structure consists of the water yield occurring in its drainage area, calculated with the proportion of the structure's drainage area over the total area of the HYDSB.

The drainage area of WCMO in each HYDSB is calculated using a linear regression defining water storage site's drainage area as a function of its surface area developed by Mitchell (2015). This linear regression is defined through spatial analysis with 9-m digital elevation model (DEM): the drainage areas of individual WCMO sites are estimated from its flow accumulation values sampled at the farthest downstream outlets of these sites, then the sampled values are defined as a function of their surface areas. It is determined that the drainage area of a WCMO is approximately 9 times is surface area and this simple linear relationship is applied in this module to estimate the drainage area of the average WCMO in each HYDSB. The drainage area of ICMO is calculated in the similar manner but the coefficient for the linear relationship depending on the surface area of ICMO is a user input that can be changed in MOSM.

The outflow from a water storage structure depends on its effective length of crest (L) and the total head over the crest (h). We use the spillway discharge equation to calculate the outflow: $Q = CLh^{3/2}$ (Chow et al., 1988) where C is a variable coefficient of discharge that can be specified for different outflow structures. Effective length, L will depend on the storage structure's spillway design. Thus, we assigned an input parameter in MOSM, α that determines the fraction of the WCMO's circumference where water would spill out. For ICMO, the outflow depends on the user-specified design weir width (WW) over which water would flow out during significant flow events. During low to moderate flow days; the water flows out through the notch (smaller opening in the weir shown in Figure 6.4). Notch design can be specified in the MOSM including the design notch width (NW) and notch height (NH).

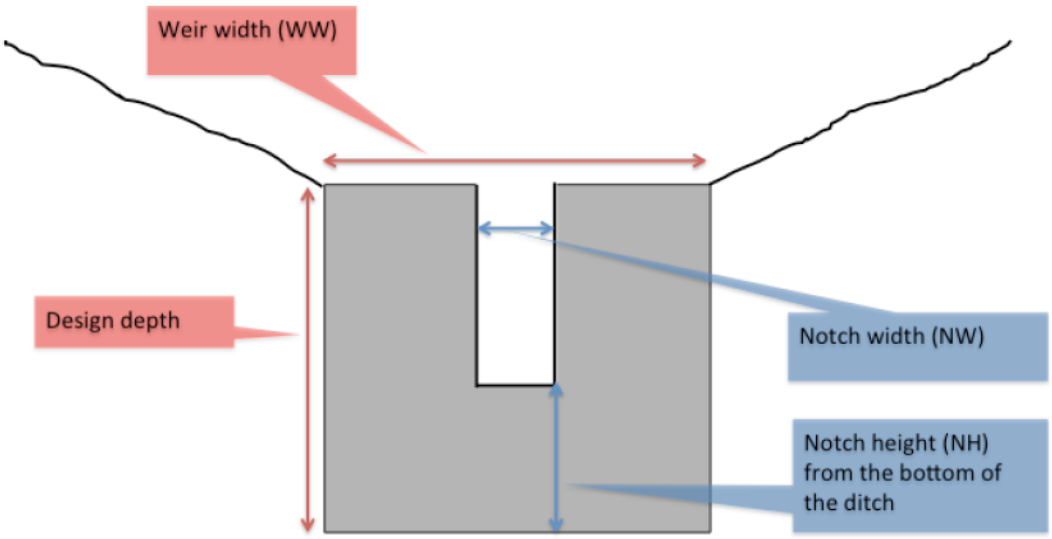

Figure 6.8: ICMO design specification in MOSM includes design weir width and storage depth, and notch design elements that allow discharge during low flow events.

At each HYDSB *j*, water storage ($S_{t,j}$) during the current time step (hour *t*) is calculated based on storage, inflow, and outflow from the previous time step ($S_{t-1,j}$, $I_{t-1,j}$, and $Q_{t-1,j}$, respectively). The initial water storage is assumed to be zero at *t*=0. Water loss from seepage and evaporation over the surface area of the storage structure in HYDSB *j* ($\overline{A_{s_j}}$) is allowed, given the input hydraulic conductivity (*K*) and evaporation rate (*ET*), which for simplicity we assume is the same for all *t* and all *j*.[2]

$$S_{t,j} = \left[S_{t-1,j} + I_{t-1,j} - Q_{t-1,j} - \overline{A_{s_j}}(K + ET)\right]\Delta t \qquad [6.23]$$

The total head of water in current time step ($H_{t,j}$) is calculated based on the volume of water to be stored in the current time step ($S_{t,j}$) and mean surface area ($\overline{A_{s_j}}$) of WCMO and/or ICMO of SEDSB *j*. If the total head of water is greater than the depth of the storage structure (i.e., $H_{t,j} > D_j$), outflow for the current time step ($Q_{t,j}$) is calculated using the spillway discharge equation, $Q_{t,j} = C \cdot \overline{L_j} \cdot (H_{t,j} - D_j)^{3/2}$ where $\overline{L_j}$ is the

[2] Future research could differentiated these values by season and soil type.

average length of crest calculated based $\overline{A_{s_j}}$ for HYDSB j and input value α determining the effective crest length over the circumference of WCMO as described above. This calculation is iterated at daily time step from 1/1/1985 to 12/31/2009.

6.4.2.2. Hydrologic river routing: Muskingum-Cunge method

After calculating the water yield from each HYDSB with and without WCMO and/or ICMO implementation, water is routed downstream. A lumped hydrologic routing method is used to route water through the river network to the watershed outlet. The Muskingum-Cunge (Mg-Cg) method is used to estimate the routing parameters in Figure 6.5 (Chow et al., 1988). K expresses the travel time of a flood wave through the length of reach (Δx) in a HYDSB; this time is assumed to be constant irrespective of flow. X is a weighting factor ranging [0, 0.5] where X=0 indicates reservoir-type storage with no wedge and no backwater, and X=0.5 indicates full wedge storage.

$$K = \frac{\Delta x}{c_k} = \frac{\Delta x}{\frac{dQ}{dA}} \qquad [6.24]$$

$$X = \frac{1}{2}\left(1 - \frac{Q}{Bc_k S_o \Delta x}\right) \qquad [6.25]$$

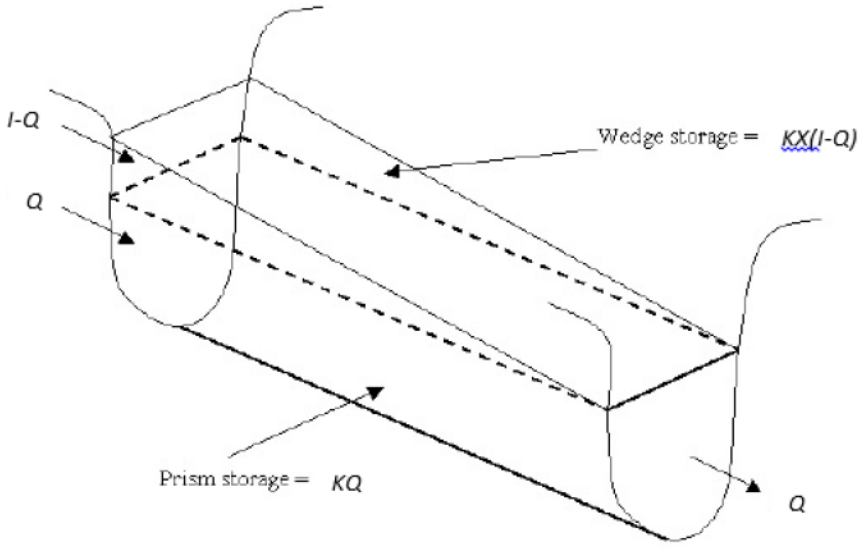

Figure 6.9: prismatic channel with wedge storage analogous to the Mg-Cg method with model parameters described in [6.26] through [6.34] (figure adopted from Chow et al., (1988)).

To express the celerity (c_k) in [6.24] and [6.26] and the weighting factor (X) in [6.25] in terms of quantifiable hydraulic geometric measures of the river system, we substitute the expression for river discharge (Q) with Manning's formula [S.I.] in [6.27], given the hydraulic geometry inputs (n= Manning's n; A= cross section area; h= depth of water; P= wetted perimeter; S_o= slope of the channel; B=channel width) at each HYDSB. These parameters are sampled and extrapolated from the surveyed river cross sections of the Maple and Le Sueur Rivers (Belmont, 2011). [6.28] expresses the unit river discharge in terms of hydraulic geometry of the channels:

$$c_k = \frac{dQ}{dA} = \frac{d}{dA}(Q) \qquad [6.26]$$

$$Q = \frac{S_o^{\frac{1}{2}}}{n} AR^{\frac{2}{3}} = \frac{S_o^{\frac{1}{2}}}{nP^{\frac{2}{3}}} A^{\frac{5}{3}} \ where\ R = \frac{A}{P} \qquad [6.27]$$

$$\frac{d}{dA}(Q) = \frac{5}{3}\left(\frac{S_o^{\frac{1}{2}}}{nP^{\frac{2}{3}}}\right) A^{\frac{2}{3}} \approx \frac{5}{3}\left(\frac{S_o^{\frac{1}{2}} h^{\frac{2}{3}}}{n}\right) \text{for a wide channel} \qquad [6.28]$$

Substituting c_k in [6.24] and [6.25], with [6.28] expressed in terms of hydraulic geometry:

$$K = \frac{\Delta x}{c_k} = \frac{\Delta x}{\frac{5}{3}\left(\frac{S_o^{\frac{1}{2}} h^{\frac{2}{3}}}{n}\right)} \quad [6.29]$$

$$X = \frac{1}{2}\left(1 - \frac{A^{\frac{5}{3}}}{nP^{\frac{2}{3}} B c_k S_o^{\frac{1}{2}} \Delta x}\right) \quad [6.30]$$

The outflow in a single time-step forward, Q_{t+1} is then expressed with the Muskingum coefficients, C_1, C_2, and C_3:

$$Q_{t+1} = C_1 I_{t+1} + C_2 I_t + C_3 Q_t \quad [6.31]$$

where the Muskingum coefficients are calculated using the terms in [6.29] and [6.30] for time step, Δt (Chow et al., 1988):

$$C_1 = \frac{\Delta t - 2KX}{2K(1-X) + \Delta t} \quad [6.32]$$

$$C_2 = \frac{\Delta t + 2KX}{2K(1-X) + \Delta t} \quad [6.33]$$

$$C_3 = \frac{2KX(1-X) - \Delta t}{2K(1-X) + \Delta t} \quad [6.34]$$

To summarize, we use the hydraulic geometry to calculate celerity and consequent discharge using Mg-Cg formulation to route the water yield at each HYDSB affected by WCMOs or ICMOs downstream.

6.4.2.3. Water routing map by HYDSB

Water yield from each HYDSB is routed to its downstream HYDSB using the Mg-Cg method described above along with data on the river network, and is applied to successive stream reaches until reaching the watershed outlet. For instance, along the Maple River before the confluence with the Le Sueur River, there are nine HYDSBs

(Figure 6.10). The model begins water routing from the uppermost HYDSBs (e.g., HYDSB 30, 28, 29, and 23 in Figure 6.10), and the downstream HYDSBs (e.g., HYDSB 25) collect inflow from all upstream HYDSBs (e.g., HYDSBs 30 and 28), subsequently routing the water yield downstream all the way to the watershed outlet.

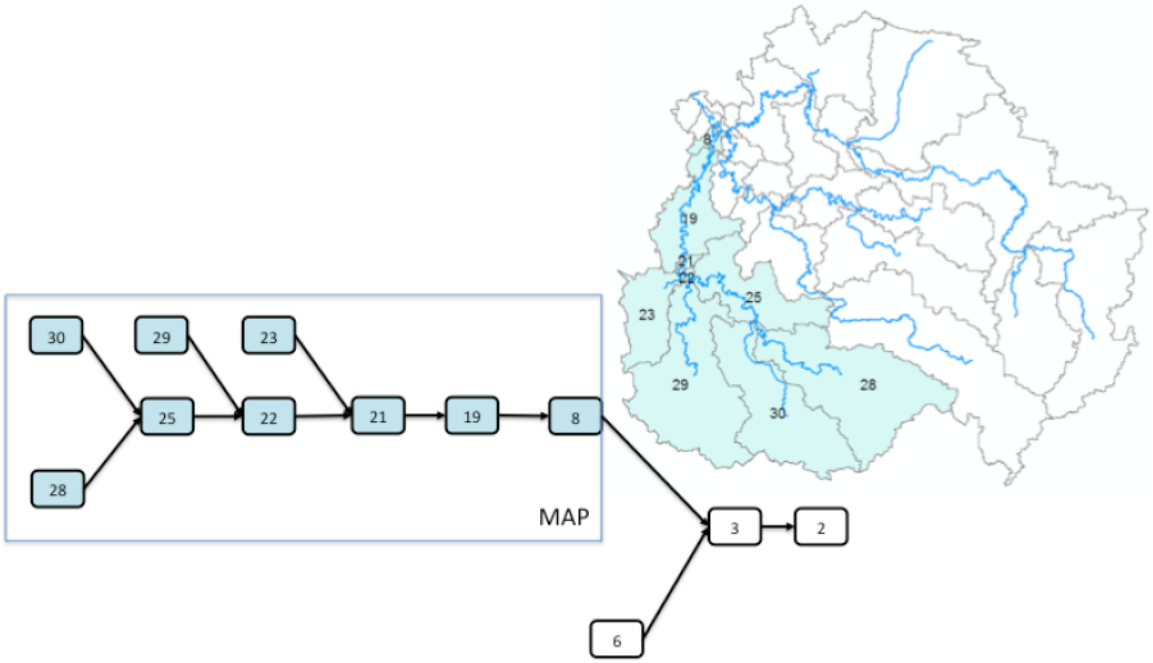

Figure 6.10: Water routing along the Maple River HYDSB before the confluence with the Le Sueur River in HYDSB 3

As an example of the above procedure, when 7,871 acres of WCMO is implemented in zone1 of Maple (Figure 6.2), the model simulates the peak flow attenuation at the lower gage location below the incised zone (location of "LM" in Figure 4.2, the outlet of HYDSB 19 in Figure 6.10). Figure 6.11 shows the daily flow from 3/3/2008 to 7/30/2008 with no WCMO implemented (orange chart) and with WCMOs implemented (blue chart), along with threshold river discharge (Q_t defined in Chapter 5.4.5, converted cubic meters per second (cms)). With 7,871 acres of WCMO sites implemented (all available WCMO sites in zone 1 of Maple subwatershed of 98,288 acres in Figure 6.1), flow above

the threshold river discharge (see Chapter 5.5.5) has been reduced by 42% throughout the whole simulation period.

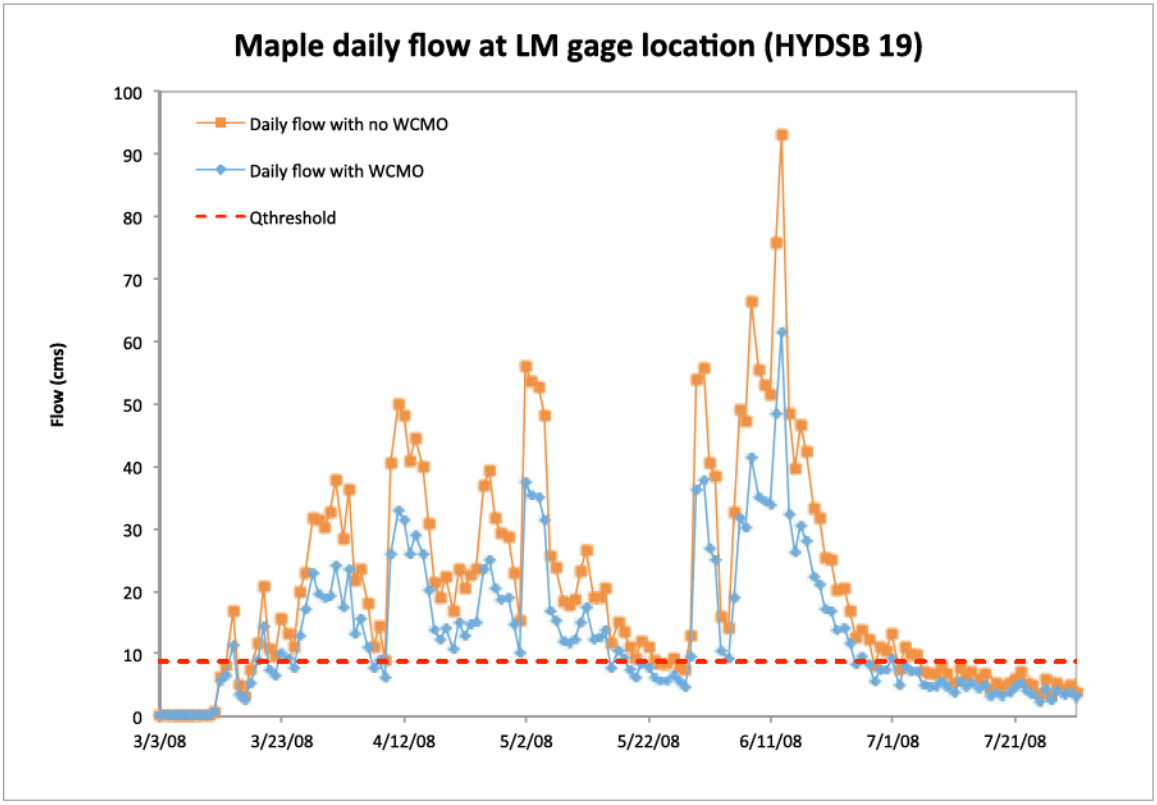

Figure 6.11: Daily river flow at the outlet of HYDSB 19 at the Lower Maple (LM) gage location when no WCMO is implemented (orange chart) and with WCMO implemented (blue chart) with threshold river discharge (red dotted line) from 3/3/2008 to 7/1/2008

6.4.3. Sediment loading reduction from peak flow reduction

The water routing algorithm simulates daily flow at each HYDSB from water conservation actions (WCMO and ICMO) using the level-pool routing for water storage MOs within each HYDSB (see Step 1 in Figure 6.12). Then, the outflows from all HYDSBs are routed downstream using the Mg-Cg method through the river network to obtain the hydrographs at the lower gage locations (e.g., Figure 6.11) along each river (see Step 2 in Figure 6.12).

MOSM calculates the simulated daily flows (Q_{LG}) in the HYDSBs where lower gages (LG) along the Maple, Cobb, and Le Sueur Rivers (LM, BC, and LL in Figure 4.2) are

located. Then the model applies the SL_{NCS} model for the flow above the threshold river discharge (Q_t) to calculate the sediment loading reduction from NCSs in the incised zone[3]. We calculate the percent sediment loading reduction in the incised zone compared to reference period when Q_{LG} wasn't affected. This percent reduction is applied to all streambanks and bluffs, including the ones outside of the incised zone to estimate the overall effects on sediment loading from water storage (Figure 6.12).

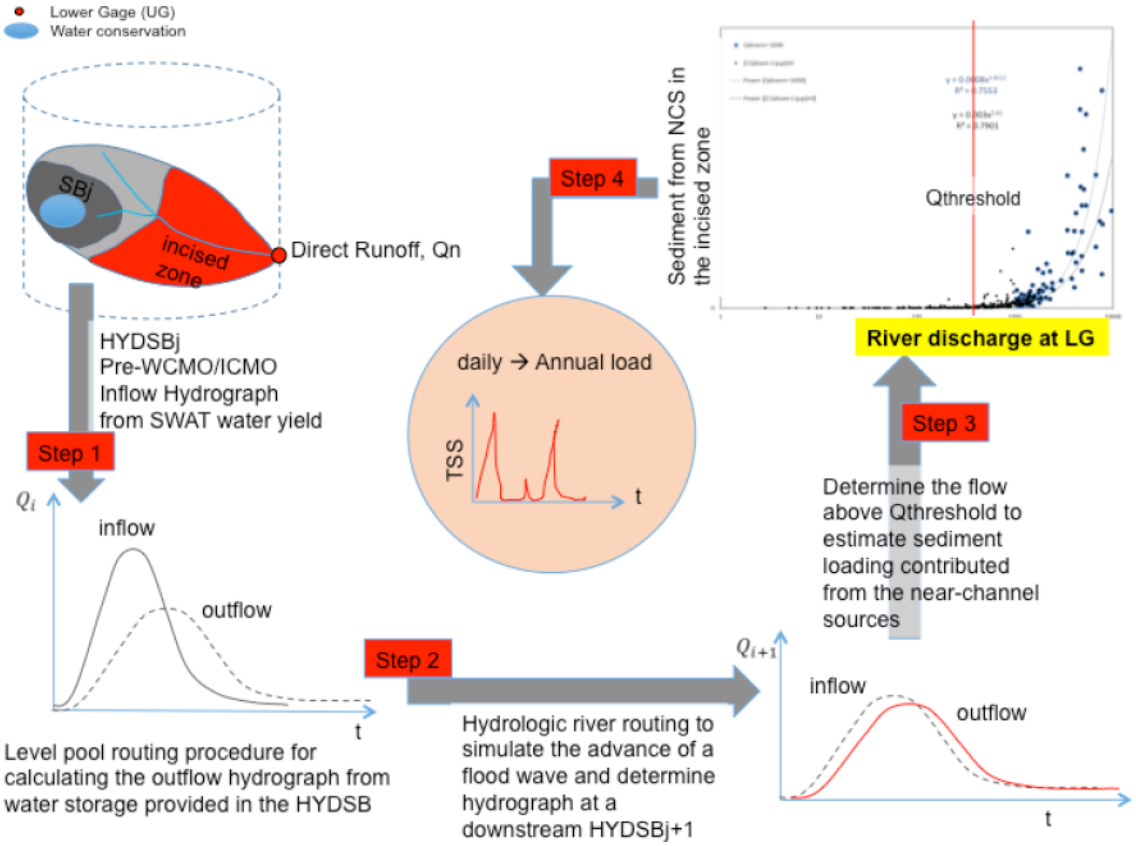

Figure 6.12: a schematic describing evaluation of water conservation management on peak flow reduction and consequent reduction in annual sediment loading from NCSs. Step1 illustrates the simulation of water yield affected by WCMO or ICMO using storage-outflow procedure. Step2 is water routing from HYDSB to downstream to simulate daily discharge at the lower gage location in each rivers of the subwatersheds. Step3 indicates application of SL_{NCS} model to estimate reduction in near-channel sediment supply. Step4 is calculation of mean annual sediment loading reduction aggregated daily estimates.

[3] Chapter 5.5.5 defines the functional relationship between peak river discharge and sediment loading (Figure 5.13): $y = 0.5386x\text{^}2.137$ where the independent variable x indicate simulated peak river discharge greater than the threshold river discharge, Q_t at 1mm/day and y indicates sediment loading from near-channel sources in the incised zone.

6.5. MO allocation module

MOSM is designed to predict changes in sediment loading as a function of type, extent, and location of MO implementation. In this section, we describe the MO database and how MO sitess are allocated across the watershed.

We expect that the performance and influence of MOs should vary with their location, and that users will wish to specify where MOs are implemented. Model users will specify extent of MO at each zone of the subwatersheds; thus, we need to calculate upper bounds to the amount of each MO of each type that can be selected at each location, which is an important category of information provided in the MO database. The MO database consists of candidate MO sites of each type in each location identified through spatial analysis using a number of spatial data including topographic, land cover, and soil maps (procedures are detailed in Appendix 6.A). The MO database defines the total available MO extents in the 1) watershed's geomorphic zones for MO allocation, 2) HYDSBs for water routing, and 3) SEDSBs for sediment loading calculations.

A user of MOSM needs to specify the MO extents for implementation in each zone of the three subwatersheds: Maple, Cobb, and Le Sueur (i.e., nine extent inputs for each MO). The purpose of the allocation algorithm is to then assign the extent of MO to individual HYDSBs and SEDSBs within each of those nine subwatershed zones. Although we could make the allocation a user-specified input, for ease of use we have implemented an automated procedure. There are various ways that this automated allocation could take place, and furthermore once allocated to a zone, rules are needed to determine which MO sites are selected within the zone. The options we have implemented for within-zone MO allocation among potential sites are as follows:

- AFMOs may be selected based on each site's upstream drainage area, soil type (hydric soil), or proximity to stream
- BFMOs may be selected based on each site's upstream drainage area, location (zone), or stream type.
- WCMOs may be selected based on each site's crop productivity index (CPI), topography, soil type, or proximity to exiting wetlands and conservation reserve program sites.
- ICMOs may be selected based on each site's extent, distance to HYDSB outlet, or location (zone).
- RAMOs may be selected base on each site's sediment loading rate or ravine evolution stage.
- NCMOs may be selected based on each site's dimension (bluff height), or sediment loading rate.

The MO allocation algorithm uses the *greedy adding heuristics* (Cohon, 2004) to prioritize candidate site selection by sorting the individual MO sites in a zone according to user-specified selection criteria. Then, the model adds up the candidate sites discretely starting from the highest priority site until the cumulative total reaches the user-specified extent for implementation in each zone of the subwatersheds. After the allocation is completed, the model calculates the total extent of allocated MOs in each HYDSB and SEDSB to execute the water routing module (Section 6.4) and the sediment loading and delivery module (Section 6.3) described earlier in this chapter.

6.6. Annual MO implementation cost

An important objective in non-point pollution management is the cost of the management practices selected. We calculate the annualized cost (C_{ann}) for each MO, which is defined as the uniform end-of-year payment over the lifetime of a MO that would have the same present worth as the actual time series of cash expenditures. These expenditures include installation and maintenance costs over the lifetime of the MO, as well as opportunity costs (foregone net revenues from crops if productivity is lowered or land is taken out of production, as measured by the land value) with default interest rate (i) of 5%:

$$C_{ann} = \left[\left(\frac{P_{inst} + P_{land}}{1+i}\right)\left(\frac{(1+i)^n \cdot i}{(1+i)^n - 1}\right) + P_{mntn}\right] * A \qquad [6.35]$$

where P_{inst}, P_{land}, and P_{mntn} are installation, land acquisition, and annual maintenance costs per extent for each MO. MOs on agricultural fields (AFMO and WCMO (agricultural land cost), and BFMO (marginal land cost) are assumed to take land out of agricultural production when implemented; thus, the land acquisition cost (P_{land}) is included in the annual cost calculation. The default cost of agricultural and marginal land is assumed to be $8,297/acre in 2016 based on the farmland values determined from crop productivity index (CPI) rating and web soil survey data in Blue Earth County ("Blue Earth County, MN Farmland Prices and Values | AcreValue," 2016).

6.7. Summary

MOSM is a reduced-complexity watershed management simulation model with its components built from the work described in previous chapters: Chapters 3 and 4 provide a framework to simulate sediment loading and delivery, and Chapter 5 supplies the

foundation for estimating the effects of water storage and peak flow attenuation on near-channel sediment supply.

MOSM utilizes high-resolution topography to route sediment using sediment delivery ratios calculated based on gaging data, soil loss map data, and a watershed sediment budget where the model's estimates of sediment loading are constrained by observed data. The model accounts for near-channel sediment supply, which is the dominant sediment source in the study watershed, in the overall evaluation of sediment loading and delivery. MOSM provides results over a wide range of conditions and inputs, and the predictions are consistent with independent observation; this is confirmed in the next chapter where we evaluate the model outputs against independent data and observations to check the reasonableness of its predictions. Lastly, the model is accessible to stakeholders because of its relatively simple structure, and allows them to evaluate a range of plausible management option in the watershed rapidly within seconds.

Appendix 6.A: MO database development—definitions and quantification of potential extent of implementation

A.1. Introduction

The Management Option Simulation Model (MOSM) evaluates the sediment reduction and cost of various MO scenarios. Modeling the watershed-scale impacts on sediment loading and cost from implementing MO scenarios requires information about management options (MOs). Therefore, the goal of the MO database development was to collect data on MOs, cost, effectiveness, and potential spatial extent. The process was iterative in that data were assembled for a wide array of management options, and this list was then reduced based on conversations with stakeholders at semi-annual meetings.

For modeling purposes, MOs were sorted into management types based on how they physically prevent erosion and/or trap sediment. The final MO types used in the MOSM are defined in Table 6.2, along with the primary mechanism through which they reduce erosion. For each of these general MO types, installation costs, maintenance costs, and estimated lifespan are noted in Table 6.3. The model outputs evaluated in Chapter 7 are results of the model inputs noted in this table. It was very difficult to find robust data on effectiveness, so we utilize a sliding scale in the MOSM that allows users to input estimated effectiveness for each management option.

Table 6.2: Description of the MO categories used in the MOSM and the primary function in reducing sediment loading evaluated by the model

MO Types	Definition	Location of implementation	Example MO	Primary Function in Sediment Reduction
TLMO	Tillage MO	Field	Conservation tillage, reduced tillage	-Reduce erosion on fields
AFMO	Agricultural field erosion MO	Field	Grassed water ways	-Trap sediment on fields (reduce sediment delivery ratio)
WCMO	Water control MO	Field	Water Retention ponds, wetland restoration	-Reduce flow to reduce near-channel erosion -Trap sediment on fields
ICMO	In-channel storage MO	Channel	Temporary water storage in ditches	-Reduce flow to reduce near-channel erosion
BFMO	Buffer MO	Field near channel	Buffer strips along channels	-Trap sediment (reduce sediment delivery ratio)
RAMO	Ravine MO	Ravines	Ravine tip stabilization to reduce branch growth	-Reduce erosion from ravines
NCMO	Near-channel MO	Bluffs	Bluff stabilization, toe protection	-Reduce erosion from bluffs

Table 6.3: Installation and annual maintenance (Mntnc) cost summary for MOs

Tillage Management Option (TLMO)				Install range	Install assumptions	Maintenance details
Extent of all farm land (ac)	Install. ($/ac)	Mntnc [$/(ac*yr)]	(yr)			
Conventional till (%)	26	8	1	19/acre moldboard plow (Iowa State University, 2016)		
Reduced till (%)	28	11	1	16/acre chisel plow (Iowa State University, 2016)		
Conservation till (%)	14	6	1			
Agricultural Field Management Option (AFMO)						
Extent of all MOs (ft)	Install. ($/ac)	Mntnc [$/(ac*yr)]	Life Span			
Input extent (ft)	3,200	64 (Center for Watershed Protection, 2004)	10	1,900-4500/acre (Tonn, 2016) 2000-3000/acre (Lewandowski et al., 2015)	35' width	Mow 2x per year. Inspect/seed after heavy rain. Control weeds. Control vermin.
Buffer Strip Management Option (BFMO)						
Extent of all MOs (ft)	Install. ($/ac)	Mntnc [$/(ac*yr)]	Life Span			
Input extent (ft)	1,000	45(Center for Watershed Protection, 2004)	10	500-2000/acre (Lewandowski et al., 2015) 750-1150/acre(Tonn, 2016)		Mowing 2x per year. Remove sediment at upper end of gradient every 2 years.
Water Conservation Management Option (WCMO)						
Extent of all MOs (ac)	Install. ($/ac)	Mntnc [$/(ac*yr)]	Life Span			
Input extent (ac)	3,000	574 (Center for Watershed Protection, 2004; Iowa State University, 2016)		6000 (ea) (Nelson, 2016) 300-5,300/acre(Tonn, 2016) 100-150/ln ft, 12,000-17,000/acre (Lewandowski et al., 2015)		Inspect embankment/ridge and repair if necessary after heavy rain. Control weeds. Control vermin. Periodically clean channel with heavy equipment.
In-Channel Management Option (ICMO)						
Extent of all MOs (ft)	Install. ($/ft)	Mntnc [$/(ft*yr)]	Life Span			
Input extent (ft)	250	1.4 (Center for Watershed Protection, 2004)		1000-3000 (ea) for structure (Tonn, 2016) 15,000-20,000 (ea) for rate control weir (Lewandowski et al., 2015)	cost based on flap gate structure	Grease gate annually. Paint every few years.
Ravine Management Option (RAMO)						
number of ravine tips	Install. ($/TIP)	Mntnc [$/(tip*yr)]	Life Span			
Input number of tips	6,000	35(Center for Watershed Protection, 2004)		1,000-11,500 (ea) (Nelson, 2016) 571-2,100/ft; 3,750-60,000 (ea) (Miller and Peterson, 2012) 1,000-21,000 (ea) (Tonn, 2016)		Check for pipe blockage
Near-Channel Source Management Option (NCMO)						
Extent of all MOs (ft)	Install. ($/ft)	Mntnc [$/(ft*yr)]	Life Span			
Input extent (ft)	200	0.7 (Center for Watershed Protection, 2004)		11-77/ft (Tonn, 2016) 500-1000/ft (Lewandowski et al., 2015) 26-208/ft (Melchoir 2014, personal communication) 62-226/ft (Nelson, 2016)		Inspection, planting shrubs

A.2. Spatial analysis to identify candidate MO site extents

In this section, we describe the spatial analysis methodology in ArcGIS to identify and characterize MOs in the Le Sueur River Basin (LSRB). Factors considered include geographic location, landcover and landuse, soil properties, and crop productivity evaluated from the following data sources. Using this data sources in the spatial analysis, we define the maximum extent of available MO sites that constrains the MO extent input in the MOSM. We also collected the geophysical characteristics, such as soil type, landuse, distance to waterways and existing conservation sites, to inform the site allocation algorithm described in Section 6.3. These geophysical characteristics are used for site prioritization in the allocation algorithm as described in Section 6.3, and they reflect stakeholder inputs during stakeholder meetings, particularly 2014 summer and winter meetings (see Table 2.1) about each MO type. A further discussion on the geophysical characteristics collected for each MO type can be found in the following sections.

Data used in the spatial analysis

- 3-m and 30-m Digital Elevation Model (DEM)[4]
- National Conservation Easements Database (NCED)[5]
- Soil Survey Geographic database (SSURGO)[6]
- Identification and classification of wetlands and deep-water habitats of the Contiguous US (CONUS wet polygons)[7].

[4] USGS The National Map Viewer, http://viewer.nationalmap.gov/viewer/

[5] National public conservation easement map layer is obtained from the National Conservation Easement Database (NCED) https://s3.amazonaws.com/nced/20130911/NCED_metadata_7_01_2012.htm. Phase I completed on July 31, 2011 and predict a nearly complete (>90%) mapping of publicly held easement in Minnesota.

[6] USDA web soil survey, http://websoilsurvey.sc.egov.usda.gov/App/HomePage.htm

[7] U.S. Fish and wildlife Service and National wetlands Inventory, http://www.fws.gov/wetlands/

- National land cover database 2011 (NLCD)[8]
- National hydrography dataset (NHD) blue lines[9]
- University of Minnesota Water Resource Center (WRC) ditch shape file[10]
- 2009 and 2010 Aerial photographs[11]

Although we strived to develop an accurate spatial analysis method, the goal of this analysis is *not* to identify specific sites for restoration, but to develop a reliable *summary* of the available MO extents across the watershed as a part of the MO database. Consequently, the MO database consists of individual MO extent, its location in the watershed, and the site characteristics that will be used in the MOSM to allocate MOs in three geomorphic regions of the watershed, and to simulate the effects on the watershed hydrology and sediment loading.

A.2.1. TLMO

A Tillage Management Option (TLMO) acts on the landscape by reducing the reference period erosion rates on field, estimated using the 33-year average USLE calculation (see Chapter 3.2.3), through reduced till or conservation till. Thus, MOSM evaluates effects of different proportions of these tillage methods on sediment erosion along with conventional method of tillage. Thus, TLMO would be applied to all agricultural fields that require tillage. In this section, we describe spatial analysis method to quantify total area where TLMO would be implemented.

Available TLMO sites are identified as "cultivated crops" in NLCD data, excluding

[8] National land cover product created by Multi-Resolution Land Characteristics (MRLC) Consortium obtained from http://www.mrlc.gov/nlcd2011.php

[9] USGS The National Map Viewer, http://viewer.nationalmap.gov/viewer/

[10] WRC ditch shape file received from Paul Davis of the Minnesota Pollution Control Agency on June 24, 2013

[11] National Agriculture Imagery Program (NAIP) in support of USDA farm service agency programs, http://www.mngeo.state.mn.us/chouse/meta.html

areas in conservation easement as shown in NCED data or wet polygons in CONUS data. Approximately 80% of the LSRB area is classified as “cultivated crops,” thus except for small urban areas near the watershed outlets and waterbodies or existing conservation sites (note the small blank spaces in Figure 6.14), most of the LSRB will be subjected TLMO implementation. Figure 6.14 shows the candidate TLMO site as tan polygons within the SEDSB boundary shown in red lines. Since the MOSM’s sediment loading calculation operates in the spatial scale of SEDSB, total available TLMO site extent within each SEDSB is calculated as discussed in Section 6.6.

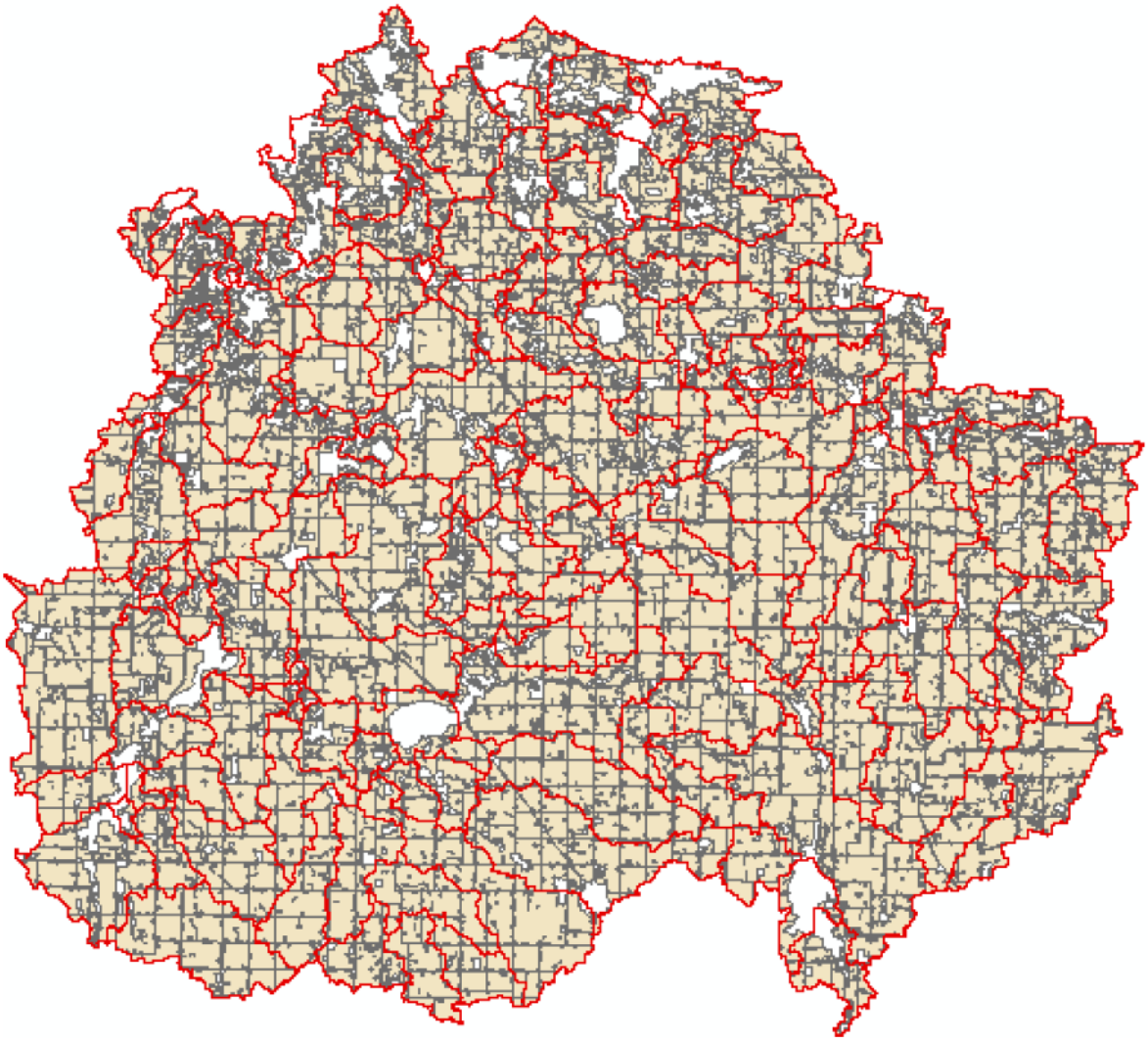

Figure 6.13: Le Sueur River Basin with available agricultural area for TLMO implementation (tan polygons) with SEDSB boundary (red outlines)

A.2.2. AFMO

An Agricultural Field Management Option (AFMO) includes treatments designed to trap sediment already eroded from fields and includes practices such as installation of grassed waterways. Ideal sites for AFMO would be along surface runoff paths where water carries sediment from upstream contributing area. In this section, we describe spatial analysis method used to identify potential AFMO sites, calculation of upstream contributing are (i.e., drainage area) from which AFMO would intercept sediment, and

collection of appropriate geophysical characteristics to be used in allocation algorithm.

Sites available for AFMOs were delineated using Stream Power Index (SPI), a product of upstream contributing area and site slope using 30-m DEM:

$$SPI = \ln(\alpha * tan\beta) \qquad [A.1]$$

where α is upstream contributing area (flow accumulation) and β is slope at each raster cell of the 30-m DEM. SPI is used to identify surface runoff paths that are more likely to scour. For example, grassed waterways can placed along runoff paths on agricultural field with high SPI values to prevent scouring and capture sediment from upstream contributing area (Pike et al., 2009).

According to our aerial photograph analysis, paths with $SPI \geq 7$ were identified as sites susceptible to water erosion on fields. Figure 6.15 shows two example sites in our aerial photograph analysis. Figure 6.15 (site1.a) and Figure 6.15 (site2.a) show the aerial photographs of the example sites where we can identify runoff paths that show indications of scouring (indicated with red dotted circles). These runoff paths with evidences of scouring have $SPI \geq 7$ as indicated by the green raster cells in Figure 6.15 (site1.b) and Figure 6.15 (site2.b). Runoff paths with $SPI \geq 11$ are often areas of existing ditches or channels. For example, in Figure 6.15 (site2.b), the raster cells with $SPI \geq 11$ coincide with stream shown in Figure 6.15 (site2.a). Thus, areas with $7 \geq SPI \geq 11$ were used to identify potential AFMO treatment sites.

However, as the aerial photographs of Figure 6.15 (site1.a) and Figure 6.15 (site1.b) illustrate, *SPI* value for some existing ditches is less than 11, indicating that these ditches are candidate sites for AFMO. This is obviously not feasible. To remedy this, we used the NHD blue lines and ditch shape files to remove sites identified on existing waterways and

lakes while only keeping the raster cells identified on "cultivated crops" land cover areas using the NLCD data.

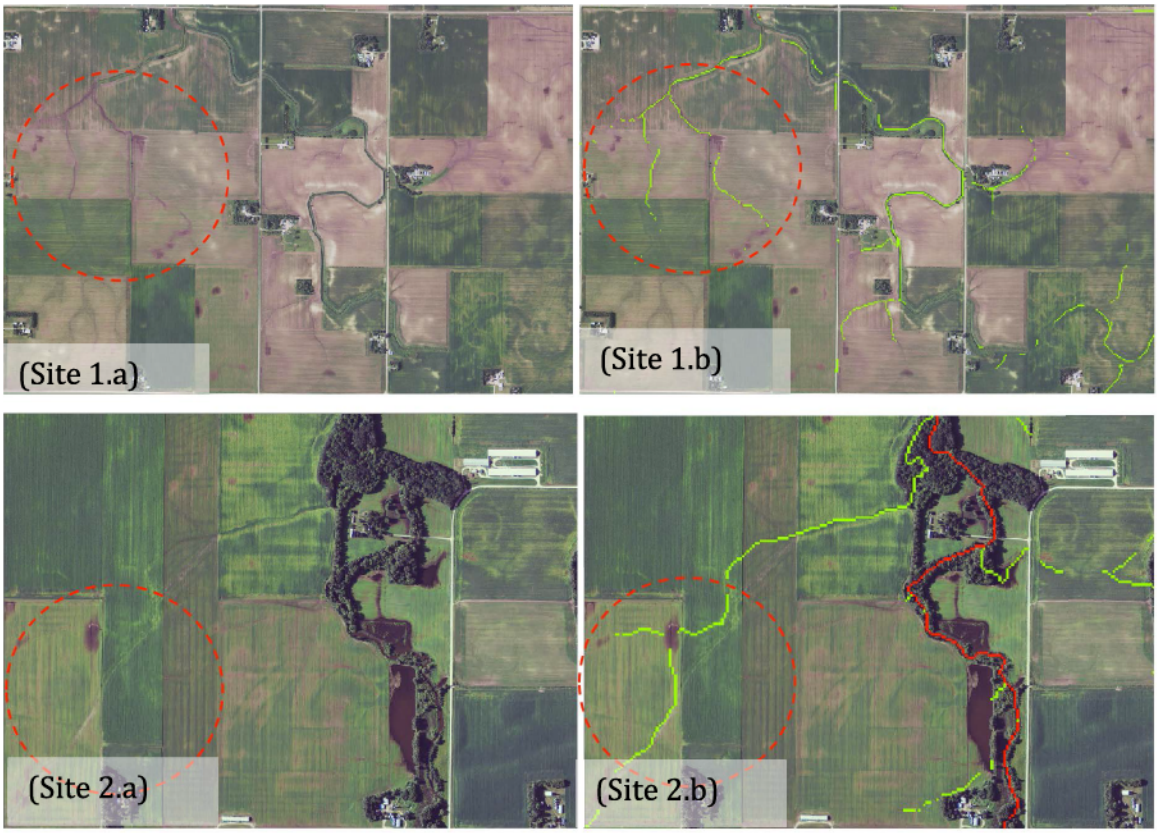

Figure 6.14: Aerial imageries of randomly selected agricultural areas in the LSRB with raster cells with 7<=SPI<=11 (green raster cells) and SPI>11 (red raster cells)

Subsequently, contiguous raster cells identified using the *SPI* method, trimmed with NHD blue lines, ditch shape files, and NLCD data, are converted to individual line feature to identify individual AFMO site. It is assumed that minimum treatable site length is 100 meters, so any line features identified as AFMO sites that are shorter than 100 meter are eliminated from the candidate sites. Finally, total available extent of AFMO sites in each SEDSB is calculated as a part of MO database to be used in the MOSM.

We surveyed the Greater Blue Earth River Basin (GBERB) stakeholders during our regular meetings to determine different criteria for site selection. According to this

survey, soil type plays a significant role in deciding whether a site would be selected for AFMO application. Therefore, the SSURGO data is used to characterize each AFMO site based on its soil type. This information is a part of the database and used in the MO allocation algorithm described in Section 6.3.

A.2.3. BFMO

An additional moanagement option, the Buffer management option (BFMO), was added after the January 2016 stakeholder meeting at the request of stakeholders following a Minnesota state-wide buffer initiative.[12] Minnesota Department of Natural Resources (MNDNR) proposed an official buffer map to accommodate Minnesota's buffer law requiring perennial vegetation buffers up to 50 feet along rivers and streams and 16.5 feet along artificial waterways such as ditches[13]. Unfortunately, at the time BFMO was added to MOSM, the official map of affected waterways was not yet available. Thus, we created our own map for buffer implementation. In this section, we describe spatial analysis method used to identify BFMO sites, and calculation of contributing areas.

NHD blue line data with FTYPE classification (describes the types of stream), as shown in Figure 6.17, were used to identify all natural streams and rivers and artificial waterways where all natural streams and rivers are given a 50-foot buffer, and artificial waterways are given a 16.5-foot buffer.

[12] Buffer Program, http://www.bwsr.state.mn.us/buffers/

[13] Buffer Mapping Project, http://dnr.state.mn.us/buffers/index.html

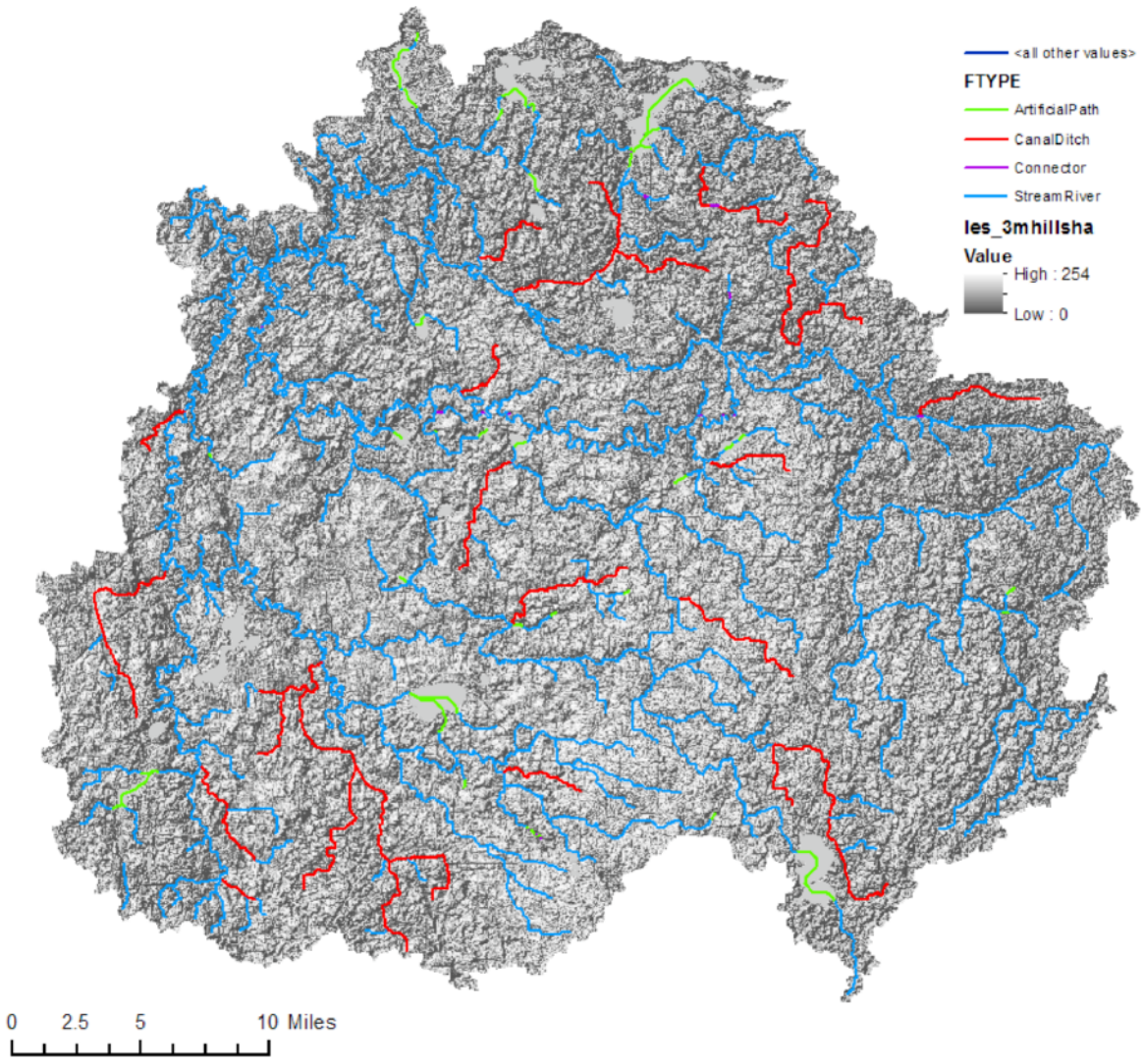

Figure 6.15 NHD data with stream classification where FTYPE attributes (stream and rivers shown in blue lines, and artificial streams and ditches are shown in other colors) are used to determine the buffer width.

A.2.4. WCMO

A Water Conservation Management Option (WCMO) broadly refers to any wetland restoration or temporary water storage basin not in a ditch or channel. WCMOs can store water in the uplands and attenuate peak river discharge in order to reduce sediment loading from NCSs (see Chapter 5). In addition, WCMOs can trap sediment from upstream contributing area in the field. This is a part of an effort to reverse the changes made in the watershed that has attributed to changes in the watershed hydrology (see

Chapter 2 for further discussion). Thus, WCMOs can be placed in areas where wetlands were removed characterized by natural depressions in the landscape or site with soil characterized by low permeability (Hammer, 1992). In this section, we describe the spatial analysis method to identify potential WCMO sites, calculation of DA, and collection of appropriate geophysical characteristics to be used in allocation algorithm.

WCMO sites are identified as topographic depressions on 3-m DEM (filled DEM minus raw DEM). Only topographic depressions with high topographic index (*TI*) values were used. *TI* is a steady state wetness index. Raster cells with high *TI* values indicate areas with large upstream contributing area on a flat terrain indicating areas likely to saturate (Beven, 2001).

$$TI = \ln\left(\frac{\alpha}{tan\beta}\right) \qquad [A.2]$$

where α is upstream contributing area (flow accumulation) and β is slope at each raster cell. The sites identified on urban areas, existing wetland, or existing conservation easement areas were eliminated using the NLCD, CONUS wet polygon, and NCED data. Stakeholder survey during stakeholder meetings revealed that any WCMO sites smaller than 3000m^2 would interfere with everyday farm operations. Accordingly, the final compilation of WCMO database is filtered by its surface area and is show in Figure 6.18. Finally, total available extent of WCMO sites in each SEDSB is calculated to be utilized in sediment loading algorithm, and total available extent in each HYDSB is calculated to be utilized in the hydrologic routing algorithm.

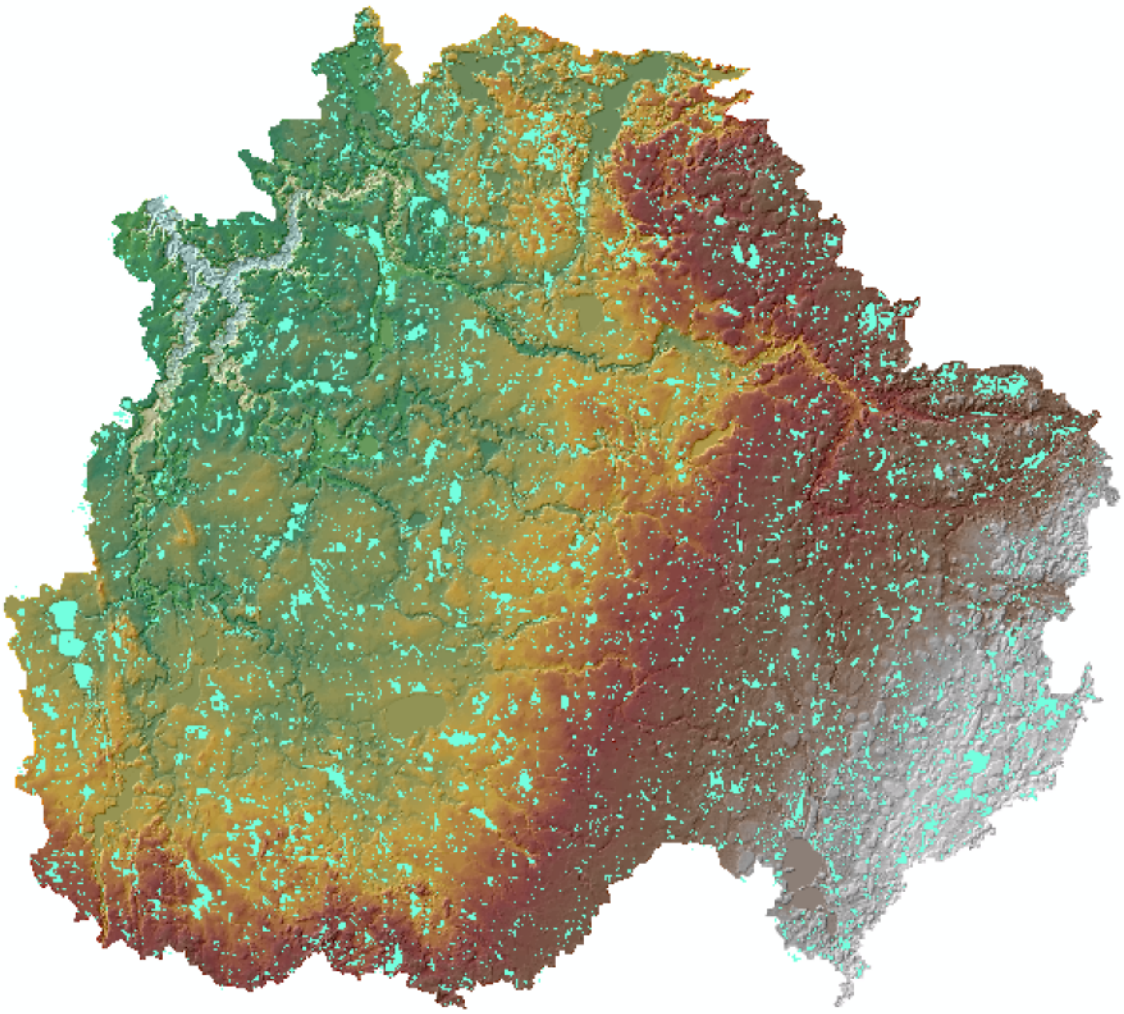

Figure 6.16: Candidate WCMO sites are shown in green polygons over the LSRB

A.2.5. ICMO

An In-Channel Management Option (ICMO) refer to in-channel water storage with outflow control structure. This option is added in response to stakeholders' request following a number of ditch restorations in the watershed in an effort to attenuate flooding. Candidate sites for ICMOs include all mapped ditches in the watershed. Specifically, we classified the "public open ditch" lines from the WRC ditch shape files (shown in blue lines in Figure 6.19) as candidate ICMO sites. Subsequently, total

available extent of ICMO sites in each HYDSB is calculated, and is utilized in the hydrologic routing algorithm.

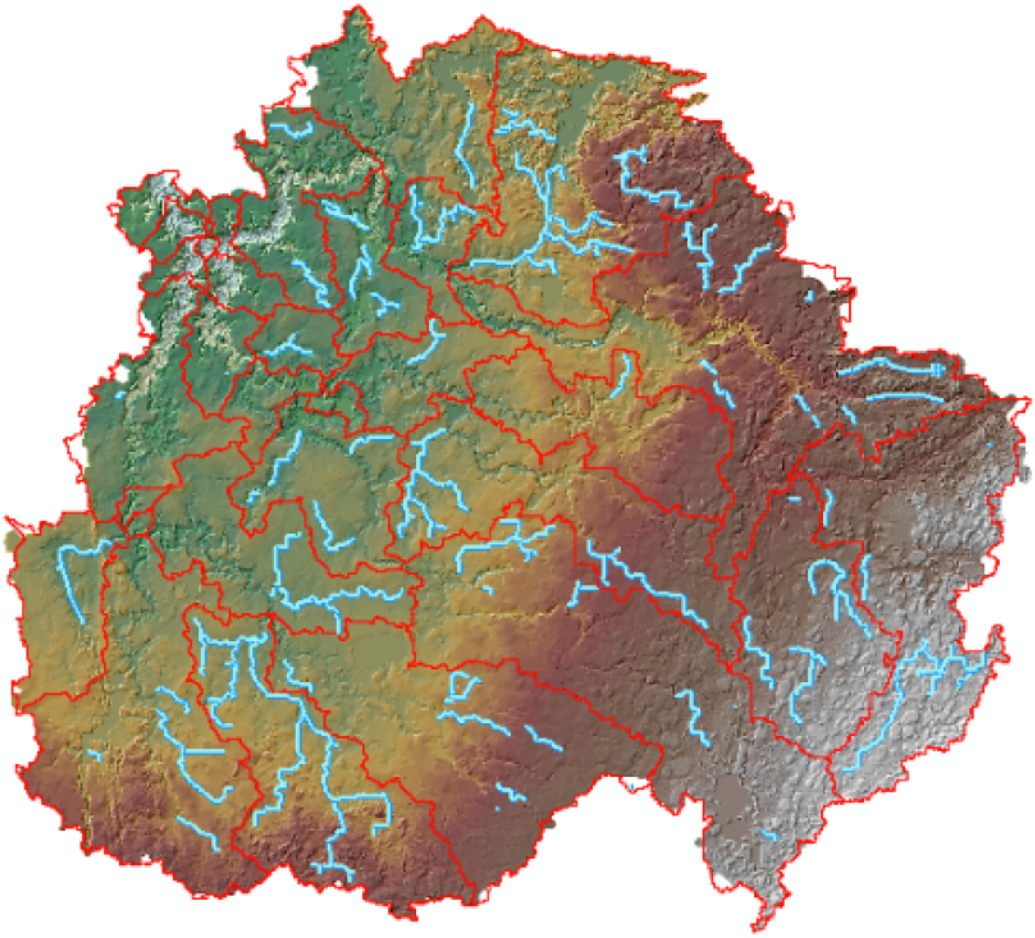

Figure 6.17: Open ditch lines extracted from WRC ditch shape file

A.2.6. RAMO

A Ravine management option (RAMO) is modeled as management that provide additional stability to ravine tips, preventing ravine growth. Examples include berms or water and soil conservation basins (WSCOBs) place around ravine tips. Candidate RAMO sites are identified using the ravine map developed for the LSRB sediment budget (Gran et al., 2011) as shown in Figure 6.20. All ravines were mapped by hand from LiDAR data, noting the sharp slope break between the low-gradient uplands and the steep ravine walls (Ibid.). The figure shows all ravines over the LSRB on the bottom. The

top figure is zoomed over the confluence of the Le Sueur, Cobb, and Maple River where abundant presence of ravines is observed in the incised zone. All mapped ravines are identified as candidate RAMO sites. The map of ravines includes area of individual ravine and its number of tips. The MOSM selects tips of individual selected ravine for RAMO implementation. The map of ravines also includes individual ravine's growth stage, indicated by the "evolution stage" in Figure 6.20. Evolution stage is a classification of ravines where 0=ravine empties into channel, 1=ravine ends on a terrace/abandoned channel, 2=ravine has an alluvial fan, and 3=ravine captured by another ravine (I. Treat and K. Gran 2016, personal communication, February 18). This classification is used in MO allocation algorithm as site selection criteria input in the MOSM.

A.2.7. NCMO

Near channel management option (NCMO) specifically refer to actions that directly stabilize bluffs along rivers in the LSRB. For the sediment budget, Gran et al. (2011) mapped all bluffs adjacent to rivers and quantified the annual sediment loading rate using aerial photographs from two different periods. Figure 6.21 shows all mapped bluffs over the LSRB on the bottom. The top figure zooms over the confluence of the Le Sueur, Cobb, and Maple Rivers where bluffs are more prevalent in the incised zone. Sediment loading rate from the sediment budget is also displayed in the figure. The bluff map also include individual bluff's surface area and height which are used as selection criteria in the MO allocation algorithm.

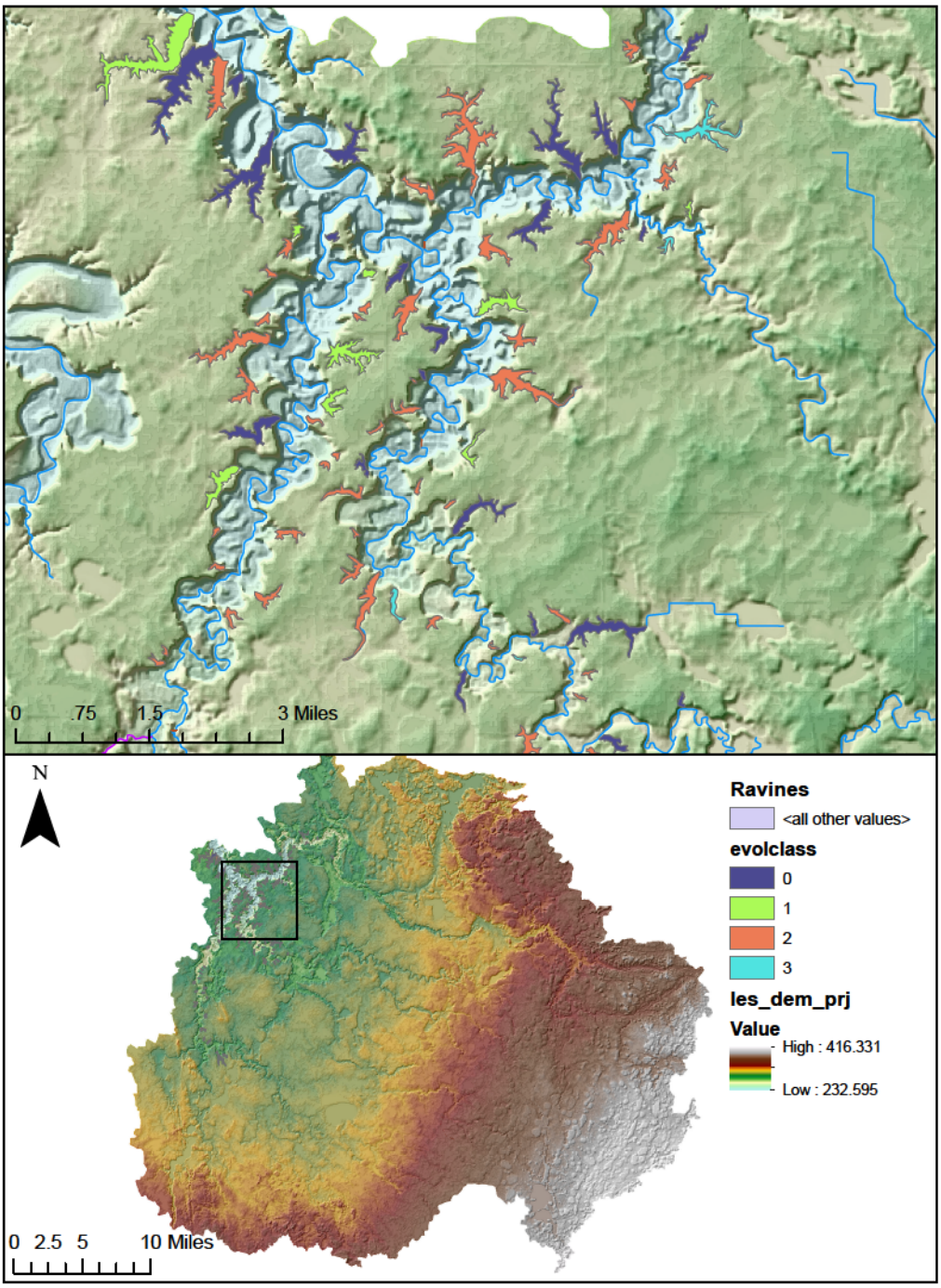

Figure 6.18: Ravines in the LSRB with evolution class (evolclass) indication

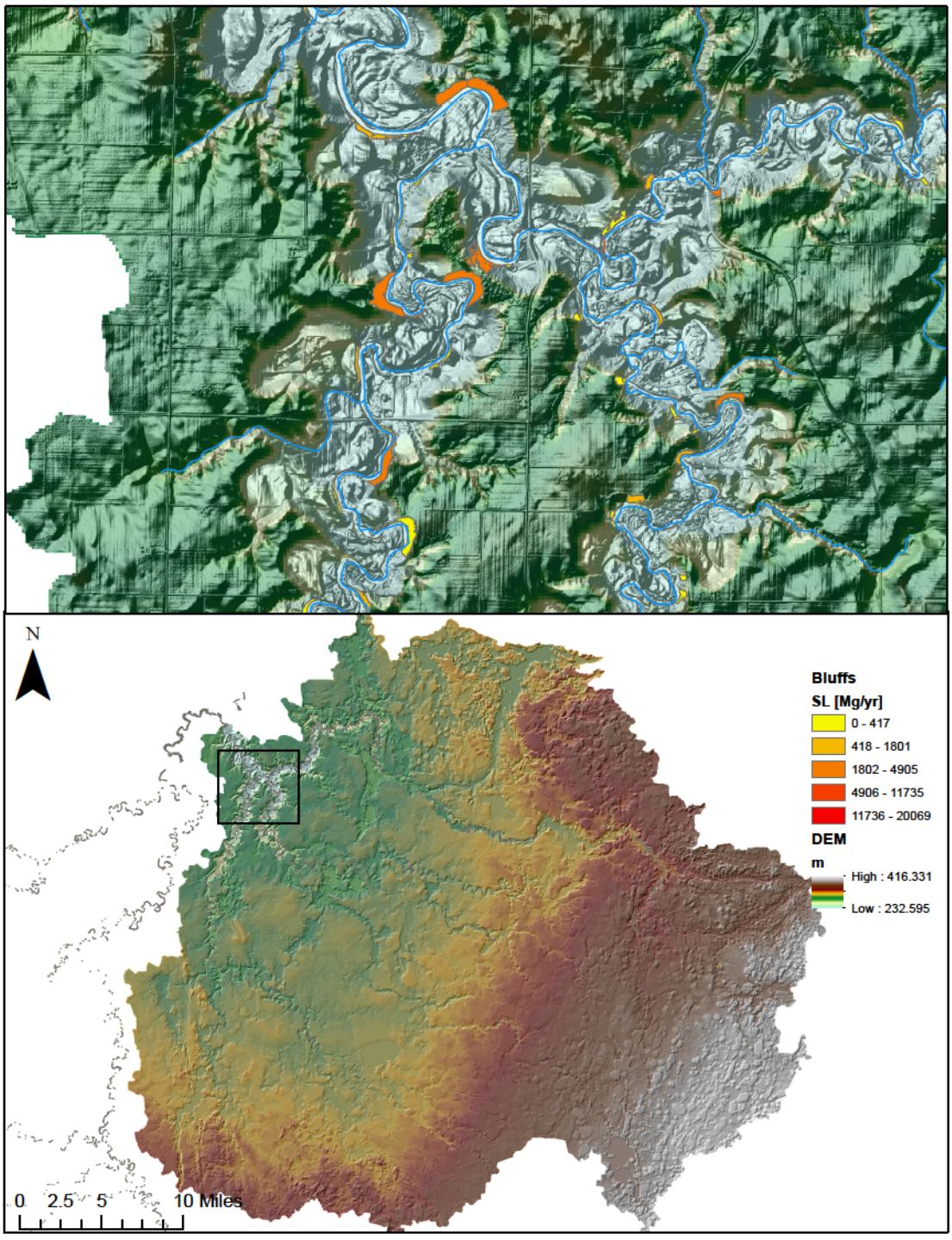

Figure 6.19: Mapped bluffs and the sediment loading class

Appendix 6.B: MOSM subroutines

The MOSM subroutines consists of 1) MO allocation, 2) water routing, and 3) sediment loading with input database for each subroutine as illustrated in Figure 6.12. The subroutines are written in Visual Basics Application (VBA). The code for each are provided below:

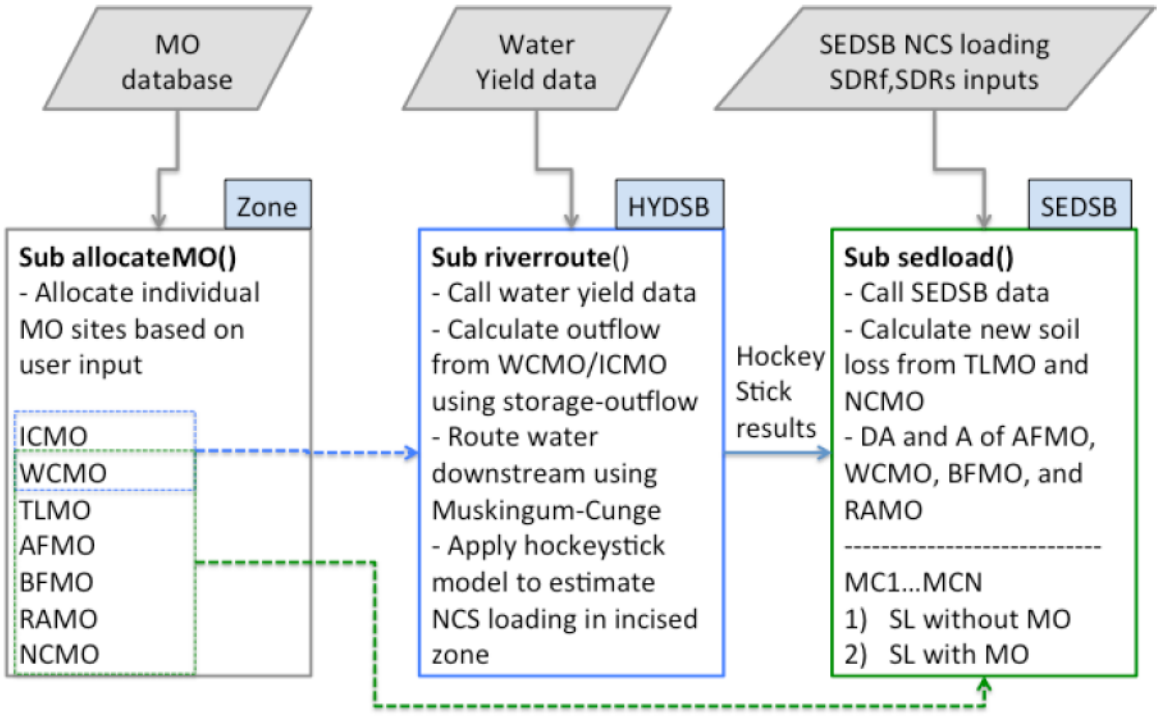

Figure 6.20: MOSM algorithms and simulation routine with input database

B.1. MO allocation subroutine

```
Option Explicit

Sub allocateMO()

Application.StatusBar = "MOSM is running..."
'SECTION1: Import MO database
    'define MO variables and selection criteria
'SECTION 2: allocation MOs
    '''TLMO
    '''AFMO
    '''BFMO
    '''WCMO
    '''ICMO
    '''RAMO
    '''NCMO
'SECTION3: call riverrouting sub and sedloading sub

''''''
```

```
''User input of MO data sort protocol by selection criteria
'TLMOsortcrit = Worksheets("I|O Detail").Range("M5")
AFMOsortcrit = Worksheets("I|O Detail").Range("M23")
BFMOsortcrit = Worksheets("I|O Detail").Range("M37")
WCMOsortcrit = Worksheets("I|O Detail").Range("M51")
ICMOsortcrit = Worksheets("I|O Detail").Range("M65")
RAMOsortcrit = Worksheets("I|O Detail").Range("M79")
NCMOsortcrit = Worksheets("I|O Detail").Range("M93")

''''''''''''''''TLMO''''''''''''''''''''''''''''''''''''''''''''''''''''
'sort the database before defining datavariant
'If TLMOsortcrit = "A" Then 'choose sites with large soil loss rates
first
'    Worksheets("TLMO").Range("A2:AZ4627").Sort _
'    key1:=Worksheets("TLMO").Range("P2"), order1:=xlDescending
'Else 'choose less hydric soil first (rate 1 =hydric...0=not hydric)
'    Worksheets("TLMO").Range("A2:AZ4627").Sort _
'    key1:=Worksheets("TLMO").Range("Z2")
'End If

TLMO_N = Worksheets("TLMO").Range("A1") 'number of MOs
TLMOdata = Worksheets("TLMO").Range("B2:AZ4627") 'estblished the sorted
MOdata for allocation

''''''''''''''''AFMO''''''''''''''''''''''''''''''''''''''''''''''''''''
Worksheets("AFMO").Range("A2:AZ2120").Sort _
key1:=Worksheets("AFMO").Range("B2")
'sort the database before defining datavariant
If AFMOsortcrit = "A" Then 'choose sites with large upstream drainage
area
    Worksheets("AFMO").Range("A2:AZ2120").Sort _
    key1:=Worksheets("AFMO").Range("P2"), order1:=xlDescending
ElseIf AFMOsortcrit = "B" Then 'choose sites on hydric soil first
    Worksheets("AFMO").Range("A2:AZ2120").Sort _
    key1:=Worksheets("AFMO").Range("AB2"), order1:=xlDescending
Else 'choose sites that are closer to open ditch first
    Worksheets("AFMO").Range("A2:AZ2120").Sort _
    key1:=Worksheets("AFMO").Range("R2")
End If

AFMO_N = Worksheets("AFMO").Range("A1") 'number of MOs
AFMOdata = Worksheets("AFMO").Range("B2:AZ2120") 'estblished the sorted
MOdata for allocation

''''''''''''''''BFMO''''''''''''''''''''''''''''''''''''''''''''''''''''
Worksheets("BFMO").Range("A2:AZ518").Sort _
    key1:=Worksheets("BFMO").Range("B2")
'sort the database before defining datavariant
If BFMOsortcrit = "A" Then 'choose sites with large upstream drainage
area
    Worksheets("BFMO").Range("A2:AZ518").Sort _
    key1:=Worksheets("BFMO").Range("T2"), order1:=xlDescending
ElseIf BFMOsortcrit = "B" Then 'choose zone 1, 2, then 3
    Worksheets("BFMO").Range("A2:AZ518").Sort _
    key1:=Worksheets("BFMO").Range("D2")
Else 'choose by stream type
    Worksheets("BFMO").Range("A2:AZ518").Sort _
```

```
    key1:=Worksheets("BFMO").Range("Q2"), order1:=xlDescending
End If

BFMO_N = Worksheets("BFMO").Range("A1") 'number of MOs
BFMOdata = Worksheets("BFMO").Range("B2:AZ518") 'estblished the sorted
MOdata for allocation

''''''''''''''WCMO''''''''''''''''''''''''''''''''''''''''''''''''''''
Worksheets("WCMO").Range("A2:AZ7875").Sort _
    key1:=Worksheets("WCMO").Range("B2")
'sort the database before defining datavariant
If WCMOsortcrit = "A" Then 'CPI/depth (smaller is more desirable)
    Worksheets("WCMO").Range("A2:AZ7875").Sort _
    key1:=Worksheets("WCMO").Range("AL2")
ElseIf WCMOsortcrit = "B" Then 'higher natural depth on hydric soil
    Worksheets("WCMO").Range("A2:AZ7875").Sort _
    key1:=Worksheets("WCMO").Range("AD2"), order1:=xlDescending, _
    key2:=Worksheets("WCMO").Range("U2"), order2:=xlDescending
Else 'closer to existing wetlands and CRP sites
    Worksheets("WCMO").Range("A2:AZ7875").Sort _
    key1:=Worksheets("WCMO").Range("AJ2")
End If

WCMO_N = Worksheets("WCMO").Range("A1") 'number of MOs
WCMOdata = Worksheets("WCMO").Range("B2:AZ7875") 'estblished the sorted
MOdata for allocation

''''''''''''''ICMO''''''''''''''''''''''''''''''''''''''''''''''''''''
Worksheets("ICMO").Range("A2:AZ538").Sort _
key1:=Worksheets("ICMO").Range("B2")
'sort the database before defining datavariant
If ICMOsortcrit = "A" Then 'longest ditch selected first
    Worksheets("ICMO").Range("A2:AZ538").Sort _
    key1:=Worksheets("ICMO").Range("O2"), order1:=xlDescending
ElseIf ICMOsortcrit = "B" Then 'Largest contributing area selected
first
    Worksheets("ICMO").Range("A2:AZ538").Sort _
    key1:=Worksheets("ICMO").Range("P2"), order1:=xlDescending
Else 'further upstream selected first (zone 1 first)
    Worksheets("ICMO").Range("A2:AZ538").Sort _
    key1:=Worksheets("ICMO").Range("D2")
End If

ICMO_N = Worksheets("ICMO").Range("A1") 'number of MOs
ICMOdata = Worksheets("ICMO").Range("B2:AZ538") 'estblished the sorted
MOdata for allocation

''''''''''''''RAMO''''''''''''''''''''''''''''''''''''''''''''''''''''
Worksheets("RAMO").Range("A2:AZ107").Sort _
    key1:=Worksheets("RAMO").Range("B2")
'sort the database before defining datavariant
If RAMOsortcrit = "A" Then 'choose sites with larger load/tip
    Worksheets("RAMO").Range("A2:AZ107").Sort _
    key1:=Worksheets("RAMO").Range("T2"), order1:=xlDescending
Else 'choose sites based on evolutionary stage
    Worksheets("RAMO").Range("A2:AZ107").Sort _
    key1:=Worksheets("RAMO").Range("R2")
```

```
End If

RAMO_N = Worksheets("RAMO").Range("A1") 'number of ravines
RAMOdata = Worksheets("RAMO").Range("B2:AZ107") 'estblished the sorted
MOdata for allocation

''''''''''''''''NCMO''''''''''''''''''''''''''''''''''''''''''''''''''
Worksheets("NCMO").Range("A2:AZ1113").Sort _
    key1:=Worksheets("NCMO").Range("B2")
'sort the database before defining datavariant
If NCMOsortcrit = "A" Then 'choose sites with larger surface area
    Worksheets("NCMO").Range("A2:AZ1113").Sort _
    key1:=Worksheets("NCMO").Range("R2"), order1:=xlDescending
Else 'choose sites with larger load_pTex
    Worksheets("NCMO").Range("A2:AZ1113").Sort _
    key1:=Worksheets("NCMO").Range("S2"), order1:=xlDescending
End If

NCMO_N = Worksheets("NCMO").Range("A1") 'number of MOs
NCMOdata = Worksheets("NCMO").Range("B2:AZ1113") 'estblished the sorted
MOdata for allocation

''''''''''''''''''''''''''''''''''''''
```

```
''''''
```

```
            selectedMOextent2 = selectedMOextent2 + TLMOdata(j2, 14) *
0.000247105 * Worksheets("CONTROL").Cells(11, 1 + i) / 100 'add extent
[ac] up if watershed and zone match
            'MOoutput2(i) = selectedMOextent2

            k2 = k2 + 1 'count the number of sites selected
            TLMOdata(j2, 41) = TLMOdata(j2, 14) *
Worksheets("CONTROL").Cells(11, 1 + i) / 100 'save the extent reserved
for conservation till [m2]
            TLMOdata(j2, 51) = 1 'indicator (2)conservation till is
selected
        End If
    Loop

    MOoutput2(i) = selectedMOextent2
    MOoutput3(i) = allMOextent - MOoutput1(i) - MOoutput2(i)

Next i

'record outputs on I|O Detail
Worksheets("I|O Detail").Range("B15:J15") = MOoutput1 'reduced till
Worksheets("I|O Detail").Range("B16:J16") = MOoutput2 'conservation
Worksheets("I|O Detail").Range("B14:J14") = MOoutput3 'conventional

 'conventional tillage = all tillable land - reduced till -
conservation till
For j = 1 To TLMO_N
    TLMOdata(j, 39) = TLMOdata(j, 14) - TLMOdata(j, 40) - TLMOdata(j,
41) 'conventional till=ag-reduced-conservation
Next j
''''''''''''''''''''''''''''''''''''''''''''''''''''''''''''''''''''''
''''''''''''''''''''''''''''''''''''''''''''''''''''''''''''''''''''''
'End of TLMO allocation
''''''''''''''''''''''''''''''''''''''''''''''''''''''''''''''''''''''
''''''''''''''''''''''''''''''''''''''''''''''''''''''''''''''''''''''
''''''''''''''''''''''''''''''''''''''''''''''''''''''''''''''''''''''SECTION
Allocate AFMOs
''''''''''''''''''''''''''''''''''''''
```

```
    If Worksheets("CONTROL").Cells(14, 1 + i) = 0 Then
          selectedMOextent = 0
          selectedMODA = 0
          k = 0
          j = 1
    Else

    '   while loop to count selected MO based on "acre input UB"
        selectedMOextent = 0
        selectedMODA = 0
        j = 0 'index for MOs
        k = 0 'index for selected sites

        Do While selectedMOextent < Worksheets("CONTROL").Cells(14, 1 +
i) And j + 1 <= AFMO_N ' AND selectedMOextent<SB area 'or add SB area
constraint-->need another loop for SB1...SB30
            j = j + 1
            If AFMOdata(j, 2) = Worksheets("I|O Detail").Cells(6, 1 +
i) And AFMOdata(j, 11) = Worksheets("I|O Detail").Cells(7, 1 + i) Then
'check river and zone
                selectedMOextent = selectedMOextent + AFMOdata(j, 14) *
3.28084 'add extent [ft] up if watershed and zone match
                selectedMODA = selectedMODA + AFMOdata(j, 15) *
0.000247105 'selected DA in acres
                k = k + 1 'count the number of sites selected
                AFMOdata(j, 50) = 1 'indicator that MO is selected
            End If
        Loop

    End If

    'k = k - 1
    'selectedMOextent = selectedMOextent - AFMOdata(j, 14) * 3.28084
    'AFMOdata(j, 50) = 0

    MOoutput1(i) = selectedMOextent
    MOoutput2(i) = allMOextent - selectedMOextent
    MOoutput3(i) = k
    MOoutput4(i) = AFMOdata(j, 14) * 3.28084 'next best site length
(ft)
    MOoutput6(i) = selectedMODA

Next i

'record outputs on I|O Detail
Worksheets("I|O Detail").Range("B30:J30") = MOoutput1 'lengthselected
(ft)
Worksheets("I|O Detail").Range("B31:J31") = MOoutput2 'remaining extent
(ft)
Worksheets("I|O Detail").Range("B32:J32") = MOoutput3 'number of sites
(#)
Worksheets("I|O Detail").Range("B33:J33") = MOoutput4 'next best site's
lenth (ft)
Worksheets("I|O Detail").Range("B34:J34") = MOoutput6 'DA of selected
sites
''''''''''''''''''''''''''''''''''''''''''''''''''''''''''''''''''''''''
''''''''''''''''''''''''''''''''''''''''''''''''''''''''''''''''''''''''
```

```
'End of AFMO allocation
''''''
```

```
    'k = k - 1
    'selectedMOextent = selectedMOextent - BFMOdata(j, 14) * 3.28084
    'selectedMOextent2 = selectedMOextent2 - BFMOdata(j, 18) *
0.000247105
    'BFMOdata(j, 50) = 0



    MOoutput1(i) = selectedMOextent
    MOoutput2(i) = allMOextent - selectedMOextent
    MOoutput3(i) = k
    MOoutput4(i) = BFMOdata(j, 14) * 3.28084 'next best site length
(ft)
    MOoutput5(i) = selectedMOextent2
    MOoutput6(i) = selectedMODA

Next i

'record outputs on I|O Detail
Worksheets("I|O Detail").Range("B44:J44") = MOoutput1 'lengthselected
(ft)
Worksheets("I|O Detail").Range("B45:J45") = MOoutput2 'remaining
extent(ft)
Worksheets("I|O Detail").Range("B46:J46") = MOoutput3 'number of sites
(#)
Worksheets("I|O Detail").Range("B47:J47") = MOoutput4 'next best site's
lenth (ft)
Worksheets("I|O Detail").Range("B48:J48") = MOoutput5 'selected extent
(ac)
Worksheets("I|O Detail").Range("B49:J49") = MOoutput6 'selected
MODA(ac)
''''''''''''''''''''''''''''''''''''''''''''''''''''''''''''''''''''''''
''''''''''''''''''''''''''''''''''''''''''''''''''''''''''''''''''''''''
'End of BFMO allocation
''''''''''''''''''''''''''''''''''''''''''''''''''''''''''''''''''''''''
''''''''''''''''''''''''''''''''''''''''''''''''''''''''''''''''''''''''
'Allocate WCMOs
''''''''''''''''''''''''''''''''''''''''''''''''''''''''''''''''''''''''
''''''''''''''''''''''''''''''''''''''''''''''''''''''''''''''''''''''''
Worksheets("I|O Detail").Range("B58:J62") = "" 'clear the output table

For i = 1 To 9 'go thourgh watershed and zones on inputable
    allMOextent = Worksheets("I|O Detail").Cells(55, 1 + i)
'sum of all available MO areas
    allMOnum = Worksheets("I|O Detail").Cells(56, 1 + i)

    'if the input total extent > available extent then correct the user
input as the available extent
    If Worksheets("CONTROL").Cells(20, 1 + i) > allMOextent Then
        Worksheets("CONTROL").Cells(20, 1 + i) = allMOextent  'this
over-writes the user-input
    End If

    'check if the input is 0 then allocate none
    If Worksheets("CONTROL").Cells(20, 1 + i) = 0 Then
          selectedMOextent = 0
```

```
            selectedMODA = 0
            k = 0
            j = 1
    Else

    'while loop to count selected MO based on "acre input UB"
    selectedMOextent = 0
    selectedMODA = 0
    j = 0
    k = 0

        Do While selectedMOextent < Worksheets("CONTROL").Cells(20, 1 +
i) And j + 1 <= WCMO_N
            j = j + 1
            If WCMOdata(j, 2) = Worksheets("I|O Detail").Cells(6, 1 +
i) And WCMOdata(j, 11) = Worksheets("I|O Detail").Cells(7, 1 + i) Then
'check river and zone
                selectedMOextent = selectedMOextent + WCMOdata(j, 14) *
0.000247105  'add extent (ac) up if watershed and zone match
                selectedMODA = selectedMODA + WCMOdata(j, 15) *
0.000247105
                k = k + 1 'count the number of sites selected
                WCMOdata(j, 50) = 1 'indicator that MO is selected
            End If
        Loop
    End If

    'k = k - 1
    'selectedMOextent = selectedMOextent - WCMOdata(j, 14) *
0.000247105
    'WCMOdata(j, 50) = 0

    MOoutput1(i) = selectedMOextent
    MOoutput2(i) = allMOextent - selectedMOextent
    MOoutput3(i) = k
    MOoutput4(i) = WCMOdata(j, 14) * 0.000247105 'next best site ac
    MOoutput6(i) = selectedMODA

Next i

'record outputs on I|O Detail
Worksheets("I|O Detail").Range("B58:J58") = MOoutput1 'lengthselected
(ft)
Worksheets("I|O Detail").Range("B59:J59") = MOoutput2 'remaining
extent(ft)
Worksheets("I|O Detail").Range("B60:J60") = MOoutput3 'number of sites
(#)
Worksheets("I|O Detail").Range("B61:J61") = MOoutput4 'next best site's
lenth (ft)
Worksheets("I|O Detail").Range("B62:J62") = MOoutput6 'next best site's
lenth (ft)

'End of WCMO allocation
''''''''''''''''''''''''''''''''''''''''''''''''''''''''''''''''''''''''
''''''''''''''''''''''''''''''''''''''''''''
''''''''''''''''''''''''''''''''''''''''''''''''''''''''''''''''''''''''Allocate
ICMOs
```

```
''''''
```

```
    MOoutput6(i) = selectedMODA * 0.000247105 'converted to acres


Next i

'record outputs on I|O Detail
Worksheets("I|O Detail").Range("B72:J72") = MOoutput1
Worksheets("I|O Detail").Range("B73:J73") = MOoutput2
Worksheets("I|O Detail").Range("B74:J74") = MOoutput3
Worksheets("I|O Detail").Range("B75:J75") = MOoutput4
Worksheets("I|O Detail").Range("B76:J76") = MOoutput6

'End of ICMO allocation
''''''
```

```
            End If
        Loop
    End If

    'k = k - 1
    'selectedMOextent = selectedMOextent - RAMOdata(j, 14)
    'RAMOdata(j, 50) = 0
    'outputs

    MOoutput1(i) = selectedMOextent 'tips selected
    MOoutput2(i) = allMOextent - selectedMOextent 'number of remaining
tips
    MOoutput3(i) = k 'number of ravines selected
    MOoutput4(i) = RAMOdata(j, 18) 'next best ravine's load per tip

Next i

'record outputs on I|O Detail
Worksheets("I|O Detail").Range("B86:J86") = MOoutput1
Worksheets("I|O Detail").Range("B87:J87") = MOoutput2
Worksheets("I|O Detail").Range("B88:J88") = MOoutput3
Worksheets("I|O Detail").Range("B89:J89") = MOoutput4

'''End of RAMO
allocation''''''''''''''''''''''''''''''''''''''''''''''''''''''''''''''''
''''''''''''''''''''''''''''''''''''''''''''''''''''''''''''''''''''''''''
''''''''''''''''''''''''''''''''''
'Allocate NCMOs
''''''''''''''''''''''''''''''''''''''''''''''''''''''''''''''''''''''''''
''''''''''''''''''''''''''''''''''''''''''''''

Worksheets("I|O Detail").Range("B100:J104") = "" 'clear the output
table

For i = 1 To 9 'go thourgh watershed and zones on input table

    allMOextent = Worksheets("I|O Detail").Cells(97, 1 + i) ' sum of MO
areas
    allMOnum = Worksheets("I|O Detail").Cells(98, 1 + i)

'''if the input total extent > available extent then correct the user
input as the available extent
    If Worksheets("CONTROL").Cells(29, 1 + i) > allMOextent Then
        Worksheets("CONTROL").Cells(29, 1 + i) = allMOextent  'this
over-writes the user-input
    End If

    'check if the input is 0 then allocate none
    If Worksheets("CONTROL").Cells(29, 1 + i) = 0 Then
          selectedMOextent = 0
          k = 0
          j = 1
    Else

    'while loop to count selected MO based on "acre input UB"
    selectedMOextent = 0
    j = 0 'index for MOs
```

```
    k = 0 'index for selected sites

        Do While selectedMOextent < Worksheets("CONTROL").Cells(29, 1 +
i) And j + 1 <= NCMO_N
            j = j + 1
            If NCMOdata(j, 2) = Worksheets("I|O Detail").Cells(6, 1 +
i) And NCMOdata(j, 11) = Worksheets("I|O Detail").Cells(7, 1 + i) Then
'check river and zone
                selectedMOextent = selectedMOextent + NCMOdata(j, 14) *
3.28084  'add extent [ft] up if watershed and zone match
'reachdata(j,14)=active length
                k = k + 1 'count the number of sites selected
                NCMOdata(j, 50) = 1 'indicator that NCMO is selected
            End If
        Loop
    End If

    'k = k - 1
    'selectedMOextent = selectedMOextent - ReachData(j, 14) * 3.28084
'convert m to ft
    'ReachData(j, 51) = 0

    MOoutput1(i) = selectedMOextent 'bluff length selected
    MOoutput2(i) = allMOextent - selectedMOextent 'number of remaining
bluff sites
    MOoutput3(i) = k 'number of bluffs selected
    MOoutput4(i) = NCMOdata(j, 14) * 3.28084 'next best bluff length

Next i

'record outputs on I|O Detail
Worksheets("I|O Detail").Range("B100:J100") = MOoutput1
Worksheets("I|O Detail").Range("B101:J101") = MOoutput2
Worksheets("I|O Detail").Range("B102:J102") = MOoutput3
Worksheets("I|O Detail").Range("B103:J103") = MOoutput4
''''''''''''''''''''''''''''''''''''''''''''''''''''''''''''''''''''''''
''''''''''''''''''''''''''''''''''''''''''''''''''''''''''''''''''''''''
'''End of NCMO allocation
''''''''''''''''''''''''''''''''''''''
```

```
Sub riverrouting(WCMO_N, WCMOdata, ICMO_N, ICMOdata)

'Section 1: allocate WCMO and ICMO to each HYDSB
'Section 2: call water yield data
'Section 3: River routing (Mg-Cg)
'''''CALL: sub storage outflow
'Section 4: Hockey Stick application

''Define global variable
Dim i As Integer, ii As Integer, j As Integer, m As Integer, o As
Integer

''''''''''''''''''''''''''''''''''''''''''''''''''''''''''''''''''''''''''''''''
''''''''''''''''''''''''''''''''''''''''''''''''''''''''''''''''''''''''''''''''
''''''''''''''''''''''''''''''''''
'''''''''1: ALLOCATE TO HYDSB
''''''''''''''''''''''''''''''''''''''''''''''''''''''''''''''''''''''''''''''''
''''''''''''''''''''''''''''''''''''''''''''''
''''''''''''''''''''''''''''''''''''''''''''''''''''''''''''''''''''''''''''''''
''''''''''''''''''''''''''''''''''''''''''''''''''''''''''''''''''''''''''''''''
''''''''''''''''''''''''''''''''''
''allocate WCMO to each HYDSB 1...30
''''''''''''''''''''''''''''''''''''''''''''''''''''''''''''''''''''''''''''''''
''''''''''''''''''''''''''''
Dim SB_WCMOselected(1 To 30) As Double
Dim SB_WCMOselectedm2(1 To 30) As Double

For i = 1 To 30
    For j = 1 To WCMO_N 'go through all MO from MOdata

        If WCMOdata(j, 13) = i And WCMOdata(j, 50) = 1 Then 'check if
MO is located in SB_i AND check MO_j is selected
            SB_WCMOselected(i) = SB_WCMOselected(i) + 1 'number of MO
selected
            SB_WCMOselectedm2(i) = SB_WCMOselectedm2(i) + WCMOdata(j,
14) 'MO area in m2
        End If

    Next j
Next i
''''''''''''''''''''''''''''''''''''''''''''''''''''''''''''''''''''''''''''''''
''''''''''''''''''''''''''''''''''''''''''''''''''''''''''''''''''''''''''''''''
''Allocate ICMOs to each HYDSB 1...30
''''''''''''''''''''''''''''''''''''''''''''''''''''''''''''''''''''''''''''''''
''''''''''''''''''''''''''''
Dim SB_ICMOselected(1 To 30) As Double
Dim SB_ICMOselectedm(1 To 30) As Double

For i = 1 To 30
    For j = 1 To ICMO_N 'go through all MO from MOdata

        If ICMOdata(j, 13) = i And ICMOdata(j, 50) = 1 Then 'check if
MO is located in SB_i AND check MO_j is selected
            SB_ICMOselected(i) = SB_ICMOselected(i) + 1
            SB_ICMOselectedm(i) = SB_ICMOselectedm(i) + ICMOdata(j, 14)
'MO length in [m]
        End If
```

```
    Next j
Next i

''''''''''''''''''''''''''''''''''''''''''''''''''''''''''''''''''''''''''''''''
''''''''''''''''''''''''''''''''''''''''''''''''''''''''''''''''''''''''''''''''
''''''''''''''''''''''''''''''''''
''''''''2: CALL WATER YIELD DATA
''''''''''''''''''''''''''''''''''''''''''''''''''''''''''''''''''''''''''''''''
''''''''''''''''''''''''''''''''''''''''''''
''''''''''''''''''''''''''''''''''''''''''''''''''''''''''''''''''''''''''''''''
''''''''''''''''''''''''''''''''''''''''''''''''''''''''''''''''''''''''''''''''
''''''''''''''''''''''''''''''''''
Dim databasepath$, flowdatabase$
Dim flowdata As Variant

'databasepath = "Macintosh HD:Users:sejongee:Documents:JHU-mac:CSSR-
Research:MOSM:v6:"
'flowdatabase = "SWATdata.xlsx" 'Daily water yield from each SB to
stream
'Application.ScreenUpdating = False
'Workbooks.Open Filename:=databasepath & flowdatabase 'open destination
workbook

'flowdata = ActiveSheet.Range("B3:AE9133") 'SWAT WATER YIELD data SB1-
30 on columns 1(B) though 30(AE) from 1985 to 2003 from row1 to 9133
flowdata = Worksheets("SWAT_WY").Range("B3:AE9133")

'ActiveWorkbook.Close savechanges:=False 'close the flow database
workbook and don't save changes
'Application.ScreenUpdating = True


''''''''''''''''''''''''''''''''''''''''''''''''''''''''''''''''''''''''''''''''
''''''''''''''''''''''''''''''''''''''''''''''''''''''''''''''''''''''''''''''''
''''''''''''''''''''''''''''''''''
'3: RIVER ROUTING
''''''''''''''''''''''''''''''''''''''''''''''''''''''''''''''''''''''''''''''''
''''''''''''''''''''''''''''''''''''''''''''''
''''''''''''''''''''''''''''''''''''''''''''''''''''''''''''''''''''''''''''''''
''''''''''''''''''''''''''''''''''''''''''''''''''''''''''''''''''''''''''''''''
''''''''''''''''''''''''''''''''''
'define SB variables''''''''''''''''''''''''''''''''''
Dim SBarea(1 To 30) As Double
Dim river(1 To 30) As String, headwater(1 To 30) As String
Dim nexti(1 To 30) As Integer, count(1 To 30) As Integer, upSBs(1 To
30) As Integer
''''''''''''''''''''''''''''''''''''''''''''''''''''''''''''''''''''''''''''''''
''''''''''''''''''''''''''''''''''''''''''''''''''''''''''''''''''''''''''''''''
'define Mg-Cg variables''''''''''''''''''''''''''''''''
Dim dx(1 To 30) As Double, So(1 To 30) As Double, B(1 To 30) As Double,
h(1 To 30) As Double, Pwet(1 To 30) As Double, XSarea(1 To 30) As
Double, N(1 To 30) As Double 'reach data
Dim dt As Double
Dim ck(1 To 30), k(1 To 30), X(1 To 30) As Double 'output Mg-Cg
variables constant over discharge record
```

```
Dim C1(1 To 30), C2(1 To 30), C3(1 To 30) As Double 'Mg-Cg parameters
depend on dt, K, and X
Dim sigma As Double
Dim Qtnout(9131, 30) As Double 'surface runoff outflow from SB (called
from storage-discharge subroutine)
Dim Qtnoutriver(9131, 30) As Double 'pre-routed discharge in river
including Qtnout and Mg-Cg routed flow from upstream SBs
Dim QtnoutriverMCrouted(9131, 30) As Double 'Mg-Cg routed Qtnoutriver
from each SB idt

''''''''''''''''''''''''Read SB input data and M-C parameters''''''''''
dt = 86400 'dt=1day ---> [sec]=[24hr]*[3600sec/hr]
sigma = 0.7 'estimate of the initial outflow as fraction of the initial
inflow (I.C.)

'Obtain river routing parameters for HYDSB 1...30
For i = 1 To 30

    SBarea(i) = Worksheets("SB I|O Detail").Cells(1 + i, 3) * 4046.86
'converted from acre to m2
    headwater(i) = Worksheets("SB I|O Detail").Cells(1 + i, 7) 'binary
    river(i) = Worksheets("SB I|O Detail").Cells(1 + i, 8) 'string
    nexti(i) = Worksheets("SB I|O Detail").Cells(1 + i, 9) 'next SB
    upSBs(i) = Worksheets("SB I|O Detail").Cells(1 + i, 10) 'number os
upper SBs

    dx(i) = Worksheets("SB I|O Detail").Cells(1 + i, 11) 'reach length
    So(i) = Worksheets("SB I|O Detail").Cells(1 + i, 12) 'reach slope
from reach shape file used for SWAT
    B(i) = Worksheets("SB I|O Detail").Cells(1 + i, 13) 'reach width
    h(i) = Worksheets("SB I|O Detail").Cells(1 + i, 14) 'reach depth
    Pwet(i) = Worksheets("SB I|O Detail").Cells(1 + i, 15)
    XSarea(i) = Worksheets("SB I|O Detail").Cells(1 + i, 16)
    N(i) = Worksheets("SB I|O Detail").Cells(1 + i, 18) 'Manning's n
guessed from handbooks referring to channels

    ck(i) = (5 / 3) * (So(i) ^ 0.5 * XSarea(i) ^ (2 / 3)) / (N(i) *
Pwet(i) ^ (2 / 3)) 'ck=dQ/dA [m/s] with Manning sub [m^(2/3)]
    k(i) = dx(i) / ck(i) '[m/m/s]=[s]
    X(i) = 0.5 * (1 - (XSarea(i) ^ (5 / 3) / (N(i) * Pwet(i) ^ (2 / 3)
* B(i) * ck(i) * So(i) ^ 0.5 * dx(i)))) '[-] parameter of shape of
wedge storage (reach width, celerity, slope, and length)

    C1(i) = (dt - 2 * k(i) * X(i)) / (2 * k(i) * (1 - X(i)) + dt)
    C2(i) = (dt + 2 * k(i) * X(i)) / (2 * k(i) * (1 - X(i)) + dt)
    C3(i) = (2 * k(i) * (1 - X(i)) - dt) / (2 * k(i) * (1 - X(i)) + dt)

    'Recording of the calculated Mg-Cg parameters
    'Worksheets("SB I|O Detail").Cells(i + 1, 20) = ck(i)
    'Worksheets("SB I|O Detail").Cells(i + 1, 21) = k(i)
    'Worksheets("SB I|O Detail").Cells(i + 1, 22) = x(i) 'test.
0<=X<=0.5

    'Worksheets("SB I|O Detail").Cells(i + 1, 23) = C1(i)
    'Worksheets("SB I|O Detail").Cells(i + 1, 24) = C2(i)
    'Worksheets("SB I|O Detail").Cells(i + 1, 25) = C3(i)
```

```
    'Worksheets("SB I|O Detail").Cells(i + 1, 26) = C1(i) + C2(i) +
C3(i) 'should =1

Next i
''''''''''''''''''''''''''''''''''''''''''''''''''''''''''''''''''''
''''''''''''''''''''''''''''''''''''''''''''''''''''''''''''''''''''
'Move down river starting from uppermost SB
''''''''''''''''''''''''''''''''''''
'Qtnoutriver(9131, 30) = 0

For m = 30 To 1 Step -1 'go backward from SB30 (larger SB# typically
mean upstream SBs) 'test with 9 for two routing

    If headwater(m) = "Y" Then

        i = m 'i=m=30 'set the first SB
        'Worksheets("SB_data").Cells(i + 1, 30) = i 'check

        count(i) = count(i) + 1  'count the number of times that goes
through SB. This should always be 1 for headwater SBs
        'Worksheets("SB_data").Cells(i + 1, 30) = count(i) 'check
''''''''''''''''''''''''''''''''''''''''''''''''''''''''''''''''''''
''''''''''''''''''''''''''''''''''''''''''''''''''''''''''''''''''''
'do storage-outflow for the headwater SB
''''''''''''''''''''''''''''''''''''''
```

```
'end of headwater SB
''''''
```

```
                                            + C3(i) *
QtnoutriverMCrouted(j - 1, i)
            Next j

            'end of Mg-Cg routing
''''''''''''''''''''''''''''''''''''''''''''''''''''''''''''''''''''''''''''''''
''''''''''''''''''''''''''''''''''''''''''''''''''''''''''''''''''''''''''''''''
            o = i 'o-i=4
            ii = nexti(i) 'l=nexti(4)=7, l=nexti(7)=6
            i = ii 'i=7

        Loop Until i = 0

'Do-Loop over''''''''''''''''''''''''''''''''''''''''''''''''''''''''''''''''''''
    End If

Next m

'End of 2a: RIVER ROUTING
''''''''''''''''''''''''''''''''''''''
```

```
CQ_a = Worksheets("I|O Detail").Range("X61")
CQ_b = Worksheets("I|O Detail").Range("X62")

'Calcuate sediment loading [Mg/day]
Qs_LESsum = 0
Qs_COBsum = 0
Qs_MAPsum = 0

For j = 1 To 9131
    'populate LES sediment loading from incised zone
    If QtnoutriverMCrouted(j, 4) > Qth * LES_DA Then
        Qs_LES(j) = CQ_a * (QtnoutriverMCrouted(j, 4) / LES_DA) ^ CQ_b
* LES_L
    Else
        Qs_LES(j) = 0
    End If
    'populate COB sediment loading from incised zone
    If QtnoutriverMCrouted(j, 13) > Qth * COB_DA Then
        Qs_COB(j) = CQ_a * (QtnoutriverMCrouted(j, 13) / COB_DA) ^ CQ_b
* COB_L
    Else
        Qs_COB(j) = 0
    End If
    'populate MAP sediment loading from incised zone
    If QtnoutriverMCrouted(j, 19) > Qth * MAP_DA Then
        Qs_MAP(j) = CQ_a * (QtnoutriverMCrouted(j, 19) / MAP_DA) ^ CQ_b
* MAP_L
    Else
        Qs_MAP(j) = 0
    End If

    Qs_LESsum = Qs_LESsum + Qs_LES(j)
    Qs_COBsum = Qs_COBsum + Qs_COB(j)
    Qs_MAPsum = Qs_MAPsum + Qs_MAP(j)

Next j

'End of 2b: HOCKEY STICK APPLICATION
''''''''''''''''''''''''''''''''''''''''''''''''''''''''''''''''''''''''''''''
''''''''''''''''''''''''''''''''''''''''''''''''''''''''''''''''''''''''''''''
''''''''''''''''''''''''''''''''''

'sediment loadingoutputs
''''''''''''''''''''''''''''''''''''''''''''''''''''''''''''''''''''''''''''''
''''''''''''''''''''''''''''''''''''''''''''''

'''Record daily sediment loading

Worksheets("SBincisedSED").Range("F3:H9133") = ""

Worksheets("SBincisedSED").Range("F3:F9133") =
Application.Transpose(Qs_LES)
Worksheets("SBincisedSED").Range("G3:G9133") =
Application.Transpose(Qs_COB)
Worksheets("SBincisedSED").Range("H3:H9133") =
Application.Transpose(Qs_MAP)
```

```
'''Record the mean annual results on Outputs tab
Worksheets("Output Detail").Range("D8") = Qs_MAPsum / (2010 - 1985)
Worksheets("Output Detail").Range("D9") = Qs_COBsum / (2010 - 1985)
Worksheets("Output Detail").Range("D10") = Qs_LESsum / (2010 - 1985)

''''''''''''''''''MsgBox "Water routing is complete. Please see the
Outputs tab for results"

End Sub

''''''''''''''''''''''''''''''''''''''''''''''''''''''''''''''''''''''''''''''''
''''''''''''''''''''''''''''''''''''''''''''''''''''''''''''''''''''''''''''''''
''''''''''''''''''''''''''''''''''
'Subroutine to estimate the storage-discharge of MOs
''''''''''''''''''''''''''''''''''''''''''''''''''
''''''''''''''''''''''''''''''''''''''''''''''''''''''''''''''''''''''''''''''''''
''''''''''''''''''''''''''''''''''''''''''''''

Sub storageoutflow(i, j, flowdata, SBarea, Qtnout, WCMOsumarea,
WCMOcount, ICMOsumlength, ICMOcount)

''''''''''''''''''''''''''''''''define input parameters and
variables''''''''''''''''''''''''''''''''''''''
```

```
Dim It(9131, 30) As Double 'inflow in cms
Dim St(9131, 30) As Double 'storage m^3
Dim Ht(9131, 30) As Double 'depth m
Dim Qt(9131, 30) As Double 'outflow from wetlad in cms

'variables for n MOs
Dim Itn(9131, 30) As Double 'inflow in cms
Dim Stn(9131, 30) As Double 'storage m^3
Dim Htn(9131, 30) As Double 'depth m
Dim Qtn(9131, 30) As Double 'outflow from wetlad in cms

''''''
```

```
''''''
```

```
            St(j, i) = St(j - 1, i) + (It(j - 1, i) - Qt(j - 1, i) -
WCMO_SAbar(i) * (1 * k + ET)) * dt '[m3]+[m3/s-m3/s-m3/s][s]=[m3]:
Current storage (to determine H)=previous storage + inflow-outflow-
seeapage-ET
            Ht(j, i) = St(j, i) / WCMO_SAbar(i) '[m3]/[m2]=[m]

            If Ht(j, i) > WCMO_D Then
                Qt(j, i) = C * L * (Ht(j, i) - WCMO_D) ^ 1.5 'outflow
fcalculated for head over the crest with depth, WCMO_D for ONE average
WCMO
            Else
                Qt(j, i) = 0 'no outflow over the rim of WCMO thus
outflow to stream system that will be routed using Mg-Cg is 0
            End If
        Next j

    '''Multiply the average wetland by the number of wetlands in SB
        For j = 1 To 9131 'set j from 5479(year 2000)
            Itn(j, i) = It(j, i) * WCMOcount(i)
            Stn(j, i) = St(j, i) * WCMOcount(i)
            Htn(j, i) = Ht(j, i) * WCMOcount(i)
            Qtn(j, i) = Qt(j, i) * WCMOcount(i) 'outflow through
wetland.
            Qtnout(j, i) = Qtn(j, i) + (flowdata(j, i) - Itn(j, i))
'Water flowing out of SB=outflow from wetland + water that didn't go
through water storage MO. This will be used in the river routing
            flowdata(j, i) = Qtnout(j, i) 'overwrite the flow data for
SBi
        Next j

End If

''''''''''''2. route the water through the
ICMO''''''''''''''''''''''''''''''''''''''''''''''''''''''''''''''''''''''
''''''''''''''''''''''''''''''''

If ICMOcount(i) = 0 Then ''check if the ICMO is empty (none selected)--
>Qtnout(j) = flowdata(j) for SB(i)
    For j = 1 To 9131
        Qtnout(j, i) = flowdata(j, i)
    Next j
Else ''''''''''''storage-outflow
calculation''''''''''''''''''''''''''''''''''''''''''''''''''''''''''''

    ICMO_SAbar(i) = ICMOsumlength(i) / ICMOcount(i) * designW '[m2]
average area of wetlands selected in a SB in meters

    'Test with IF contributing area > SB area then set the maximum
contributing area=SBarea
    If ICMOsumlength(i) * designW * beta > SBarea(i) Then
        beta = SBarea(i) / ICMOsumlength(i) * designW
    End If

        '''set initial condition: storage=1ft of water
        It(1, i) = flowdata(1, i) * (ICMO_SAbar(i) * beta /
(SBarea(i)))  '[cms] inflow to wetland is proportional to flow in SB-->
```

```
Q/I = SBarea/(wetland drainge area)-->I=Q*(wetland drainage
area)/SBarea
        St(1, i) = designNH * ICMO_SAbar(i) 'initial condition [m^3] is
1 ft of water at the bottom of reservoir
        Ht(1, i) = St(1, i) / ICMO_SAbar(i) '[m] = 0.3m
        Qt(1, i) = 0 'C * designLC * Ht(1, i) ^ 1.5 '[cms]

        ''iteration begins
        For j = 2 To 9131 'for all flow record from 1985-2009,j=1--
>1/1/1985
            It(j, i) = flowdata(j, i) * beta * ICMO_SAbar(i) /
(SBarea(i))  '[m3/s][-][m2]/[m2]=[m3/s]
            St(j, i) = St(j - 1, i) + (It(j - 1, i) - Qt(j - 1, i) -
ICMO_SAbar(i) * (1 * k + ET)) * dt '[m3]+[m3/s-m3/s-m2*m/s][s]=[m3]:
current storage=previous storage+inflow-coutflow-ET
            Ht(j, i) = St(j, i) / ICMO_SAbar(i) '[m3]/[m2]=[m]

            If Ht(j, i) > designD Then
                Qt(j, i) = C * designLC * (Ht(j, i) - designD) ^ 1.5
'outflow over the weir
            ElseIf Ht(j, i) > designNH Then
                Qt(j, i) = C * designNW * (Ht(j, i) - designNH) ^ 1.5
'outflow through the notch during small storm events when water is not
overtopping the structure
            Else
                Qt(j, i) = 0
            End If

        Next j

    '''Multiply the average wetland by the number of wetlands in SB
        For j = 1 To 9131
            Itn(j, i) = It(j, i) * ICMOcount(i)
            Stn(j, i) = St(j, i) * ICMOcount(i)
            Htn(j, i) = Ht(j, i) * ICMOcount(i)
            Qtn(j, i) = Qt(j, i) * ICMOcount(i) 'outflow through
wetland.
            Qtnout(j, i) = Qtn(j, i) + (flowdata(j, i) - Itn(j, i))
'Water flowing out of SB=outflow from wetland + water that didn't go
through water storage MO. This will be used in the river routing

        'Worksheets("Sheet2").Cells(1 + j, 2) = flowdata(j, i) 'inflow
in cms

        'Worksheets("Sheet2").Cells(1 + j, 8) = Itn(j, i)
        'Worksheets("Sheet2").Cells(1 + j, 9) = Stn(j, i)
        'Worksheets("Sheet2").Cells(1 + j, i) = Ht(j, i)
        'Worksheets("Sheet2").Cells(1 + j, 11) = Qtn(j, i)
        'Worksheets("Sheet2").Cells(1 + j, 12) = Qtnout(j, i)

        Next j

    'Worksheets("Sheet1").Range("T1") = ICMO_SAbar(i)
    'Worksheets("Sheet1").Range("T2") = L(i)

End If
```

```
'the product is the box variable Qtnout(j=1/1/1985-12/31/2009,i=SB1-
SB30)


'end of storage outflow''''''''''''''''''''''''''''''''''''''''
''''''''''''''''''''''''''''''''''''''''''''''''''''''''''''''''''''''''''''''''
''''''''''''''''''''
End Sub
```

B.3. Sediment loading algorithm

```
Option Explicit

Sub sedloading(TLMO_N, TLMOdata, AFMO_N, AFMOdata, BFMO_N, BFMOdata,
WCMO_N, WCMOdata, RAMO_N, RAMOdata, NCMO_N, NCMOdata)

'SECTION1: import reach database

'SECTION 2: calculate MO extents in each SEDSB
    'TLMO: calculate SE*-save as->ReachData(j,30)

    'AFMO: calculate DA, Ag
    'WCMO: calculate DA, Aw
    'Agw
    'Ag'=Ag_Agw
    'Aw'=Aw-Agw
    'Calculate SDRf reduction factor (SDRfeff) with above -save as-
>ReachData(j,31)

    'RAMO: calculate SL*-save as->ReachData(j,32)
    'NCMO: calculate SL*-save as->ReachData(j,33)

'SECTION 3: sediment loading algorithm
    'sediment loading without MOs
    'sedimetn loading with MOs: Go through Reach contributing area and
Calculate MO effect


Dim i As Integer, j As Integer, k As Integer

''''''''''''''''''''''''''''''''''''''''''''''''''''''''''''''''''''''''''''''''
''''''''''''''''''''''''''''''''''''''''''''''''''''''''''''''''''''''''''''''''SECTION 1:
Import Reachdatabase
''''''''''''''''''''''''''''''''''''''''''''''''''''''''''''''''''''''''''''''''
```

```
'Reach data access
'databasepath = "Macintosh HD:Users:sejongee:Documents:JHU-mac:CSSR-
Research:MOSM:v6:"
'ReachDatabase = "Reachdata.xlsx"
'Application.ScreenUpdating = False 'to prevent slowing down operation
'Workbooks.Open Filename:=databasepath & ReachDatabase 'open
destination workbook (database workbook)

'''''
Dim Reach_N As Integer, UM_N As Integer, MC_N As Integer, LC_N As
Integer, UL_N As Integer, LO_N As Integer
Reach_N = Worksheets("Reachdata").Range("A1") 'number of reach segments
UM_N = Worksheets("Reachdata").Range("D3")
MC_N = Worksheets("Reachdata").Range("E3")
LC_N = Worksheets("Reachdata").Range("F3")
UL_N = Worksheets("Reachdata").Range("G3")
LO_N = Worksheets("Reachdata").Range("H3")

Dim UMtoLO As Integer, MCtoLO As Integer, LCtoLO As Integer, ULtoLO As
Integer
'define the Reach/SB locations where the reaches make connection
UMtoLO = Worksheets("Reachdata").Range("D5") '510
MCtoLO = Worksheets("Reachdata").Range("E5") '377
LCtoLO = Worksheets("Reachdata").Range("F5") '377
ULtoLO = Worksheets("Reachdata").Range("G5") '105

ReachData = Worksheets("Reachdata").Range("B10:AZ538") 'import reach
database including area, soilloss, and loadings
SDRfparam = Worksheets("SDRf").Range("E6:G534") 'import SDRf
distribution parameters
SDRfpparam = Worksheets("SDRf").Range("H6:J534") 'import SDRf
distribution parameters
SDRffparam = Worksheets("SDRf").Range("K6:M534") 'import SDRf
distribution parameters
'BESTSDRf = Worksheets("SDRf").Range("G6:G534")
SDRsparam = Worksheets("SDRsparam").Range("D5:G9") 'import SDRs
parameters
BESTparam = Worksheets("SDRsparam").Range("H5:J9") 'best parameter for
1 MC situation

'ActiveWorkbook.Close savechanges:=False 'close the database
'Application.ScreenUpdating = True
''''''''''''''''''''''''''''''''''''''''''''''''''''''''''''''''''''''''''
''''''''''''''''''''''
'end of importing input Data
''''''''''''''''''''''''''''''''''''''''''''''''''''''''''''''''''''''''''
''''''''''''''''''''''''''''''''''''''''''''''''''''''''''''''''''''''''''
'SECTION2: go through Reach contributing area and Calculate MO effect
'''calculate soil loss reduction from TLMO
'''calculate extent of AFMO
'''calculate sediment loading reduction from RAMO and NCMO
'''calculate SDRf reduction from AFMO

''''''''''''''''''''''''''''''''''''''''''''''''''''''''''''''''''''''''''
''''''''''''''''''''''''''''''''''''''''''''''''''''''''''''''''''''''''''

'MO efficiency variable and definitions
```

```
Dim Anmin_factor As Double
Dim alpha As Variant
Dim X As Double 'proportion of AFMO DA (Ag) and WCMO DA (Aw) overlap
Dim BFMO_DF As Double 'drainage extent
Dim Fr As Double 'Ravine seidment source addressed

Dim BFMOeff As Double
Dim AFMOeff As Double
Dim WCMOeff As Double
Dim RAMOeff As Double
Dim NCMOeff As Double

Anmin_factor = Worksheets("I|O Detail").Range("P3") / 100
alpha = Worksheets("I|O Detail").Range("T20:AB22")
X = Worksheets("I|O Detail").Range("M30")
BFMO_DF = Worksheets("I|O Detail").Range("M42")
Fr = Worksheets("I|O Detail").Range("M87") / 100

BFMOeff = Worksheets("CONTROL").Range("M17") / 100
AFMOeff = Worksheets("CONTROL").Range("M14") / 100
WCMOeff = Worksheets("CONTROL").Range("M20") / 100
RAMOeff = Worksheets("CONTROL").Range("M26") / 100
NCMOeff = Worksheets("CONTROL").Range("M29") / 100

''''''''''''''''''''''''''''''''''''''''''''''''''''''''''''''''''''''''''''''
'''Calculate soil loss reduction from 1) TLMO, 2) BFMO 3) AFMOs, 4)
WCMO 5) Agw 6) sed loading reduction from RAMO and 7)NCMO
'Loop thorugh SEDSB
''''''''''''''''''''''''''''''''''''''''''''''''''''''''''''''''''''''''''''''
''''''''''''''''''''''''''''''''''''''''''''''''''''
Dim A As Double
Dim Anmin As Double
Dim TLMO_SE As Double
Dim Ab As Double
Dim Ag As Double
Dim WCMO_A As Double
Dim Aw As Double
Dim Agw As Double
Dim Ag_ As Double
Dim Aw_ As Double
'Dim SDRfeff As Double '----------->store as reachdata(i,31)
Dim RAMO_SL As Double '----------->store as reachdata(i,32)
Dim NCMO_SL As Double '----------->store as reachdata(i,33)

For i = 1 To Reach_N '1 to Reach_N

    A = ReachData(i, 6)
    Anmin = A * Anmin_factor
    TLMO_SE = 0
    Ab = 0
    Ag = 0
    WCMO_A = 0
    Aw = 0
    Agw = 0
    Ag_ = 0
    Aw_ = 0
    'SDRfeff = 0
```

```
    RAMO_SL = 0
    NCMO_SL = 0

    ''''''''''''1) Calculate new soil loss after TLMO---
>ReachData(i,30)''''''''''''''''''''''''''''''''''''''''''''''''''''''''''''''''
''''''''''''''''''''''''''''''''''''''''''''''''''''''''''''''''''''''''''''''''
    ''calculate SE=(alpha1*A1+alpha2*A2+alpha3*A3)*Xbar for M, C, L for
j=1 to TLMO_N <--if River =M,C,L

    For j = 1 To TLMO_N 'go through each TLMO in the database

        If ReachData(i, 1) = TLMOdata(j, 5) Then 'check TLMO_j is
located in SEDSB_i

            If ReachData(i, 3) = "LES" Then 'check River=LES

                'Calculate new SE for zone1, zone2, or zone 3
                TLMO_SE = TLMO_SE _
                    + (alpha(1, 1) * TLMOdata(j, 39) + alpha(2, 1) *
TLMOdata(j, 40) + alpha(3, 1) * TLMOdata(j, 41)) * ReachData(i, 26) *
ReachData(i, 27) _
                    + (alpha(1, 2) * TLMOdata(j, 39) + alpha(2, 2) *
TLMOdata(j, 40) + alpha(3, 2) * TLMOdata(j, 41)) * ReachData(i, 26) *
ReachData(i, 28) _
                    + (alpha(1, 3) * TLMOdata(j, 39) + alpha(2, 3) *
TLMOdata(j, 40) + alpha(3, 3) * TLMOdata(j, 41)) * ReachData(i, 26) *
ReachData(i, 29)

            ElseIf ReachData(i, 3) = "COB" Then

                TLMO_SE = TLMO_SE _
                    + (alpha(1, 4) * TLMOdata(j, 39) + alpha(2, 4) *
TLMOdata(j, 40) + alpha(3, 4) * TLMOdata(j, 41)) * ReachData(i, 26) *
ReachData(i, 27) _
                    + (alpha(1, 5) * TLMOdata(j, 39) + alpha(2, 5) *
TLMOdata(j, 40) + alpha(3, 5) * TLMOdata(j, 41)) * ReachData(i, 26) *
ReachData(i, 28) _
                    + (alpha(1, 6) * TLMOdata(j, 39) + alpha(2, 6) *
TLMOdata(j, 40) + alpha(3, 6) * TLMOdata(j, 41)) * ReachData(i, 26) *
ReachData(i, 29)

            Else 'if river=MAP

                TLMO_SE = TLMO_SE _
                    + (alpha(1, 7) * TLMOdata(j, 39) + alpha(2, 7) *
TLMOdata(j, 40) + alpha(3, 7) * TLMOdata(j, 41)) * ReachData(i, 26) *
ReachData(i, 27) _
                    + (alpha(1, 8) * TLMOdata(j, 39) + alpha(2, 8) *
TLMOdata(j, 40) + alpha(3, 8) * TLMOdata(j, 41)) * ReachData(i, 26) *
ReachData(i, 28) _
                    + (alpha(1, 9) * TLMOdata(j, 39) + alpha(2, 9) *
TLMOdata(j, 40) + alpha(3, 9) * TLMOdata(j, 41)) * ReachData(i, 26) *
ReachData(i, 29)

            End If

        End If
```

```
    Next j

    'calculate new soil loss (SE*) with TLMO application plus soil loss
from non-tilled area (=ReachData(i,10)-ReachData(i,25)) for each SEDSB
i
    ReachData(i, 30) = TLMO_SE + ReachData(i, 10) - ReachData(i, 25)
    'Worksheets("Sheet1").Cells(1 + i, 1) = ReachData(i, 30)
    'Worksheets("Reachdata").Cells(9 + i, 31) = ReachData(i, 30)

        ''''''''''''''2) Calculate (DA of BFMO)---
>ReachData(i,33)''''''''''''''''''''''''''''''''''''''''''''''''''''''''''
''''''''''''''''''''''''''''''''''''''''''''''''''''''''''''''''''''''''''
    For j = 1 To BFMO_N
        If ReachData(i, 1) = BFMOdata(j, 5) And BFMOdata(j, 50) = 1
Then 'check BFMO_j is located inSEDSB_i and BFMO_j is selected
            'Ab = Ab + BFMOdata(j, 18) * BFMO_DF 'sum BFMO_DA=L*DL in
SEDSB_i
            Ab = Ab + BFMOdata(j, 19)
        End If
    Next j

   'set the upper bound of BFMO drainage area to Ap
    If Ab > ReachData(i, 40) Then
        Ab = ReachData(i, 40)
    End If

    'Worksheets("Reachdata").Cells(9 + i, 48) = Ab

    ''''''''''''''3) Calculate (DA of AFMO)---
>ReachData(i,31)''''''''''''''''''''''''''''''''''''''''''''''''''''''''''
''''''''''''''''''''''''''''''''''''''''''''''''''''''''''''''''''''''''''
    For j = 1 To AFMO_N
        If ReachData(i, 1) = AFMOdata(j, 5) And AFMOdata(j, 50) = 1
Then 'check AFMO_j is located inSEDSB_i and AFMO_j is selected
            Ag = Ag + AFMOdata(j, 15) 'sum AFMO_DA in SEDSB_i
        End If
    Next j

    ''''''''''''''4) Calculate (DA of WCMO)---
>ReachData(i,32)''''''''''''''''''''''''''''''''''''''''''''''''''''''''''
''''''''''''''''''''''''''''''''''''''''''''''''''''''''''''''''''''''''''
    For j = 1 To WCMO_N
        If ReachData(i, 1) = WCMOdata(j, 5) And WCMOdata(j, 50) = 1
Then 'check AFMO_j is located inSEDSB_i and AFMO_j is selected
            WCMO_A = WCMO_A + WCMOdata(j, 14) 'sum allocated WCMO_A in
SEDSB_i
        End If
    Next j

    'calculate WCMO DA, Aw given the WCMO Area selected for each SEDSB
i
    Aw = (ReachData(i, 41) - Anmin) * (1 - Exp(-1e-06 * WCMO_A))
'calculate DA of WCMO as function of Af-Anmin and selected SA of WCMO
    'Worksheets("Reachdata").Cells(9 + i, 43) = Aw
```

```
     ''''''''''''''5) Calculate Agw, Ag', and Aw and SDRfN elements
''''''''''''''
```

```
    ReachData(i, 33) = NCMO_SL
    'Worksheets("Sheet1").Cells(1 + i, 6) = ReachData(i, 33)
Next i
''''''''''''''''''''''''''''''''''''''''''''''''''''''''''''''''''''''''''''''''
'''''''END OF MO IMPACT
''''''''''''''''''''''''''''''''''''''''''''''''''''''

'SECTION3: Calculate stochastic sediment loading using
MC''''''''''''''''''''''''''''''''''''''''''''''''''''''''''''''''''''''''''''''''
''''''''''''''''''''''''
'''Determine SDRf and SDRs from random
selection''''''''''''''''''''''''''''''''''''''''''''''''''''''''''''''''''''''''
''''''''''''''''''''''''''''''''''''''''''''''''''''
'''Calculate SL without MOs
''''''''''''''''''''''''''''''''''''''''''''''''''''''''''''''''''''''''''''''''''''
''''''''''''''''''''''''''''''''''''''''''''''''''
'''Calculate SL with MOs
''''''''''''''''''''''''''''''''''''''''''''''''''''''''''''''''''''''''''''''''''''
''''''''''''''''''''''''''''''''''''''''''''''''''

'Define and read input param
Dim MCn As Integer
MCn = Worksheets("CONTROL").Range("M2") 'number of MC iterations
Dim density As Double
Dim perc As Double
perc = Worksheets("I|O Detail").Range("M3") 'MC percentile output
density = Worksheets("I|O Detail").Range("M4") 'soil density to
calculate volume of storage

'define variables to generate SDRf and SDRs
'Dim UMrndi As Integer, MCrndi As Integer, LCrndi As Integer, ULrndi As
Integer, LOrndi As Integer
Dim UM_a2 As Double, UM_b2 As Double
Dim MC_a2 As Double, MC_b2 As Double
Dim LC_a2 As Double, LC_b2 As Double
Dim UL_a2 As Double, UL_b2 As Double
Dim LO_a2 As Double, LO_b2 As Double

Dim RndProb As Double
Dim SDRf As Double
Dim SDRfN As Double
Dim SDRs As Double
Dim SLf As Double

Dim Hockeystick_MAP As Double, Hockeystick_COB As Double,
Hockeystick_LES As Double, Hockeystick As Double

Hockeystick_MAP = Worksheets("Output Detail").Range("E8")
Hockeystick_COB = Worksheets("Output Detail").Range("E9")
Hockeystick_LES = Worksheets("Output Detail").Range("E10")
Hockeystick = (Hockeystick_MAP + Hockeystick_COB + Hockeystick_LES) / 3

'''define output variables
'Sediment Loading (SL) outputs with no MO input
Dim SL_UM_noMO() As Double, SL_MC_noMO() As Double, SL_LC_noMO() As
Double, SL_UL_noMO() As Double, SL_LO_noMO() As Double
ReDim SL_UM_noMO(1 To MCn) As Double
```

```
ReDim SL_MC_noMO(1 To MCn) As Double
ReDim SL_LC_noMO(1 To MCn) As Double
ReDim SL_UL_noMO(1 To MCn) As Double
ReDim SL_LO_noMO(1 To MCn) As Double

'Sediment Loading (SL) outputs with MO input
Dim SL_UM() As Double, SL_MC() As Double, SL_LC() As Double, SL_UL() As
Double, SL_LO() As Double
ReDim SL_UM(1 To MCn) As Double
ReDim SL_MC(1 To MCn) As Double
ReDim SL_LC(1 To MCn) As Double
ReDim SL_UL(1 To MCn) As Double
ReDim SL_LO(1 To MCn) As Double

'Sediment Loading Reduction (SLR) outputs with MO input
Dim SLR_UM() As Double, SLR_MC() As Double, SLR_LC() As Double,
SLR_UL() As Double, SLR_LO() As Double
ReDim SLR_UM(1 To MCn) As Double
ReDim SLR_MC(1 To MCn) As Double
ReDim SLR_LC(1 To MCn) As Double
ReDim SLR_UL(1 To MCn) As Double
ReDim SLR_LO(1 To MCn) As Double

'SDf and SDs outputs with MOs
Dim SDfmm_UM() As Double, SDfmm_MC() As Double, SDfmm_LC() As Double,
SDfmm_UL() As Double, SDfm_LO() As Double
ReDim SDfmm_UM(1 To MCn) As Double
ReDim SDfmm_MC(1 To MCn) As Double
ReDim SDfmm_LC(1 To MCn) As Double
ReDim SDfmm_UL(1 To MCn) As Double
ReDim SDfmm_LO(1 To MCn) As Double

Dim SDsmm_UM() As Double, SDsmm_MC() As Double, SDsmm_LC() As Double,
SDsmm_UL() As Double, SDsmm_LO() As Double
ReDim SDsmm_UM(1 To MCn) As Double
ReDim SDsmm_MC(1 To MCn) As Double
ReDim SDsmm_LC(1 To MCn) As Double
ReDim SDsmm_UL(1 To MCn) As Double
ReDim SDsmm_LO(1 To MCn) As Double

For i = 1 To MCn

    If MCn = 1 Then ''''''''''''''''''''''''''''''''''''''''''''''Dfine
DETERMINISTIC SDR parmaeters WITH BEST
PARAM''''''''''''''''''''''''''''''
    'to calculate the best SDRs
    UM_a2 = BESTparam(1, 2)
    UM_b2 = BESTparam(1, 3)
    MC_a2 = BESTparam(2, 2)
    MC_b2 = BESTparam(2, 3)
    LC_a2 = BESTparam(3, 2)
    LC_b2 = BESTparam(3, 3)
    UL_a2 = BESTparam(4, 2)
    UL_b2 = BESTparam(4, 3)
    LO_a2 = BESTparam(5, 2)
    LO_b2 = BESTparam(5, 3)
```

```
    Else ''''''
```

```
                    - (ReachData(j, 34) *
Exp(WorksheetFunction.NormInv(RndProb, SDRffparam(j, 1), SDRffparam(j,
2))) _
                    + ReachData(j, 35) *
Exp(WorksheetFunction.NormInv(RndProb, SDRfpparam(j, 1), SDRfpparam(j,
2)))) _
                    / ReachData(j, 6)

            If SDRfN < 0 Then
                SDRfN = 1e-05
            End If

        End If

        'Worksheets("Reachdata").Cells(9 + j, 33) = SDRf
        'Worksheets("Reachdata").Cells(9 + j, 34) = SDRfN

        If ReachData(j, 4) = "UM" Then
            '1) no MO SL calculation
            SDRs = Exp(UM_a2 * (ReachData(j, 9) / ReachData(j, 7)) ^
UM_b2 * ReachData(j, 8))
            SL_UM_noMO(i) = SL_UM_noMO(i) + (ReachData(j, 10) * SDRf +
ReachData(j, 22)) * SDRs 'ReachData(j,10) is the input soil loss
'Reachdata(j,22)=net NCS loading

            '2) MO SL calculation
            SLf = ReachData(j, 30) * SDRfN

            SDfmm_UM(i) = SDfmm_UM(i) + (ReachData(j, 30) - SLf) /
(density * ReachData(j, 6)) * 1000 'sediment deposition over entire
SEDSB area (j,6)
            SL_UM(i) = SL_UM(i) + (SLf + ReachData(j, 32) +
(ReachData(j, 18) + ReachData(j, 33)) * (1 - Hockeystick_MAP)) * SDRs
'apply effects of water conservation to bluff (j,33) and stream
banks(j,18)
            'SDsmm_UM(i) = SDsmm_UM(i) + (SLf + ReachData(j, 32) +
ReachData(j, 18) + ReachData(j, 33) - SL_UM(i)) / (density *
ReachData(j, 8)) * 1000
            SDsmm_UM(i) = SDsmm_UM(i) + (SLf + ReachData(j, 32) +
(ReachData(j, 18) + ReachData(j, 33)) * (1 - Hockeystick_MAP)) * (1 -
SDRs) / (density * ReachData(j, 8)) * 1000

            '3) MO SL reduction  (SLR) calculation
            SLR_UM(i) = SL_UM_noMO(i) - SL_UM(i)

        ElseIf ReachData(j, 4) = "MC" Then
            '1) no MO SL calculation
            'SDRf = SDRf1000(j, MCrndi)
            SDRs = Exp(MC_a2 * (ReachData(j, 9) / ReachData(j, 7)) ^
MC_b2 * ReachData(j, 8))
            SL_MC_noMO(i) = SL_MC_noMO(i) + (ReachData(j, 10) * SDRf +
ReachData(j, 22)) * SDRs 'ReachData(j,10) is the input soil loss

            '2) MO SL calculation
            SLf = ReachData(j, 30) * SDRfN
```

```
            SDfmm_MC(i) = SDfmm_MC(i) + (ReachData(j, 30) - SLf) /
(density * ReachData(j, 6)) * 1000 'sediment deposition over entire
SEDSB area (j,6)
            SL_MC(i) = SL_MC(i) + (SLf + ReachData(j, 32) +
(ReachData(j, 18) + ReachData(j, 33)) * (1 - Hockeystick_COB)) * SDRs
'apply effects of water conservation to bluff (j,33) and stream
banks(j,18)
            SDsmm_MC(i) = SDsmm_MC(i) + (SLf + ReachData(j, 32) +
(ReachData(j, 18) + ReachData(j, 33)) * (1 - Hockeystick_COB)) * (1 -
SDRs) / (density * ReachData(j, 8)) * 1000

            '3) MO SL reduction  (SLR) calculation
            SLR_MC(i) = SL_MC_noMO(i) - SL_MC(i)

        ElseIf ReachData(j, 4) = "LC" Then
            '1) no MO SL calculation
            'SDRf = SDRf1000(j, LCrndi)
            SDRs = Exp(LC_a2 * (ReachData(j, 9) / ReachData(j, 7)) ^
LC_b2 * ReachData(j, 8))
            SL_LC_noMO(i) = SL_LC_noMO(i) + (ReachData(j, 10) * SDRf +
ReachData(j, 22)) * SDRs 'ReachData(j,10) is the input soil loss

            '2) MO SL calculation
            SLf = ReachData(j, 30) * SDRfN
            SDfmm_LC(i) = SDfmm_LC(i) + (ReachData(j, 30) - SLf) /
(density * ReachData(j, 6)) * 1000 'sediment deposition over entire
SEDSB area (j,6)
            SL_LC(i) = SL_LC(i) + (SLf + ReachData(j, 32) +
(ReachData(j, 18) + ReachData(j, 33)) * (1 - Hockeystick_COB)) * SDRs
'apply effects of water conservation to bluff (j,33) and stream
banks(j,18)
            SDsmm_LC(i) = SDsmm_LC(i) + (SLf + ReachData(j, 32) +
(ReachData(j, 18) + ReachData(j, 33)) * (1 - Hockeystick_COB)) * (1 -
SDRs) / (density * ReachData(j, 8)) * 1000

             '3) MO SL reduction  (SLR) calculation
            SLR_LC(i) = SL_LC_noMO(i) - SL_LC(i)

        ElseIf ReachData(j, 4) = "UL" Then
            '1) no MO SL calculation
            'SDRf = SDRf1000(j, UMrndi)
            SDRs = Exp(UL_a2 * (ReachData(j, 9) / ReachData(j, 7)) ^
UL_b2 * ReachData(j, 8))
            SL_UL_noMO(i) = SL_UL_noMO(i) + (ReachData(j, 10) * SDRf +
ReachData(j, 22)) * SDRs 'ReachData(j,10) is the input soil loss

            '2) MO SL calculation
            SLf = ReachData(j, 30) * SDRfN
            SDfmm_UL(i) = SDfmm_UL(i) + (ReachData(j, 30) - SLf) /
(density * ReachData(j, 6)) * 1000 'sediment deposition over entire
SEDSB area (j,6)
            SL_UL(i) = SL_UL(i) + (SLf + ReachData(j, 32) +
(ReachData(j, 18) + ReachData(j, 33)) * (1 - Hockeystick_LES)) * SDRs
'apply effects of water conservation to bluff (j,33) and stream
banks(j,18)
```

```
            SDsmm_UL(i) = SDsmm_UL(i) + (SLf + ReachData(j, 32) +
(ReachData(j, 18) + ReachData(j, 33)) * (1 - Hockeystick_LES)) * (1 -
SDRs) / (density * ReachData(j, 8)) * 1000

            '3) MO SL reduction  (SLR) calculation
            SLR_UL(i) = SL_UL_noMO(i) - SL_UL(i)

        End If

        'Worksheets("Reachdata").Cells(j + 9, 35) = SDRs

    Next j

    ''''''Go through LO with outputs from UM, MC, LC, and
UL''''''''''''''''''''''''''''''''''''''''''''''''''''''''

    For j = 1 To Reach_N 'go through LO and add inflows from upstream
watersheds

        'look up SDRf 1)optimal solution 2) calculated from lognomarl
distribution outputs from Topofilter
        If MCn = 1 Then
            SDRf = SDRfparam(j, 3)
            SDRfN = (SDRf _
                    - (ReachData(j, 34) * SDRffparam(j, 3) _
                    + ReachData(j, 35) * SDRfpparam(j, 3)) _
                    / ReachData(j, 6))
        Else
            SDRf = Exp(WorksheetFunction.NormInv(RndProb, SDRfparam(j,
1), SDRfparam(j, 2))) 'calculate SDRf from
            SDRfN = (SDRf _
                    - (ReachData(j, 34) *
Exp(WorksheetFunction.NormInv(RndProb, SDRffparam(j, 1), SDRffparam(j,
2))) _
                    + ReachData(j, 35) *
Exp(WorksheetFunction.NormInv(RndProb, SDRfpparam(j, 1), SDRfpparam(j,
2)))) _
                    / ReachData(j, 6))

            If SDRfN < 0 Then
                SDRfN = 1e-05
            End If
        End If

        If ReachData(j, 4) = "LO" Then

            'Calculate the SDR for each SEDSB j
            'SDRf = SDRf1000(j, LOrndi)
            SDRs = Exp(LO_a2 * (ReachData(j, 9) / ReachData(j, 7)) ^
LO_b2 * ReachData(j, 8))

            '2) MO SL calculation
            SLf = ReachData(j, 30) * SDRfN
            SDfmm_LO(i) = SDfmm_LO(i) + (ReachData(j, 30) - SLf) /
(density * ReachData(j, 6)) * 1000

            'check the SEDSB that confluence with upstream watersheds:
```

```
            If ReachData(j, 1) = UMtoLO Then 'UM to LO junction
                '1) no MO SL calculation
                SL_LO_noMO(i) = SL_LO_noMO(i) + (ReachData(j, 10) *
SDRf + ReachData(j, 22) + SL_UM_noMO(i)) * SDRs 'Input at UG from UM

                '2) MO SL calculation
                SL_LO(i) = SL_LO(i) + (SLf + ReachData(j, 32) +
(ReachData(j, 18) + ReachData(j, 33)) * (1 - Hockeystick) + SL_UM(i)) *
SDRs
                SDsmm_LO(i) = SDsmm_LO(i) + (SLf + ReachData(j, 32) +
(ReachData(j, 18) + ReachData(j, 33)) * (1 - Hockeystick) + SL_UM(i)) *
(1 - SDRs) / (density * ReachData(j, 8)) * 1000

                '3) MO SL reduction  (SLR) calculation
                SLR_LO(i) = SL_LO_noMO(i) - SL_LO(i)

            ElseIf ReachData(j, 1) = MCtoLO Then 'MC, LC to LO junction
                 '1) no MO SL calculation
                SL_LO_noMO(i) = SL_LO_noMO(i) + (ReachData(j, 10) *
SDRf + ReachData(j, 22) + SL_MC_noMO(i) + SL_LC_noMO(i)) * SDRs 'Input
at UG from MC and LC

                '2) MO SL calculation
                SL_LO(i) = SL_LO(i) + (SLf + ReachData(j, 32) +
(ReachData(j, 18) + ReachData(j, 33)) * (1 - Hockeystick) + SL_MC(i) +
SL_LC(i)) * SDRs
                SDsmm_LO(i) = SDsmm_LO(i) + (SLf + ReachData(j, 32) +
(ReachData(j, 18) + ReachData(j, 33)) * (1 - Hockeystick) + SL_MC(i) +
SL_LC(i)) * (1 - SDRs) / (density * ReachData(j, 8)) * 1000

                '3) MO SL reduction  (SLR) calculation
                SLR_LO(i) = SL_LO_noMO(i) - SL_LO(i)

            ElseIf ReachData(j, 1) = ULtoLO Then
                '1) no MO SL calculation
                SL_LO_noMO(i) = SL_LO_noMO(i) + (ReachData(j, 10) *
SDRf + ReachData(j, 22) + SL_UL_noMO(i)) * SDRs 'Input at UG from UL

                '2) MO SL calculation
                SL_LO(i) = SL_LO(i) + (SLf + ReachData(j, 32) +
(ReachData(j, 18) + ReachData(j, 33)) * (1 - Hockeystick) + SL_UL(i)) *
SDRs
                SDsmm_LO(i) = SDsmm_LO(i) + (SLf + ReachData(j, 32) +
(ReachData(j, 18) + ReachData(j, 33)) * (1 - Hockeystick) + SL_UL(i)) *
(1 - SDRs) / (density * ReachData(j, 8)) * 1000

            Else
                '1) no MO SL calculation
                SL_LO_noMO(i) = SL_LO_noMO(i) + (ReachData(j, 10) *
SDRf + ReachData(j, 22)) * SDRs

                '2) MO SL calculation
                SL_LO(i) = SL_LO(i) + (SLf + ReachData(j, 32) +
(ReachData(j, 18) + ReachData(j, 33)) * (1 - Hockeystick)) * SDRs
                SDsmm_LO(i) = SDsmm_LO(i) + (SLf + ReachData(j, 32) +
(ReachData(j, 18) + ReachData(j, 33)) * (1 - Hockeystick)) * (1 - SDRs)
/ (density * ReachData(j, 8)) * 1000
```

```
                '3) MO SL reduction  (SLR) calculation
                SLR_LO(i) = SL_LO_noMO(i) - SL_LO(i)

            End If

          'Worksheets("Reachdata").Cells(j + 9, 35) = SDRs

        End If
    Next j

SDfmm_UM(i) = SDfmm_UM(i) / UM_N
SDsmm_UM(i) = SDsmm_UM(i) / UM_N
SDfmm_MC(i) = SDfmm_MC(i) / MC_N
SDsmm_MC(i) = SDsmm_MC(i) / MC_N
SDfmm_LC(i) = SDfmm_LC(i) / LC_N
SDsmm_LC(i) = SDsmm_LC(i) / LC_N
SDfmm_UL(i) = SDfmm_UL(i) / UL_N
SDsmm_UL(i) = SDsmm_UL(i) / UL_N
SDfmm_LO(i) = SDfmm_LO(i) / LO_N
SDsmm_LO(i) = SDsmm_LO(i) / LO_N

'Application.StatusBar = "calculating sediment loading"

Next i

'Application.StatusBar = False

''''''
```

```
Worksheets("Output Detail").Range("C34") = SLR_LC
Worksheets("Output Detail").Range("C35") = SLR_UL
Worksheets("Output Detail").Range("C36") = SLR_LO
'SDf mm/yr
Worksheets("Output Detail").Range("C41") = SDfmm_UM
Worksheets("Output Detail").Range("C42") = SDfmm_MC
Worksheets("Output Detail").Range("C43") = SDfmm_LC
Worksheets("Output Detail").Range("C44") = SDfmm_UL
Worksheets("Output Detail").Range("C45") = SDfmm_LO
'SDs mm/yr
Worksheets("Output Detail").Range("C49") = SDsmm_UM
Worksheets("Output Detail").Range("C50") = SDsmm_MC
Worksheets("Output Detail").Range("C51") = SDsmm_LC
Worksheets("Output Detail").Range("C52") = SDsmm_UL
Worksheets("Output Detail").Range("C53") = SDsmm_LO

Else

''NO MO
'''SL outputs
'mean
Worksheets("Output Detail").Range("C15") = mean(MCn, SL_UM_noMO)
Worksheets("Output Detail").Range("C16") = mean(MCn, SL_MC_noMO)
Worksheets("Output Detail").Range("C17") = mean(MCn, SL_LC_noMO)
Worksheets("Output Detail").Range("C18") = mean(MCn, SL_UL_noMO)
Worksheets("Output Detail").Range("C19") = mean(MCn, SL_LO_noMO)

'Standard deviation
Worksheets("Output Detail").Range("D15") = StdDev(MCn, SL_UM_noMO,
mean(MCn, SL_UM_noMO))
Worksheets("Output Detail").Range("D16") = StdDev(MCn, SL_MC_noMO,
mean(MCn, SL_MC_noMO))
Worksheets("Output Detail").Range("D17") = StdDev(MCn, SL_LC_noMO,
mean(MCn, SL_LC_noMO))
Worksheets("Output Detail").Range("D18") = StdDev(MCn, SL_UL_noMO,
mean(MCn, SL_UL_noMO))
Worksheets("Output Detail").Range("D19") = StdDev(MCn, SL_LO_noMO,
mean(MCn, SL_LO_noMO))

'min
Worksheets("Output Detail").Range("E15") =
WorksheetFunction.Min(SL_UM_noMO)
Worksheets("Output Detail").Range("E16") =
WorksheetFunction.Min(SL_MC_noMO)
Worksheets("Output Detail").Range("E17") =
WorksheetFunction.Min(SL_LC_noMO)
Worksheets("Output Detail").Range("E18") =
WorksheetFunction.Min(SL_UL_noMO)
Worksheets("Output Detail").Range("E19") =
WorksheetFunction.Min(SL_LO_noMO)

'max
Worksheets("Output Detail").Range("F15") =
WorksheetFunction.Max(SL_UM_noMO)
Worksheets("Output Detail").Range("F16") =
WorksheetFunction.Max(SL_MC_noMO)
```

```
Worksheets("Output Detail").Range("F17") =
WorksheetFunction.Max(SL_LC_noMO)
Worksheets("Output Detail").Range("F18") =
WorksheetFunction.Max(SL_UL_noMO)
Worksheets("Output Detail").Range("F19") =
WorksheetFunction.Max(SL_LO_noMO)

'95 percentile
Worksheets("Output Detail").Range("G15") =
WorksheetFunction.Percentile(SL_UM_noMO, perc / 100)
Worksheets("Output Detail").Range("G16") =
WorksheetFunction.Percentile(SL_MC_noMO, perc / 100)
Worksheets("Output Detail").Range("G17") =
WorksheetFunction.Percentile(SL_LC_noMO, perc / 100)
Worksheets("Output Detail").Range("G18") =
WorksheetFunction.Percentile(SL_UL_noMO, perc / 100)
Worksheets("Output Detail").Range("G19") =
WorksheetFunction.Percentile(SL_LO_noMO, perc / 100)

'75 percentile
Worksheets("Output Detail").Range("H15") =
WorksheetFunction.Percentile(SL_UM_noMO, 1 - perc / 100)
Worksheets("Output Detail").Range("H16") =
WorksheetFunction.Percentile(SL_MC_noMO, 1 - perc / 100)
Worksheets("Output Detail").Range("H17") =
WorksheetFunction.Percentile(SL_LC_noMO, 1 - perc / 100)
Worksheets("Output Detail").Range("H18") =
WorksheetFunction.Percentile(SL_UL_noMO, 1 - perc / 100)
Worksheets("Output Detail").Range("H19") =
WorksheetFunction.Percentile(SL_LO_noMO, 1 - perc / 100)

'record all the MC outputs
'Worksheets("Output Detail").Range("J15:ALU15") = SL_UM_noMO

''with MO
''''SL outputs
'mean
Worksheets("Output Detail").Range("C23") = mean(MCn, SL_UM)
Worksheets("Output Detail").Range("C24") = mean(MCn, SL_MC)
Worksheets("Output Detail").Range("C25") = mean(MCn, SL_LC)
Worksheets("Output Detail").Range("C26") = mean(MCn, SL_UL)
Worksheets("Output Detail").Range("C27") = mean(MCn, SL_LO)

'STD
Worksheets("Output Detail").Range("D23") = StdDev(MCn, SL_UM, mean(MCn,
SL_UM))
Worksheets("Output Detail").Range("D24") = StdDev(MCn, SL_MC, mean(MCn,
SL_MC))
Worksheets("Output Detail").Range("D25") = StdDev(MCn, SL_LC, mean(MCn,
SL_LC))
Worksheets("Output Detail").Range("D26") = StdDev(MCn, SL_UL, mean(MCn,
SL_UL))
Worksheets("Output Detail").Range("D27") = StdDev(MCn, SL_LO, mean(MCn,
SL_LO))

'min
Worksheets("Output Detail").Range("E23") = WorksheetFunction.Min(SL_UM)
```

```
Worksheets("Output Detail").Range("E24") = WorksheetFunction.Min(SL_MC)
Worksheets("Output Detail").Range("E25") = WorksheetFunction.Min(SL_LC)
Worksheets("Output Detail").Range("E26") = WorksheetFunction.Min(SL_UL)
Worksheets("Output Detail").Range("E27") = WorksheetFunction.Min(SL_LO)

'max
Worksheets("Output Detail").Range("F23") = WorksheetFunction.Max(SL_UM)
Worksheets("Output Detail").Range("F24") = WorksheetFunction.Max(SL_MC)
Worksheets("Output Detail").Range("F25") = WorksheetFunction.Max(SL_LC)
Worksheets("Output Detail").Range("F26") = WorksheetFunction.Max(SL_UL)
Worksheets("Output Detail").Range("F27") = WorksheetFunction.Max(SL_LO)

'95 percentile
Worksheets("Output Detail").Range("G23") =
WorksheetFunction.Percentile(SL_UM, perc / 100)
Worksheets("Output Detail").Range("G24") =
WorksheetFunction.Percentile(SL_MC, perc / 100)
Worksheets("Output Detail").Range("G25") =
WorksheetFunction.Percentile(SL_LC, perc / 100)
Worksheets("Output Detail").Range("G26") =
WorksheetFunction.Percentile(SL_UL, perc / 100)
Worksheets("Output Detail").Range("G27") =
WorksheetFunction.Percentile(SL_LO, perc / 100)

'75 percentile
Worksheets("Output Detail").Range("H23") =
WorksheetFunction.Percentile(SL_UM, 1 - perc / 100)
Worksheets("Output Detail").Range("H24") =
WorksheetFunction.Percentile(SL_MC, 1 - perc / 100)
Worksheets("Output Detail").Range("H25") =
WorksheetFunction.Percentile(SL_LC, 1 - perc / 100)
Worksheets("Output Detail").Range("H26") =
WorksheetFunction.Percentile(SL_UL, 1 - perc / 100)
Worksheets("Output Detail").Range("H27") =
WorksheetFunction.Percentile(SL_LO, 1 - perc / 100)

'Record SL reduction
''''SLR outputs
'mean
Worksheets("Output Detail").Range("C32") = mean(MCn, SLR_UM)
Worksheets("Output Detail").Range("C33") = mean(MCn, SLR_MC)
Worksheets("Output Detail").Range("C34") = mean(MCn, SLR_LC)
Worksheets("Output Detail").Range("C35") = mean(MCn, SLR_UL)
Worksheets("Output Detail").Range("C36") = mean(MCn, SLR_LO)

'STD
Worksheets("Output Detail").Range("D32") = StdDev(MCn, SLR_UM,
mean(MCn, SLR_UM))
Worksheets("Output Detail").Range("D33") = StdDev(MCn, SLR_MC,
mean(MCn, SLR_MC))
Worksheets("Output Detail").Range("D34") = StdDev(MCn, SLR_LC,
mean(MCn, SLR_LC))
Worksheets("Output Detail").Range("D35") = StdDev(MCn, SLR_UL,
mean(MCn, SLR_UL))
Worksheets("Output Detail").Range("D36") = StdDev(MCn, SLR_LO,
mean(MCn, SLR_LO))
```

```
'min
Worksheets("Output Detail").Range("E32") =
WorksheetFunction.Min(SLR_UM)
Worksheets("Output Detail").Range("E33") =
WorksheetFunction.Min(SLR_MC)
Worksheets("Output Detail").Range("E34") =
WorksheetFunction.Min(SLR_LC)
Worksheets("Output Detail").Range("E35") =
WorksheetFunction.Min(SLR_UL)
Worksheets("Output Detail").Range("E36") =
WorksheetFunction.Min(SLR_LO)

'max
Worksheets("Output Detail").Range("F32") =
WorksheetFunction.Max(SLR_UM)
Worksheets("Output Detail").Range("F33") =
WorksheetFunction.Max(SLR_MC)
Worksheets("Output Detail").Range("F34") =
WorksheetFunction.Max(SLR_LC)
Worksheets("Output Detail").Range("F35") =
WorksheetFunction.Max(SLR_UL)
Worksheets("Output Detail").Range("F36") =
WorksheetFunction.Max(SLR_LO)

'100-X percentile
Worksheets("Output Detail").Range("G32") =
WorksheetFunction.Percentile(SLR_UM, perc / 100)
Worksheets("Output Detail").Range("G33") =
WorksheetFunction.Percentile(SLR_MC, perc / 100)
Worksheets("Output Detail").Range("G34") =
WorksheetFunction.Percentile(SLR_LC, perc / 100)
Worksheets("Output Detail").Range("G35") =
WorksheetFunction.Percentile(SLR_UL, perc / 100)
Worksheets("Output Detail").Range("G36") =
WorksheetFunction.Percentile(SLR_LO, perc / 100)

'X percentile
Worksheets("Output Detail").Range("H32") =
WorksheetFunction.Percentile(SLR_UM, 1 - perc / 100)
Worksheets("Output Detail").Range("H33") =
WorksheetFunction.Percentile(SLR_MC, 1 - perc / 100)
Worksheets("Output Detail").Range("H34") =
WorksheetFunction.Percentile(SLR_LC, 1 - perc / 100)
Worksheets("Output Detail").Range("H35") =
WorksheetFunction.Percentile(SLR_UL, 1 - perc / 100)
Worksheets("Output Detail").Range("H36") =
WorksheetFunction.Percentile(SLR_LO, 1 - perc / 100)


 ''''SDf [mm/yr]
 'mean
Worksheets("Output Detail").Range("C41") = mean(MCn, SDfmm_UM)
Worksheets("Output Detail").Range("C42") = mean(MCn, SDfmm_MC)
Worksheets("Output Detail").Range("C43") = mean(MCn, SDfmm_LC)
Worksheets("Output Detail").Range("C44") = mean(MCn, SDfmm_UL)
Worksheets("Output Detail").Range("C45") = mean(MCn, SDfmm_LO)
```

```
'STD
Worksheets("Output Detail").Range("D41") = StdDev(MCn, SDfmm_UM,
mean(MCn, SDfmm_UM))
Worksheets("Output Detail").Range("D42") = StdDev(MCn, SDfmm_MC,
mean(MCn, SDfmm_MC))
Worksheets("Output Detail").Range("D43") = StdDev(MCn, SDfmm_LC,
mean(MCn, SDfmm_LC))
Worksheets("Output Detail").Range("D44") = StdDev(MCn, SDfmm_UL,
mean(MCn, SDfmm_UL))
Worksheets("Output Detail").Range("D45") = StdDev(MCn, SDfmm_LO,
mean(MCn, SDfmm_LO))

'min
Worksheets("Output Detail").Range("E41") =
WorksheetFunction.Min(SDfmm_UM)
Worksheets("Output Detail").Range("E42") =
WorksheetFunction.Min(SDfmm_MC)
Worksheets("Output Detail").Range("E43") =
WorksheetFunction.Min(SDfmm_LC)
Worksheets("Output Detail").Range("E44") =
WorksheetFunction.Min(SDfmm_UL)
Worksheets("Output Detail").Range("E45") =
WorksheetFunction.Min(SDfmm_LO)

'max
Worksheets("Output Detail").Range("F41") =
WorksheetFunction.Max(SDfmm_UM)
Worksheets("Output Detail").Range("F42") =
WorksheetFunction.Max(SDfmm_MC)
Worksheets("Output Detail").Range("F43") =
WorksheetFunction.Max(SDfmm_LC)
Worksheets("Output Detail").Range("F44") =
WorksheetFunction.Max(SDfmm_UL)
Worksheets("Output Detail").Range("F45") =
WorksheetFunction.Max(SDfmm_LO)

'95 percentile
Worksheets("Output Detail").Range("G41") =
WorksheetFunction.Percentile(SDfmm_UM, perc / 100)
Worksheets("Output Detail").Range("G42") =
WorksheetFunction.Percentile(SDfmm_MC, perc / 100)
Worksheets("Output Detail").Range("G43") =
WorksheetFunction.Percentile(SDfmm_LC, perc / 100)
Worksheets("Output Detail").Range("G44") =
WorksheetFunction.Percentile(SDfmm_UL, perc / 100)
Worksheets("Output Detail").Range("G45") =
WorksheetFunction.Percentile(SDfmm_LO, perc / 100)

'75 percentile
Worksheets("Output Detail").Range("H41") =
WorksheetFunction.Percentile(SDfmm_UM, 1 - perc / 100)
Worksheets("Output Detail").Range("H42") =
WorksheetFunction.Percentile(SDfmm_MC, 1 - perc / 100)
Worksheets("Output Detail").Range("H43") =
WorksheetFunction.Percentile(SDfmm_LC, 1 - perc / 100)
Worksheets("Output Detail").Range("H44") =
WorksheetFunction.Percentile(SDfmm_UL, 1 - perc / 100)
```

```
Worksheets("Output Detail").Range("H45") =
WorksheetFunction.Percentile(SDfmm_LO, 1 - perc / 100)

 ''''SDs [mm/yr]
 'mean
Worksheets("Output Detail").Range("C49") = mean(MCn, SDsmm_UM)
Worksheets("Output Detail").Range("C50") = mean(MCn, SDsmm_MC)
Worksheets("Output Detail").Range("C51") = mean(MCn, SDsmm_LC)
Worksheets("Output Detail").Range("C52") = mean(MCn, SDsmm_UL)
Worksheets("Output Detail").Range("C53") = mean(MCn, SDsmm_LO)

'STD
Worksheets("Output Detail").Range("D49") = StdDev(MCn, SDsmm_UM,
mean(MCn, SDsmm_UM))
Worksheets("Output Detail").Range("D50") = StdDev(MCn, SDsmm_MC,
mean(MCn, SDsmm_MC))
Worksheets("Output Detail").Range("D51") = StdDev(MCn, SDsmm_LC,
mean(MCn, SDsmm_LC))
Worksheets("Output Detail").Range("D52") = StdDev(MCn, SDsmm_UL,
mean(MCn, SDsmm_UL))
Worksheets("Output Detail").Range("D53") = StdDev(MCn, SDsmm_LO,
mean(MCn, SDsmm_LO))

'min
Worksheets("Output Detail").Range("E49") =
WorksheetFunction.Min(SDsmm_UM)
Worksheets("Output Detail").Range("E50") =
WorksheetFunction.Min(SDsmm_MC)
Worksheets("Output Detail").Range("E51") =
WorksheetFunction.Min(SDsmm_LC)
Worksheets("Output Detail").Range("E52") =
WorksheetFunction.Min(SDsmm_UL)
Worksheets("Output Detail").Range("E53") =
WorksheetFunction.Min(SDsmm_LO)

'max
Worksheets("Output Detail").Range("F49") =
WorksheetFunction.Max(SDsmm_UM)
Worksheets("Output Detail").Range("F50") =
WorksheetFunction.Max(SDsmm_MC)
Worksheets("Output Detail").Range("F51") =
WorksheetFunction.Max(SDsmm_LC)
Worksheets("Output Detail").Range("F52") =
WorksheetFunction.Max(SDsmm_UL)
Worksheets("Output Detail").Range("F53") =
WorksheetFunction.Max(SDsmm_LO)

'95 percentile
Worksheets("Output Detail").Range("G49") =
WorksheetFunction.Percentile(SDsmm_UM, perc / 100)
Worksheets("Output Detail").Range("G50") =
WorksheetFunction.Percentile(SDsmm_MC, perc / 100)
Worksheets("Output Detail").Range("G51") =
WorksheetFunction.Percentile(SDsmm_LC, perc / 100)
Worksheets("Output Detail").Range("G52") =
WorksheetFunction.Percentile(SDsmm_UL, perc / 100)
```

```
Worksheets("Output Detail").Range("G53") =
WorksheetFunction.Percentile(SDsmm_LO, perc / 100)

'75 percentile
Worksheets("Output Detail").Range("H49") =
WorksheetFunction.Percentile(SDsmm_UM, 1 - perc / 100)
Worksheets("Output Detail").Range("H50") =
WorksheetFunction.Percentile(SDsmm_MC, 1 - perc / 100)
Worksheets("Output Detail").Range("H51") =
WorksheetFunction.Percentile(SDsmm_LC, 1 - perc / 100)
Worksheets("Output Detail").Range("H52") =
WorksheetFunction.Percentile(SDsmm_UL, 1 - perc / 100)
Worksheets("Output Detail").Range("H53") =
WorksheetFunction.Percentile(SDsmm_LO, 1 - perc / 100)

End If
''''''''''''''''''''''''''''''''''''''''''''''''''''''''''''''''''''''''''''''''
''''''''''''''''''''''''''''''''''''''''''''''''''''''''''''''''''''''''''''''''
Application.StatusBar = False

''''''''''''''''''''''''''''''''''''''
```

7. Model evaluation

7.1. Introduction

The management option simulation model (MOSM) developed in Chapter 6 is intended to support evaluation of alternative management investments to reduce sediment loading from a large, agricultural watershed and their cost effectiveness. Rather than applying existing watershed models to the problem, we developed MOSM through a collaborative process in order to create a model that is accessible to a wide range of users and responsive to various policy questions on a watershed-wide mitigation strategy. This simulation model has a simple, accessible structure that supports informed stakeholder use, a rapid run time to allow analysis of multiple scenarios, and computational modules that are strongly constrained by available observations of flow and sediment delivery.

The core of the model is defined in terms of the sediment delivery ratio, or the fraction of eroded sediment that is delivered to the watershed outlet. By its nature, this approach constrains the model outputs to be a fraction of observed sediment source loading. For the management options included in the model, output is generally constrained to fall between the observed sediment load and zero, a strong constraint. For example, if no management options are selected, the model simply returns an annual sediment delivery that is the average annual delivery determined from gaging data.

Even though the conceptual basis of the model is quite simple, the number of interacting parts is large and it is useful to ensure that clearly aberrant behavior does not occur. The primary approach to evaluate the reasonability of MOSM's results is to compare them to detailed elements of the sediment mass balance developed for the watershed (Gran et al., 2011). Although the sediment budget and MOSM rely on some of

the same information, their development and operation are distinct, providing opportunities to evaluate model consistency and plausibility. Therefore, in Section 7.2, we evaluate the model outputs against sediment budget and other independent data. We do this by simulating the effects of individual management options at various extent and spatial allocation. This section also reports on cost calculation of individual management options.

In Section 7.3, we conduct a sensitivity analysis on different management site selection criteria (defined Chapter 6.5) and allocation in different geomorphic regions of the watershed. In section 7.4, we compare individual management's cost per unit of load reduction based on different management cost structures.

We developed MOSM in a stakeholder framework with the specific goal of developing stakeholder support and understanding. Part of this challenge was to develop a basis for evaluating the effects of different management alternatives on reducing sediment loading. This requires a format for model output that can be understood by stakeholders and a model that runs sufficiently fast so that a range of scenarios can be evaluated quickly. In Section 7.5, we develop a management option portfolio (MOP) representing different management strategies with a range of potential management option implementation scenarios across the watershed, and demonstrate how the outputs of MOSM may be interpreted and applied. In Section 7.6, we describe the implication of multiple objectives in environmental management decision-making before concluding the chapter in Section 7.7.

7.2. Model outputs: evaluation of sediment loading prediction against independent data and the corresponding cost calculation of individual management options

In this section, we evaluate management option simulation outputs against independent sediment budget data by simulating each management measure in isolation for various extents and spatial allocations, along with the respective cost calculation. Section 7.2.1 revisits the MOSM user-input interface to illustrate how individual management options at various extents and locations are inputted. A part of the MOSM user-input interface is MO cost and effectiveness.

At the heart of MOSM are sediment delivery ratios developed using Topofilter (Chapters 3 and 4). Both Topofilter and the sediment budget rely on gaged observations of sediment loading and estimates of near-channel sediment supply (NCSS). For field-derived sediment, Topofilter introduces the added element of USLE estimates of soil erosion from agricultural field and topographically driven values of field (*SDRf*) and stream (*SDRs*) sediment delivery ratio (*SDR*). This introduces a high degree of spatial resolution that must remain consistent with the sediment budget's upland sediment supply rates determined from gage observations and verified from sediment fingerprinting (Gran et al., 2011).

First, sediment load reductions when agricultural field management options are implemented at all available sites are compared to other independent sources' estimates of field sediment losses (Section 7.2.2). Second, we evaluate the MOSM's simulation of hydrographs resulting from water conservation against a calibrated SWAT model simulations (Section 7.2.3).

For NCS sediment supply, MOSM introduces a sediment delivery ratio driven by the channel length, slope, and floodplain area between source and watershed outlet, and two options for reducing sediment loading: local stabilization of bluff toes or reduction in high river discharges. These combined influences should remain consistent with the sediment budget estimates of the fraction of watershed sediment load derived from NCSS. So, we compare sediment load reductions with management implemented at all ravines or bluffs against the sediment budget's estimates to evaluate the reasonableness of *SDRs* values used in the simulation model (Section 7.2.4).

7.2.1. Model interface and input values

MOSM interface includes management allocation in three zones: upland (zone 1), transitional (zone 2), and incised (zone 3) zones within each of the three main subwatersheds of the Le Sueur River Basin (LSRB): Maple (MAP), Cobb (COB), and Le Sueur (LES) subwatersheds (Figure 6.1). There are seven management option (MO) groups: tillage MO (TLMO), agricultural field MO (AFMO), water conservation MO (WCMO), in-channel water storage MO (ICMO), ravine MO (RAMO), and near-channel MO (NCMO). The model interface allows users to specify MO extents for allocation in green cells and the model records the allocated extents in the yellow cells after executing the MO allocation module (Table 7.1).

We use MOSM's deterministic simulation setting that uses the set of *SDRf* and *SDRs* values that yield sediment load predictions that match the observed sediment load. We use 100% efficiency for all MO evaluation in this section (i.e., the first column in Table 7.2(a) is set at 100% for each MO) to quantify the controllable part of each source's contribution. This way, we calculate reduction of all sediment sourced from each MO's

contributing area. For example, setting 100% efficiency for AFMO results in zero *SDRf* in its contributing area so no sediment is contributed from its contributing area, which is a fraction of the total watershed area as will be discussed in Section 7.2.2.

MOSM's allocation algorithm calculates MO extents (Section 6.5) based on available site extents and selection criteria. For the evaluation in this section, default site selection criteria are used to allocate management options (Table 7.3). We include a sensitivity analysis to demonstrate the general response of cost and effectiveness resulting from different MO selection criteria in Section 7.3.

MO cost and life span inputs are determined from literature review and expert elicitations (Table 6.3), and these values are used in this evaluation (columns 2 to 4 of Table 7.2 (a)). The implications of an alternative MO cost structure (Table 7.2(b)) are included in Section 7.4.

Table 7.1: MOSM input table for MO extent and location inputs (green cells) for the LSRB, consisting of three subwatersheds, Le Sueur, Cobb, and Maple with three geomorphic zones, upland, transitional, and incised. Maximum available MO sites are shown in the rows above the input cells. After the allocation algorithm is executed, selected MO extents are displayed in the yellow cells.

River	LeSueur			Cobb			Maple			Extent	Extent
Zone	Upland	Trans	Incised	Upland	Trans	Incised	Upland	Trans	Incised	inputed	selected
Tillage Management Option (TLMO) ALLOCATION											
Extent of all farm land (ac)	131,976	37,736	50,961	76,825	58,506	28,588	84,280	81,556	19,711	570,138	acre
Conventional till (%)	33	33	33	33	33	33	33	33	33	190,046	190,046
Reduced till (%)	33	33	33	33	33	33	33	33	33	190,046	190,046
Conservation till (%)	33	33	33	33	33	33	33	33	33	190,046	190,046
Agricultural Field Management Option (AFMO) ALLOCATION											
Extent of all MOs (ft)	489,638	153,344	163,291	259,759	192,325	94,596	254,013	230,363	44,849	1,882,178	AFMO*W [ac]
Input extent (ft)	-	-	-	-	-	-	-	-	-	-	-
Buffer Strip Management Option (BFMO) ALLOCATION											
Extent of all MOs (ft)	1,070,389	332,417	600,050	615,745	475,117	379,555	647,512	647,400	175,287	4,943,473	BFMO*W [ac]
Input extent (ft)	-	-	-	-	-	-	-	-	-	-	-
Water Conservation Management Option (WCMO) ALLOCATION											
Extent of all MOs (ac)	15,424	4,676	6,637	7,791	5,142	3,324	7,871	8,158	1,553	60,577	WCMO [ac]
Input extent (ac)	-	-	-	-	-	-	-	-	-	-	-
In-Channel Management Option (ICMO) ALLOCATION											
Extent of all MOs (ft)	358,396	196,427	154,818	146,696	135,845	34,959	293,607	181,222	3,064	1,505,034	ICMO [ft]
Input extent (ft)	-	-	-	-	-	-	-	-	-	-	-
Ravine Management Option (RAMO) ALLOCATION											
number of ravine tips	-	-	275	-	-	132	-	14	196	617	RAMO [tips]
Input number of tips	-	-	-	-	-	-	-	-	-	-	-
Near-Channel Source Management Option (NCMO) ALLOCATION											
Extent of all MOs (ft)	69,774	3,061	60,676	8,222	4,091	44,997	3,520	11,175	46,831	252,346	NCMO [ft]
Input extent (ft)	-	-	-	-	-	-	-	-	-	-	-

Table 7.2: MO effectiveness and cost input table (green cells). Cost input consists of MO's installation cost ($/extent), maintenance cost ($/extent), and life span (year). TLMO effectiveness is calculated internally based on soil loss estimates, reference period tillage practice, and gage data. WCMO and ICMO's effectiveness on sediment loading reduction from near-channel sources are calculated internally through hydrologic routing algorithm; while WCMO also has effectiveness on capturing and storing sediment on agricultural field. Thus, effectiveness inputs are required for AFMO, BFMO, and WCMO on sediment delivery reduction (%); and for RAMO and NCMO on sediment erosion reduction (%). (a) Default input values from Chapter 6, Appendix A that result in outputs discussed in section 7.2 to 7.3, and 7.5; continued next page

MO efficiency	Installation	Ann. Maintenance	Life Span	Total
%	Cost	Cost	(yr)	Cost ($/yr)
Tillage Management (TLMO) EFFECTIVENESS & COST				
	Install. ($/ac)	Mntnc [$/(ac*yr)]	(yr)	Total ($/yr)
Conventional	26	8	1	6,461,562
Reduced	28	11	1	7,411,791
Conservation	14	6	1	3,800,919
Agricultural Field Management (AFMO) EFFECTIVENESS & COST				
Sed. Delivery	Install. ($/ac)	Mntnc [$/(ac*yr)]	Life Span	Cost ($/yr)
75 %	3,200	64	10	0
Buffer Strip Management (BFMO) EFFECTIVENESS & COST				
Sed. Delivery	Install. ($/ac)	Mntnc [$/(ac*yr)]	Life Span	Cost ($/yr)
100 %	1,000	45	10	0
Water Conservation Management (WCMO) COST				
Sed. Delivery	Install. ($/ac)	Mntnc [$/(ac*yr)]	Life Span	Cost ($/yr)
90 %	3,000	574	25	0
In-Channel Management (ICMO) COST				
	Install. ($/ft)	Mntnc [$/(ft*yr)]	Life Span	Total ($/yr)
	250	1	10	0
Ravine Management (RAMO) EFFECTIVENESS & COST				
Sed. Erosion	Install. ($/TIP)	Mntnc [$/(tip*yr)]	Life Span	Total ($/yr)
75 %	6,000	35	10	0
Near-Channel Source Management (NCMO) EFFECTIVENESS & COST				
Sed. Erosion	Install. ($/ft)	Mntnc [$/(ft*yr)]	Life Span	Total ($/yr)
70 %	200	1	5	0

(a)

Table 7.2: MO effectiveness and cost input table (green cells). Cost input consists of MO's installation cost ($/extent), maintenance cost ($/extent), and life span (year). TLMO effectiveness is calculated internally based on soil loss estimates, reference period tillage practice, and gage data. WCMO and ICMO's effectiveness on sediment loading reduction from near-channel sources are calculated internally through hydrologic routing algorithm; while WCMO also has effectiveness on capturing and storing sediment on agricultural field. Thus, effectiveness inputs are required for AFMO, BFMO, and WCMO on sediment delivery reduction (%); and for RAMO and NCMO on sediment erosion reduction (%). (b) This alternate cost input will be discussed in section 7.4

	Installation	Ann. Maintenance	Life Span	Total
% Reduction	Cost	Cost	(yr)	Cost ($/yr)
Tillage Management (TLMO) EFFECTIVENESS & COST				
	Install. ($/ac)	Mntnc [$/(ac*yr)]	(yr)	
	50	0	1	
	25	25	1	
	0	50	1	
Agricultural Field Management (AFMO) EFFECTIVENESS & COST				
Sed. Delivery	Install. ($/ac)	Mntnc [$/(ac*yr)]	Life Span	
75 %	3,000	50	10	
Buffer Strip Management (BFMO) EFFECTIVENESS & COST				
Sed. Delivery	Install. ($/ac)	Mntnc [$/(ac*yr)]	Life Span	
100 %	3,000	50	10	
Water Conservation Management (WCMO) COST				
Sed. Delivery	Install. ($/ac)	Mntnc [$/(ac*yr)]	Life Span	
90 %	1,000	50	25	
In-Channel Management (ICMO) COST				
	Install. ($/ft)	Mntnc [$/(ft*yr)]	Life Span	
	50	0	10	
Ravine Management (RAMO) EFFECTIVENESS & COST				
Sed. Erosion	Install. ($/TIP)	Mntnc [$/(tip*yr)]	Life Span	
75 %	1,500	25	10	
Near-Channel Source Management (NCMO) EFFECTIVENESS & COST				
Sed. Erosion	Install. ($/ft)	Mntnc [$/(ft*yr)]	Life Span	
70 %	400	20	5	

(b)

Table 7.3: MO site selection criteria inputs based on individual site's geophysical characteristics. In general, the default site selection criterion lead to selecting sites with highest effectiveness (e.g., NCMO default input leads the model to select the bluffs with highest estimated sediment loading) while the other criteria chooses sites based on other landuse and topographic characteristics.

AFMO	A*	Select sites with largest upstream drainage area first
	B	Select larger sites located on hydric soil first
	C	Select sites that are closest to stream network first.
BFMO	A	Select sites with largest upstream drainage area first
	B*	Furthest upstream selected first (i.e. BFMO in zone 1)
	C	Select sequentially: stream, canal ditch, connector, then artificial path
WCMO	A	Select sites with lower CPI value with higher natural depth (Crop Productivity Index (CPI) / Depth of WCMO)
	B*	Select sites with higher natural depth located on Hydric soil first)
	C	Select sites closer to existing wetlands and CRP sites first
ICMO	A	Longest ditches selected first
	B*	Closest to SEDSB outlet (i.e., larger flow accumulation)
	C	Furthest upstream selected first (i.e. ICMO in zone 1)
RAMO	A*	Select the ravines with largest load per tip
	B	Select ravine by its evolution stages (0-3)
NCMO	A	Select tallest bluffs with largest open surface area
	B*	Select bluffs with larger loads first

*Indicates the default inputs

7.2.2. AFMO and BFMO: sediment impacts and cost results

Agricultural field MO (AFMO) and stream buffer MO (BFMO) act on agricultural fields to capture sediment eroded from their contributing areas before entering the stream network. Thus, AFMO and BFMO implementation reduces sediment input from fields to streams, consequently reducing sediment load at the watershed outlet. We implement AFMO and BFMO in isolation to examine the resulting sediment loads from field compared to the sediment budget estimates. Corresponding costs of implementing these individual management options are included in this section.

Sediment input from field to stream in the sediment budget is 77,380 Mg/yr before discounting the lake and floodplain deposits (Gran et al., 2011). These sediment sinks should correspond to the decreases in sediments achieved by *SDRf* (this factor accounts for deposition in both field and lake) and *SDRs* (this factor accounts for deposition in floodplains). The sediment budget estimates lake deposit at 17,240 Mg/yr (a partial estimate of field source deposition since sediment can be stored on field as well as in lakes) and floodplain deposit at 25,260 Mg/yr. The sediment budget estimates sediment loading (*SL*) at the watershed outlet from field sources with both lake and floodplain deposits removed at 34,880 Mg/yr (=77,380 -17,240-25,260).

The floodplain deposit rate estimated in the sediment budget includes sediment deposits from ravines (but not sediment from streambanks and bluffs as the sediment budget discounts streambanks' and bluffs' floodplain deposits in their source input rates), so we have to estimate the floodplain deposition from ravines to partition the field sediment along floodplain. Ravines produce 20,009 Mg/yr of sediment. Assuming *SDRs* of 0.84 for all ravine sources (see Section 7.2.4), the ravines' floodplain deposit is about

3,201 Mg/year. This implies that the sediment loading from agricultural field, discounting appropriate amount field sediment deposited in lakes and floodplain, should be about 38,081 Mg/yr (=77,380-17,240-25,260+3,201). Note that 38,081 Mg/yr calculated from sediment budget does not discount field deposition, so this may be an overestimate.

MOSM estimates sediment loading from fields at 37,533 Mg/yr: the annual soil production from field is discounted by *SDRf* and *SDRs* across the 529 SEDSBs in the LSRB (the sediment subbasin (SEDSB) is the spatial unit at which sediment loading is calculated in MOSM) to represent sediment trapped on field and in floodplains. Although we do not match the exact amount of sediment loading from the field from the sediment budget, these estimates are generally in agreement.

There isn't a direct way to verify the simulation results of implementing all AFMO and BFMO sites other than showing that implementing all sites result in sediment reduction that is proportional to the total loading from field source. Contributing areas of all potential AFMO and BFMO sites cover about 7% and 10% of the watershed areas, respectively. When all AFMO sites are implemented, MOSM predicts a sediment reduction at 2,035 Mg/yr, about 5% of total sediment loading from field (Figure 7.1). AFMO acts on upper part of the agricultural field, where *SDRf* is smaller than the areas adjacent to stream network; while BFMO acts on the area adjacent to stream network to trap and store sediment (See Chapter 4 for more discussion). As a result, when all BFMO sites are implemented, sediment loading reduction is 7,456 Mg/yr, about 20% of total sediment loading from field (Figure 7.2). *SDRf* within 100 m of the stream (i.e., contributing area of BFMO) is about 2-13 times larger (Chapter 4.4.2) than in further upland, thus amplifying the effects of BFMO and reducing the effects of AFMO.

Implementing AFMO or BFMO at their full extent results in sediment reductions that are fractions of total sediment loading from field because these management options influence only small fractions of the total agricultural field area.

Turning to the costs associated with these potential reductions, we estimate that the unit cost of individual MOs (i.e., annual MO implementation cost divided by sediment loading reduction, $/Mg) gradually increases as more AFMO sites are implemented. This indicates that it becomes more expensive to remove a unit mass of sediment with more AFMO sites implemented. The default site selection criterion dictates that the model selects sites with largest upstream drainage first, therefore trapping more sediment initially (see Section 7.3 for an analysis of the sensitivity of the model to selection criteria). Therefore, the unit cost (i.e., cost of removing a metric ton of sediment) increases with increasing site allocation because as the area implemented increases, the model is forced to select more sites with smaller upstream drainage area.

Compared to BFMO, implementation of AFMO is expensive at about $2,000-$3,000 versus $1,200-$1,600 per metric ton of sediment reduced. Because BFMO is implemented in areas where the *SDRf* is larger, BFMO has opportunity to trap sediment more effectively than AFMO.

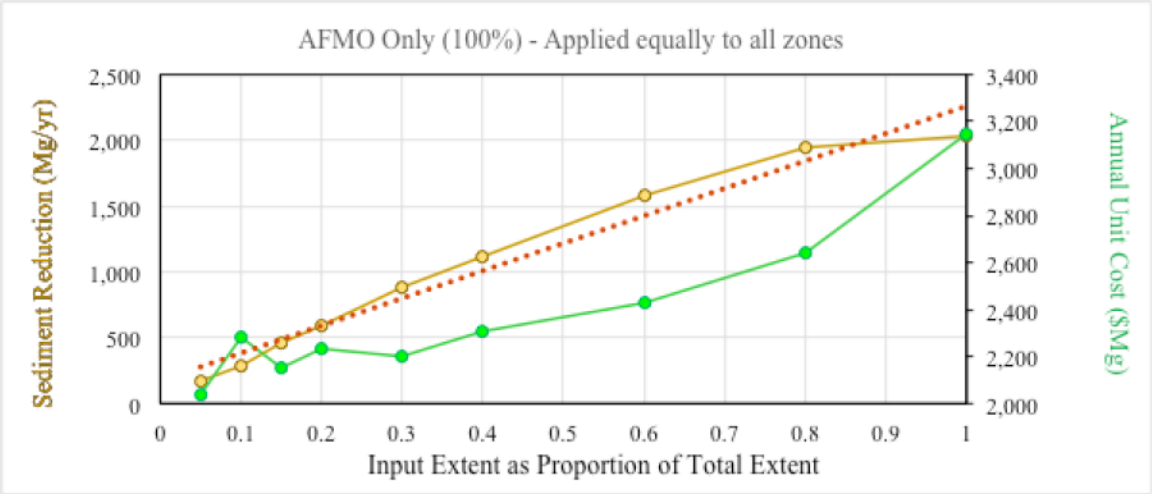

Figure 7.1: Plots showing sediment loading reduction at the watershed outlet (Mg/yr, left y-axis) and annual unit cost ($/Mg, right y-axis) in response to MOs implemented at various increments of all available sites. Linear interpolation of the sediment reduction at various extents is shown in red dotted lines. The linear interpolation highlights the concavity of the sediment reduction over increasing total extent of sites selected.

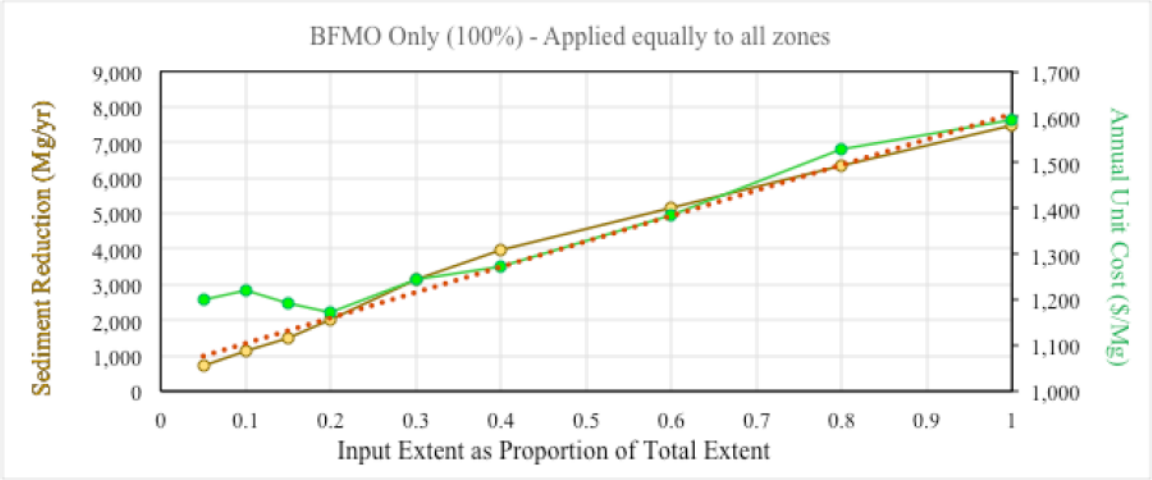

Figure 7.2: Plots showing sediment loading reduction at the watershed outlet (Mg/yr, left y-axis) and annual unit cost ($/Mg, right y-axis) in response to MOs implemented at various increments of all available sites. Linear interpolation of the sediment reduction at various extents is shown in red dotted lines. The linear interpolation highlights the concavity of the sediment reduction over increasing total extent of sites selected.

7.2.3. WCMO: sediment impacts and cost results

Implementation of water conservation MO (WCMO) provides water storage in the uplands. Water storage attenuates peak flows in the river system downstream, consequently reducing the sediment eroded from streambanks and bluffs. WCMO also provides storage for sediment from their contributing area in the uplands. MOSM calculates both effects of peak flow reduction and sediment storage.

With the design depth at 6.6 feet and surface area determined from the spatial analysis (Chapter 6, Appendix A), total storage volume of all WCMO sites is 399,807 ac-ft, and the consequent sediment reduction achieved is 137,550 Mg/yr (Figure 7.3). According to the sediment budget, sediment loading from streambanks and bluffs is 130,735 Mg/year(Gran et al., 2011).

Additional sediment reduction may be attributed to WCMO's capacity to store sediment sourced from field in its contributing area: when all WCMO sites are implemented, their contributing areas make up about 37% of the watershed area. Sediment loading from WCMO's contributing area is 9,716 Mg/yr, which is calculated by multiplying the sediment produced in the contributing area by *SDRf* and *SDRs* at SEDSBs. WCMO's function to trap sediment from its contributing area is minor compared to its function to reduce peak river discharge and NCSS.

This calculation indicates MOSM's estimate of sediment reduction from streambanks and bluffs from flow reduction only is less than the sediment budget's estimate of sediment loading from these sources (sediment reduction from streambanks and bluffs via flow reduction estimated by MOSM is 137,550-9,716=127,834 Mg/yr, versus total loading from these sources at 130,735 Mg/year estimated by the sediment budget). In other words, not all sediment loading from streambanks and bluffs is addressed by peak flow attenuation. This makes sense since the hockey stick relation developed in Chapter 5 evaluates the occurrences of sediment supply from near-channel source only when river discharge is high; while there are occurrences of sediment loading from these sources during low to moderate flows.

Turning to costs, WCMO's unit cost ranges from $300-$600 per metric ton of sediment reduction, and steadily increases with extent (Figure 7.3). Concavity of the total sediment reduction as a function of WCMO extent indicates that sediment loading reduction is more effective with the first sites selected because as more WCMO sites are selected, available contributing areas is limited within the field areas (i.e., WCMO contributing area cannot exceed the subbasin area). Therefore, sediment loading reduction become less effective as more sites are selected.

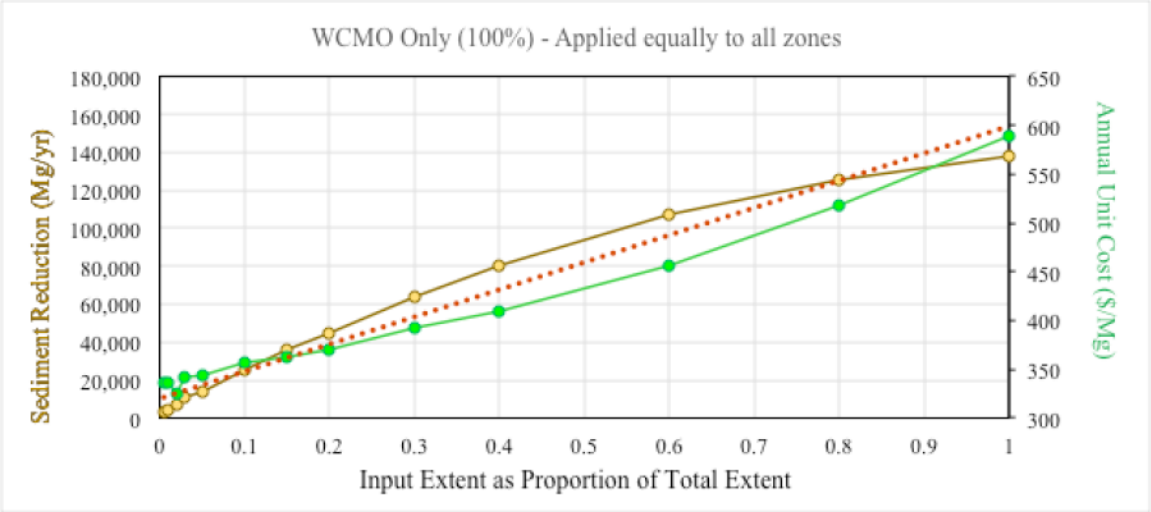

Figure 7.3: Plots showing sediment loading reduction at the watershed outlet (Mg/yr, left y-axis) and annual unit cost ($/Mg, right y-axis) in response to MOs implemented at various increments of all available sites. Linear interpolation of the sediment reduction at various extents is shown in red dotted lines. The linear interpolation highlights the concavity of the sediment reduction over increasing total extent of sites selected.

In order to confirm that MOSM's flow routing algorithm and prediction of flow reduction are simulated realistically, we refer to calibrated SWAT model simulations with various wetland restoration implementation in different parts of the watershed since SWAT has proven to be reliable in water yield simulations (Borah, 2004). The calibrated SWAT model (Mitchell, 2015) simulation utilizes the same WCMO sites (see Mitchell, 2015 for full discussion of SWAT model simulation), so we compare the peak flow reductions simulated by MOSM to the SWAT model with the same fractions of available

WCMO sites implemented (Table 7.4). Note that MOSM utilizes this SWAT model's water yield data at each HYDSB (spatial scale used to run flow routing algorithm in MOSM; see Chapter 6.4); however, our simulation algorithm's calculations of water storage and flow routing from individual HYDSB are independent from the SWAT model's algorithms.

Both models yield comparable amount of peak flow reductions at sediment subbasin 4 (SEDSB 4) (lower gage (gage: LL) location along the Le Sueur River (LES)), SEDSB 13 (lower gage (gage: BC) location along the Cobb River (COB)), and SEDSB 19 (lower gage (gage: LM) location along the Maple River (MAP)) (see Chapter 4, Figure 4.2 for these gage locations).

Table 7.4: MOSM's river routing results from implementing equal percentages of WCMO in different zones (various extents of WCMO in zone 1 and zones 2&3 shown in second column) of the watershed as the impact of wetland restoration simulated using calibrated SWAT model, conducted by Mitchell (2015)

		Peak flow (Q>Qth) reduction [%] =					
Scenario	extent (%)	SEDSB4 (LES)	SEDSB13 (COB)	SEDSB19 (MAP)	SEDSB 4 (LES)	SEDSB13 (COB)	SEDSB19 (MAP)
Zone1	0.50%	1.98%	2.14%	1.45%	2.04%	1.00%	0.94%
	1.00%	4.04%	3.04%	3.05%	4.02%	2.11%	1.92%
	4.00%	7.48%	6.47%	5.13%	8.03%	4.36%	3.94%
	7.50%	28.70%	21.05%	18.22%	30.36%	16.53%	14.40%
Zones 2&3	0.50%	1.54%	1.17%	1.67%	1.02%	0.75%	1.16%
	1.00%	2.73%	2.09%	3.25%	2.14%	1.60%	2.36%
	4.00%	10.22%	9.24%	12.98%	8.62%	6.83%	9.70%
	7.50%	17.56%	17.77%	20.57%	16.45%	12.91%	17.70%

7.2.4. RAMO and NCMO: sediment impacts and cost results

Ravine MO (RAMO) stabilizes and prevents further growth of ravine tips. According to the watershed sediment budget (Gran et al., 2011), sediment input from ravines, before floodplain deposits have been discounted, is 20,009 Mg/yr. We estimate the sediment loading from ravines minus the floodplain deposit (SL_R) using *SDRs* from Topofilter. Most of the ravines are located in the incised zone where average *SDRs* is about 0.84

(i.e., 16% of sediment from ravines are deposited in floodplains) (see Table 4.3). The average S*DRs* value is calculated by averaging over 118 SEDSBs located in the incised zone. Since 80% of sediment loading from ravines is addressed by RAMO (20% of sediment is sourced from outside of ravine according to the watershed sediment budget (Gran et al., 2011)), the total amount of sediment from ravines that could be captured by RAMO should be about 13,446 Mg/year (=20,009*0.8*0.84). This means that about 6,563 Mg/year (=20,009-13,446) of sediment from ravine is deposited along floodplain before reaching watershed outlet. However we speculate that considering many of the ravines are located closer to the mouth of the Le Sueur River Basin where *SDRs* values are generally greater than 0.84 (see Figure 6.18), the average estimate of 13,446 Mg/yr is an underestimate. MOSM estimates that ravine loading captured by RAMO is 14,616 Mg/yr when all sites are implemented (Figure 7.4). This is calculated by multiplying the 80% of ravine loading by *SDRs* at all SEDSBs in MOSM. Since we speculate that sediment budget's ravine load discounted by average *SDRs* in the incised zone (13,446 Mg/yr) is an underestimate, MOSM's simulation of sediment captured by RAMO is reasonable.

With the default site selection criteria, the model selects RAMO sites with largest sediment loading rates first, so the annual unit cost increases as more RAMO sites are selected within the range of $17-$33 per metric ton of sediment loading reduction (Figure 7.4).

Near channel MO (NCMO) reduces sediment production from bluffs. According to an aerial photograph analysis, the total sediment production from bluffs is 118,089 Mg/yr, and according to sediment fingerprinting and gaging, the sediment loading after

floodplain deposit is 74,278 Mg/yr (Gran et al., 2011). MOSM estimates total sediment-loading reduction of 79,241 Mg/yr (this value is effectively bluff loading times *SDRs* at all SEDSBs across the watershed) when all mapped bluffs are addressed with NCMO (Figure 7.5). Based on this comparison, MOSM seems to be overestimating the effects of *SDRs* and sediment loading from bluffs by about 7% compared to the sediment budget.

MOSM selection criteria are set up to select bluffs with largest sediment production rates first; thus, the sediment reduction as a function of NCMO extent is concave and annual cost increases with extent. Unit costs of NCMO are larger than for RAMO ($17-$33 per metric ton of sediment reduction), particularly due to relatively high cost of operation, ranging from about $35-$140 per metric ton of sediment reduction.

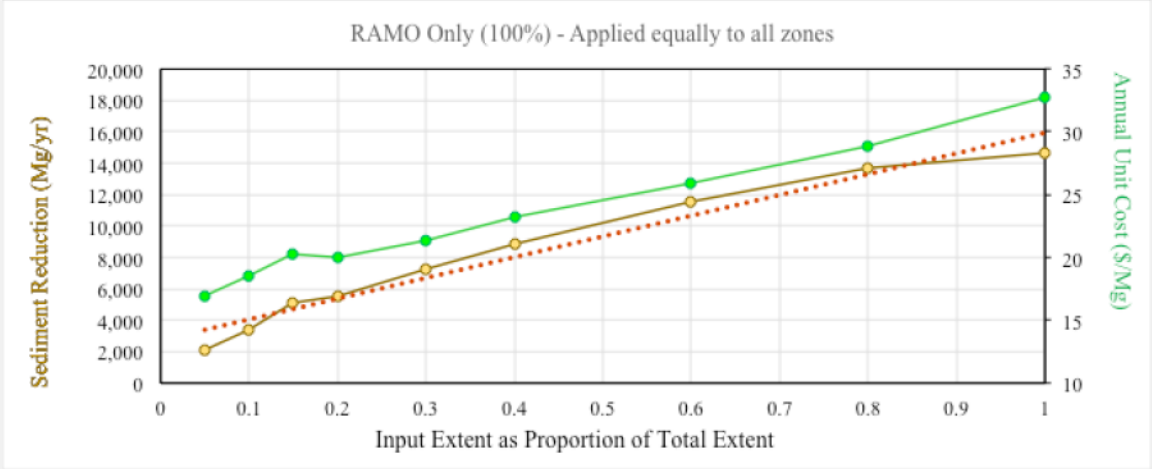

Figure 7.4: Plots showing sediment loading reduction at the watershed outlet (Mg/yr, left y-axis) and annual unit cost ($/Mg, right y-axis) in response to MOs implemented at various increments of all available sites. Linear interpolation of the sediment reduction at various extents is shown in red dotted lines. The linear interpolation highlights the concavity of the sediment reduction over increasing total extent of sites selected.

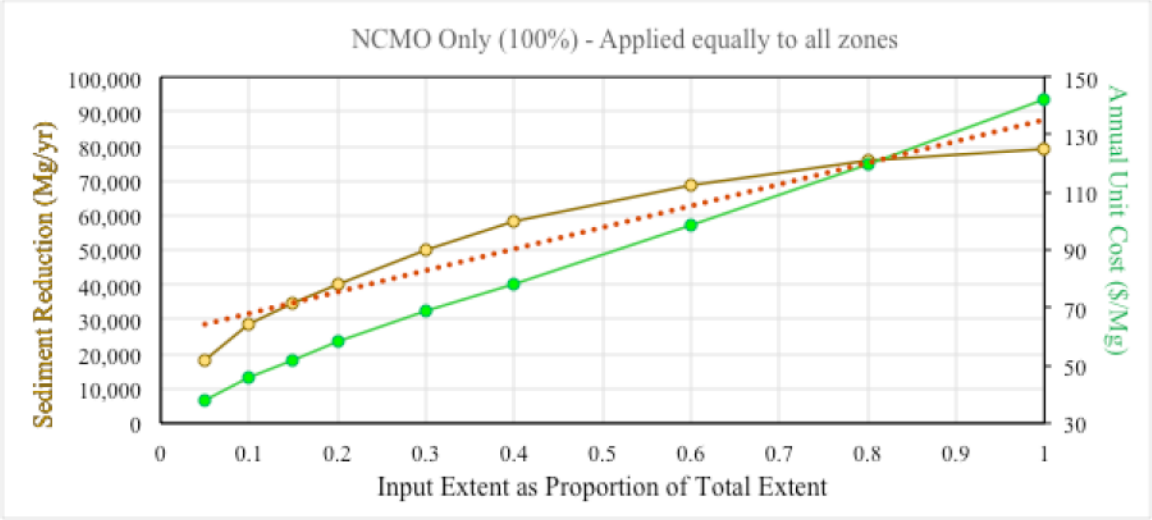

Figure 7.5: Plots showing sediment loading reduction at the watershed outlet (Mg/yr, left y-axis) and annual unit cost ($/Mg, right y-axis) in response to MOs implemented at various increments of all available sites. Linear interpolation of the sediment reduction at various extents is shown in red dotted lines. The linear interpolation highlights the concavity of the sediment reduction over increasing total extent of sites selected.

7.3. Sensitivity analysis on site selection criteria and MO cost structure

MOSM outputs are sensitive to user inputs and model parameters that dictate sediment delivery and loading, and MO implementation cost. For instance, location of MO implementation and cost inputs (Table 7.2 (a)) would impact the sediment reduction in the affected sediment sources and calculation of annual cost. In this section sensitivities to a number of model inputs are assessed. First, we investigate the model's sensitivity to management option site selection criteria (Section 7.3.1). Second, we investigate the model's sensitivity to management allocation in different geomorphic zones (Section 7.3.2). Finally, we investigate model's sensitivity to different management option cost structure (Table 7.2 b) in Section 7.3.3.

7.3.1. Site selection criteria

MOSM provides different choices for how individual sites are selected to fulfill the user-specified extent of different management options. Choosing different site selection criteria affects the sediment loading reduction and cost calculations. With default site

selection criteria (criteria set A in Table 7.3), the model selects sites with larger potential to reduce sediment loading first; therefore, the unit cost (cost of removing 1 Mg of sediment) generally increases with increasing extents with inclusion of sites with less potential to reduce sediment loading (Figure 7.6, see "default" site selection unit cost plot).

On the other hand, with alternate site selection criteria, the model may select more costly sites first. For instance, in the case of AFMO, MOSM selects individual AFMO sites based on soil type or proximity to stream network, respectively if B or C are used. These choices have little influence on effectiveness of sediment loading reduction. As a result, unit costs for these choices are larger at the beginning because the model is calculating less sediment reduction with same amount of investment, but as more sites are selected those sites with more potential to reduce sediment begin to play a role in the overall sediment reduction, and the unit costs of these choices begin to converge with the default rule choice (Figure 7.6 (a)). There are reasons to choose site selection criteria B or C even if they are not as cost effective as criterion A. For instance, when the objectives for implementing management options include utilizing sites that are less suitable for agricultural production (criterion B) or in marginal land near the stream (criterion C), these alternative choices may be more desirable.

Similar patterns of unit cost emerge for the other management options. If the model first picks sites with a larger potential to store sediment (AFMO (Fig. 7.6(a) and BFMO (Fig. 7.6(b)), or sites that offer more water storage capacity (WCMO) (Figure 7.6 (c)), or sites with more observed sediment erosion (RAMO and NCMO) (Figure 7.6 (d) and (e),

respectively), the initial unit cost is small at beginning and increases with extent of implementation compared to alternative choices for MO site selection.

(a)

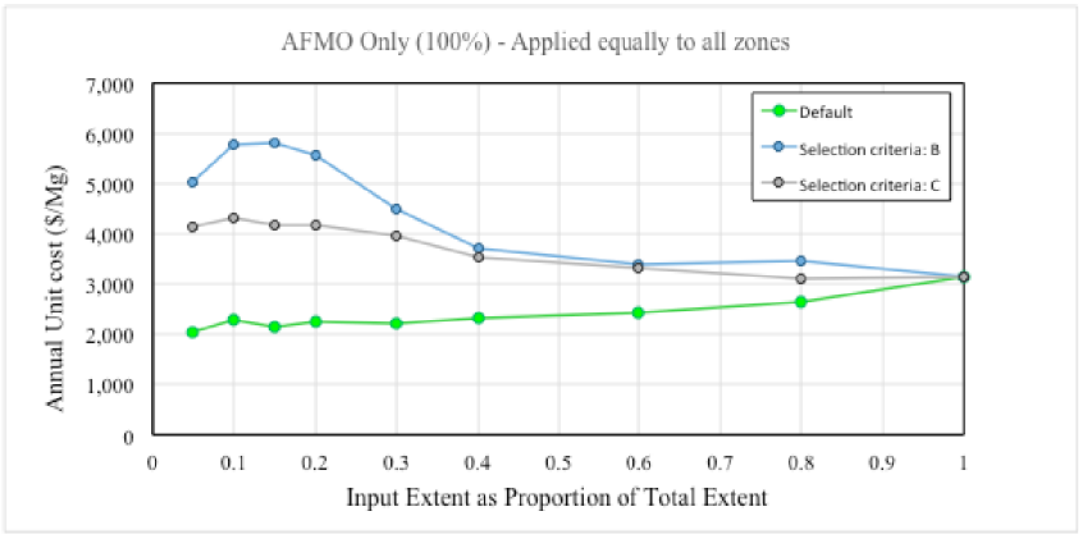

(b)

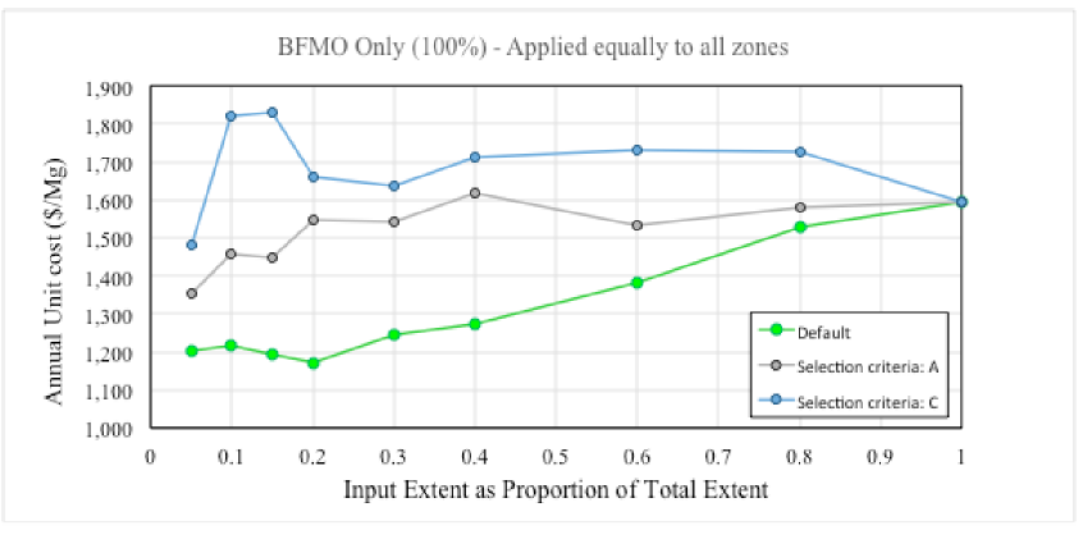

(c)

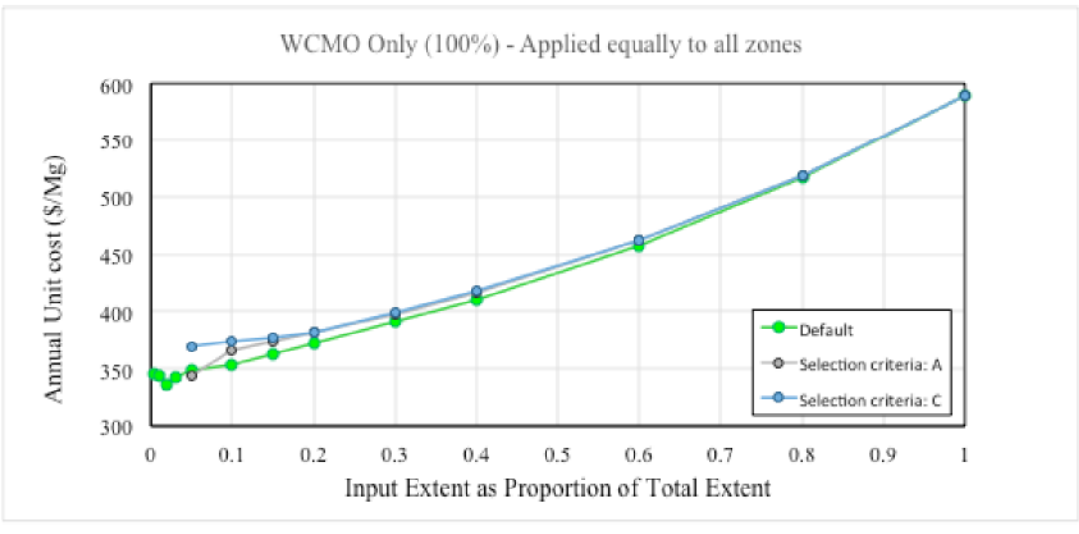

(d)

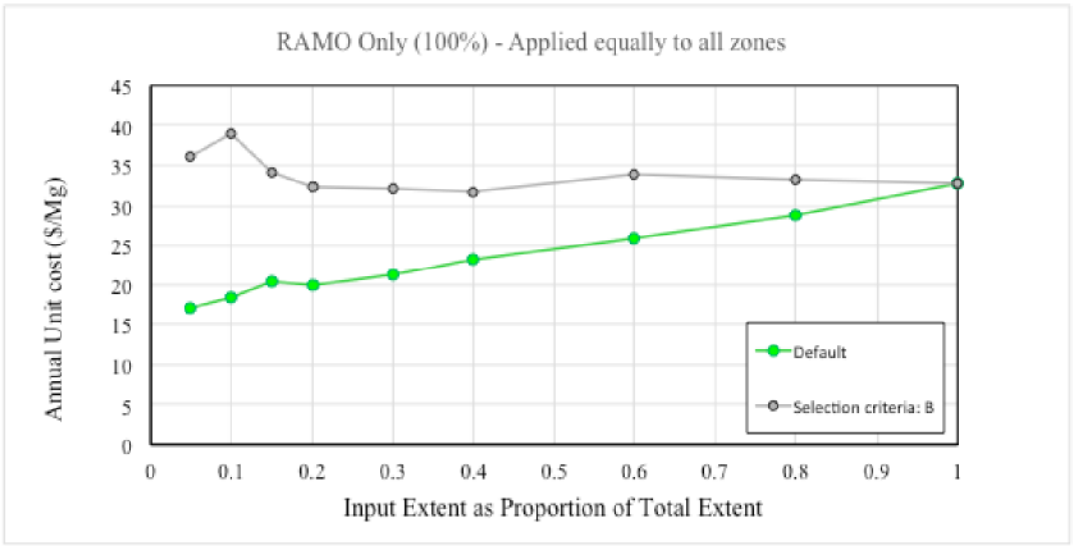

(e)

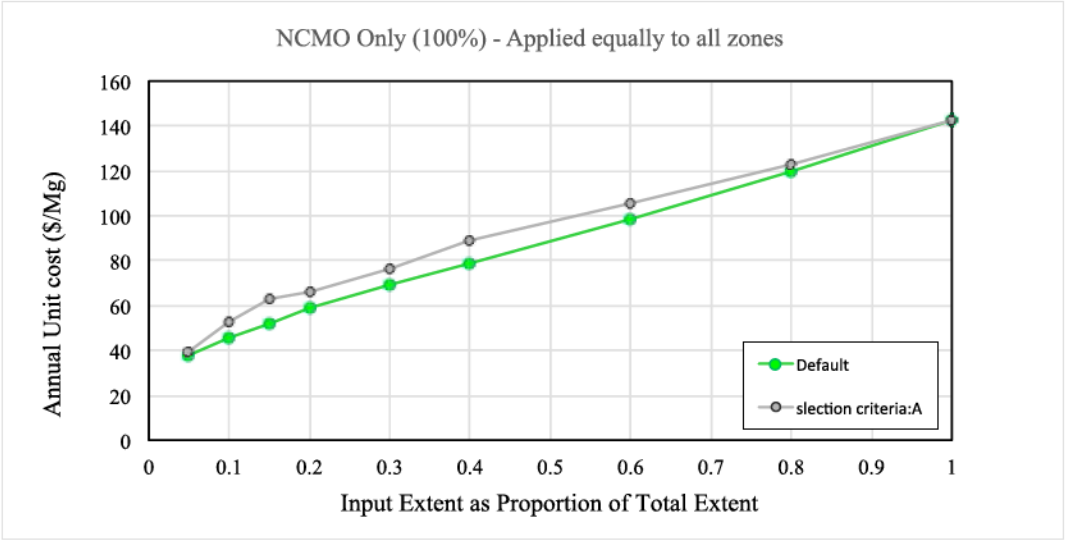

Figure 7.6: Comparison of annual unit cost for MO implementation with different site selection criteria for (a) AFMO; (b) BFMO; (c) WCMO; (d) RAMO; and (e) NCMO. Default site selection is most cost effective because this criterion force the model to choose sites with the most potential to remove sediment first while the other criteria chooses sites based on various other site characteristics.

7.3.2. Allocation of management options among geomorphic zones

MOSM can simulate effects of choosing to implement management options in different geomorphic zones (flat upland, transitional, and incised zones; see Figure 6.1). Management options acting in different parts of the watershed will have different effects in part because of spatially distributed sediment delivery ratio (*SDR*) values and in part because of dependence of hydrologic impact on water storage location. For instance, *SDR* is generally large in the incised zone where sediment will travel shorter distance over steeper terrain compared to further upland. Also, water storage in further upland will impact downstream hydrograph at different stages of storm compared to water storage near the watershed outlet. This is already demonstrated in Section 7.2.3 (Table 7.4), but here we take a closer look.

First, we evaluate the sensitivity in unit cost (i.e., cost of removing a metric ton of sediment) of implementing sediment trapping with AFMO in different geomorphic zones. There are more AFMO sites in the upland: 2,304 acres compared to 1,322 acres in the transitional zone and 695 acres in the incised zone. However, sediment-loading reduction from implementing AFMO in the upland zone is less effective than in zones closer to the watershed outlet (Figure 7.7). While large portions of sediment generated in the upland are deposited along the way (i.e., smaller *SDR*), sediment from transitional and incised zones are more likely to travel all the way to the mouth of the watershed (i.e., larger *SDR*); thus, AFMO is more effective in the lower portions of the watershed. However, many AFMO sites in the transitional zone have larger upstream drainage areas than the sites in the incised zone with compact field areas due to topography. For this reason, even though *SDR* is generally larger, AFMO is less cost-effective in the incised zone than in

the transitional zone. In sum, spatial location of management options affects the estimated sediment-loading reduction, but individual site characteristics, such as sediment trapping potential or erosion rates from drainage area, can also affect the sediment loading reduction at the watershed outlet.

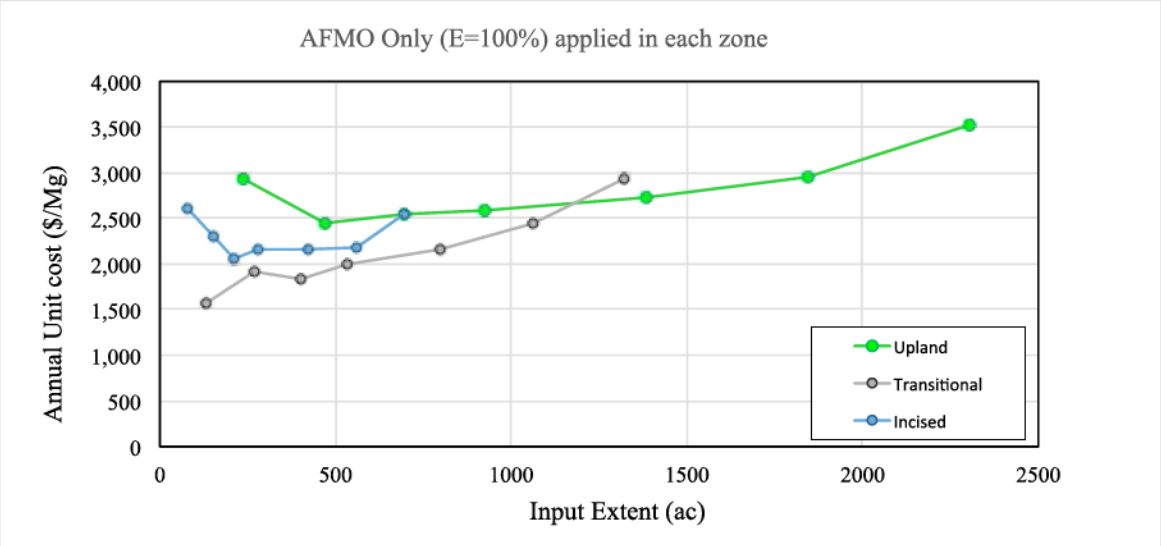

Figure 7.7: This plot compares annual unit cost (cost of removing 1 Mg of sediment) of implementing AFMO in upland versus transitional versus incised zone. Implementation of AFMO in different zones have different unit costs because sediment reduction varies as a result of spatially variable sediment delivery ratios over the watershed as well as individual site characteristics

Second, we evaluated the impact of spatial location of water conservation with WCMO with no other management options in place. There are more WCMO sites in the upland of 31,086 acres compared to 17,977 acres in the transitional zone and 11,514 acres in the incised zone. Cost-effectiveness of sediment-loading reduction from water storage is larger in the upland than the transitional and incised zones (Figure 7.8).

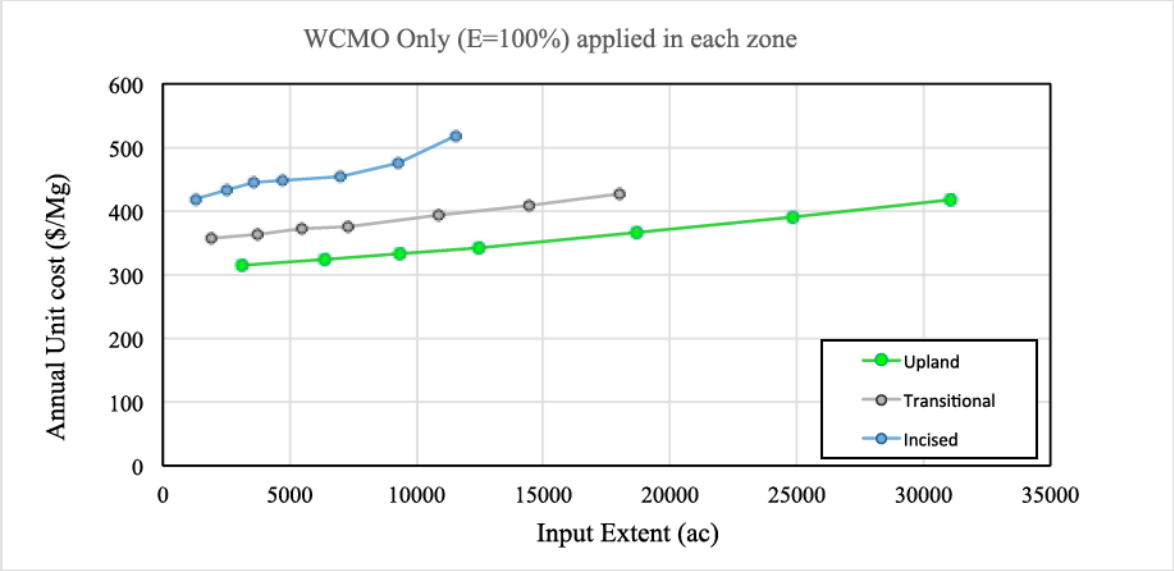

Figure 7.8: Implementation of WCMO in different zones have different unit costs because sediment reduction effectiveness varies as a result of water storage, hydrologic routing, and peak flow attenuation

Placing water storage in different locations, near or far from the incised zone, will affect the peak river charge in the incised zone differently as well as consequent reduction in near-channel sediment supply (NCSS). Flood wave from the upland zone has to travel further and contributes to downstream hydrograph at a different time than flood wave traveling from the incised zone. Based on this analysis, peak flow attenuation is most effective with water conserved further upland than near the incised zone resulting in more significant sediment-loading reduction. For instance, unit cost of removing a metric tone of NCSS from storing water in the upland is about $100 cheaper than storing water in the incised zone. By reducing the flood wave contribution from further upland seems to put more water out of phase with storm peaks. This is consistent with an observation of flood wave attenuation by wetlands in Boreal watersheds: downstream hydrograph is affected by movement of water within the watersheds that is influenced by the flood peaks, volumes of water storage, water storage location, flood wave travel time, and outflow (Hillman, 1998).

7.3.3. Summary of sensitivity analysis of individual management options

Unit cost evaluation of management options depends on management option cost inputs. For example, consider a management option cost structure with a conservative estimate for water conservation actions ($3000/ac) and relatively inexpensive near-channel source management ($200/ft) (Table 7.2 (a)). Annual unit cost evaluation of individual management options indicates that it is more desirable to focus investment on near-channel management with NCMO to reduce NCSS than to implement water storages with WCMO (Figure 7.9 (a)). On the other hand, with different cost assumptions (inexpensive water conservation ($1000/ac) (i.e., simpler water storage mitigation method compared to a full wetland restoration) and more costly near-channel management option ($400/ft) (i.e., due to accessibility and type of specific mitigation method), Table 7.2 (b)), water storage with WCMO becomes a more desirable alternative than addressing the source directly with NCMO (Figure 7.9(b)).

With either of those two extreme sets of cost assumptions (Table 7.2), ravine management with RAMO is significantly more cost effective than other managements (Figure 7.9). However, the total possible sediment removal by RAMO is limited at 14,000 Mg/yr. Field management options, AFMO and BFMO, are unattractive sediment reduction measures because they are relatively expensive and their maximum capacity to remove sediment is even smaller than RAMO at about 2000 Mg/yr and 7000 Mg/yr, respectively.

Development of a management option portfolio (MOP) would consider the effectiveness of individual management options. For instance, inclusion of RAMO in a MOP can help to target the most cost-effective sources, but if the goal of sediment

removal is greater than 14,000 Mg/yr, other management options will need to be included, such as near-channel management or water conservation depending on costs and effectiveness of these options.

(a)

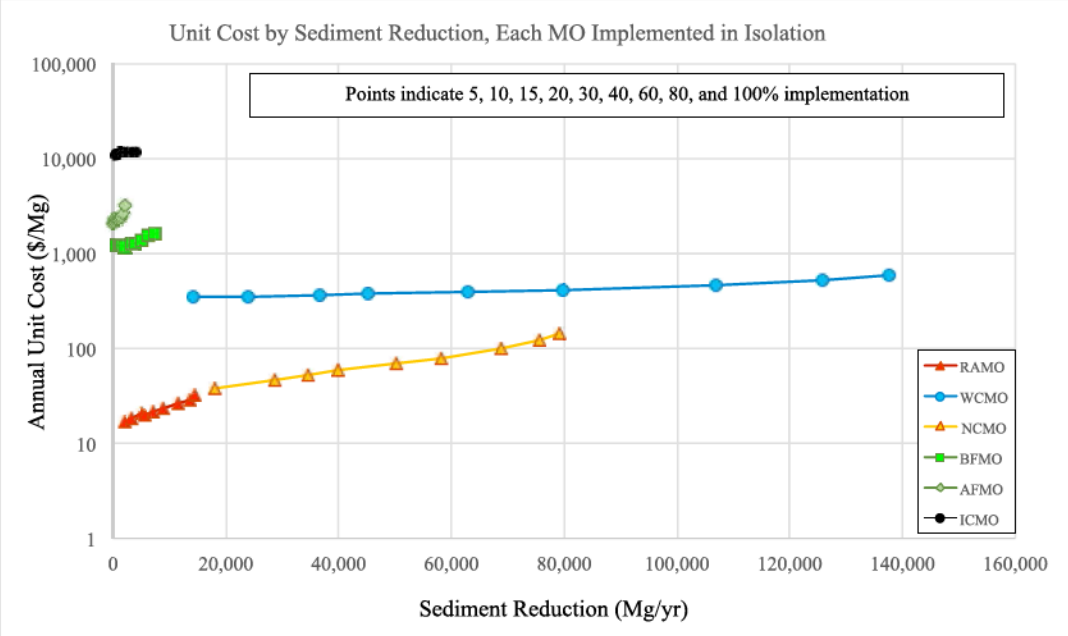

(b)

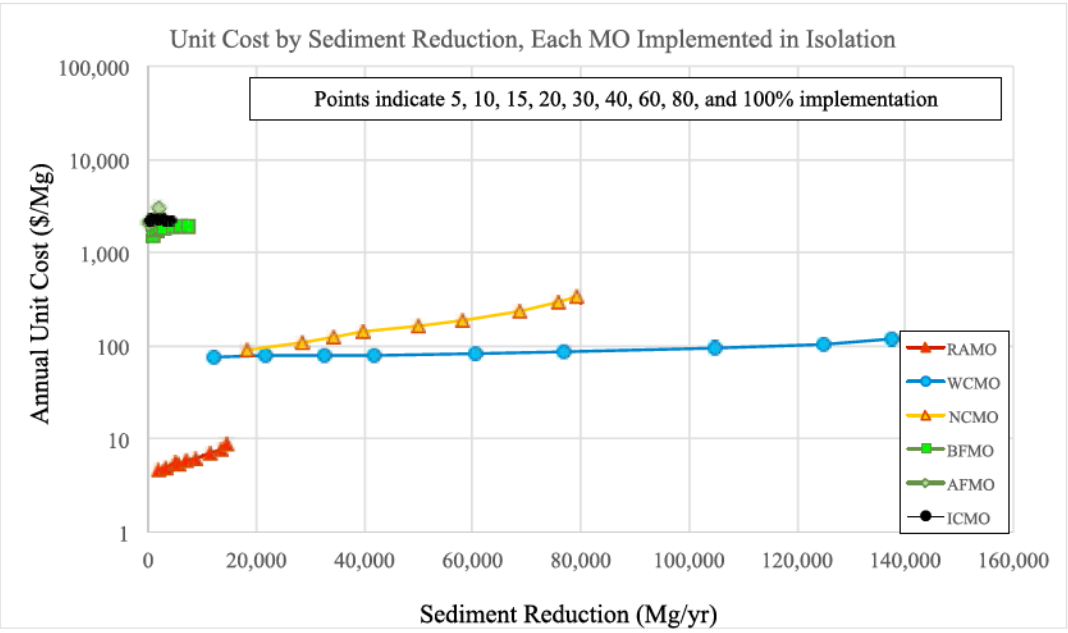

Figure 7.9: (a) Incremental annual unit cost of individual management options implemented in isolation at different extent with 100% efficiency using the cost inputs specified in Table 7.2(a); (b) incremental annual unit cost of individual management calculated using the cost inputs specified in Table 7.2(b). Unit costs of individual management options reveal how effectively each option addresses sediment loading.

7.4. Management option portfolio

In this section, we develop a sample management option portfolio to evaluate the impacts of different management strategies. In Section 7.4.1, we define various management scenarios, and in Section 7.4.2, we evaluate the outputs of MOSM on these scenarios. In Section 7.4.3, we identify dominant management scenarios and discuss the implication on these solutions with management constraints. In Section 7.4.4, we consider multiple objectives and their impact on evaluation of these management option scenarios.

7.4.1. Definition of management option scenarios

Combinations of individual management options are likely to be the most attractive strategies to reduce sediment loadings. With an understanding gained from the individual management option evaluations in the previous two sections, a MO portfolio (MOP) is developed where multiple management scenarios are analyzed. This analysis is conducted with management cost and effectiveness inputs specified in Table 7.2 (a) with default site selection criteria in Table 7.3. Note that this is not an optimization analysis, in which a formal optimization model is used to identify management scenarios that minimize the total cost of meeting a sediment-loading target; rather, we simulate potentially attractive scenarios in a heuristic manner. Future work will address optimization, which may identify scenarios that have lower total costs of achieving a given reduction.

Insight from the above analyses leads to developing *site-specific* and *hydrologic* strategies. Any *site-specific strategy* will address one of the two major sediment sources,

which originate from distinct areas: 1) agricultural field and 2) near-channel sources. Therefore, most of the scenarios we construct emphasize one or the other sources.

Agricultural field management scenarios include different combinations of tillage MO (TLMO), agricultural field MO (AFMO), and stream buffer MO (BFMO). Various TLMO implementation scenarios are considered in combination with other managements. These are designated as follows: T1 indicates equal distribution of the tillage practices, 33% of conventional till, 33% of reduced till, and 33% of conservation till across the watershed, which is the assumed present practice (Chapter 6.3.1); T2 indicates conservation till at 50% with conventional and reduced till at 25% each across the watershed; and T3 indicates reduced and conservation till at 50% each across the watershed. Spatial location of management can also influence the effectiveness of sediment reduction as discussed in Section 7.3.2. Thus, we developed scenarios where AFMO and BFMO are allocated in the transitional and incised zones (zones 2 and 3) at various extents in addition to all zones, in combination with various TLMO implementations ("Ag field" and "Stream buffer" strategies in Table 7.5). AF1, AF2, and AF3 indicate implementing AFMO at 10%, 50%, and 100% of all available sites in all zones. AF1z2, AF2z2, AF3z2 indicate implementing AFMO at 10%, 50%, and 100% of all available sites in zone 2. Similarly, BF1, BF2, and BF3 indicate implementing BFMO at 10%, 50%, and 100% of all available sites in all zones. BF1z3, BF2z3, BF3z3 indicate implementing BFMO at 10%, 50%, and 100% of all available sites in zone 3 (Table 7.5).

Near-channel source management scenarios include mitigation of ravine tip erosion with RAMO, and mitigation of bluff erosion with NCMO. Ravines and bluffs are significant contributors of sediment, so the site-specific strategies include targeting of

these near-channel sources ("NCS" in Table 7.5). Scenarios T2RA1, T2RA2, and T2RA3 indicate T2 tillage scenario (no change from present practice) plus varying extents of RAMO implementation at 10%, 50%, and 100% of all available RAMO sites. Similarly, Scenarios T2NC1, T2NC2, and T2NC3 indicate T2 tillage scenario plus varying extents of NCMO implementation at10%, 50%, and 100% of all available sites. T2RA1NC1, T2RA2NC2, and T2RA3NC3 indicate T2 tillage scenarios plus varying extents of RAMO and NCMO together at 10%, 50%, and 100% each of all available sites.

A second insight from the analyses earlier in this chapter is that WCMO has the potential to cost-effectively achieve large sediment reductions. We consider *hydrologic strategies* where different combinations of water conservation and near-channel source managements are considered: 1) water conservation management only, and 2) water conservation plus near-channel source managements (Table 7.6).

Water conservation management scenarios include implementation of WCMO at various extents: WC1, WC2, WC3, WC4, and WC5 indicate implementing WCMO at 5%, 10%, 30%, 50%, and 100% of all available sites across all zones. The effectiveness of reducing river discharge differs depending on the location of the water storage as discussed in Section 7.3.2; thus, scenarios include implementation of WCMO to various degrees in zones 1 or 2 of the watershed. WC1z1, WC2z1, and WC3z1 indicate implementing WCMO at 10%, 50%, and 100% of all available sites in zone 1; and WC1z2, WC2z2, and WC3z2 indicate implementing WCMO at 10%, 50%, and 100% of all available sites in zone 2. These scenarios are combined with tillage practice scenario T2.

Another set of scenarios worth exploring is combinations of water storage with direct erosion control at the bluffs with NCMO. Under this strategy, we developed a number of scenarios consisting of WCMO and NCMO implementation at various extents and spatial locations. NC1, NC2, and NC3 indicate implementing NCMO at 10%, 50%, and 100% of all available sites across all zones; and NC1z3, NC2z3, and NC3z3 indicate implementing NCMO at 10%, 50%, and 100% of all available sites in zone 3. For the coupled WCMO and NCMO scenarios, WCMO is implemented in the upland zone (zone 1) only in order to identify dominant solutions since WCMO is more effective further in the upland (see Section 7.3.2).

Table 7.5: Summary of site-specific strategies with total extent selected, annual sediment loading (SL) reduction, annual cost, and unit cost of reducing a metric ton of sediment loading

Management Option Portfolio			Total extent selected			SL reduction	Annual Cost	Unit cost
Strategy	Scenario	Description	ac	ft	tips	Mg/yr	$/yr	$/Mg
Ag Field	T1AF1	TLMO: 33%-33%-33% (T1), AFMO10% all zones (AF1)	450	196,064		219	667,056	3,046
	T1AF2	T1, AFMO50% all zones (AF2)	2,167	943,994		1,008	3,211,682	3,186
	T1AF3	T1, AFMO100% all zones (AF3)	4,321	1,882,178		1,527	6,403,599	4,194
	T1AF1BF1	T1, AF1, BFMO10% all zone (BF1)	1,804	857,520		1,038	2,220,319	2,139
	T1AF1BF2	T1, AF1, BFMO50% all zone (BF2)	5,640	3,528,109		3,896	6,841,386	1,756
	T1AF1BF3	T1, AF1, BFMO100% all zone (BF3)	10,414	6,825,651		7,675	12,541,034	1,634
	T2AF1	TLMO: 25%-25%-50% (T2), AFMO10% all zones (AF1)	450	196,064		3,767	-900,823	-239
	T2AF2	T2, AFMO50% all zones (AF2)	2,167	943,994		4,468	1,643,803	368
	T2AF3	T2, AFMO100% all zones (AF3)	4,321	1,882,178		4,930	4,835,720	981
	T2AF1BF1	T2, AF1, BFMO10% all zone (BF1)	1,804	857,520		4,505	652,440	145
	T2AF2BF2	T2, AF2, BFMO50% all zone (BF2)	7,348	3,528,109		7,786	7,818,133	1,004
	T2AF3BF3	T2, AF3, BFMO100% all zone (BF3)	14,285	6,825,651		11,634	16,709,698	1,436
	T3AF1	TLMO: 0%-50%-50% (T3), AFMO10% all zones (AF1)	450	196,064		9,090	-188,151	-21
	T3AF2	T3, AFMO50% all zones (AF2)	2,167	943,994		9,658	2,356,475	244
	T3AF3	T3, AFMO100% all zones (AF3)	4,321	1,882,178		10,035	5,548,392	553
	T3AF1BF1	T3, AF1, BFMO10% all zone (BF1)	1,804	857,520		9,705	1,365,112	141
	T3AF2BF2	T3, AF2, BFMO50% all zone (BF2)	7,348	3,528,109		12,437	8,530,805	686
	T3AF3BF3	T3, AF3, BFMO100% all zone (BF3)	14,285	6,825,651		15,610	17,422,370	1,116
	T2AF1z2	T2, AFMO10% in zone 2 (AF1z2)	77	33,706		3,656	-1,398,736	-383
	T2AF2z2	T2, AFMO50% in zone 2 (AF2z2)	348	151,653		3,807	-1,188,241	-312
	T2AF3z2	T2, AFMO100% in zone 2 (AF3z2)	695	302,735		3,902	-929,690	-238
	T2AF1z2BF1z3	T2, AF1z2, BFMO10% zone 3 (BF1z3)	476	207,424		4,098	-1,072,497	-262
	T2AF2z2BF2z3	T2, AF2z2, BFMO50% zone 3 (BF2z3)	1,652	751,188		5,961	500,765	84
	T2AF3z2BF3z3	T2, AF3z2, BFMO100% zone 3 (BF3z3)	3,189	1,457,627		7,537	2,041,765	271
Stream Buffer	T2BF1	T2, BFMO10% all zone (BF1)	1,354	661,455		4,312	-14,616	-3
	T2BF2	T2, BFMO50% all zone (BF2)	5,190	2,584,116		6,891	4,606,451	668
	T2BF3	T2, BFMO100% all zone (BF3)	9,964	4,943,473		10,278	10,306,099	1,003
	T3BF1	T3, BF1	1,354	661,455		9,550	698,056	73
	T3BF2	T3, BF2	5,190	2,584,116		11,712	5,319,123	454
	T3BF3	T3, BF3	9,964	4,943,473		14,509	11,018,771	759
	T2BF1z3	T2, BF1z3	399	173,718		4,015	-1,241,640	-309
	T2BF2z3	T2, BF2z3	1,304	599,535		5,728	121,127	21
	T2BF3z3	T2, BF3z3	2,494	1,154,892		7,209	1,403,576	195
NCS	T2RA1	T2, RAMO10% all zone (RA1)			80	6,092	-1,505,877	-247
	T2RA2	T2, RAMO50% all zone (RA2)			338	11,547	-1,305,920	-113
	T2RA3	T2, RAMO100% all zone (RA3)			617	14,534	-1,089,688	-75
	T2NC1	T2, NCMO10% all zone (NC1)		26,227		23,569	-258,697	-11
	T2NC2	T2, NCMO50% all zone (NC2)		128,120		48,534	4,177,097	86
	T2NC3	T2, NCMO100% all zone (NC3)		252,346		59,042	9,710,767	164
	T2RA1NC1	T2, RAMO10%, NCMO10% all zone		26,227	80	26,088	-196,695	-8
	T2RA2NC2	T2, RAMO50%, NCMO 50% all zone		128,120	338	56,507	4,439,056	79
	T2RA3NC3	T2, RAMO100%, NCMO 100% all zone		252,346	617	70,002	10,188,958	146

Table 7.6: Summary of hydrologic strategies with total extent selected, annual sediment loading (SL) reduction, annual cost, and unit cost of reducing a metric ton of sediment loading

Management Option Portfolio			Total extent selected			SL reduction	Annual Cost	Unit cost
Strategy	Scenario	Description	ac	ft	tips	Mg/yr	$/yr	$/Mg
Water conser-vation	T2WC1	T2, WCMO5% all zone (WC1)	3,681			17,817	3,354,872	188
	T2WC2	T2, WCMO10% all zone (WC2)	6,370			27,490	6,950,900	253
	T2WC3	T2, WCMO30% all zone (WC3)	18,380			65,954	23,013,279	349
	T2WC4	T2, WCMO 50% all zone (WC4)	30,549			97,088	39,287,634	405
	T2WC5	T2, WCMO100% all zone (WC5)	60,577			139,415	79,446,424	570
	T2WC1z1	T2, WCMO10% zone1 (WC1z1)	3,134			16,818	2,623,005	156
	T2WC2z1	T2, WCMO50% zone1 (WC2z1)	15,608			62,163	19,306,271	311
	T2WC3z1	T2, WCMO100% zone1 (WC3z1)	31,086			102,548	40,005,736	390
	T2WC1z2	T2, WCMO10% zone2 (WC1z2)	1,929			10,757	1,011,316	94
	T2WC2z2	T2, WCMO50% zone2 (WC2z2)	9,048			34,753	10,532,515	303
	T2WC3z2	T2, WCMO100% zone2 (WC3z2)	17,977			59,465	22,473,972	378
	T2WC1z3	T2, WCMO10% zone3 (WC1z3)	1,308			7,705	180,822	23
	T2WC2z3	T2, WCMO50% zone3 (WC2z3)	5,893			20,919	6,313,090	302
	T2WC3z3	T2, WCMO100% zone3 (WC3z3)	11,514			32,989	13,830,959	419
Water Conservation & NCS	T2WC1z1NC1	T2, WCMO10% zone1, NCMO10% all zone	3,134	29,291		34,914	3,932,187	113
	T2WC1z1NC2	T2, WCMO10% zone1, NCMO50% all zone	3,134	128,537		57,471	8,367,981	146
	T2WC1z1NC3	T2, WCMO10% zone1, NCMO100% all zone	3,134	252,346		66,969	13,901,651	208
	T2WC2z1NC1	T2, WCMO50% zone1, NCMO10% all zone	15,608	29,291		73,753	20,615,454	280
	T2WC2z1NC2	T2, WCMO50% zone1, NCMO50% all zone	15,608	128,537		88,087	25,051,247	284
	T2WC2z1NC3	T2, WCMO50% zone1, NCMO100% all zone	15,608	252,346		94,135	30,584,918	325
	T2WC3z1NC1	T2, WCMO100% zone1, NCMO10% all zone	31,086	29,291		108,373	41,314,918	381
	T2WC3z1NC2	T2, WCMO100% zone1, NCMO50% all zone	31,086	128,537		115,478	45,750,711	396
	T2WC3z1NC3	T2, WCMO100% zone1, NCMO100% all zone	31,086	252,346		118,486	51,284,382	433
	T2WC1z1NC1z3	T2, WCMO10% zone1, NCMO10%zone3 (NC1z3)	3,134	17,536		34,113	3,406,784	100
	T2WC1z1NC2z3	T2, WCMO10% zone1, NCMO50%zone3 (NC2z3)	3,134	780,445		54,510	6,111,225	112
	T2WC1z1NC3z3	T2, WCMO10% zone1, NCMO100% zone3 (NC3z3)	3,134	152,503		62,965	9,439,170	150
	T2WC2z1NC1z3	T2, WCMO50% zone1, NCMO10% zone3	15,608	17,536		73,270	20,090,050	274
	T2WC2z1NC2z3	T2, WCMO50% zone1, NCMO50% zone3	15,608	78,045		86,360	22,794,491	264
	T2WC2z1NC3z3	T2, WCMO50% zone1, NCMO100% zone3	15,608	152,503		91,797	26,122,436	285
	T2WC3z1NC1z3	T2, WCMO100% zone1, NCMO10%zone3	31,086	17,536		108,156	40,789,515	377
	T2WC3z1NC2z3	T2, WCMO100% zone1, NCMO50% zone3	31,086	77,192		114,758	43,493,956	379
	T2WC3z1NC3z3	T2, WCMO100% zone1, NCMO100% zone3	31,086	152,503		117,509	46,821,900	398

7.4.2. Identification of dominant management option scenarios and resulting cost-reduction tradeoffs

Management scenarios are evaluated in terms of two objectives: minimize annual investment and maximize sediment-loading reduction (Tables 7.5 and 7.6). Tradeoffs between these objectives among various scenarios can be communicated by plotting the simulation outputs in the objective space: sediment loading reduction (x-axis) versus total annual cost of MO implementation (y-axis) (Figure 7.10). In this tradeoff plot, the dominant scenarios populate the southeast quadrant in the objective space since the corresponding objectives are to maximize on the x-axis and minimized on the y-axis.

The tradeoff plot illustrates that the site-specific strategies that focus management on agricultural field have limited capacity to reduce sediment. A maximum reduction of 15,610 Mg/yr is achieved with reduced and conservation tillage scenario (T3), 100% of AFMO (AF3), and 100% of BFMO (BF3) sites implemented at all zones of the watershed (T3AF3BF3 in Table 7.5 and green circles in Figure 7.10). This strategy is costly at about $17 million/yr. In general, for field-based measures, BFMO or a mixture of BFMO and AFMO are more effective than AFMO alone.

Addressing near-channel sources, with management of ravines (RAMO) and of bluffs (NCMO), is generally more cost-effective and far-reaching than addressing just field sources alone. However, the capacity of NCMO and RAMO to remove sediment is limited at 70,002 Mg/yr with an implementation cost at about $10M/yr when 100% of these management sites are implemented. If the sediment reduction goal is larger than 70,002 Mg/yr, scenarios combining WCMO and NCMO should be considered. For example, the scenario, where conventional (25%), reduced (25%), and conservation till

(50%) (T2) are implemented with water conservation implemented in 50% of all sites in the upland zone, and bluffs managed in 100% of all sites in in the incised zone (T2WC2z1NC3z3 in Table 7.6), reduces sediment loading by 91,797 Mg/yr.

A water conservation strategy with WCMO implementation generally reduces more sediment than the scenarios under site-specific strategy. With 100% of WCMO sites are implemented in all zones (WC5 in Table 7.6), the sediment-loading reduction is 139,415 Mg/yr (blue circles in Figure 7.10). Because we used a conservative cost estimate for water conservation (Table 7.2a), WCMO implementation is less desirable than both NCMO alone and combination of WCMO and NCMO.

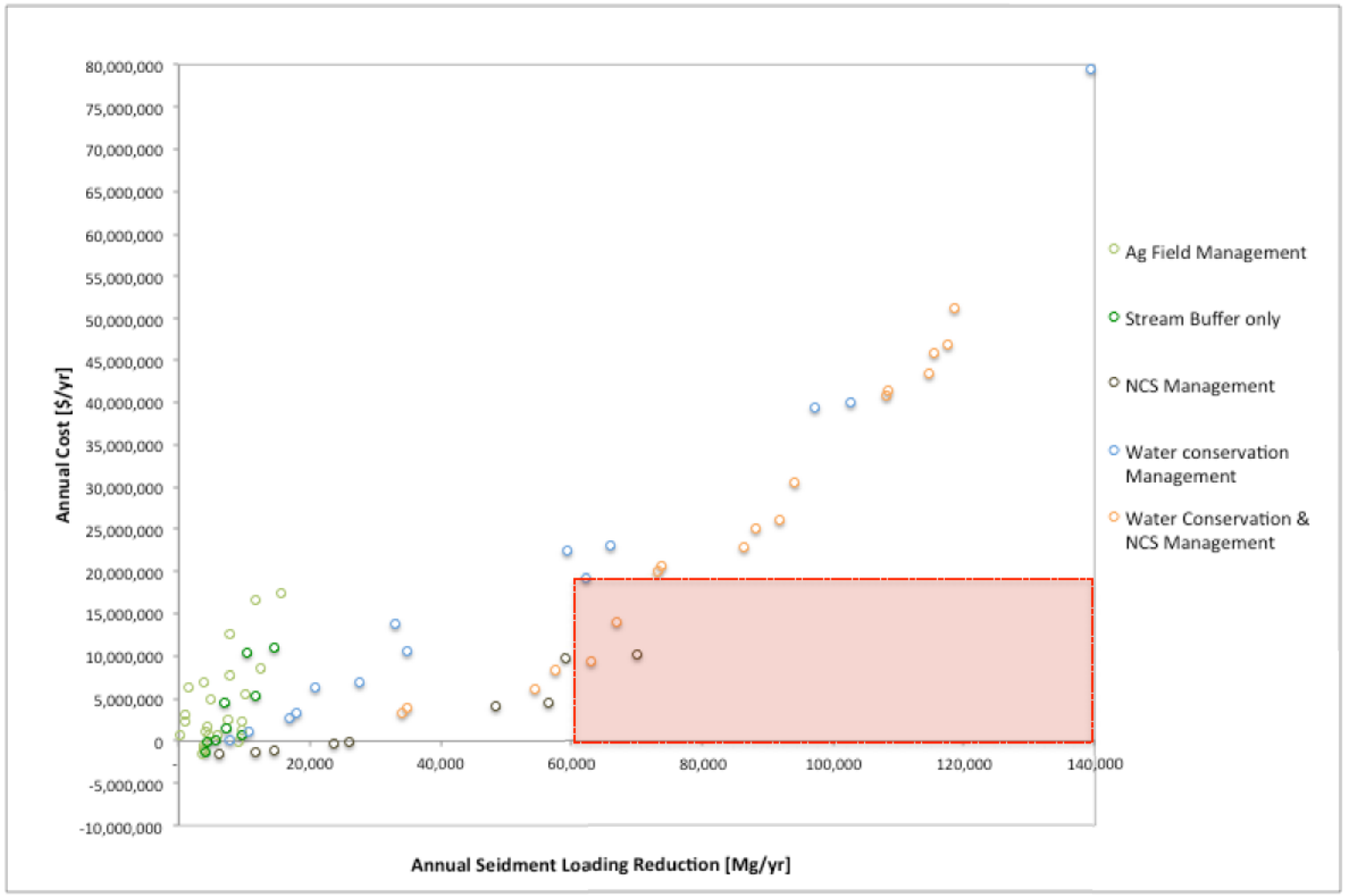

Figure 7.10: a tradeoff curve evaluating the objectives to 1) maximize annual sediment loading reduction on the x-axis and 2) minimize annual cost of land acquisition, implementation, and maintenance on the y-axis. The plot imposes a cost constraint at $20 Million/year and sediment loading reduction constraint at 60,000 Mg/yr where feasible solutions are populated in the red box.

7.4.3. Management constraints and feasible solutions

In this section, we consider scenarios that expend a particular amount of annual expenditure and/or achieve a minimum sediment loading reduction requirement. For example, if a maximum cost constraint is imposed at $20 Million/year and minimum sediment reduction constraint is set at 60,000 Mg/year (Figure 7.10 illustrates this feasible area with red square), then four scenarios remain as feasible solutions that satisfy both constraints (Table 7.7).

Table 7.7: list of feasible solutions with cost constraint at $20 Million/year and sediment reduction constraint at 60,000 Mg/year

Scenario	SL reduction [Mg/yr]	Annual Cost [$/yr]	Unit Cost [$/Mg]
T2WC1z1NC3z3	62,965	9,439,170	150
T2RA3NC3	70,002	10,188,958	146
T2WC1z1NC3	66,969	13,901,651	208
T2WC2z1	62,163	19,306,271	311

Among these solutions, T2RA3NC3 (T2 plus RAMO and NCMO implemented at 100% in all zones) has the lowest cost per metric ton of sediment reduced; thus, this solution might be viewed as an attractive relative the other three solutions. However, a management scenario with a mixture of water conservation and NCS management, T2WC1z1NC3z3 (T2 plus 10% WCMO sites in zone 1 and 100% NCMO sites in zone 3), is almost as desirable with a slightly lower cost and less sediment reduction. These feasible solutions may be evaluated in terms of tradeoff between sediment reduction and cost; for example, scenario T2RA3NC3 can reduce additional 7,037 Mg/yr sediment with an additional cost of $749,788/yr compared to T2WC1z1NC3z3. In choosing among these four solutions, managers and stakeholders would likely wish to consider other objectives as well. In the next section, we discuss implication of multiple objectives in evaluating various management scenarios and environmental decision-making.

7.4.4. Consideration of multiple objectives

There are other benefits (environmental, economic, and social) that could be used to evaluate different management strategies and differentiate among scenarios with similar costs and sediment reductions. An evaluation of effects of alternative land use change in Minnesota on the joint provision of ecosystem services, species habitat, and return to landowner illustrates the importance of taking ecosystem services into account in land use decisions (Polasky et al., 2011). Therefore, we evaluate multiple objectives, highlighting ecosystem services and recreational returns of management option alternatives in this section.

At the first stakeholder meeting (see Chapter 2, Appendix 2.B), we surveyed the stakeholders on what "goals" of environmental management they would wish to be considered. We compiled the following list of objectives from the stakeholder inputs from this meeting:

Objective 1. Decrease sediment loading in the water system

Objective 2. Impose reasonable costs for environmental management

Objective 3. Create clean ecosystem/nutrient management

Objective 4. Facilitate recreation area

Objective 5. Grow non-row crops for bio-fuel

We selected the first two objectives to quantify the impacts of various management scenarios in the previous section because they are directly related to sediment mitigation, a definitive goal of the Collaborative for Sediment Source Reduction (CSSR) project. However, management scenarios considered in this study can address these other objectives concurrently. For example, implementation of water conservation, such as

wetland restoration, not only stores water, but they also provides ecosystem services (e.g., biodiversity support, endangered species protection, and protection of ecological infrastructure) and recreation areas (e.g., fishing, swimming, hiking, nature viewing, hunting, birding, and boating) (King et al., 2000).

In the rest of this section, we illustrate how these other objectives could be considered in a general multi-objective tradeoff analysis, using one particular method as an example. There are many possible multi-objective decision methods and environmental economic methods that might be used (e.g., the survey of multi-criteria decision-making (MCDM) methods in Marler and Arora (2004)). One approach is to define additional axes in plots like Figure 7.10 representing other objectives, so that the tradeoff curves instead become tradeoff surfaces in three or more dimensions. This can be followed by valuation using, e.g., multicriteria weighting methods (Hobbs and Meier, 2012).

Another approach to include these additional social and environmental objectives is to quantify other objectives in dollar terms and then combine them with the cost objective in Figure 7.10. For instance, the monetization might be undertaken using the contingent valuation method (CVM) (Hackett, 2010). CVM would involve the use of survey questionnaires to quantify the values of achieving each of these objectives. For example, in the first CVM study, non-market values for hunting and recreation services of Maine woods were estimated (Davis, 1963). Likewise, management options in this research can be evaluated for their values associated with achieving the objectives 3 through 5.

Simulating the use of the CVM method, we assigned monetary values added to WCMO, RAMO, and NCMO per extent for each of these objectives from literature review. For example, wetland restoration's effectiveness (i.e., WCMO) in reducing

nutrients and providing clean ecosystem services might be translated into social economic value (the perceived nonmarket values the public ascribes to ecosystem, aesthetics, and recreation services (USGS, 2015): Nitrogen mitigation at $1,248 and Waterfowl recreation at $16 (estimates in $/ha/yr) (Jenkins et al., 2010) (Table 7.8 shows these values in terms of $/ac/yr). River restoration's values (i.e., NCMO) were estimated using a survey method in North Carolina (Holmes et al., 2004), where restoration's annual benefit is estimated at $89.5/ft for full restoration including riparian reestablishment, or at $23.1/ft for partial restoration done at piecemeal along the stream. In that study, the annual benefits were described in terms of five indicators of ecosystem service: abundance of game fish, water clarity, wildlife habitat, allowable water use, and ecosystem naturalness (thus, objectives 3 and 4 combined) (Holmes et al., 2004). Since NCMO will be applied to discrete bluffs addressing parts of the river system, we applied the partial restoration value in this analysis (Table 7.8). Valuation of ravine management on ecosystem services and nutrient management is not as common as the other types of management options, but typically ravine management focuses only on erosion control from flood events ("Blue Earth County water management plan 2017-2027: Priority concerns scoping document," 2016) so for this analysis we didn't attribute any ecosystem services, nutrient management, or recreational values to RAMO.

Table 7.8: A hypothetical contingent valuation of management options for objectives 3 through 5

MOs\Objectives	Obj.3	Obj.4	Obj.5
WCMO [$/yr-ac]	505	7	0
RAMO [$/tip]	0	0	0
NCMO [$/yr-ft]	23.08	0	0

We will need further work (i.e., independent surveys among Minnesotans in the study watershed) to appropriately assign values to these other benefits achieved by management options. Thus, in this section we simply describe how a vertical shift and tilting in the tradeoff curve resulting from adding dollar estimates for other objectives may affect decision-making instead of describing the detailed implication of adding the values in Table 7.8. With the monetary values considered for these extra objectives, we can adjust the cost of implementing each management option as a way to include the values of other objectives achieved by the management scenarios.

With the inclusion of the valuations of objectives 3 through 5 from Table 7.8, the tradeoff curve is shifted down and consequent tradeoff relations among different scenarios have been altered (Figure 7.11 shows management scenarios with only two objectives considered in open circles and those with multiple objectives considered in closed circles). Compared to the case in which only two objectives were considered, WCMO becomes relatively more desirable when other objectives are considered (notice the closer proximity between WCMO scenarios and NCMO scenarios with multiple objectives). Since NCMO has relatively little value with respect to the other objectives, this also implies that WCMO and NCMO (orange circles) become more desirable for a number of scenarios than the scenarios with NCMO only when multiple objectives are considered.

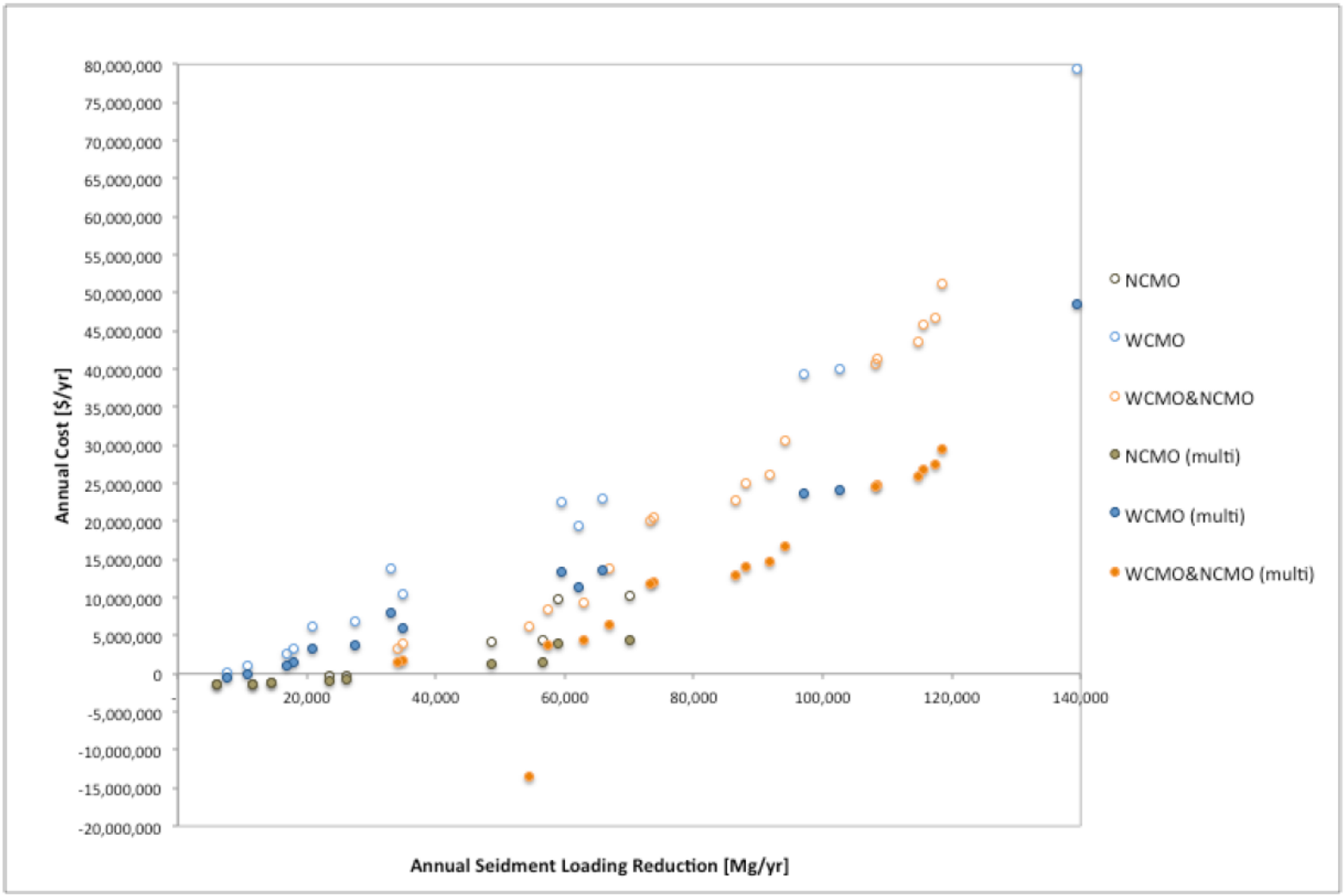

Figure 7.11: This chart illustrates how the tradeoff curve of various management scenarios may be shifted with addition of multiple objective evaluations using the CVM that assigns monetary values to managements in achieving other social and environmental objective

7.5. Summary

In this chapter, we examined the behavior of MOSM in terms of credibility and utility for environmental management decision-making processes. Important challenges in managing agricultural nonpoint source pollution include difficulties in reliably predicting pollution and incorporating the complexity of agricultural system in pollution control system (Chapter 1). We have demonstrated that MOSM's prediction of sediment loading from various dominant sediment sources is consistent with data represented by the watershed sediment budget and within the constraints provided by observed information.

The simulation model considers relevant management options in the study site and predicts the impacts of implementing management options in different areas of the watershed in terms of sediment reduction and annual management cost. Other objectives can be used to augment the two-objective structure of model outputs, and further inform social and environmental implications of various management scenarios. This can be done, for instance, by assigning dollar values to other categories of benefits and costs and then netting from the original installation costs. We found that this increased the attractiveness of portfolios that included WCMO, which have other ecological benefits, relative to portfolios including NCMO.

8. Conclusion

8.1. Research motivation and chapter review

There is a need for an accessible, reliable, and robust modeling approach to address agricultural nonpoint source (NPS) sediment pollution. In this dissertation, we developed a watershed modeling approach to help guide management strategies for efficiently distributing environmental investment funds to address agricultural NPS sediment pollution across the Le Sueur River Basin (LSRB), an agricultural watershed in south-central Minnesota that contributes the highest amount of sediment of any Minnesota River tributary (Wilcock, 2009).

Environmental modeling may bridge the scientific approaches and monitoring of various environmental processes to the need for making measurable progress toward water quality improvement (Thomann, 1998; Tomer et al., 2015). But many environmental simulation models have become increasingly complex over the years, introducing an important separation between model predictions and decision-makers (Gaddis, 2010). The model complexity has contributed to the fundamental source of historical conflict in environmental management: "the lack of reliable, trustworthy, and mutually agreed upon information on the causes of problems and the consequences of environmental control actions (Thomann, 1998)." A solution would be to develop an approach to support environmental decision-making that offers transparency and participation of decision-makers, and to provide context-sensitive knowledge for specific management decisions (Haag and Kaupenjohann, 2001).

We developed a watershed modeling approach to evaluate NPS sediment pollution across the watershed (Topofilter models in Chapters 3&4), to quantify near-channel

source sediment supply (Chapter 5), and to simulate the environmental and economic impacts of various management alternatives (Management Option Simulation Model (MOSM) in Chapters 6&7) through a collaborative modeling process involving various scientific experts and stakeholders (Chapter 2).

In the following sections, we revisit the research objectives and contributions made by the watershed modeling approach presented in this dissertation.

8.2. Research objective and corresponding outcomes

The overarching research objective set forth in Chapter 1 was to *develop a watershed-modeling framework for assessing conservation actions intended to reduce sediment loading from an agricultural watershed*. This objective was addressed by a number of modeling components:

1) Routing and delivery of sediment is simulated using a sediment delivery ratio (SDR) approach. The model combines a high-resolution digital elevation model (DEM) and spatially explicit soil erosion rates with spatially integrated information on sediment loading measured at stream gages (Chapters 3&4). The model specifically addresses the *sediment delivery problem* that stands between estimates of distributed soil erosion and the often small fraction of that erosion that is delivered from the watershed (Walling, 1983);
2) A model for near-channel sediment supply (NCSS) is developed using sediment load information at paired gages that bracket the incised zone, where near-channel sources dominate. A single relation between river discharge and NCSS is observed to hold for six different streams with paired gages. The relation supports estimates of the change in NCSS that can be achieved with

reductions in peak river discharge through water conservation actions (chapter 5);

3) The sediment delivery and NCSS models are combined in a simulation model with reduced list of management options that either reduce sediment sources or sediment delivery from the watershed (Chapters 6).

The sediment delivery problem links distributed soil erosion estimates with actual sediment delivery at a point in the watershed. We extracted the dominant effect of topography on this linkage using high-resolution topography from aerial LiDAR in a model called TopoFilter. The approach uses a simple relation to express the effect on sediment delivery of slope and distance from field source to stream, and another similar relation applied to transport along the stream channel. The model parameters are conditioned to eliminate parameter space that does not provide a reasonable match to the observed loading at stream gages. The conditioned parameter space provides a distribution of sediment loading predictions that account for uncertainties in the model structure, observed data, and natural variability.

The NCSS problem is addressed using a set of near-synchronous observations of sediment load at pairs of stream gages that bracket large parts of the incised zone of their watersheds, where NCSS have been shown to predominate. Rather than attempting to estimate and cumulate all different sources of sediment loading in the incised zone, the paired-gage approach provides a direct estimate of the net sediment input. The rate of NCSS is found to increase as a power function of river discharge. This model provides a predictive foundation for evaluating the effects of water storage management on peak flow attenuation versus direct mitigation to reduce NCSS.

The results of these research projects, along with updates on the sediment budget (Gran et al., 2011), were reported to the stakeholders during the Collaborative for Sediment Source Reduction (CSSR) meetings. The meetings were intended to build a concrete understanding and agreement among stakeholders on the major causes of the NPS sediment pollution and their implication for management in the study watershed.

The management option simulation model (MOSM) combines the SDR and NCSS models with a reduced list of management options in order to support evaluation of management actions to reduce sediment loading. Management options are defined according to their role in sediment loading. Some actions reduce sediment erosion on the field, or through bluff or ravine stabilization in the near-channel zone, and other actions reduce the delivery of sediment from field sources to the stream network. The core of the model is spatially distributed SDR from TopoFilter that, in effect, discounts sediment production rates from various sources (field, ravines, streambanks, and bluffs) as well as management actions to reduce sediment production and delivery. The model includes a water routing module that estimates the effect of water storage management. The estimated river discharge is then applied to the NCSS model to estimate the reduction of sediment loading from waters storage management.

The model results are strongly constrained by the use of SDR approach. When no management is in place, the model simply returns the measured annual sediment loading. When additional management actions are implemented, the estimated sediment loading is constrained between the existing loading and zero.

We demonstrated that simulation outputs of the models agree well with observations at stream gages and with a watershed-scale sediment budget that incorporates a range of

independent data (Belmont et al., 2011; Gran et al., 2011). Also, in order to demonstrate how the model outputs can be used to evaluate effects of multiple different management alternatives, we developed a management option portfolio including strategies to address specific sources, provide water storage, or combinations of these strategies. Tradeoffs between two objectives – minimize annual management investment and maximize sediment load reduction – are evaluated for different management scenarios along with identification of more dominant solutions (Chapter 7).

8.3. Contribution of the data-driven, reduced complexity modeling

The goal of this research was to provide information about agricultural NPS sediment pollution from field and near-channel sources, and to develop a watershed simulation model that is transparent and accessible to stakeholders. Data-driven, reduced-complexity modeling approach is central to the watershed modeling framework presented in this dissertation. We demonstrated that the models built using the data-driven, reduced complexity approach provide *relevant, reliable* and *robust* predictions by making an effective use of information on soil, topography, and gage information throughout the dissertation.

The data-driven, reduced-complexity modeling approach represents the watershed processes by capturing only the essential and measurable information relevant to management questions while effectively using available data to inform model structure and simulation. We accomplished this through collaboration with scientific experts and stakeholders, where we obtained available information and determined appropriate model structure to reflect the management needs. The data-driven, reduced-complexity approach is, therefore, *relevant* to environmental and social needs in that the focus of model

development is in fostering stakeholder involvement and understanding, and supporting environmental decision-making. This approach is *reliable* in that model development is strongly constrained by observational data, and its predictions are credible and consistent with observations at the watershed scale. Also, this framework provides a basis for determining uncertainty in the simulation outputs by using multiple model runs with plausible variation in the sediment delivery input parameters. The approach is *robust* in that individual processes and model uncertainties are traceable within the simple model structure, and model outputs are strongly constrained by observation over a wide range of inputs. Because the management simulation model is not burdened with the computation of complex natural processes, the model is simple and accessible to a wide range of users, and simulation time is rapid. It produces results in seconds, thereby allowing immediate feedback for users, and permits multiple runs that can illustrate changes in sediment reduction with various extents of management options over different geomorphic regions of the watershed.

References:

Amore, E., Modica, C., Nearing, M.A., Santoro, V.C., 2004. Scale effect in USLE and WEPP application for soil erosion computation from three Sicilian basins. J. Hydrol. 293, 100–114. doi:10.1016/j.jhydrol.2004.01.018

Arnold, J.G., Kiniry, J.R., Srinivasan, R., Williams, J.R., 2011. Soil and Water Assessment Tool: input / output file documentation (version 2009) (No. TR-365).

Ascough II, J.C., Maier, H.R., Ravalico, J.K., Strudley, M.W., 2008. Future research challenges for incorporation of uncertainty in environmental and ecological decision-making. Ecological Modelling, The Importance of Uncertainty and Sensitivity Analysis in Process-based Models of Carbon and Nitrogen Cycling in Terrestrial Ecosystems with Particular Emphasis on Forest EcosystemsSelected Papers from a Workshop Organized by the International Society for Ecological Modelling (ISEM) at the Third Biennal Meeting of the International Environmental Modelling and Software Society (IEMSS) in Burlington, Vermont, USA, August 9-13, 2006 219, 383–399. doi:10.1016/j.ecolmodel.2008.07.015

Beach, T., 1994. The fate of eroded soil: sediment sinks and sediment budgets of agrarian landscapes in Southern Minnesota, 1851-1988. ann. Assoc. Am. Geogr. 84, 5–28.

Beeson, P.C., 2014. Sediment delivery estimates in water quality models altered by resolution and source of topographic data. J. Environ. Qual. 43, 26. doi:10.2134/jeq2012.0148

Belmont, P., 2011. Floodplain width adjustments in response to rapid base level fall and knickpoint migration. Geomorphology 128, 92–102. doi:10.1016/j.geomorph.2010.12.026

Belmont, P., Gran, K., Hobbs, B., Kozarek, J., Marr, J., Wilcock, P., 2012. Collaborative for Sediment Source Reduction: Greater Blue Earth River Basin-EPA 319 Grant scope of work and work plan (Proposal).

Belmont, P., Gran, K.B., Schottler, S.P., Wilcock, P.R., Day, S.S., Jennings, C., Lauer, J.W., Viparelli, E., Willenbring, J.K., Engstrom, D.R., Parker, G., 2011. Large shift in source of fine sediment in the upper Mississippi River. Environ. Sci. Technol. 45, 8804–8810. doi:10.1021/es2019109

Beven, K., 2001. Rainfall-runoff modelling. Wiley, The Atrium, Southern Gate, Chichester, West Sussex PO19 8SQ, England.

Beven, K., 2006. A manifesto for the equifinality thesis. J. Hydrol. 320, 18. doi:10.1016/j.jhydrol.2005.07.007

Beven, K., Freer, J., 2001. Equifinality, data assimilation, and uncertainty estimation in mechanistic modelling of complex environmental systems using the GLUE methodology. J. Hydrol. 249, 11. doi:10.1016/S0022-1694(01)00421-8

Bevis, M., 2015. Pleistocene base-level fall is a fundamental driver of erosion in southern Minnesota's Greater Blue Earth River Basin. University of Minnesota Duluth.

Blue Earth County water management plan 2017-2027: Priority concerns scoping document [WWW Document], 2016. URL http://www.co.blue-earth.mn.us/DocumentCenter/View/1529 (accessed 1.14.17).

Blue Earth County, MN Farmland Prices and Values | AcreValue [WWW Document], 2016. URL https://www.acrevalue.com/map/MN/Blue-Earth/ (accessed 8.29.16).

Boomer, K.B., 2008. Empirical models based on the universal soil loss equation fail to predict sediment discharges from Chesapeake Bay catchments. J. Environ. Qual. 37, 79. doi:10.2134/jeq2007.0094

Borah, D.K., 2004. Watershed-scale hydrologic and nonpoint-source pollution models: Review of applications. Trans. ASABE. 47, 789.

Boyce, R.C., 1975. Sediment routing with sediment delivery ratios. Present and prospective technology for predicting sediment yield and sources, ARS-S-40, 61–65.

Center for Watershed Protection, 2004. pondwetlandguidebookdraft.pdf (No. EPA contract 68-C-99-253).

Chow, V.T., Maidment, D.R., Mays, L.W., 1988. Applied Hydrology. McGraw-Hill Education.

Christiaens, K., Feyen, J., 2001. Analysis of uncertainties associated with different methods to determine soil hydraulic properties and their propagation in the distributed hydrological MIKE SHE model. J. Hydrol. 246, 63–81. doi:10.1016/S0022-1694(01)00345-6

Cohon, J.L., 2004. Multiobjective Programming and Planning. Courier Dover Publications, Mineola, N.Y.

Daly, L., Bourke, G.J., 2008. Interpretation and Uses of Medical Statistics. John Wiley & Sons.

Dalzell, Pennington, Derric, Polasky, Stephen, Mulla, David, Taff, Steve, Nelson, Erik,

2012. Lake Pepin Watershed full cost accounting project-final report prepared for the MPCA.

Davis, R.K., 1963. The value of outdoor recreation: an economic study of the Maine Woods (Ph.D. Dissertation). Harvard University, Cambridge.

Day, S.S., Gran, K.B., Belmont, P., Wawrzyniec, T., 2013. Measuring bluff erosion part 1: terrestrial laser scanning methods for change detection. Earth Surf. Process. Landforms 38, 1055–1067. doi:10.1002/esp.3353

Day, S.S., Gran, K.B., Belmont, P., Wawrzyniec, T., 2013b. Measuring bluff erosion part 2: pairing aerial photographs and terrestrial laser scanning to create a watershed scale sediment budget. Earth Surf. Process. Landf. 38, 1068–1082. doi:10.1002/esp.3359

de Vente, J., Poesen, J., 2005. Predicting soil erosion and sediment yield at the basin scale: Scale issues and semi-quantitative models. Earth-Sci. Rev. 71, 95–125. doi:10.1016/j.earscirev.2005.02.002

De Vente, J., Poesen, J., Arabkhedri, M., Verstraeten, G., 2007. The sediment delivery problem revisited. Prog. Phys. Geogr. 31, 155. doi:10.1177/0309133307076485

de Vente, J., Poesen, J., Verstraeten, G., Van Rompaey, A., Govers, G., 2008. Spatially distributed modelling of soil erosion and sediment yield at regional scales in Spain. Global and Planetary Change 60, 393–415. doi:10.1016/j.gloplacha.2007.05.002

Desmet, P.J.J., 1996. A GIS procedure for automatically calculating the USLE LS factor on topographically complex landscape units. J. Soil Water Conserv. 51, 427.

Dooge, J.C.I., 1986. Looking for hydrologic laws. Water Resour. Res. 22, 46S–58S.

doi:10.1029/WR022i09Sp0046S

Downer, C.W., 2009. Simulation of reactive constituent rate and transport in hydrologic simulator GSSHA (No. ERDC TN-SWWRP-09-2), System-wide water resources program. U.S. army engineer research and development center, coastal and hydraulics Laboratory, Vicksburg, MS.

Downer, C.W., Ogden, F.L., 2003. Prediction of runoff and soil moistures at the watershed scale: Effects of model complexity and parameter assignment. Water Resour. Res. 39, 1045. doi:10.1029/2002WR001439

Downer, C.W., Ogden, F.L., 2006. Gridded Surface Subsurface Hydrologic Analysis (GSSHA) User's Manual; Version 1.43 for Watershed Modeling System 6.1.

Drumm, E.C., 1997. Subgrade resilient modulus correction for saturation effects. J. Geotech. Eng. 123, 663–670. doi:10.1061/(ASCE)1090-0241(1997)123:7(663)

Engstrom, D.R., 2009. Historical changes in sediment and phosphorus loading to the upper Mississippi River: mass-balance reconstructions from the sediments of Lake Pepin. J. Paleolimnol. 41, 563–588. doi:10.1007/s10933-008-9292-5

Fernandez, C., Wu, J.Q., McCool, D.K., Stöckle, C.O., 2003. Estimating water erosion and sediment yield with GIS, RUSLE, and SEDD. J. Soil Water Conserv. 58, 128–136.

Ferro, V., 1995. Sediment delivery processes at basin scale. Hydrol. Sci. Bull. 40, 703. doi:10.1080/02626669509491460

Fiener, P., Auerswald, K., 2003. Effectiveness of Grassed Waterways in Reducing Runoff and Sediment Delivery from Agricultural Watersheds. J. Environ. Qual. 32, 927–936. doi:10.2134/jeq2003.9270

Fisher, S., Moore, R., 2008. 2007 Tillage Transect Survey--Final Report [WWW Document]. Tillage Transect 2007 Final Report LowRes. URL http://mrbdc.mnsu.edu/sites/mrbdc.mnsu.edu/files/public/transect/pdf/Tillage_Transect_2007_Final_Report_LowRes.pdf (accessed 6.13.16).

Fistikoglu, O., 2002. Integration of GIS with USLE in assessment of soil erosion. Water resour. manag. 16, 447. doi:10.1023/A:1022282125760

Folle, S., Dalzell, B., Mulla, D., 2009. Evaluation of Best Management Practices (BMPs) in impaired watersheds using the SWAT model. Minnesota Department of Agriculture Clean Legacy Fund.

Gaddis, E.J.B., 2010. Effectiveness of a participatory modeling effort to identify and advance community water resource goals in St. Albans, Vermont. Environ. Model.Softw. 25, 1428. doi:10.1016/j.envsoft.2009.06.004

Garbrecht, J., Liew, M.V., Brown, G.O., 2004. Trends in precipitation, streamflow, and evapotranspiration in the Great Plains of the United States. J. Hydrol. Eng. 9, 360–367. doi:10.1061/(ASCE)1084-0699(2004)9:5(360)

Gassman, 2007. The soil and water assessment tool: historical development, applications, and future research directions. Trans. ASABE. 1211–1250.

Gatto, L.W., 1995. Soil Freeze-Thaw Effects on Bank Erodibility and Stability. (No. CRREL-SR-95-24), COLD REGIONS RESEARCH AND ENGINEERING LAB HANOVER NH.

Gran, K., Belmont, P., Day, S., Jennings, C., Johnson, A., Perg, L., Wilcock, P., 2009. Geomorphic evolution of the Le Sueur River, Minnesota, USA, and implications for current sediment loading. Geol. Soc. Am. Spec. Pap. 451, 119–130.

Gran, K., Belmont, P., Day, S., Jennings, C., Lauer, J.W., Viparelli, E., Wilcock, P., Parker, G., Azmera, L., Etcherling, C., others, 2011. An integrated sediment budget for the Le Sueur River Basin (No. MPCA Report wq-iw7-29o).

Gran, K., Finnegan, N., Johnson, A., Belmont, P., Wittkop, C., Rittenour, T., 2013. Landscape evolution, valley excavation, and terrace development following abrupt postglacial base-level fall. Geol. Soc. Am. Bull. 125, 1851–1864. doi:10.1130/B30772.1

Gupta, H.V., 1998. Toward improved calibration of hydrologic models: Multiple and noncommensurable measures of information. Water Resour. Res. 34, 751–763. doi:10.1029/97WR03495

Haag, D., Kaupenjohann, M., 2001. Parameters, prediction, post-normal science and the precautionary principle—a roadmap for modelling for decision-making. Ecol. Model. 144, 45–60. doi:10.1016/S0304-3800(01)00361-1

Hackett, S.C., 2010. Environmental and Natural Resources Economics: Theory, Policy, and the Sustainable Society. M.E. Sharpe.

Hammer, D.A., 1992. Designing constructed wetlands systems to treat agricultural nonpoint source pollution. Ecological Engineering 1, 49–82. doi:10.1016/0925-8574(92)90025-W

Hillman, G.R., 1998. Flood wave attenuation by a wetland following a beaver dam failure on a second order boreal stream. Wetlands 18, 21–34. doi:10.1007/BF03161439

Hirsch, R.M., Costa, J.E., 2004. U.S. stream flow measurement and data dissemination improve. Eos Trans. Am. Geophys. Union 85, 197–203.

doi:10.1029/2004EO200002

Hobbs, B.F., Meier, P., 2012. Energy Decisions and the Environment: A Guide to the Use of Multicriteria Methods. Springer Science & Business Media.

Holmes, T.P., Bergstrom, J.C., Huszar, E., Kask, S.B., Orr III, F., 2004. Contingent valuation, net marginal benefits, and the scale of riparian ecosystem restoration. Ecological Economics 49, 19–30. doi:10.1016/j.ecolecon.2003.10.015

Hooke, J.M., 1979. An analysis of the processes of river bank erosion. J. Hydrol. 42, 39–62. doi:10.1016/0022-1694(79)90005-2

Houston Engineering Inc., 2016. PTMApp: Theory and development documentation (Model documentation No. 6059_051).

Ian Treat, Karen Gran, 2016. Ravine shape file.

Iowa State University, 2016. Iowa Farm Custom Rate Survey | Ag Decision Maker [WWW Document]. URL https://www.extension.iastate.edu/AGDM/crops/html/a3-10.html (accessed 1.22.17).

Jain, S.K., Singh, V.P., 2003. Water resources systems planning and management. Elsevier.

Jenkins, W.A., Murray, B.C., Kramer, R.A., Faulkner, S.P., 2010. Valuing ecosystem services from wetlands restoration in the Mississippi Alluvial Valley. Ecological Economics 69, 1051–1061. doi:10.1016/j.ecolecon.2009.11.022

Jenson, S., Dominque, J., 1988. Extracting topographic structure from digital elevation data foar geographic information system analysis. Photogrammetric Engineering and Remote Sensing 54.

Jia, Y., 2006. Robust optimization for total maximum daily load allocations. Water Resour. Res. 42, W02412. doi:10.1029/2005WR004079

Johnson, T.C., Cole, D.M., Chamberlain, E.J., 1978. Influence of Freezing and Thawing on the Resilient Properties of a Silt Soil Beneath an Asphalt Concrete Pavement, (No. CRREL-78-23), COLD REGIONS RESEARCH AND ENGINEERING LAB HANOVER NH.

Jørgensen, S.E., 2002. Integration of Ecosystem Theories: A Pattern: A Pattern. Springer Science & Business Media.

Juracek, K.E., Fitzpatrick, F.A., 2009. Geomorphic applications of stream-gage information. River Res. Appl. 25, 329–347. doi:10.1002/rra.1163

Kelley, D.W., Nater, E.A., 2000. Historical sediment flux from three watersheds into Lake Pepin, Minnesota, USA. J. Environ. Qual. 29, 561–568. doi:10.2134/jeq2000.00472425002900020025x

King, D.M., Wainger, L.A., Bartoldus, C.C., Wakeley, J.S., 2000. Expanding Wetland Assessment Procedures: Linking Indices of Wetland Function with Services and Values (No. ERDC/EL TR-00-17), Environmental laboratory. US Army Corps of Engineers.

Kirchner, J.W., 2006. Getting the right answers for the right reasons: Linking measurements, analyses, and models to advance the science of hydrology. Water Resour. Res. 42, W03S04. doi:10.1029/2005WR004362

Korfmacher, K.S., 2001. The Politics of Participation in Watershed Modeling. Environ. Manage. 27, 161–176. doi:10.1007/s002670010141

Krysanova, V., Arnold, J., 2008. Advances in ecohydrological modelling with SWAT—

a review. Hydrol. Sci. J. 53, 939–947. doi:10.1623/hysj.53.5.939

Krysanova, V., Müller-Wohlfeil, D.-I., Becker, A., 1998. Development and test of a spatially distributed hydrological/water quality model for mesoscale watersheds. Ecol. Model. 106, 261–289. doi:10.1016/S0304-3800(97)00204-4

Kumarasamy, K., Belmont, P., 2014. Quantifying uncertainty and variability in sediment yield estimates in Le Sueur River Basin. AGU Fall Meeting Abstracts 51.

Lane, S.N., Brookes, C.J., Kirkby, M.J., Holden, J., 2004. A network-index-based version of TOPMODEL for use with high-resolution digital topographic data. Hydrol. Process. 18, 191–201. doi:10.1002/hyp.5208

Leopold, L.B., Langbein, W.B., 1962. The concept of entropy in landscape evolution (USGS Numbered Series No. 500–A), Professional Paper.

Lewandowski, A., Everett, L., Lenhart, C., Terry, K., Origer, M., Moore, R., 2015. Fields to Streams: Managing Water in Rural Landscapes. Part One, Water Shaping the Landscape. Water Resources Center, University of Minnesota Extension.

Lim, K.J., 2005. GIS-based sediment assessment tool. Catena 64, 61. doi:10.1016/j.catena.2005.06.013

Marler, R.T., Arora, J.S., 2004. Survey of multi-objective optimization methods for engineering. Struct Multidisc Optim 26, 369–395. doi:10.1007/s00158-003-0368-6

MATLAB and Statistics Toolbox, 2016.

Matteson, S., 2006. Fecal coliform TMDL assessment for 21 impaired streams in the Blue Earth River Basin (No. 6–1). Minnesota State University, Mankato Water

Resource Center Publication.

McDonnell, J.J., Sivapalan, M., Vaché, K., Dunn, S., Grant, G., Haggerty, R., Hinz, C., Hooper, R., Kirchner, J., Roderick, M.L., Selker, J., Weiler, M., 2007. Moving beyond heterogeneity and process complexity: A new vision for watershed hydrology. Water Resour. Res. 43, W07301. doi:10.1029/2006WR005467

McMillan, H.K., Brasington, J., 2007. Reduced complexity strategies for modelling urban floodplain inundation. Geomorphology, Reduced-Complexity Geomorphological Modelling for River and Catchment Management 90, 226–243. doi:10.1016/j.geomorph.2006.10.031

Melchoir, M., 2014. Personal communication.

Merritt, W.S., Letcher, R.A., Jakeman, A.J., 2003. A review of erosion and sediment transport models. Envi. Model. Softw., The Modelling of Hydrologic Systems 18, 761–799. doi:10.1016/S1364-8152(03)00078-1

Miller, T., Peterson, J., 2012. Ag BMP Handbook for Minnesota.

Minnesota State University, Mankato Water Resources Center, 2012. Turbidity Total Maximum Daily Load study - Greater Blue Earth River Basin (No. wq-iw7-29b).

Mitchell, N., 2015. Achieving peak flow and sediment loading reduction through increased water storage in the Le Sueur Watershed, Minnesota: a modeling approach (Master of Science Thesis). University of Minnesota, Duluth.

MNDNR, 2017. Buffer Mapping Project: Minnesota DNR [WWW Document]. URL http://dnr.state.mn.us/buffers/index.html (accessed 6.14.16).

Montgomery, D.R., 2007. Dirt: The Erosion of Civilizations. University of California Press.

MPCA, 2012. Ditches and blue lines of the Greater Blue Earth River Basin.

Munro, R.N., Deckers, J., Haile, M., Grove, A.T., Poesen, J., Nyssen, J., 2008. Soil landscapes, land cover change and erosion features of the Central Plateau region of Tigrai, Ethiopia: Photo-monitoring with an interval of 30 years. Catena, Environmental change, geomorphic processes and land degradation in tropical highlands 75, 55–64. doi:10.1016/j.catena.2008.04.009

Nelson, P., 2016. Personal communication.

Novotny, E.V., Stefan, H.G., 2007. Stream flow in Minnesota: Indicator of climate change. J. Hydrol. 334, 319. doi:10.1016/j.jhydrol.2006.10.011

Oreskes, N., Shrader-Frechette, K., Belitz, K., 1994. Verification, Validation, and Confirmation of Numerical Models in the Earth Sciences. Science 263, 641–646.

Osmanoğlu, B., Dixon, T.H., Wdowinski, S., 2014. Three-Dimensional Phase Unwrapping for Satellite Radar Interferometry, I: DEM Generation. IEEE Transactions on Geoscience and Remote Sensing 52, 1059–1075. doi:10.1109/TGRS.2013.2247043

Palmer, M.A., Covich, A.P., Lake, S., Biro, P., Brooks, J.J., Cole, J., Dahm, C., Gibert, J., Goedkoop, W., Martens, K., Verhoeven, J., Bund, W.J.V.D., 2000. Linkages between aquatic sediment biota and life above sediments as potential drivers of biodiversity and ecological processes: a disruption or intensification of the direct and indirect chemical, physical, or biological interactions between aquatic sediment biota and biota living above the sediments may accelerate biodiversity loss and contribute to the degradation of aquatic and riparian habitats. BioScience 50, 1062–1075. doi:10.1641/0006-

3568(2000)050[1062:LBASBA]2.0.CO;2

Parysow, P., Wang, G., Gertner, G., Anderson, A.B., 2003. Spatial uncertainty analysis for mapping soil erodibility based on joint sequential simulation. CATENA 53, 65–78. doi:10.1016/S0341-8162(02)00198-4

Phillips, J.D., 2006. Evolutionary geomorphology: thresholds and nonlinearity in landform response to environmental change. Hydrol. Earth Syst. Sci. Discuss. 3, 365–394.

Pike, A.C., Mueller, T.G., Schörgendorfer, A., Shearer, S.A., Karathanasis, A.D., 2009. Erosion Index Derived from Terrain Attributes using Logistic Regression and Neural Networks. Agronomy Journal 101, 1068. doi:10.2134/agronj2008.0207x

Polasky, S., Nelson, E., Pennington, D., Johnson, K.A., 2011. The Impact of Land-Use Change on Ecosystem Services, Biodiversity and Returns to Landowners: A Case Study in the State of Minnesota. Environ. Resour. Econ. 48, 219–242. doi:http://link.springer.com/journal/volumesAndIssues/10640

Ponce, V.M., Lohani, A.K., Scheyhing, C., 1996. Analytical verification of Muskingum-Cunge routing. J. Hydrol. 174, 235–241. doi:10.1016/0022-1694(95)02765-3

Renard, K., 1991. RUSLE: Revised Universal Soil Loss Equation. J. Soil Water Conserv. 46, 30.

Schaffrath, K.R., Belmont, P., Wheaton, J.M., 2015. Landscape-scale geomorphic change detection: quantifying spatially variable uncertainty and circumventing legacy data issues. Geomorphology 250, 334–348. doi:10.1016/j.geomorph.2015.09.020

Schottler, S.P., Ulrich, J., Belmont, P., Moore, R., Lauer, J.W., Engstrom, D.R.,

Almendinger, J.E., 2013. Twentieth century agricultural drainage creates more erosive rivers. Hydrol. Process. 1–11. doi:10.1002/hyp.9738

Segerson, K., 1988. Uncertainty and incentives for nonpoint pollution control. J. Environ. Econ. Manage. 15, 87–98. doi:10.1016/0095-0696(88)90030-7

Shepard, L., Westmoreland, P., 2011. This perennial land : third crops, blue earth, and the road to a restorative agriculture. Perennial Lands, Minneapolis, Minn.

Shortle, J.S., Horan, R.D., 2001. The Economics of Nonprofit Pollution Control. J. Econ. Surv. 15, 255–289.

Simon, A., Curini, A., Darby, S.E., Langendoen, E.J., 2000. Bank and near-bank processes in an incised channel. Geomorphology 35, 193–217. doi:10.1016/S0169-555X(00)00036-2

Singh, A.K., Singh, A., Engelhardt, M., 1997. The lognormal distribution in environmental applications. Washington, DC: US Environmental Protection Agency, Office of Solid Waste and Emergency Response.

Singh, J., Knapp, H.V., Arnold, J.G., Demissie, M., 2005. Hydrological modeling of the Iroquois River Watershed using HSPF and SWAT. J. Am. Water. Resour. Assoc. 41, 343–360.

Singh, V.P., Frevert, D.K., 2005. Watershed Models. CRC Press.

Skaggs, R.W., Youssef, M.A., Chescheir, G.M., 2012. DRAINMOD: Model Use, Calibration, and Validation. Transactions of the ASABE 55, 1509–1522. doi:10.13031/2013.42259

Smith, S.M.C., Belmont, P., Wilcock, P.R., 2011. Closing the gap between watershed modeling, sediment budgeting, and stream restoration, in: Simon, A., Bennett,

S.J., Castro, J.M. (Eds.), Stream Restoration in Dynamic Fluvial Systems. American Geophysical Union, pp. 293–317.

Sørensen, R., Seibert, J., 2007. Effects of DEM resolution on the calculation of topographical indices: TWI and its components. Journal of Hydrology 347, 79–89. doi:10.1016/j.jhydrol.2007.09.001

Stone, R.P., Hilborn, D., 2000. Universal Soil Loss Equation, USLE. Ministry of Agriculture, Rood and Rural Affairs.

Stoorvogel, J.J., Antle, J.M., Crissman, C.C., Bowen, W., 2004. The tradeoff analysis model: integrated bio-physical and economic modeling of agricultural production systems. Agric. Syst. 80, 43–66. doi:10.1016/j.agsy.2003.06.002

The Minnesota State Legislative Coordinating Commission, 2016. About the Funds | Minnesota's Legacy [WWW Document]. URL http://www.legacy.leg.mn/about-funds (accessed 11.22.16).

Thomann, R.V., 1998. The future "Golden Age" of predictive models for surface water quality and ecosystem management. J. Environ. Eng. 124, 94–103. doi:10.1061/(ASCE)0733-9372(1998)124:2(94)

Tomer, M.D., Porter, S.A., Boomer, K.M.B., James, D.E., Kostel, J.A., Helmers, M.J., Isenhart, T.M., McLellan, E., 2015. Agricultural conservation planning framework: 1. developing multipractice watershed planning scenarios and assessing nutrient reduction potential. J. Environ. Qual. 44, 754–767. doi:10.2134/jeq2014.09.0386

Tonn, B., 2016. Environmental Quality Incentives Program | NRCS Minnesota [WWW Document]. URL

https://www.nrcs.usda.gov/wps/portal/nrcs/detail/mn/programs/financial/eqip/ (accessed 1.22.17).

Tran, A.M.-T., 2015. Analyses of Potential Ravine and Bluff Stabilization Sites within the Blue Earth and Le Sueur River Basins (Master of Science Thesis). Minnesota State University Mankato, Mankato, MN.

Trimble, S.W., 1981. Changes in Sediment Storage in the Coon Creek Basin, Driftless Area, Wisconsin, 1853 to 1975. Science 214, 181–183. doi:10.1126/science.214.4517.181

Trimble, S.W., 1997. Contribution of stream channel erosion to sediment yield from an urbanizing watershed. Science 278, 1442–1444.

Trimble, S.W., 1999. Decreased Rates of Alluvial Sediment Storage in the Coon Creek Basin, Wisconsin, 1975-93. Science 285, 1244–1246. doi:10.1126/science.285.5431.1244

Trimble, S.W., 2000. US soil erosion rates--myth and reality. Science 289, 248. doi:10.1126/science.289.5477.248

US EPA, 2012a. Impaired waters and Total Maximum Daily Loads [WWW Document]. URL http://water.epa.gov/lawsregs/lawsguidance/cwa/tmdl/index.cfm (accessed 10.26.12).

US EPA, 2012b. Impaired waters and Total Maximum Daily Loads [WWW Document]. URL http://water.epa.gov/lawsregs/lawsguidance/cwa/tmdl/index.cfm (accessed 10.26.12).

USDA, 1975. Sediment sources, yields, and delivery ratios, National Engineering Handbook, Section 3 Sedimentation.

USDA, 2016. USLE Database Research [WWW Document]. URL https://www.ars.usda.gov/midwest-area/west-lafayette-in/national-soil-erosion-research/docs/usle-database/research/ (accessed 1.10.17).

USGS, 2015. Social Values for Ecosystem Services (SolVES) [WWW Document]. URL https://solves.cr.usgs.gov/ (accessed 1.14.17).

Van Buren, M.A., Watt, W.E., Marsalek, J., 1997. Application of the log-normal and normal distributions to stormwater quality parameters. Water Res. 31, 95–104. doi:10.1016/S0043-1354(96)00246-1

Vanoni, V.A., 2006. Manuals and reports on engineering practice. American Society of Civil Engineers.

Vaze, J., Teng, J., Spencer, G., 2010. Impact of DEM accuracy and resolution on topographic indices. Environ. Model. Softw. 25, 1086–1098. doi:10.1016/j.envsoft.2010.03.014

Voinov, A., Bousquet, F., 2010. Modelling with stakeholders. Envi. Model. Softw. 25, 1268–1281. doi:10.1016/j.envsoft.2010.03.007

W. C. Hession, D. E. Storm, C. T. Haan, 1996. Two-phase Uncertainty Analysis: An Example Using the Universal Soil Loss Equation. Transactions of the ASAE 39, 1309–1319. doi:10.13031/2013.27622

Wahl, K., Thoas, Jr., W., Hirsch, R., 1995. Stream-gaging program of the USGS (overview of the program) (USGS Circular No. 1123). USGS, Reston, Virginia.

Walling, D.E., 1983. The sediment delivery problem. J. Hydrol. 65, 209. doi:10.1016/0022-1694(83)90217-2

Westoby, M.J., Brasington, J., Glasser, N.F., Hambrey, M.J., Reynolds, J.M., 2012.

"Structure-from-Motion" photogrammetry: A low-cost, effective tool for geoscience applications. Geomorphology 179, 300–314. doi:10.1016/j.geomorph.2012.08.021

Wilcock, P., 2009. Synthesis Report for Minnesota River Sediment Col- loquium. (Report for MPCA).

Wilcock, P., Cho, S., Gran, K., Hobbs, B., Belmont, P., Bevis, M., Heitkamp, B., Jeff Marr, Mielke, S., Mitchell, N., Kumarasamy, K., 2016. Collaborative for sediment source reduction Greater Blue Earth River Basin (EPA 319 Grant Final Report).

Wischmeier, W.H., Smith, D.D., 1978. Predicting rainfall erosion losses - a guide to conservation planning. Agriculture Handbooks (USA), No. 537 62 pp.

Wu, J., 2006. Uncertainty analysis for coupled watershed and water quality modeling systems. J WATER RESOUR PLAN MANAGE ASCE 132, 351–361. doi:10.1061/(ASCE)0733-9496(2006)132:5(351)

Xepapadeas, A.P., 1992. Environmental policy design and dynamic nonpoint-source pollution. J. Environ. Econ. Manage. 23, 22–39. doi:10.1016/0095-0696(92)90039-Y

Yearley, S., 1999. Computer models and the public's understanding of science: a case-study analysis. Soc. Stud. Sci. 29, 845–866.

Zhang, W., Montgomery, D.R., 1994. Digital elevation model grid size, landscape representation, and hydrologic simulations. Water Resour. Res. 30, 1019–1028. doi:10.1029/93WR03553

Zhang, Y., Degroote, J., Wolter, C., Sugumaran, R., 2009. Integration of modified

universal soil loss equation (MUSLE) into a gis framework to assess soil erosion risk. Land Degrad. Dev. 20, 84–91. doi:10.1002/ldr.893

Biographical sketch

Se Jong Cho was born in Seoul, South Korea on December 18, 1978. She moved to the United States in 1996 and became a naturalized citizen in 2002. She graduated from Northwestern University in 2003 with a Bachelor of Science in Civil Engineering. Se Jong completed her Master of Science in Engineering from Johns Hopkins University while working full time as a hydraulic engineer in May 2009. Shortly after completing her Master's, she began her doctoral program and delved into full time study in Environmental Engineering in September 2009.